

Aus dem NeuroCure Clinical Research Center
der Medizinischen Fakultät Charité – Universitätsmedizin Berlin

DISSERTATION

Afferent visual system changes in patients with
Neuromyelitis Optica Spectrum Disorders

Veränderungen des afferenten visuellen Systems bei
Patienten mit Neuromyelitis Optica Spektrum-Erkrankungen

zur Erlangung des akademischen Grades
Medical Doctor - Doctor of Philosophy (M.D./Ph.D.)

vorgelegt der Medizinischen Fakultät
Charité – Universitätsmedizin Berlin

von

Frederike Cosima Oertel

aus Berlin

Datum der Promotion:05.03.2021.....

Table of contents

1. TABLE OF ABBREVIATIONS	6
2. ABSTRACT [ENGLISH]	9
3. ABSTRACT [GERMAN]	11
4. INTRODUCTION	13
4.1 AIMS	14
5. METHODS	15
5.1 PARTICIPANTS	15
5.2 ETHICS	16
5.3 CLINICAL EXAMINATION AND FUNCTIONAL TESTING	17
5.4 OPTICAL COHERENCE TOMOGRAPHY (OCT)	17
5.5 MAGNETIC RESONANCE IMAGING (MRI)	19
5.6 PROBABILISTIC TRACTOGRAPHY	20
5.7 TRACT-BASED SPATIAL STATISTICS (TBSS)	21
5.8 STATISTICAL ANALYSIS	21
6. RESULTS	22
6.1 METHOD-OCT [18]	22
6.1.1 COHORT DESCRIPTION	22
6.1.2 CONTRIBUTION OF BLOOD VESSELS TO RETINAL NERVE FIBER LAYER THICKNESS	22
6.2 METHOD-DTI [19]	23
6.2.1 COHORT DESCRIPTION	23
6.2.2 METHOD COMPARISON	23
6.2.3 COMPARISON OF NMOSD PATIENTS AGAINST HEALTHY CONTROLS	23

6.3 AQP4-CROSS-SECTIONAL [20]	24
6.3.1 COHORT DESCRIPTION	24
6.3.2 OCT ANALYSIS	24
6.3.3 MRI ANALYSIS	25
6.3.4 CORRELATION OF OCT AND MRI PARAMETERS	25
6.3.5 FUNCTIONAL MEASUREMENTS	25
6.4 AQP4-LONGITUDINAL [21]	26
6.4.1 COHORT DESCRIPTION	26
6.4.2 GROUP DIFFERENCES AT BASELINE	26
6.4.3 OCT CHANGES DURING FOLLOW-UP	26
6.4.4 FUNCTIONAL MEASUREMENTS	27
6.5 MOG-CROSS-SECTIONAL [22]	27
6.5.1 COHORT DESCRIPTION	27
6.5.2 OCT ANALYSIS	28
6.5.3 FUNCTIONAL MEASUREMENTS	28
6.6 MOG-LOGITUDINAL [23]	28
6.6.1 COHORT DESCRIPTION	28
6.6.2 GROUP DIFFERENCES AT BASELINE	29
6.6.3 OCT CHANGES DURING FOLLOW-UP	29
7. DISCUSSION	30
7.1 METHOD-OCT [18]	30
7.2 METHOD-DTI [19]	30
7.3 AQP4-CROSS-SECTIONAL [20]	31
7.4 AQP4-LONGITUDINAL [21]	33
7.5 MOG-CROSS-SECTIONAL [22]	34
7.6 MOG-LONGITUDINAL [23]	35
7.7 PROJECT OUTCOMES AND OUTLOOK	36
7.8 CONCLUSIONS	38

8. REFERENCES	39
9. STATUTORY DECLARATION	47
10. CONTRIBUTIONS	48
11. PUBLICATIONS	50
11.1 METHOD-OCT [18]	50
<p>F.C. Oertel, H. Zimmermann, J. Mikolajczak, M. Weinhold, E.M. Kadas, T. Oberwahrenbrock, F. Pache, J. Bellmann-Strobl, K. Ruprecht, F. Paul, A.U. Brandt, Contribution of blood vessels to retinal nerve fiber layer thickness in NMOSD, <i>Neurol. - Neuroimmunol. Neuroinflammation</i>. (2017) e338.</p>	
11.2 METHOD-DTI [19]	54
<p>J. Kuchling, Y. Backner, F.C. Oertel, N. Raz, J. Bellmann-Strobl, K. Ruprecht, F. Paul, N. Levin, A.U. Brandt, M. Scheel, Comparison of probabilistic tractography and tract-based spatial statistics for assessing optic radiation damage in patients with autoimmune inflammatory disorders of the central nervous system, <i>NeuroImage Clin</i>. (2018) 538–550.</p>	
11.3 AQP4-CROSS-SECTIONAL [20]	69
<p>F.C. Oertel, J. Kuchling, H. Zimmermann, C. Chien, F. Schmidt, B. Knier, J. Bellmann-Strobl, T. Korn, M. Scheel, A. Klistorner, K. Ruprecht, F. Paul, A.U. Brandt, Microstructural visual system changes in AQP4-antibody–seropositive NMOSD, <i>Neurol. - Neuroimmunol. Neuroinflammation</i>. 4 (2017) e334.</p>	
11.4 AQP4-LONGITUDINAL [21]	79
<p>F.C. Oertel, J. Havla, A. Roca-Fernández, N. Lizak, H. Zimmermann, S. Motamedi, N. Borisow, O.B. White, J. Bellmann-Strobl, P. Albrecht, K. Ruprecht, S. Jarius, J. Palace, M.I. Leite, T. Kuempfel, F. Paul, A.U. Brandt, Retinal ganglion cell loss in neuromyelitis optica: a longitudinal study, <i>J Neurol Neurosurg Psychiatry</i>. (2018) 1259-1265.</p>	
11.5 MOG-CROSS-SECTIONAL [22]	88
<p>F. Pache, H. Zimmermann, J. Mikolajczak, S. Schumacher, A. Lacheta, F.C. Oertel, J. Bellmann-Strobl, S. Jarius, B. Wildemann, M. Reindl, A. Waldman,</p>	

K. Soelberg, N. Asgari, M. Ringelstein, O. Aktas, N. Gross, M. Buttman, T. Ach, K. Ruprecht, F. Paul, A.U. Brandt, in cooperation with the Neuromyelitis Optica Study Group (NEMOS), MOG-IgG in NMO and related disorders: a multicenter study of 50 patients. Part 4: Afferent visual system damage after optic neuritis in MOG-IgG-seropositive versus AQP4-IgG-seropositive patients, J. Neuroinflammation. 13 (2016) 282.

11.6 MOG-LONGITUDINAL [23] 101

F.C. Oertel, O. Outteryck, B. Knier, H. Zimmermann, N. Borisow, J. Bellmann-Strobl, A. Blaschek, S. Jarius, M. Reindl, K. Ruprecht, E. Meinl, R. Hohlfeld, F. Paul, A.U. Brandt, T. Kümpfel, J. Havla, Optical coherence tomography in myelin-oligodendrocyte-glycoprotein antibody-seropositive patients: a longitudinal study, J. Neuroinflammation. 16 (2019) 154.

12. CURRICULUM VITAE 113

Mein Lebenslauf wird aus datenschutzrechtlichen Gründen in der elektronischen Version meiner Arbeit nicht veröffentlicht.

13. PUBLICATION LIST 114

14. ACKNOWLEDGMENTS 121

1. Table of abbreviations

3D FLAIR	Volumetric high-resolution fluid-attenuated inversion recovery sequence
AD	Axial diffusivity
ANOVA	Analysis of variance
AQP4-IgG	Aquaporin-4 antibodies
AQP4-eyes ^{ON-}	Eyes of aquaporin-4-antibody seropositive patients with Neuromyelitis Optica Spectrum Disorders without an ipsilateral history of optic neuritis
AQP4-eyes ^{ON+}	Eyes of aquaporin-4-antibody seropositive patients with Neuromyelitis Optica Spectrum Disorders with an ipsilateral history of optic neuritis
AQP4-patients ^{ON-}	Aquaporin-4-antibody seropositive patients with Neuromyelitis Optica Spectrum Disorders without a history of optic neuritis
AQP4-patients ^{ON+}	Aquaporin-4-antibody seropositive patients with Neuromyelitis Optica Spectrum Disorders with a history of optic neuritis
ART	Automatic real time function for image averaging
AUC	Area under the curve
B	Estimate
BCAN	Berlin Center for Advanced Neuroimaging
BHC	Bonferroni Holm correction
BL	Baseline
BV	Retinal blood vessels
CIS	Clinically isolated syndrome
CNS	Central nervous system
CON-PROB	ConTrack-based probabilistic tractography
CSD	Constrained spherical deconvolution
CSD-PROB	Constrained spherical deconvolution-based probabilistic tractography
DTI	Diffusion tensor imaging
EDSS	Expanded disability status scale
ETDRS	Early Treatment Diabetic Retinopathy charts

FA	Fractional anisotropy
FOV	Field-of-view
FT	Foveal thickness
F/U	Follow-up
GCIP	Combined ganglion cell and inner plexiform layer
GEE	Generalized estimating equation
HC	Healthy control
INL	Inner nuclear layer
JHU-TBSS	Tract-based spatial statistics approach based on Johns Hopkins University 1mm white matter tractography probabilistic atlas
JUEL-TBSS	Tract-based spatial statistics approach based on Jülich 1mm probabilistic atlas
LETM	Longitudinally extensive transverse myelitis
LGN	Lateral geniculate nucleus
LMM	Linear mixed models
logMAR	$-\log_{10}$ of decimal visual acuity values
LST	Lesion segmentation toolbox
NMOSD	Neuromyelitis Optica Spectrum Disorders
MD	Mean diffusivity
MOG-IgG	Myelin-oligodendrocyte-glycoprotein antibodies
MOG-eyes ^{ON-}	Eyes of myelin-oligodendrocyte-glycoprotein antibody seropositive patients without an ipsilateral history of optic neuritis
MOG-eyes ^{ON+}	Eyes of myelin-oligodendrocyte-glycoprotein antibody seropositive patients with an ipsilateral history of optic neuritis
MNI-152	3D coordinate system of the Montreal Neurological Institute
MPRAGE	Volumetric high-resolution T1 weighted magnetization prepared rapid acquisition gradient echo sequence
MS	Multiple sclerosis
MV	Macular volume (3 mm diameter)
NCRC	NeuroCure Clinical Research Center
OCT	Optical coherence tomography
ON	Optic neuritis
OR	Optic radiation
p	p-value

pRNFL	Peripapillary retinal nerve fiber layer
pRNFL _{with vessels}	pRNFL measurement including blood vessel positions
pRNFL _{without vessels}	pRNFL measurement excluding blood vessel positions
r	Pearson's correlation coefficient
R ² _{cond}	Conditional coefficient of determination estimated by pseudo-r-squared for mixed-effects models
R ² _{marg}	Marginal coefficient of determination estimated by pseudo-r-squared for mixed-effects models
RD	Radial diffusivity
ROC	Receiver operating characteristic
ROI	Region of interest
SD	Standard deviation
SD-OCT	Spectral-domain optical coherence tomography
SE	Standard error
TBSS	Tract-based spatial statistics
TE	Echo time
TI	Inversion time
TMV	Total macular volume (6 mm diameter)
TR	Repetition time
V1	Primary visual cortex
VA	High contrast visual acuity

2. Abstract [English]

The neuromyelitis optica spectrum comprises chronic inflammatory disorders of the central nervous system (CNS). In 55 % of the patients, optic neuritis is the primary clinical manifestation. Longitudinally extensive transverse myelitis (LETM) including three or more vertebral segments and brainstem syndromes are other important hallmarks of neuromyelitis optica spectrum disorders (NMOSD). The NMOSD-specific antibody targets aquaporin-4 (AQP4-IgG), an astrocytic water channel, and can be detected in serum of up to 80 % of the patients. It has been proposed that accumulation of irreversible disability in AQP4-IgG seropositive NMOSD occurs exclusively in response to attacks. Nevertheless, recent data from animal experiments and human autopsy studies also suggest attack-independent changes, possibly mediated by astrocytic degeneration, in AQP4-IgG seropositive NMOSD. In a subset of AQP4-IgG seronegative patients, myelin-oligodendrocyte-glycoprotein-antibodies (MOG-IgG) can be detected. It is still under debate whether MOG-IgG seropositive disease is part of the NMO-spectrum or rather a separate disease entity.

The aim of this work was to evaluate and to quantify attack-independent alterations of the afferent visual system in AQP4-IgG seropositive NMOSD and to characterize different retinal disease patterns in AQP4-IgG and MOG-IgG seropositive patients. Therefore, modern imaging techniques, such as optical coherence tomography and diffusion weighted imaging based probabilistic tractography were applied. First, these methods were established and evaluated for investigations in the afferent visual system. Second, by utilizing the established methods, microstructural attack-independent changes in the afferent visual system of AQP4-IgG seropositive NMOSD patients were investigated cross-sectionally as well as longitudinally. Key findings were an attack-independent thinning of the fovea and microstructural changes of the optic radiation as well as a longitudinal ganglion cell layer thinning as a potential marker of neuro-axonal damage in comparison to healthy controls. The localization and extent of these changes suggested a widespread astrocytopathy of the CNS with subsequent neuro-axonal degeneration. Lastly, a similar retinal neurodegeneration after optic neuritis but no longitudinal ganglion cell loss was found in MOG-IgG seropositive patients.

The results reported in this thesis challenge the paradigm of pure attack-dependent tissue damage in AQP4-IgG NMOSD and favor the notion that AQP4-IgG and MOG-IgG disorders may represent distinct disease entities. These findings demand - if further substantiated - an adaption of therapeutic strategies, which are at the moment very similar between both patient groups and usually solely based on attack frequency. The functional and diagnostic relevance of the reported findings as well as their translatability to other functional systems of the CNS still needs to be elucidated.

3. Abstract [German]

Das Neuromyelitis Optica Spektrum umfasst chronische inflammatorische Erkrankungen des zentralen Nervensystems (ZNS), die sich zu 55 % zuerst als Sehnervenentzündung (ON) manifestieren. Andere häufige Manifestationen der Patienten mit Neuromyelitis optica-Spektrum-Erkrankungen (*Neuromyelitis optica spectrum disorders*, NMOSD) sind langstreckige transverse Myelitiden über drei oder mehr vertebrale Segmente und Affektionen des Hirnstamms, wie z.B. das Area-postrema-Syndrom. Der NMOSD-spezifische Antikörper bindet Aquaporin-4 (AQP4-IgG), einen astrozytären Wasserkanal, und kann im Serum von bis zu 80% der NMOSD-Patienten nachgewiesen werden. Seit der Definition der NMOSD bestand das Paradigma einer reinen schub-assoziierten klinischen Verschlechterung ohne chronisch-progressiven Verlauf. Daten aus Tierexperimenten und Autopsie-Studien lassen jedoch eine mikrostrukturelle schub-unabhängige Komponente der NMOSD-Pathologie vermuten, die möglicherweise durch die Degeneration von Astrozyten induziert ist.

In einem Teil der AQP4-IgG seronegativen NMOSD-Patienten lässt sich ein Antikörper gegen das Myelin-Oligodendrozyten-Glykoprotein (MOG-IgG) nachweisen. Zurzeit wird diskutiert, ob sich MOG-IgG seropositive Patienten dem NMO-Spektrum zuordnen lassen oder ob es sich um eine davon abzugrenzende Erkrankung handelt.

Zur Evaluation und Quantifizierung schub-unabhängiger Veränderungen des afferenten visuellen Systems in AQP4-IgG seropositiver NMOSD und zur vergleichenden Charakterisierung retinaler Veränderungen in AQP4-IgG und MOG-IgG seropositiven Patienten wurden im Rahmen dieser Dissertation moderne bildgebende Methoden wie die Optische Kohärenztomographie und Probabilistische Traktographie im diffusionsgewichteten MRT angewendet. Nach einer Kontext-spezifischen Evaluation und Weiterentwicklung der Methoden konnten schub-unabhängige mikrostrukturelle Veränderungen bei Patienten mit AQP4-IgG seropositiver NMOSD sowohl in Querschnittsuntersuchungen, als auch longitudinal im afferenten visuellen System erstmalig nachgewiesen werden. Dabei zeigten sich u.a. eine schub-unabhängige Ausdünnung der Fovea, mikrostrukturelle Veränderungen der Sehstrahlung sowie eine longitudinale Abnahme der retinalen Ganglienzellschicht als Marker neuro-axonalen Schadens im Vergleich zu gesunden Kontrollen. Die Lokalisation und das Ausmaß der

Veränderungen suggeriert eine ausgedehnte Astrozytopathie des ZNS mit folgender neuro-axonaler Degeneration. Außerdem zeigte sich in MOG-IgG seropositiven Patienten ein mit AQP4-IgG seropositiven Patienten vergleichbarer neuraxonaler Schaden nach ON, aber kein longitudinaler Verlust von Ganglienzellen.

Diese Ergebnisse stellen die Paradigmen eines rein schub-abhängigen Schädigungsmusters der AQP4-IgG seropositiven NMOSD und einer gemeinsamen Spektrum-Diagnose für AQP4-IgG und MOG-IgG seropositive Patienten infrage und befürworten - sofern weiter bestätigt - eine Überarbeitung der Therapiestrategie, die aktuell bei beiden Patientengruppen sehr ähnlich ist und v.a. auf der Reduktion der Schubfrequenz beruht. Die Klärung der funktionellen und diagnostischen Relevanz der nachgewiesenen Veränderungen im afferenten visuellen System und deren Übertragbarkeit auf andere funktionelle Systeme des ZNS steht noch aus.

4. Introduction

Neuromyelitis optica spectrum disorders (NMOSD) are chronic inflammatory diseases of the central nervous system (CNS) [1]. In 55 % of NMOSD patients, optic neuritis (ON) is the first clinical attack, which may lead to severe visual impairment, especially after the occurrence of several subsequent ON episodes over time [2]. Longitudinally extensive transverse myelitis (LETM) including three or more vertebral segments and brain stem syndromes are further hallmarks of the disease. Secondary symptoms include depression, fatigue and neuropathic pain, which are often undervalued and insufficiently treated in NMOSD [3,4].

Historically, NMOSD were considered a subtype of multiple sclerosis (MS). It was only after 2004, when a pathogenic antibody against the astrocytic water channel aquaporin-4 (AQP4-IgG) was detected in patients with ON and myelitis, that NMOSD was considered as a separate disease entity, apart from MS. AQP4-IgG can be detected in serum of up to 80% of the NMOSD patients [5]. In ca. 40 % of AQP4-IgG seronegative patients myelin-oligodendrocyte-glycoprotein-antibodies (MOG-IgG) can be detected, whereas 60% are double-negative NMOSD patients [6,7]. In this context, it is still a matter of debate whether MOG-IgG seropositive patients are part of the NMO-spectrum or rather a separate disease entity termed MOG-IgG seropositive encephalomyelitis or MOG-IgG seropositive autoimmunity [8,9]. For example, Havla et al. and Chien et al. recently suggested a different disease pattern between MOG-IgG and AQP4-IgG seropositive patients pointing towards a separation of the two entities [10,11]. However, further studies on structural and clinical differences are needed to clarify this diagnostic dilemma.

In contrast to MS, a purely attack-related disability worsening in AQP4-IgG seropositive NMOSD has been proposed and a clinically progressive disease course is considered highly uncommon [12]. Nevertheless, animal and human autopsy studies recently suggested microstructural attack- and lesion-independent damage in NMOSD, pointing towards a direct degenerative influence of AQP4-IgG and AQP4-specific T-cells targeting retinal and cerebral astrocytic cells [13–15]. Against this background, the intention of this thesis was to investigate and to quantify potential attack- and lesion-independent damage

in AQP4-IgG seropositive NMOSD and to characterize differences of retinal damage between AQP4-IgG and MOG-IgG seropositive patients as well as longitudinal changes in MOG-IgG seropositive patients. The afferent visual system is a highly affected functional system and easily accessible by multiple modern imaging techniques. It was therefore used as a suitable representative pathophysiological disease model [16,17].

4.1 Aims

The starting-point was a publication by Ventura et al. [13] showing potential lesion-independent spinal cord atrophy in AQP4-IgG seropositive NMOSD suggesting attack-independent pathology in a small number of patients (N = 6) for the first time. Thereafter, the first aim of this thesis was to evaluate and to quantify attack- and lesion-independent alterations of the visual pathway in AQP4-IgG seropositive NMOSD.

Furthermore, it remains unclear, if MOG-IgG seropositive patients are part of the NMO-spectrum or part of a separate disease entity - so called MOG-IgG seropositive encephalomyelitis or autoimmunity [8]. Therefore, the second aim of this thesis was to characterize the different retinal disease patterns in AQP4-IgG and MOG-IgG seropositive patients and to investigate longitudinal changes in MOG-IgG seropositive patients. For the investigation, several modern imaging techniques, mainly optical coherence tomography (OCT) and diffusion tensor imaging (DTI), were applied [16,17]. To further improve these studies, pre-existing methods were analyzed and adapted to assure applicability in NMOSD. In detail, the objectives of the six sub-projects were:

To establish and to evaluate applied methods:

- To investigate potential influences of retinal blood vessels (BVs) on OCT analysis in NMOSD. (METHOD-OCT) [18]
- To compare the capacity of tract-based spatial statistics (TBSS) and probabilistic tractography based approaches to detect optic radiation (OR) damage in several patient cohorts compared to healthy controls (HCs). (METHOD-DTI) [19]

To characterize and to quantify attack-independent changes in AQP4-IgG seropositive NMOSD:

- To cross-sectionally identify microstructural lesion-independent afferent visual system changes in the retina and OR of AQP4-IgG seropositive NMOSD patients without a history of ON compared to HCs. (AQP4-CROSS-SECTIONAL) [20]
- To longitudinally investigate progressive retinal neuro-axonal damage in the eyes of AQP4-IgG seropositive NMOSD without a history of ON compared to HCs. (AQP4-LONGITUDINAL) [21]

To investigate retinal changes in MOG-IgG seropositive patients with and without a history of ON:

- To cross-sectionally identify differences in the retinal disease pattern after ON between AQP4-IgG and MOG-IgG seropositive patients. (MOG-CROSS-SECTIONAL) [22]
- To longitudinally investigate progressive retinal neuro-axonal damage in MOG-IgG seropositive patients compared to HCs. (MOG-LONGITUDINAL [23])

5. Methods

5.1 Participants

All participants were recruited from ongoing observational cohort studies at the NeuroCure Clinical Research Center (NCRC) at Charité-Universitätsmedizin Berlin, Germany (for all sub-projects) and

- the Technical University Munich, Germany (AQP4-CROSS-SECTIONAL [20], MOG-LONGITUDINAL [23]),
- the Ludwig Maximilians Universität Munich, Germany (AQP4-LONGITUDINAL [21], MOG-LONGITUDINAL [23])
- the Nuffield Department for Clinical Neurosciences at Oxford University, United Kingdom (AQP4-LONGITUDINAL [21]).
- the universities of Düsseldorf, Freiburg, Würzburg and Heidelberg, Germany and the Vejle Hospital and Institute of Molecular Medicine, University of Southern Denmark, Odense, Denmark (MOG-CROSS-SECTIONAL [22])
- the Roger Salengro Hospital, University of Lille, France (MOG-LONGITUDINAL [23])

The cohort of interest was AQP4-IgG seropositive NMOSD for METHOD-OCT [18], METHOD-DTI [19], AQP4-CROSS-SECTIONAL [20] and AQP4-LONGITUDINAL [21], according to the consensus diagnostic criteria 2015 [1]. Depending on the research question, the cohort was complemented by other diseases of the NMO-spectrum or by patients with LETM only (METHOD-OCT [18], METHOD-DTI [19]) and compared to HCs (METHOD-DTI [19], AQP4-CROSS-SECTIONAL [20], AQP4-LONGITUDINAL [21]), MS and clinically isolated syndrome (CIS) (METHOD-DTI [19]). The cohort of interest was MOG-IgG seropositive patients for MOG-CROSS-SECTIONAL [22] and MOG-LONGITUDINAL [23]. For MOG-CROSS-SECTIONAL [22], the cohort was compared to AQP4-IgG seropositive NMOSD. Further inclusion criteria were complete clinical and imaging data, and age between 18 and 75 years (MOG-LONGITUDINAL [23]: between 15 and 75 years). Eyes with ON within five months before participation or comorbidities potentially influencing image analysis such as ischemic cerebral and retinal pathologies and high refraction errors were excluded. HC participants were selected to match the cohort of interest in age and sex.

AQP4-IgG and MOG-IgG were determined by cell-based assays using the laboratory's cut-offs (AQP4-IgG: Euroimmun, Lübeck, Germany; MOG-IgG: Molecular Neuroimmunology Group, University Heidelberg, Heidelberg, Germany; MOG IFT, EUROIMMUN, Laboratory Stöcker, Germany; Reindl Lab, Medical University of Innsbruck, Innsbruck, Austria; Meinl Lab, LMU, Munich, Hemmer Lab, TUM, Munich) [24–26].

5.2 Ethics

All cohort studies were approved by the local ethic committees and performed in accordance with the guidelines for Good Scientific Practice, the declaration of Helsinki in its current applicable version as well as with the German and – when applicable – British, French and Danish law. All participants gave written informed consent before inclusion.

5.3 Clinical examination and functional testing

A detailed history was taken and a complete neurological examination including the Expanded Disability Status Scale (EDSS) [27] was performed for all patients at NCRC at their annual visits under supervision of a board-certified neurologist. Monocular high contrast visual acuity (VA) was acquired by ETDRS (Early Treatment Diabetic Retinopathy Study) charts in 20ft distance under habitual correction (METHOD-OCT [18], METHOD-DTI [19], AQP4-CROSS-SECTIONAL [20], MOG-CROSS-SECTIONAL [22], MOG-LONGITUDINAL [23]) or best correction (AQP4-LONGITUDINAL [21]) and reported as $-\log_{10}$ (logMAR) of decimal values to assure normal distribution (AQP4-CROSS-SECTIONAL [20], AQP4-LONGITUDINAL [21], MOG-CROSS-SECTIONAL [22], MOG-LONGITUDINAL [23]), letter acuity (METHOD-OCT [18]) or decimal values (METHOD-DTI [19]).

5.4 Optical Coherence Tomography (OCT)

OCT is a non-invasive interferometric method to generate structural cross-sectional images of the retina. Depending on the structural composition of the retina, low-coherent light is reflected and backscattered differently. The following interference with a reference beam allows anatomical reconstruction with a resolution of a few micrometers (approximately 5 μm). Due to a fixed reference mirror and a simultaneous analysis of echoes from all retinal layers by Fourier transformation, spectral-domain OCT (SD-OCT) allows 50 to 100 times faster acquisition than previous methods, highly reduces motion artifacts and gives better reproducibility [17]. All OCT data were acquired with Spectralis SD-OCT (Heidelberg Engineering, Heidelberg, Germany) using automatic real time function for image averaging (ART).

Over the last years of OCT research, the peri-papillary retinal nerve fiber layer (pRNFL) has been shown to be a reliable marker for neuro-axonal damage and is widely used for diagnostic studies and clinical trials [28]. The pRNFL consists of the unmyelinated axons of retinal ganglion cells, originating from the retina and forming the optic nerve, thereby representing the anterograde parts of axons directly affected by ON [29]. The pRNFL is usually measured within a 12° (~3.4 mm) diameter ring (1,536 A-scans; $1 \leq \text{ART} \leq 100$) around the optic nerve head and represents a cross-section of the full axonal content of

the particular optic nerve. pRNFL is reported as mean thickness (in μm) in all OCT sub-projects to quantify the severity of neuro-axonal damage after ON [29]. For METHOD-OCT [18], retinal BV positions were automatically detected by OCTSEG [30] and manually corrected; the relative BV contribution as percentage was calculated utilizing pRNFL with vessels ($\text{pRNFL}_{\text{with vessels}}$) and pRNFL without vessels ($\text{pRNFL}_{\text{without vessels}}$): $[\text{pRNFL}_{\text{with vessels}} - \text{pRNFL}_{\text{without vessels}}]/\text{pRNFL}_{\text{with vessels}} \times 100 \%$ [18]. For all sub-projects, intraretinal layer segmentation was performed semi-automatically (using Eye Explorer software, Version 1.9.10.0) and manually corrected if necessary.

The pRNFL is usually accompanied by the combined ganglion cell and inner plexiform layer (GCIP), consisting of the retinal ganglion cells and parts of retinal astrocytes. Due to poor differentiation of the ganglion cell layer and inner plexiform layer in OCT imaging, both are usually combined together as GCIP for analysis. The ganglion cells account for about 34 % of the macular volume and are therefore mostly measured as perifoveal volume (in mm^3) [17,28]. The diameter of the cylinder (AQP4-CROSS-SECTIONAL [20] and MOG-CROSS-SECTIONAL [22]: 6 mm diameter; AQP4-LONGITUDINAL [21] and MOG-LONGITUDINAL [23]: 3 mm diameter) depends on the available OCT data.

Recently, the inner nuclear layer (INL) was reported to be swollen in neuroinflammatory states in autoimmune diseases of the CNS [31] and was therefore quantified in the same scan and diameter (AQP4-LONGITUDINAL [21], MOG-CROSS-SECTIONAL [22], MOG-LONGITUDINAL [23]) as well as the total macular volume (TMV, 6 mm diameter) (AQP4-CROSS-SECTIONAL [20]) or the macular volume (MV, 3 mm diameter) (AQP4-LONGITUDINAL [21], MOG-LONGITUDINAL [23]) and the outer retinal layers (MOG-CROSS-SECTIONAL [22]). However, over the period of this work, the fovea turned out to be of particular interest in NMOSD [20,32]. It is known as the point of sharpest vision and the parafoveal area is characterized by a high density of astrocytic Müller cells, which express AQP4 and may thus serve as antibody-targets in AQP4-IgG seropositive NMOSD [14,15]. Therefore, in two sub-projects (AQP4-CROSS-SECTIONAL [20], AQP4-LONGITUDINAL [21]) the fovea thickness (FT) is reported as mean thickness of the 1-mm-cylinder around the fovea from each collected macular scan [20]. OCT scan quality was analyzed based on the OSCAR-IB criteria [33] and reported according to the APOSTEL criteria [34].

5.5 Magnetic Resonance Imaging (MRI)

All MRI data for the sub-projects METHOD-DTI [19] and AQP4-CROSS-SECTIONAL [20] were acquired on the same 3T scanner (MAGNETOM Trio Siemens, Erlangen, Germany) at the Berlin Center for Advanced Neuroimaging (BCAN). Diffusion tensor imaging (DTI) estimates displacement of water molecules, and by interpreting these data along and perpendicular to white matter tracts allows conclusions about tract integrity [16]. For each voxel, the tensor information is summarized in the following DTI-based indices, which correlate with different pathological tissue changes [16]: From all DTI-based indices, fractional anisotropy (FA) represents anisotropic diffusion as a marker of microstructural integrity and is most widely used, whereas mean diffusivity (MD) measures the total molecular water diffusion rate and seems to reflect tissue integrity on a more global level [16]. Of specific interest in the field of neuroimmunology are the radial diffusivity (RD) and axial diffusivity (AD). RD is suggested to represent demyelination, whereas AD is a potential marker of axonal damage [16]. For DTI a single-shot echo planar sequence was used (repetition time (TR) / echo time (TE) = 7,500 ms/ 86 ms; field-of-view (FOV) = 240 x 240 mm²; matrix 96 x 96, slice thickness 2.3 mm, 64 noncollinear directions, b-value = 1,000 s/ mm²).

A volumetric high-resolution fluid-attenuated inversion recovery sequence (3D FLAIR) (TR / TE / inversion time (TI) = 6,000 ms/ 388 ms/ 2,100 ms; FOV = 256 x 256 mm², slice thickness 1.0 mm) was used for white matter lesion identification. Lesions of FLAIR images were quantified manually using ITK-SNAP (www.itksnap.org) [35] (METHOD-DTI [16]) or the lesion prediction algorithm in the Lesion Segmentation Toolbox (LST) for Matlab 2013a (MathWorks, Inc., Natick, MA) [36] (AQP4-CROSS-SECTIONAL [20]). A volumetric high-resolution T1 weighted magnetization prepared rapid acquisition gradient echo (MPRAGE) sequence (TR / TE / TI = 1,900 ms/ 2.55 ms/ 900 ms; FOV = 240 x 240 mm², matrix 240 x 240; 176 slices, slice thickness 1.0 mm) was used for co-registration (METHOD-DTI [19]).

5.6 Probabilistic Tractography

Probabilistic tractography is a modern DTI-based modelling approach for analyzing and visualizing white-matter tracts based on a priori anatomical knowledge of tract terminations and course [16].

For the subprojects METHOD-DTI [19] and AQP4-CROSS-SECTIONAL [20], probabilistic tractography of the OR was performed with MRtrix 0.2 (J-D Tournier; Brain Research Institute, Melbourne, Australia) [37], as already established in our group and modified from pipelines of Martínez-Heras et al. [38] and Lim et al. [39] (CSD-PROB). Diffusion tensors were fitted by a linear least squares approach. Fiber orientation distribution was assessed by constrained spherical deconvolution (CSD) and mapped with a maximum harmonic order of 6. Lateral geniculate nucleus (LGN) as the seed region of interest (ROI) and primary visual cortex (V1) as target ROI were generated as binary masks based on the Jülich probabilistic atlas. For exclusion masks, a termination coronal plane 20 mm posterior of the temporal pole, a midline sagittal exclusion plane and a grey matter segmentation mask were generated in the 3D coordinate system of the Montreal Neurological Institute (MNI-152). All exclusion masks and inclusion ROIs were registered to individual DTI space. For each OR, 10,000 uni-directional streamlines were generated (step size: 0.2 mm; FA threshold 0.1; curvature threshold 25 %) from LGN to V1 and subsequently transferred to the Vistalab environment (vistalab.stanford.edu/, Vistalab, Stanford University, Stanford, CA) for tract profiling of weighted mean DTI values at 50 equally spaced positions [40]. For AQP4-CROSS-SECTIONAL [20] the middle 30 positions were used for statistical analysis to exclude potential confounders from LGN and V1. For METHOD-DTI [19] the complete tract was analyzed to guarantee comparability with other methodological approaches.

A second probabilistic tractography method was applied as a comparison in METHOD-DTI [19] based on the open-source MrVista package (vistalab.stanford.edu/, Vistalab, Stanford University, Stanford, CA) (CON-PROB). First, eddy current-induced distortion correction and motion correction were performed within the vistalab environment. Probabilistic tractography was then performed in parallel to the ConTrack algorithm by Sherbondy et al. [41]. Fiber tensors were fitted by a least-squares approach. LGN and V1 were identified manually in co-registered MPRAGE images. For each OR, 75,000 unidirectional streamlines were generated (no FA threshold; curvature threshold 130°)

from LGN to V1 and reduced to the 20 % (15,000) most likely streamlines. All ORs were manually corrected for erroneously identified fibers using Quench. Then, as outlined above, DTI values were derived along the OR at 50 equally-spaced positions and reported as weighted average at the node [40].

5.7 Tract-Based Spatial Statistics (TBSS)

TBSS is an approach for group comparisons of DTI data, based on tools of the FMRIB Software Library (FSL 5.0.9) and widely used as a fast and easy method to assess microstructural damage in several, atlas-derived brain regions [42]. First, diffusion tensors are calculated by a linear least squares approach and FA images are generated. The brain is extracted by the BET-function. Subsequently, FA images of all patients are aligned into a common space by a nonlinear registration tool called FNIRT. One FA-skeleton for the representation of mutual tract cores of all individuals is generated. The individual FA images can now be projected onto the FA skeleton and analyzed based on atlas masks. For METHOD-DTI [19], OR adapted masks of the Johns-Hopkins University 1 mm white matter tractography probabilistic atlas (JHU-TBSS) and the Jülich 1 mm probabilistic atlas (JUDEL-TBSS) were used for DTI methods comparison.

5.8 Statistical Analysis

Age and sex differences in patients and HCs were tested by Chi-squared test for sex and Mann-Whitney-U-Test for age. Analysis of OCT values and OR tractography results were performed cross-sectionally by generalized estimated equation models (GEEs) and longitudinally by linear mixed-effects models (LMM) to account for intra-subject inter-eye dependencies as well as for irregular intervals between visits in longitudinal analyses. Dependent on the research questions, models were corrected for age, sex, and history of ON. Also, the following statistical methods were applied: paired t-test as well as one-way and two-way repeated measures analysis of variance (ANOVA) for group differences; Pearson correlation and Bland-Altman plots for correlation analyses; Fisher's z test for correlation comparison, intraclass correlation coefficients (ICC) by two-way random-effects models for absolute agreement between methods, receiver operating characteristic (ROC) analysis for sensitivity and specificity evaluation, Fisher combined

probability test for combined p values of exploratory and confirmatory cohort results and a linear spline regression model by Ratchford et al. [43]. If necessary, statistical tests were adjusted for multiple comparisons using Bonferroni-Holm correction (BHC, for METHOD-DTI [19]).

All statistical tests were performed using R [44] with packages psych, geepack, irr, ICC, lme4, lmer, ROct, ggplot2, beeswarm, Mass, MuMIn, Rmisc and multcomp; complemented by Graphpad Prism 6.0 (for METHOD-DTI [19], AQP4-CROSS-SECTIONAL [20]). Significance was established at $p < 0.05$. All values are expressed as mean \pm standard deviation (SD), if not stated otherwise.

6. Results

6.1 METHOD-OCT [18]

6.1.1 Cohort description

Forty patients participated in the study (female/male 39/1; age 44.7 ± 15.4 years). Thirty-seven patients fulfilled the 2015 NMOSD diagnostic criteria (AQP4-IgG seropositive $n = 28$) [1]. Three patients had a diagnosis of MOG-IgG seropositive autoimmunity [8]. Twenty-five patients (42 eyes) had a history of ON. Due to insufficient OCT image quality, three eyes were excluded from the analysis [33].

6.1.2 Contribution of blood vessels to retinal nerve fiber layer thickness

pRNFL_{without vessels} ($68.3 \pm 26.2 \mu\text{m}$) was thinner than pRNFL_{with vessels} ($76.1 \pm 26.6 \mu\text{m}$; $p < 2e^{-16}$). The relative BV contribution increased with lower pRNFL ($r = -0.700$; $p = 1e^{-12}$) and was drastically lower in eyes with a pRNFL $> 60 \mu\text{m}$ ($9 \% \pm 3 \%$) than in eyes with pRNFL $< 60 \mu\text{m}$ ($16 \% \pm 5 \%$; $p = 8e^{-8}$). VA (36 ± 19 ETDRS letters) correlated with pRNFL_{with vessels} ($r = 0.621$; $p = 2e^{-9}$) as well as with pRNFL_{without vessels} ($r = 0.618$; $p = 2e^{-9}$). In eyes with a pRNFL $< 60 \mu\text{m}$, the correlation was marginally better for pRNFL_{without vessels} ($r = 0.495$; $p = 0.007$) than for pRNFL_{with vessels} ($r = 0.482$; $p = 0.009$). However, this difference did not reach significance. pRNFL and contribution of BV were not influenced by antibody-status, time since onset or therapeutic regime.

6.2 METHOD-DTI [19]

6.2.1 Cohort description

Sixty-two patients with autoimmune neuroinflammatory conditions participated in this study. Nineteen patients with AQP4-IgG seropositive NMOSD and four AQP4-IgG seronegative NMOSD patients were combined as NMOSD group for analysis (female/male 20/3; age 46.7 ± 14.5 years) [1]. All NMOSD patients had a history of ON. Furthermore, 39 patients with CIS or early relapsing-remitting MS were included. All cohorts were compared to 26 HCs (female/male 22/4, age 43.7 ± 15.7 years). For improved clarity of this summary, group differences are only reported for the comparison between NMOSD and HCs.

6.2.2 Method comparison

All methods were equally capable to generate OR tracts in all patients' MRI with the exception of one CIS patient using CSD-PROB. In HCs, the relative variability quantified by the coefficient of variation was increasing from JUEL-TBSS (4 %) over JHU-TBSS (6 %) and CSD-PROB (7 %) to highest values in CON-PROB (14 %).

The FA values generated with all four methods showed good agreement in Bland-Altman plots and were correlated with each other with correlation coefficients ranging between $r = 0.273$ (JUEL-TBSS/CON-PROB) and $r = 0.871$ (JHU-TBSS/JUEL-TBSS). However, the FA value distribution of the four methods differed drastically in all patient cohorts and absolute agreement was poor: The lowest ICC of all four methods were found for HCs with the suspected lowest damage (ICC = 0.024) and NMOSD with the suspected highest OR damage (ICC = 0.074).

6.2.3 Comparison of NMOSD patients against healthy controls

All methods revealed significant FA differences in NMOSD (JUEL-TBSS 0.44 ± 0.03 , JHU-TBSS 0.48 ± 0.04 , CON-PROB 0.38 ± 0.06 , CSD-PROB 0.50 ± 0.04) versus HCs (JUEL-TBSS 0.46 ± 0.02 , JHU-TBSS 0.52 ± 0.03 , CON-PROB 0.42 ± 0.06 , CSD-PROB 0.54 ± 0.03 , all comparisons with BHC $p < 0.05$). ROC-analysis for the comparison of HCs and NMOSD showed the highest area under the curve (AUC) for CSD-PROB

(AUC = 0.812) followed by CON-PROB (AUC = 0.742), JHU-TBSS (AUC = 0.756) and JUEL-TBSS (AUC = 0.719).

In NMOSD total T2 lesion volume and OR-specific T2 lesion volume differed from HCs (total T2 lesion volume: HC 0.38 ± 0.66 ml, NMOSD 2.15 ± 3.07 ml; OR-specific T2 lesion volume: HCs 0.04 ± 0.07 ml, NMOSD 0.44 ± 0.87 ml; both comparisons with BHC: $p < 0.05$). OR-specific T2 lesion volume was weakly correlated with OR FA values, not reaching significance in NMOSD with any method ($0.15 \leq p \leq 0.76$). Also, pRNFL (HCs 96.9 ± 7.5 μm , NMOSD 67.1 ± 19.7 μm ; with BHC $p < 0.05$) as well as VA of the worse eye ([decimal values]: HCs 1.02 ± 0.31 , NMOSD 0.74 ± 0.47 , with BHC $p < 0.05$) were severely reduced in NMOSD compared to HCs. Independent of the method, pRNFL was not correlated with OR FA values of NMOSD patients ($0.32 \leq p \leq 0.74$).

6.3 AQP4-CROSS-SECTIONAL [20]

6.3.1 Cohort description

For the initial cohort, 25 patients with AQP4-IgG seropositive NMOSD and 26 matched HCs (female/male 22/4; age 43.6 ± 15.7 years) were included at Charité-Universitätsmedizin Berlin [1]. Nineteen of these patients had a history of ON (AQP4-patients^{ON+}; female/male 17/2; age 43.7 ± 12.5 years), whereas six patients had a history of LETM without prior ON (AQP4-patients^{ON-}; female/male 6/0; age 43.1 ± 9.8 years).

For a confirmatory cohort, six additional AQP4-IgG seropositive NMOSD patients – three patients with a history of ON (female/male 3/0; age 44.0 ± 1.0 years) and three patients with a history of LETM only (female/male 3/0; age 41.3 ± 10.7 years) - and eight HCs (female/male 8/0; age 42.3 ± 1.7 years) from Technical University Munich were included [1].

6.3.2 OCT analysis

Compared to HCs (280 ± 21 μm), FT of AQP4-patients^{ON-} (260 ± 18 μm , $p = 0.015$) and AQP4-patients^{ON+} (262 ± 18 μm , $p = 2.4e^{-4}$) was equally reduced and did not differ between patient groups ($p = 0.900$). However, neither pRNFL nor GCIP – both markers of neuro-axonal damage in the retina – were thinner in AQP4-patients^{ON-} (pRNFL: 105.0 ± 6.9 μm ; GCIP: 1.93 ± 0.11 mm^3) compared to HCs (pRNFL: 97.1 ± 7.4 μm , $p = 0.005$; GCIP: 1.87 ± 0.15 mm^3 , $p = 0.210$). pRNFL was thicker than in HCs. In AQP4-

patients^{ON+}, as predicted, pRNFL ($71.7 \pm 22.8 \mu\text{m}$) and GCIP ($1.54 \pm 0.30 \text{ mm}^3$) were thinned severely compared to HCs (pRNFL: $p = 2.4e^{-10}$; GCIP: $p = 8.3e^{-8}$) as well as compared to AQP4-patients^{ON-} (pRNFL: $p = 7.0e^{-11}$; GCIP: $p = 3.9e^{-8}$). With regards to the relatively small sample size, the analysis of a second independent confirmatory cohort was conducted, which confirmed all results. Statistical combination of p values from both cohorts replicated OCT value differences between AQP4-patients^{ON+} and HCs (pRNFL: $p = 1.43e^{-18}$; GCIP: $p = 8.87e^{-22}$; FT: $p = 1.24e^{-16}$), but also between AQP4-patients^{ON-} and HCs (pRNFL: $p = 1.93e^{-9}$; FT: $p = 3.52e^{-14}$).

6.3.3 MRI analysis

Using CSD-PROB [16], ORs of AQP4-patients^{ON+} showed a reduction in FA (0.53 ± 0.04) as well as an increase in MD (0.87 ± 0.05) and RD (0.59 ± 0.06) compared to HCs (FA: 0.57 ± 0.04 ; $p = 1.5e^{-5}$; MD: 0.83 ± 0.07 , $p = 0.037$; RD: 0.53 ± 0.08 , $p = 0.003$). However, FA was also reduced in AQP4-patients^{ON-} (0.54 ± 0.03) compared to HCs ($p = 0.046$) pointing towards microstructural alterations in the OR of AQP4-patients^{ON-}. Differences in other DTI parameters did not reach significance. To exclude lesional influences on the afferent visual system in AQP4-patients^{ON-}, whole brain lesion volume and OR lesions were analyzed. Two AQP4-patients^{ON-} of the initial cohort presented with small unspecific dot-like lesions in the OR unilaterally. No OR lesions were detectable in any confirmatory AQP4-patient^{ON-}. Whole-brain lesion volume did not differ between AQP4-patients^{ON-} ($0.95 \pm 1.30 \text{ ml}$) and AQP4-patients^{ON+} ($0.95 \pm 1.23 \text{ ml}$, $p > 0.999$).

6.3.4 Correlation of OCT and MRI parameters

In AQP4-patients^{ON+}, reduced GCIP was correlated with FA values ($r = 0.361$, $p = 0.030$). However, in AQP4-patients^{ON-}, neither pRNFL ($r = -0.204$, $p = 0.500$) nor GCIP ($r = 0.261$, $p = 0.400$) showed a correlation with FA. FT was not correlated with FA in AQP4-patients^{ON-} ($r = 0.066$, $p = 0.800$) or AQP4-patients^{ON+} ($r = 0.210$, $p = 0.200$).

6.3.5 Functional measurements

AQP4-Patients^{ON-} presented with normal VA ([logMAR] -0.02 ± 0.10), where mean VA of all eyes of AQP4-patients^{ON+} was impaired ([logMAR] 0.22 ± 0.37 ; $p = 0.002$). VA was not correlated with FT or FA in AQP4-patients^{ON-} (FT: $r = -0.312$, $p = 0.300$; FA: $r = -0.445$, $p = 0.100$) or AQP4-patients^{ON+} (FT: $r = 0.082$, $p = 0.700$; FA: $r = 0.073$, $p = 0.700$).

6.4 AQP4-LONGITUDINAL [21]

6.4.1 Cohort description

Fifty-one AQP4-IgG seropositive NMOSD patients from Charité-Universitätsmedizin Berlin (N = 23), Ludwig-Maximilians University Munich (N = 11) and Oxford University (N = 17) (94 eyes, female/male 43/8; age 47.3 ± 14.4 years) were enrolled [1]. Thirty-four eyes had an ON-attack at least five months before baseline (BL) (AQP4-eyes^{ON+}). Sixty eyes had no history of ON (AQP4-eyes^{ON-}). Eyes with ipsilateral ON during F/U (N = 4), insufficient imaging data (N = 3) or ophthalmological comorbidities (N = 1) were excluded. Seven patients experienced attacks during follow-up (F/U): two patients with one LETM, one patient with four LETMs, four patients (2 eyes^{ON-}, 2 eyes^{ON+}) with contralateral ON during F/U. The NMOSD cohort was compared to 28 sex- and age-matched HCs (56 eyes, female/male 22/6; age 43.1 ± 9.8 years). Median F/U time was equal between NMOSD ([median (range)] 2.3 years (1.0 – 3.5)) and HCs ([median (range)] 2.3 (1.0 – 3.3)). VA was acquired in a subset of 22 patients with NMOSD from Berlin and Oxford (F/U ([median (range)] 1.1 years (0.7 – 3.3))).

6.4.2 Group differences at baseline

At baseline, AQP4-eyes^{ON+} showed reduced GCIP (0.43 ± 0.12 mm³), pRNFL (67.0 ± 24.2 μm) and MV (2.11 ± 0.19 mm³) compared to HCs (GCIP: 0.63 ± 0.04 mm³, $p < 2.0e^{-16}$, pRNFL: 98.5 ± 9.2 μm, $p = 5.0e^{-11}$; MV: 2.37 ± 0.10 mm³, $p = 3.7e^{-12}$). GCIP (0.59 ± 0.06 mm³) and MV (2.25 ± 0.15 mm³) was also reduced in AQP4-eyes^{ON-} compared to HCs (GCIP: $p = 0.002$; MV: $p = 6.1e^{-6}$), but still higher than in AQP4-eyes^{ON+} (GCIP: $p = 7.4e^{-12}$, MV: $p = 1.0e^{-5}$). A subset of AQP4-eyes^{ON-}, who had never experienced ON ipsi- or contralaterally, also showed reduced GCIP (0.60 ± 0.05 mm³) compared to HCs ($p = 0.016$). pRNFL did not differ between AQP4-eyes^{ON-} and HCs. Also, INL was comparable between all three groups. Compared to HCs (278 ± 19 μm), FT reduction was replicated in AQP4-eyes^{ON+} (262 ± 20 μm, $p = 3.7e^{-4}$) and AQP4-eyes^{ON-} (267 ± 21 μm, $p = 0.040$) [20,32].

6.4.3 OCT changes during follow-up

A longitudinal GCIP thinning with an annual loss of $[-0.00415 \pm 0.01200$ mm³] was observed in AQP4-eyes^{ON-} ($p = 0.022$). Compared to HCs (annual

loss - $0.00005 \pm 0.00466 \text{ mm}^3$), this thinning was significantly larger ($p = 0.044$, $R^2_{\text{marg}} = 0.123$, $R^2_{\text{cond}} = 0.995$). Also, annual loss in AQP4-eyes^{ON-} with ($-0.00413 \pm 0.00779 \text{ mm}^3$) and without a contralateral history of ON (annual loss - $0.00468 \pm 0.01310 \text{ mm}^3$) did not differ ($p = 0.805$). In contrast, AQP4-eyes^{ON+} did not show longitudinal GCIP thinning compared to HCs (annual loss - $0.00094 \pm 0.0119 \text{ mm}^3$, $p = 0.960$). Influences of ethnicity, treatment and contralateral ON in AQP4-eyes^{ON-} during F/U were excluded. In patients experiencing attacks during F/U, pRNFL thickening (pRNFL difference: $1.56 \pm 4.39 \text{ }\mu\text{m}$) was shown, compared to NMOSD patients without any attacks during F/U (pRNFL difference: $-1.04 \pm 3.21 \text{ }\mu\text{m}$; $p = 0.003$). GCIP ($p = 0.513$), MV ($p = 0.670$), INL ($p = 0.970$) or FT ($p = 0.330$) were not changed by attacks during F/U.

6.4.4 Functional measurements

At baseline, VA of AQP4-eyes^{ON+} ([logMAR] 0.41 ± 0.69) was reduced, compared to AQP4-eyes^{ON-} ([logMAR] 0.01 ± 0.25) without reaching significance ($p = 0.052$). VA improvement during F/U in AQP4-eyes^{ON+} (-0.21 ± 0.40) was more pronounced than in AQP4-eyes^{ON-} (-0.02 ± 0.07), also not reaching significance ($p = 0.054$).

6.5 MOG-CROSS-SECTIONAL [22]

6.5.1 Cohort description

Sixteen MOG-IgG seropositive patients from Charité-Universitätsmedizin Berlin ($N = 10$), the University of Freiburg ($N = 1$), the University of Würzburg ($N = 1$), the University of Düsseldorf ($N = 1$), the University of Heidelberg ($N = 1$) and the Vejle Hospital and Institute of Molecular Medicine, University of Southern Denmark, Odense, Denmark ($N = 2$) (female/male 15/1; age 44.0 ± 15.2 years) were compared to 16 age- and sex-matched AQP4-IgG-positive NMOSD patients (all female, age [mean \pm SD] 43.2 ± 13.9 years) and 16 age- and sex-matched healthy controls (female/male 15/1; age [mean \pm SD] 43.9 ± 15.4 years) from the NCRC's research database. Two MOG-seropositive patients with ophthalmologic comorbidities (glaucoma, dry macular degeneration) and two eyes with acute ON were included in the case descriptions but excluded from the statistical analysis together with their respective AQP4-IgG seropositive and healthy controls. Only eyes with a history of ON (MOG-eyes^{ON+}) were included in the statistical analysis. Thus,

23 eyes from 14 patients (Number of ON episodes [median(range)]: 4.5 (1 - 13); time since last ON [median(range)]: 16.4 (3-125) months) were included.

6.5.2 OCT analysis

In MOG-eyes^{ON+}, pRNFL thickness ($59 \pm 23 \mu\text{m}$) and GCIP volume ($1.50 \pm 0.34 \text{ mm}^3$) was reduced compared to HC (pRNFL: $99 \pm 6 \mu\text{m}$; GCIP: $1.97 \pm 0.11 \text{ mm}^3$). INL was increased in MOG-eyes^{ON+} seropositive patients ($1.03 \pm 0.10 \text{ mm}^3$) compared to HC ($0.95 \pm 0.04 \text{ mm}^3$, $p = 0.009$). No group difference was noted between MOG-eyes^{ON+} and AQP4- eyes^{ON+} regarding pRNFL, GCIP or INL.

The first ON episode caused less pRNFL loss in MOG- eyes^{ON+} ($12.8 \mu\text{m}$, $p = 0.001$) than in AQP4-eyes^{ON+} ($32.8 \mu\text{m}$, $p < 0.001$) compared to HC; In contrast, a second episode caused more pRNFL loss in MOG-eyes^{ON+} ($37.8 \mu\text{m}$, $p < 0.001$) than in AQP4-eyes^{ON+} ($20.8 \mu\text{m}$, n.s.). Of note, the MOG-eyes^{ON+} showed a higher annualized relapse rate ($p = 0.026$) and annualized ON rate ($p = 0.004$) compared to AQP4-eyes^{ON+} and a higher number of ON episodes in MOG-eyes^{ON+} was correlated with a more severe pRNFL ($B = - 4.9$, $SE = 1.40$, $p < 0.001$) and GCIP reduction ($B = -0.07$, $SE = 0.02$, $p < 0.001$), whereas retinal neurodegeneration was not associated to the number of ON episodes in AQP4-eyes^{ON+}.

6.5.3 Functional measurements

P100 latency was reduced in 60 % (12/20 eyes) of MOG-eyes^{ON+} with available VEP-data. Also, VA was reduced in MOG-eyes^{ON+} ([logMAR] 0.35 ± 0.88): 70 % (16/23) of MOG-eyes^{ON+} had a preserved VA [logMAR] of ≤ 0.1 , whereas three eyes being legally blind with a VA [logMAR] ≥ 1.0 . A preserved VA but no significant difference of VA was noted compared to AQP4-eyes^{ON+} ([logMAR] 0.72 ± 1.09 , $p = 0.300$).

6.6 MOG-LONGITUDINAL [23]

6.6.1 Cohort description

Thirty-eight eyes of 24 MOG-IgG seropositive patients without ON during follow-up (MOG-eyes^{ON-}, female/male 15/9; age 40.7 ± 13.5 years) from the NCRC, Charité-Universitätmedizin Berlin (N = 10), LMU Munich (N = 11), Klinikum rechts der Isar, TU Munich (N = 2), Germany, and from the University of Lille Hospital, France (N = 1) were

included. Patients fulfilled the diagnostic criteria for MOG-IgG seropositive NMOSD meeting the 2015 IPND criteria for seronegative NMOSD (N = 12) or MOG-IgG seropositive MS (N = 3) or MOG-IgG seropositive encephalomyelitis (N = 2) or MOG-IgG seropositive recurrent ON (N = 7). Before BL, 18 eyes had no history of ON (MOG-eye^{ON-}) and 20 eyes had a history of ON (MOG-eye^{ON+}; number of ONs [median (range)]: 0 (0 - 8); time since ON in years [median (range)] 2.2 (0.4 - 14.9)). Of the MOG-eye^{ON-}, six eyes had no attacks during F/U, whereas twelve eyes had an attack (five eyes of three patients with a myelitis, four eyes of two patients with myelitis and brainstem attacks, one eye of one patient with myelitis and contralateral ON and two eyes of two patients with contralateral ON).

Fifty-six eyes of twenty-eight age- and sex-matched HCs (female/male 18/6; age 43.1 ± 9.8 years) from NCRC, Charité-Universitätsmedizin Berlin were included. Patients with age < 15 or > 75, bilateral ON during F/U, F/U ≤ 8 months and eyes with a history of ON ≤ 5 months before BL, missing OCT data, confounding diseases or ON during F/U were excluded. Median F/U time was equal between MOG-IgG seropositive patients ([median (IQR)] 1.9 years (0.6 – 2.8)) and HCs ([median (IQR)] 1.9 (0-8 – 3.3)).

6.6.2 Group differences at baseline

At BL, MOG-eyes^{ON+} (0.39 ± 0.12 mm³, p < 0.0001) and MOG-eyes^{ON-} (0.57 ± 0.07 mm³, p = 0.008) had a thinner GCIP compared to HC (0.63 ± 0.04 mm³). MOG-eyes^{ON+} also showed a thinner pRNFL (58.25 ± 22.56 μm) and MV (2.19 ± 0.13 mm³) as well as a thicker INL (0.30 ± 0.05 mm³) compared to HC (pRNFL: 98.50 ± 9.17 μm, p < 0.0001. MV: 2.37 ± 0.10 mm³, p < 0.0001. INL: 0.27 ± 0.03 mm³, p = 0.046) and MOG-eyes^{ON-} (pRNFL: 94.33 ± 15.92 μm, p < 0.0001 MV: 2.34 ± 0.11 mm³, p = 0.0005. INL: 0.26 ± 0.03 mm³, p = 0.004). MOG-eyes^{ON-} did not show any other difference compared to HC. Thirty percent (6/20) MOG-eyes^{ON+} had macular microcysts. MOG-eyes^{ON+} ([logMAR] 0.55 ± 0.81) had a reduced VA compared to MOG-eyes^{ON-} ([logMAR] 0.05 ± 0.15, p = 0.058) and HC ([logMAR] -0.09 ± 0.14; p = 0.010).

6.6.3 OCT changes during follow-up

No longitudinal group differences (GCIP, pRNFL, INL, MV) were observed between MOG-eyes^{ON-} and MOG-eyes^{ON+}. Therefore, MOG-eyes^{ON-} and MOG-eyes^{ON+} were analyzed as a combined cohort compared to HC to investigate ON-independent damage.

Longitudinally, MOG-IgG seropositive eyes suffered from pRNFL thinning (annual loss: $-2.20 \pm 4.29 \mu\text{m}$) without progressive GCIP reduction compared to HC ($-0.35 \pm 1.17 \mu\text{m}$, $p = 0.009$). The loss was mainly observed in the twelve MOG-eyes^{ON-} with an attack within the six months before BL (not an ipsilateral ON; pRNFL: $100.2 \pm 12.7 \mu\text{m}$ vs. $82.7 \pm 16.2 \mu\text{m}$; $p = 0.019$).

7. Discussion

7.1 METHOD-OCT [18]

The contribution of BV to average pRNFL measurements increased with thinner pRNFL. Therefore, BV-induced noise might be particularly strong in low pRNFL measurements, as found in severely affected eyes of NMOSD patients with multiple ON episodes. Potential limitations of this study included the small and heterogenous NMOSD cohort and the lack of comparison to HCs. The latter would have been especially interesting, since Green et al. [45] described fundoscopic findings, suggesting an inner retinal BV wall thickening in NMOSD. However, this sub-project was neither able to specify, nor account for this effect. This small exploratory study was meant to raise awareness of the issue of potential flooring effects in pRNFL measurements. Hence, the reduced sensitivity of pRNFL measurements in low measuring range should be kept in mind, especially for longitudinal studies in highly affected NMOSD patients, as in parts of the cohort for the subproject AQP4-LONGITUDINAL [21] and MOG-LONGITUDINAL [23].

7.2 METHOD-DTI [19]

This method comparison focused on four common, widely used, and easily accessible TBSS and probabilistic tractography pipelines. An advantage of TBSS methods is the fully-automated implementation without manual intervention, but it is known to be highly susceptible to FA skewing by partial volume effects of surrounding structures [42]. In contrast, probabilistic tractography is often more time-consuming and susceptible to image artifacts leading to an insufficient tract generation, but shows higher sensitivity for microstructural changes and allows along-tract analyses [16]. Further, the newer CSD-

PROB method shows improved sensitivity for crossing and kissing fibers compared to CON-PROB, but also a higher risk of failure in tract reconstruction [16].

Despite the different approaches of TBSS-JUEL, TBSS-JHU, CSD-PROB and CON-PROB, all methods were equally capable of detecting microstructural damage in the OR of NMOSD patients compared to HCs and were highly correlated. Since the absolute agreement of FA values differed drastically between methods in our study, comparisons of FA values between different DTI studies need to be avoided. This study showed methodical differences to be most prominent in patients with suspected severe visual system damage like in NMOSD, making it mandatory to apply the same method to quantify FA values in the OR within a study and to harmonize protocols for future DTI studies in NMOSD [16].

All methods distinguished NMOSD from HCs, with the best AUC found for CSD-PROB. All NMOSD patients in this study had a history of ON, confirmed by a prominent reduction of pRNFL thickness and VA. Hence, these results are in line with previous studies showing significant FA reduction within the OR as a sign of anterograde trans-synaptic degeneration due to ON [46]. However, overall FA reduction was not correlated with pRNFL and showed only a weak correlation with OR lesion volume pointing towards a partly independent microstructural degenerative process in the OR and/or the retina of NMOSD patients.

In this method comparison approach, CSD-PROB, as a fully-automated method without manual intervention, showed the highest AUC and was therefore used in all following DTI-based OR-analyses including the subproject AQP4-CROSS-SECTIONAL [20]. Nevertheless, future studies are warranted to validate the capacity and limitations of different methods and to develop a gold standard for DTI-based OR analysis.

7.3 AQP4-CROSS-SECTIONAL [20]

AQP4-IgG seropositive NMOSD patients without a history of ON and normal visual function presented with reduced OR FA values and decreased FT suggesting ON-independent retinal and OR changes. In the past, attack-independent alterations in NMOSD have been controversially discussed [32,47]. However, this study now clearly

demonstrated attack- and lesion-independent afferent visual system changes in two independent cohorts.

The foveal and parafoveal areas are characterized by a high density of astrocytic Müller cells. Müller cells have a relevant role in neurotransmitter and photoreceptor recycling as well as in water balance and energy metabolism [48]. Apart from Müller cells, two other types of retinal astrocytes exist: elongated astrocytes located in the RNFL and star-shaped astrocytes located in the ganglion cell layer [48]. All three types of astrocytes express AQP4 and might serve as retinal targets of AQP4-IgG and also AQP4-specific T cells in NMOSD [14,15]. Subsequent astrocytic dysfunction or degeneration could change water and energy homeostasis and decrease retinal function. Also, astrocytic dysfunction would lead to neuro-axonal damage in the retina and other brain regions [15,48,49]. The equal thinning of the fovea in patients with and without a history of ON in this study suggests a Müller cell associated retinal pathology independent of previous lesions or attacks affecting the afferent visual system [20,32,50].

Beyond that, the microstructural OR changes in patients without prior ON indicate a more widespread diffuse astrocytopathy in the afferent visual system. Previously, spinal cord atrophy and astrocytic end feet changes in spinal cord lesions of AQP4-IgG seropositive patients without a history of LETM have been described [13]. Also, multiple animal studies showed the retraction of astrocytic end feet or astrocyte death suggesting a primary astrocytopathy in NMOSD outside of acute lesions [14,49]. Including this study, the detection of sub-clinical damage in multiple locations like the spinal cord, OR and retina, points to a disseminated astrocytopathy in NMOSD within the CNS.

To exclude potential confounders, only AQP4-IgG seropositive patients who presented with LETM and had no history of ON, visual symptoms or brainstem syndromes for the patients^{ON-} cohort were included; a lack of pRNFL thinning and VA reduction made sub-clinical ON further unlikely. In contrast to previous studies, eyes with contralateral ON were also excluded from this group to avoid potential carry-over effects by chiasmic involvement [2]. Two patients^{ON-} presented with small lesions near the OR, but their measurements were well positioned within the data distribution of the whole cohort and did not appear as outliers. Despite the very low sample size of the initial cohort, all OCT results were confirmed in an independent confirmatory cohort. Nevertheless, potential

environmental influences (prematurity, ethnicity etc.) on the highly variable foveal shape cannot be excluded. Also, it remained unclear if the reported differences are attack-related, for example induced by circulating antibodies or by general inflammatory states, and whether these cross-sectional findings are indeed part of longitudinal progressive processes or rather caused by discontinuous disease activity. The AQP4-LONGITUDINAL [21] analysis to follow up the reported findings was therefore needed.

7.4 AQP4-LONGITUDINAL [21]

This study reported longitudinal GCIP loss in AQP4-IgG seropositive NMOSD eyes without a history of ON. Whereas AQP-CROSS-SECTIONAL [20] and preclinical studies previously suggested microstructural attack- and lesion-independent damage in NMOSD, pointing towards a direct degenerative influence of AQP4-IgG and AQP4-specific T-cells targeting retinal astrocytic cells, previous cross-sectional studies showed conflicting results regarding the question as to whether sub-clinical neuro-axonal damage occurs in the retina of NMOSD patients independent of ON [14,15]. While some studies found ON-independent pRNFL and GCIP thinning compared to HCs [32], others did not report any difference [47]. Also, the only two previous longitudinal studies in NMOSD reported opposing results: Whereas pRNFL thinning was shown in NMOSD patients from France over 18 months [51], Manogaran et al. did not report any significant pRNFL or macular thickness reduction in a case series of nine NMOSD patients over four years [52]. Using intra-retinal layer segmentation, the current study now showed longitudinal GCIP thinning in eyes of AQP4-IgG seropositive patients without a history of ON. In eyes with a history of ON, no significant thinning was shown compared to HCs. This may be explained by the flooring effects in eyes affected by ON, as described for pRNFL in METHOD-OCT [18].

Patients without a history of ON presented with thinned GCIP and TMV at baseline, compared to HCs, suggesting pre-existing ON-independent neuro-axonal damage. Further, the FT thinning in eyes with and without a history of ON compared to HCs described in AQP4-CROSS-SECTIONAL [20] was replicated in this study. Together with the longitudinal GCIP thinning, these results suggest a primary retinopathy affecting retinal astrocytes with subsequent neuro-axonal damage in AQP4-IgG seropositive NMOSD. FT did not change longitudinally. This might be explained by the pathological

process in the fovea might have already taken place before inclusion in the longitudinal study. Other potential explanations include discontinuous thinning during inflammatory states or during transient periods of high-antibody-concentrations. Since the fovea is already the thinnest part of the retina, FT measurements could be affected by flooring effects or might be insensitive to subtle changes during longitudinal analyses with a short F/U.

The absent difference between non-ON eyes with and without a history of contralateral ON and the nonexistent influence of contralateral ON in the statistical model as well as the unreduced pRNFL and VA in non-ON eyes makes chiasmic cross-over effects and sub-clinical ONs highly unlikely. Nevertheless, other sources of retrograde neuro-axonal damage have to be considered as an alternative explanation for GCIP thinning: For example, this study did not account for potential retrograde degeneration originating from lesions in the posterior visual pathway. This should be addressed in future confirmatory studies.

In contrast to AQP4-CROSS-SECTIONAL [20] and in the light of the rarity of NMOSD in Europe, this multi-center study was strengthened by a comparable high sample size and allowed a separation of physiological (for example age-related) thinning and disease-related degeneration based on the comparison with HCs. Nevertheless, this study was still not able to evaluate influences of ethnicity and disease-modifying therapies in subgroup analyses. Further potential limitations include the lack of posterior visual pathway imaging mentioned above and the lack of HCs from all study sites.

7.5 MOG-CROSS-SECTIONAL [22]

MOG-IgG seropositive patients showed a severe neuroaxonal degeneration after ON, which was comparable to ON-induced damage in AQP4-IgG seropositive patients. This study further suggests that the comparable damage between both groups is caused by a higher relapse rate in MOG-IgG compared to AQP4-IgG seropositive patients. This would explain the contradictory results from earlier studies describing a monophasic disease, a milder clinical phenotype, less neuro-axonal damage and a better recovery in MOG-IgG compared to AQP4-IgG seropositive patients [53–56]. More recent studies support our findings in MOG-IgG seropositive patients including a relapsing disease course with a

high frequency of attacks, a retinal neuro-axonal damage after ON at least as severe as in AQP4-IgG seropositive patients and – in some patients – with severe visual impairment [57,58].

Interestingly, some MOG-IgG seropositive patients had a high VA despite a severe neuro-axonal damage. More sensitive functional tests as low-contrast letter acuity or multifocal VEP would be necessary to further investigate these findings. Further limitations of this study comprise the lack of HCs from all centers, of non-Caucasian patients and of a systematic testing for other optic neuropathies such as Leber's hereditary optic neuropathy as well as the retrospective character and the limited sample size due to the condition's rarity.

7.6 MOG-LONGITUDINAL [23]

In this small longitudinal study, we did not observe progressive ON-independent GCIP thinning in MOG-IgG seropositive patients compared to HC. This is in contrast to progressive GCIP reduction in MS and AQP4-IgG seropositive NMOSD as shown in AQP4-LONGITUDINAL [21,59].

A previous cross-sectional study by Havla et al. observed a pRNFL and GCIP reduction in MOG-eyes^{ON} compared to HC [11]. Our study now confirmed the reduced GCIP at baseline but showed pRNFL thinning only longitudinally and without accompanying GCIP loss. Potential explanations for the GCIP reduction only at baseline include a subclinical optic nerve pathology, a progressive neurodegenerative retinal involvement, an affection by subclinical ON and chiasmic crossover of contralateral ON. In light of the publication by Ramanathan et al. describing only 5 % of ONs to involve the chiasm in MOG-IgG seropositive patients, the latter however seems unlikely [2].

The longitudinal pRNFL reduction without GCIP loss might indicate a subclinical retinal involvement but could also suggest drug-induced retinal damage related to immunosuppressive treatment or a remission of pRNFL edema. This is clearly in contrast to AQP4-LONGITUDINAL [21] and therefore an additional hint towards a differentiation of MOG-IgG seropositive patients from AQP4-IgG seropositive NMOSD as a separate disease entity. Whereas a primary AQP4-IgG-induced retinopathy was also suggested

by preclinical investigations [15], an expression of MOG in the retina has not been shown so far, making a primary retinopathy in MOG-IgG seropositive patients further unlikely.

A study by Chien et al. recently suggested a swelling of the upper cervical cord area during non-myelitis attacks in MOG-IgG seropositive patients as a sign of systemic affection [10]. Our data, showing pRNFL loss especially after non-ipsilateral ON attacks, is in line with these results. Chien et al. also showed clear differences of spinal cord affection patterns, disability accumulation and myelitis attack frequency between AQP4-IgG and MOG-IgG seropositive patients further supporting our findings from MOG-CROSS-SECTIONAL [22] and MOG-LONGITUDINAL [23] pointing towards a separation of both antibody groups as distinct immunological disorders.

Apart from the small sample size due to the rarity of the condition in Europe, further limitations of the study are the heterogeneity of clinical phenotypes, of immunosuppressive treatments and of applied MOG-IgG assays. Furthermore, this project lacks MRI data to specify afferent visual pathway damage posterior to the retina.

7.7 Project outcomes and outlook

The findings, reported in this thesis, showed ON- and lesion-independent changes in the afferent visual system of patients with AQP4-IgG seropositive NMOSD for the first time, in both a cross-sectional and a longitudinal approach. These findings challenge the long prevailing paradigm of pure attack-related degeneration in NMOSD and suggest an attack- and lesion-independent process contributing to disability increase in NMOSD. However, it is still unclear, if the progressive course is limited to an astrocytic retinopathy, or if other functional pathways, like the [spinal cord – corticospinal tract – primary motor cortex]-axis, are similarly affected by a diffuse astrocytopathy. The results by Ventura et al. [13] describing LETM-independent changes in the spinal cord, as well as attack-independent symptoms, including fatigue, depression and neuropathic pain, favor the hypothesis of a widespread tissue alteration in NMOSD. They are in line with the diffuse astrocytopathy in NMOSD suggested by AQP4-CROSS-SECTIONAL [20] and AQP4-LONGITUDINAL [21], widely exceeding the confined boundaries of the afferent visual system [3,60]. Whereas the clinical relevance of fatigue, depression and pain for the

quality of life of NMOSD patients has already been reported [3,60], the clinical relevance of sub-clinical afferent visual system changes still needs to be clarified, since both studies (AQP4-CROSS-SECTIONAL [20] and AQP4-LONGITUDINAL [21]) lacked consistent and sensitive functional data, e.g. low-contrast visual acuity or visual evoked potentials. Independent of their functional relevance, these progressive sub-clinical alterations might be a sensitive marker for future disease progression and a precursor of full attacks with secondary demyelination and neuroaxonal damage. In particular, the foveal changes might provide important information on the differential diagnoses of AQP4-IgG seropositive NMOSD and MS, MOG-IgG seropositive autoimmunity and other neuroophthalmological conditions [20,32].

In contrast to AQP4-IgG seropositive NMOSD, this thesis also showed MOG-IgG seropositive patients to suffer from more frequent but milder ON attacks with a subsequent poorer long-term prognosis [22]. MOG-IgG seropositive patients seem to be preserved from progressive GCIP reduction and only showed pRNFL thinning potentially corresponding with a reduction of retinal edema during an attack-related systemic inflammatory state (MOG-LONGITUDINAL [23]). Both studies in MOG-IgG seropositive patients (MOG-CROSS-SECTIONAL [22], MOG-LONGITUDINAL [23]) are highly supportive of the theory that AQP4-IgG and MOG-IgG are in fact biomarkers of two different disease entities [8]. However, the current long-term treatment strategies of AQP4-IgG and MOG-IgG seropositive patients (oral prednisolone, rituximab, azathioprine, mycophenolate mofetil, tocilizumab) are very similar – and evidence is mostly based on retrospective studies and uncontrolled trials [61]. The progressive damage in AQP4-IgG seropositive patients as well as the striking differences between both disease groups might demand an adaption of the current approach for disease-modifying therapy (DMT) in AQP4-IgG and MOG-IgG seropositive patients, which is currently based mainly on attack frequency. Therefore, RCTs developing safe and effective drugs for AQP4-IgG and MOG-IgG seropositive patients are highly warranted. Several trials are currently conducted or planned [61]. For future studies, OCT parameters like GCIP or foveal shape characteristics should be included as endpoints to evaluate not only structural damage of ONs, but also to sensitively track effects on progressive retinal changes. The most widely used OCT parameter in clinical studies to date is pRNFL as it is easily accessible and mostly standardized [28]. Nevertheless, the application of pRNFL could be problematic in some cases, since pRNFL is known to be swollen after ON for up to three months in MS and for an unknown time period also in NMOSD [29]. In AQP4-

CROSS-SECTIONAL [20], patients without a history of ON presented with a thicker pRNFL compared to HCs. In AQP4-LONGITUDINAL [21], patients with no ipsilateral ON but other attacks during F/U even presented with a pRNFL swelling compared to patients without any attacks during F/U. Also, in MOG-LONGITUDINAL [23] pRNFL swelling was one potential explanation for our findings. Although the results of these studies should not be overstated in light of the small sample sizes, pRNFL swelling in NMOSD could indicate tissue swelling caused by astrocytic dysfunction, a systemic inflammatory state or prednisolone treatment side-effects. Mild pRNFL swelling might conceal sub-clinical neuro-axonal damage of the pRNFL and could potentially limit certain conclusions in RCTs and diagnostic trials, emphasizing the necessity of new OCT endpoints for RCTs, such as GCIP and foveal shape characteristics.

7.8 Conclusions

Methodological pre-analyses raised awareness for the potential flooring effects in OCT measurements by retinal BVs in severely affected eyes and showed CSD-PROB to be the most appropriate method for DTI-based OR evaluation in AQP4-IgG seropositive NMOSD [18,19]. Following these methodological evaluations, this thesis showed attack- and lesion-independent alterations in the afferent visual system of AQP4-IgG seropositive patients both cross-sectionally and longitudinally for the first time [20,21]. Localizations and extent of these changes suggest an underlying astrocytopathy of the CNS in AQP4-IgG seropositive NMOSD with subsequent neuro-axonal damage. These results challenge the paradigm of AQP4-IgG seropositive NMOSD-related damage to occur solely attack-dependent and demand an adaptation of therapy response markers, currently typically based on attack frequency. Furthermore, this thesis shows a severe retinal damage after ON in MOG-IgG seropositive patients and striking differences in retinal disease patterns between AQP4-IgG and MOG-IgG seropositive patients. Longitudinally, our data suggest the absence of ganglion cell loss in MOG-IgG seropositive patients independent of ON further underlining the differences of both antibody groups and lending further evidence to the pathophysiological and clinical separation of both disease entities. The functional and diagnostic relevance of the detected afferent visual system changes as well as their applicability to other functional systems of the CNS still needs to be investigated in the future.

8. References

- [1] D.M. Wingerchuk, B. Banwell, J.L. Bennett, P. Cabre, W. Carroll, T. Chitnis, J. de Seze, K. Fujihara, B. Greenberg, A. Jacob, S. Jarius, M. Lana-Peixoto, M. Levy, J.H. Simon, S. Tenembaum, A.L. Traboulsee, P. Waters, K.E. Wellik, B.G. Weinshenker, International consensus diagnostic criteria for neuromyelitis optica spectrum disorders, *Neurology*. 85 (2015) 177–189. doi:10.1212/WNL.0000000000001729.
- [2] S. Ramanathan, K. Prelog, E.H. Barnes, E.M. Tantsis, S.W. Reddel, A.P. Henderson, S. Vucic, M.P. Gorman, L.A. Benson, G. Alper, C.J. Riney, M. Barnett, J.D. Parratt, T.A. Hardy, R.J. Leventer, V. Merheb, M. Nosadini, V.S. Fung, F. Brilot, R.C. Dale, Radiological differentiation of optic neuritis with myelin oligodendrocyte glycoprotein antibodies, aquaporin-4 antibodies, and multiple sclerosis, *Mult. Scler. Houndmills Basingstoke Engl.* 22 (2016) 470–482. doi:10.1177/1352458515593406.
- [3] J.-B. Chanson, H. Zéphir, N. Collongues, O. Outteryck, F. Blanc, M. Fleury, P. Vermersch, J. de Seze, Evaluation of health-related quality of life, fatigue and depression in neuromyelitis optica, *Eur. J. Neurol.* 18 (2011) 836–841. doi:10.1111/j.1468-1331.2010.03252.x.
- [4] S. Asseyer, F. Schmidt, C. Chien, M. Scheel, K. Ruprecht, J. Bellmann-Strobl, A.U. Brandt, F. Paul, Pain in AQP4-IgG-positive and MOG-IgG-positive neuromyelitis optica spectrum disorders, *Mult. Scler. J. - Exp. Transl. Clin.* 4 (2018) 2055217318796684. doi:10.1177/2055217318796684.
- [5] A. Zekeridou, V.A. Lennon, Aquaporin-4 autoimmunity, *Neurol. Neuroimmunol. Neuroinflammation*. 2 (2015) e110. doi:10.1212/NXI.0000000000000110.
- [6] S.H.M. Hamid, D. Whittam, K. Mutch, S. Linaker, T. Solomon, K. Das, M. Bhojak, A. Jacob, What proportion of AQP4-IgG-negative NMO spectrum disorder patients are MOG-IgG positive? A cross sectional study of 132 patients, *J. Neurol.* 264 (2017) 2088–2094. doi:10.1007/s00415-017-8596-7.
- [7] S. Jarius, D. Franciotta, F. Paul, R. Bergamaschi, P.S. Rommer, K. Ruprecht, M. Ringelstein, O. Aktas, W. Kristoferitsch, B. Wildemann, Testing for antibodies to human aquaporin-4 by ELISA: sensitivity, specificity, and direct comparison with immunohistochemistry, *J. Neurol. Sci.* 320 (2012) 32–37. doi:10.1016/j.jns.2012.06.002.
- [8] Y. Hachohen, J. Palace, Time to separate MOG-Ab-associated disease from AQP4-Ab-positive neuromyelitis optica spectrum disorder, *Neurology*. (2018).

doi:10.1212/WNL.0000000000005619.

- [9] S.S. Zamvil, A.J. Slavin, Does MOG Ig-positive AQP4-seronegative opticospinal inflammatory disease justify a diagnosis of NMO spectrum disorder?, *Neurol. Neuroimmunol. Neuroinflammation*. 2 (2015) e62. doi:10.1212/NXI.0000000000000062.
- [10] C. Chien, M. Scheel, T. Schmitz-Hübsch, N. Borisow, K. Ruprecht, J. Bellmann-Strobl, F. Paul, A.U. Brandt, Spinal cord lesions and atrophy in NMOSD with AQP4-IgG and MOG-IgG associated autoimmunity, *Mult. Scler. Houndmills Basingstoke Engl.* (2018) 1352458518815596. doi:10.1177/1352458518815596.
- [11] J. Havla, T. Kümpfel, R. Schinner, M. Spadaro, E. Schuh, E. Meinl, R. Hohlfeld, O. Outteryck, Myelin-oligodendrocyte-glycoprotein (MOG) autoantibodies as potential markers of severe optic neuritis and subclinical retinal axonal degeneration, *J. Neurol.* 264 (2017) 139–151. doi:10.1007/s00415-016-8333-7.
- [12] D.M. Wingerchuk, S.J. Pittock, C.F. Lucchinetti, V.A. Lennon, B.G. Weinshenker, A secondary progressive clinical course is uncommon in neuromyelitis optica, *Neurology*. 68 (2007) 603–605. doi:10.1212/01.wnl.0000254502.87233.9a.
- [13] R.E. Ventura, I. Kister, S. Chung, J.S. Babb, T.M. Shepherd, Cervical spinal cord atrophy in NMOSD without a history of myelitis or MRI-visible lesions, *Neurol. Neuroimmunol. Neuroinflammation*. 3 (2016) e224. doi:10.1212/NXI.0000000000000224.
- [14] B. Zeka, M. Hastermann, N. Kaufmann, K. Schanda, M. Pende, T. Misu, P. Rommer, K. Fujihara, I. Nakashima, C. Dahle, F. Leutmezer, M. Reindl, H. Lassmann, M. Bradl, Aquaporin 4-specific T cells and NMO-IgG cause primary retinal damage in experimental NMO/SD, *Acta Neuropathol. Commun.* 4 (2016) 82. doi:10.1186/s40478-016-0355-y.
- [15] C.M. Felix, M.H. Levin, A.S. Verkman, Complement-independent retinal pathology produced by intravitreal injection of neuromyelitis optica immunoglobulin G, *J. Neuroinflammation*. 13 (2016) 275. doi:10.1186/s12974-016-0746-9.
- [16] J. Kuchling, A.U. Brandt, F. Paul, M. Scheel, Diffusion tensor imaging for multilevel assessment of the visual pathway: possibilities for personalized outcome prediction in autoimmune disorders of the central nervous system, *EPMA J.* 8 (2017) 279–294. doi:10.1007/s13167-017-0102-x.
- [17] F.C. Oertel, H. Zimmermann, F. Paul, A.U. Brandt, Optical coherence tomography in neuromyelitis optica spectrum disorders: potential advantages for individualized monitoring of progression and therapy, *EPMA J.* 9 (2018) 21–33.

doi:10.1007/s13167-017-0123-5.

[18] F.C. Oertel, H. Zimmermann, J. Mikolajczak, M. Weinhold, E.M. Kadas, T. Oberwahrenbrock, F. Pache, J. Bellmann-Strobl, K. Ruprecht, F. Paul, A.U. Brandt, Contribution of blood vessels to retinal nerve fiber layer thickness in NMOSD, *Neurol. - Neuroimmunol. Neuroinflammation*. 4 (2017) e338.

doi:10.1212/NXI.0000000000000338.

[19] J. Kuchling, Y. Backner, F.C. Oertel, N. Raz, J. Bellmann-Strobl, K. Ruprecht, F. Paul, N. Levin, A.U. Brandt, M. Scheel, Comparison of probabilistic tractography and tract-based spatial statistics for assessing optic radiation damage in patients with autoimmune inflammatory disorders of the central nervous system, *NeuroImage Clin*. 19 (2018) 538–550. doi:10.1016/j.nicl.2018.05.004.

[20] F.C. Oertel, J. Kuchling, H. Zimmermann, C. Chien, F. Schmidt, B. Knier, J. Bellmann-Strobl, T. Korn, M. Scheel, A. Klistorner, K. Ruprecht, F. Paul, A.U. Brandt, Microstructural visual system changes in AQP4-antibody–seropositive NMOSD, *Neurol. - Neuroimmunol. Neuroinflammation*. 4 (2017) e334.

doi:10.1212/NXI.0000000000000334.

[21] F.C. Oertel, J. Havla, A. Roca-Fernández, N. Lizak, H. Zimmermann, S. Motamedi, N. Borisow, O.B. White, J. Bellmann-Strobl, P. Albrecht, K. Ruprecht, S. Jarius, J. Palace, M.I. Leite, T. Kuempfel, F. Paul, A.U. Brandt, Retinal ganglion cell loss in neuromyelitis optica: a longitudinal study, *J Neurol Neurosurg Psychiatry*. (2018) jnnp-2018-318382. doi:10.1136/jnnp-2018-318382.

[22] F. Pache, H. Zimmermann, J. Mikolajczak, S. Schumacher, A. Lacheta, F.C. Oertel, J. Bellmann-Strobl, S. Jarius, B. Wildemann, M. Reindl, A. Waldman, K. Soelberg, N. Asgari, M. Ringelstein, O. Aktas, N. Gross, M. Buttman, T. Ach, K. Ruprecht, F. Paul, A.U. Brandt, in cooperation with the Neuromyelitis Optica Study Group (NEMOS), MOG-IgG in NMO and related disorders: a multicenter study of 50 patients. Part 4: Afferent visual system damage after optic neuritis in MOG-IgG-seropositive versus AQP4-IgG-seropositive patients, *J. Neuroinflammation*. 13 (2016) 282. doi:10.1186/s12974-016-0720-6.

[23] F.C. Oertel, O. Outteryck, B. Knier, H. Zimmermann, N. Borisow, J. Bellmann-Strobl, A. Blaschek, S. Jarius, M. Reindl, K. Ruprecht, E. Meinl, R. Hohlfeld, F. Paul, A.U. Brandt, T. Kümpfel, J. Havla, Optical coherence tomography in myelin-oligodendrocyte-glycoprotein antibody-seropositive patients: a longitudinal study, *J. Neuroinflammation*. 16 (2019) 154. doi:10.1186/s12974-019-1521-5.

- [24] S. Jarius, F. Paul, O. Aktas, N. Asgari, R.C. Dale, J. de Seze, D. Franciotta, K. Fujihara, A. Jacob, H.J. Kim, I. Kleiter, T. Kümpfel, M. Levy, J. Palace, K. Ruprecht, A. Saiz, C. Trebst, B.G. Weinshenker, B. Wildemann, MOG encephalomyelitis: international recommendations on diagnosis and antibody testing, *J. Neuroinflammation*. 15 (2018) 134. doi:10.1186/s12974-018-1144-2.
- [25] M. Spadaro, S. Winklmeier, E. Beltrán, C. Macrini, R. Höftberger, E. Schuh, F.S. Thaler, L.A. Gerdes, S. Laurent, R. Gerhards, S. Brändle, K. Dornmair, C. Breithaupt, M. Krumbholz, M. Moser, G. Krishnamoorthy, F. Kamp, D. Jenne, R. Hohlfeld, T. Kümpfel, H. Lassmann, N. Kawakami, E. Meinl, Pathogenicity of human antibodies against myelin oligodendrocyte glycoprotein, *Ann. Neurol*. 84 (2018) 315–328. doi:10.1002/ana.25291.
- [26] S. Mader, V. Gredler, K. Schanda, K. Rostasy, I. Dujmovic, K. Pfaller, A. Lutterotti, S. Jarius, F. Di Pauli, B. Kuenz, R. Ehling, H. Hegen, F. Deisenhammer, F. Aboul-Enein, M.K. Storch, P. Koson, J. Drulovic, W. Kristoferitsch, T. Berger, M. Reindl, Complement activating antibodies to myelin oligodendrocyte glycoprotein in neuromyelitis optica and related disorders, *J. Neuroinflammation*. 8 (2011) 184. doi:10.1186/1742-2094-8-184.
- [27] J.F. Kurtzke, Rating neurologic impairment in multiple sclerosis: an expanded disability status scale (EDSS), *Neurology*. 33 (1983) 1444–1452.
- [28] T. Oberwahrenbrock, M. Weinhold, J. Mikolajczak, H. Zimmermann, F. Paul, I. Beckers, A.U. Brandt, Reliability of Intra-Retinal Layer Thickness Estimates, *PLoS ONE*. 10 (2015). doi:10.1371/journal.pone.0137316.
- [29] A. Petzold, M.P. Wattjes, F. Costello, J. Flores-Rivera, C.L. Fraser, K. Fujihara, J. Leavitt, R. Marignier, F. Paul, S. Schippling, C. Sindic, P. Villoslada, B. Weinshenker, G.T. Plant, The investigation of acute optic neuritis: a review and proposed protocol, *Nat. Rev. Neurol*. 10 (2014) 447–458. doi:10.1038/nrneurol.2014.108.
- [30] M.A. Mayer, J. Hornegger, C.Y. Mardin, R.P. Tornow, Retinal Nerve Fiber Layer Segmentation on FD-OCT Scans of Normal Subjects and Glaucoma Patients, *Biomed. Opt. Express*. 1 (2010) 1358–1383. doi:10.1364/BOE.1.001358.
- [31] B. Knier, P. Schmidt, L. Aly, D. Buck, A. Berthele, M. Mühlau, C. Zimmer, B. Hemmer, T. Korn, Retinal inner nuclear layer volume reflects response to immunotherapy in multiple sclerosis, *Brain J. Neurol*. (2016). doi:10.1093/brain/aww219.
- [32] I.H. Jeong, H.J. Kim, N.-H. Kim, K.S. Jeong, C.Y. Park, Subclinical primary retinal pathology in neuromyelitis optica spectrum disorder, *J. Neurol*. 263 (2016) 1343–1348.

doi:10.1007/s00415-016-8138-8.

- [33] P. Tewarie, L. Balk, F. Costello, A. Green, R. Martin, S. Schippling, A. Petzold, The OSCAR-IB consensus criteria for retinal OCT quality assessment, *PloS One*. 7 (2012) e34823. doi:10.1371/journal.pone.0034823.
- [34] A. Cruz-Herranz, L.J. Balk, T. Oberwahrenbrock, S. Saidha, E.H. Martinez-Lapiscina, W.A. Lagreze, J.S. Schuman, P. Villoslada, P. Calabresi, L. Balcer, A. Petzold, A.J. Green, F. Paul, A.U. Brandt, P. Albrecht, IMSVISUAL consortium, The APOSTEL recommendations for reporting quantitative optical coherence tomography studies, *Neurology*. 86 (2016) 2303–2309. doi:10.1212/WNL.0000000000002774.
- [35] P.A. Yushkevich, J. Piven, H.C. Hazlett, R.G. Smith, S. Ho, J.C. Gee, G. Gerig, User-guided 3D active contour segmentation of anatomical structures: significantly improved efficiency and reliability, *NeuroImage*. 31 (2006) 1116–1128. doi:10.1016/j.neuroimage.2006.01.015.
- [36] P. Schmidt, C. Gaser, M. Arsic, D. Buck, A. Förchler, A. Berthele, M. Hoshi, R. Ilg, V.J. Schmid, C. Zimmer, B. Hemmer, M. Mühlau, An automated tool for detection of FLAIR-hyperintense white-matter lesions in Multiple Sclerosis, *NeuroImage*. 59 (2012) 3774–3783. doi:10.1016/j.neuroimage.2011.11.032.
- [37] J.-D. Tournier, F. Calamante, A. Connelly, Robust determination of the fibre orientation distribution in diffusion MRI: non-negativity constrained super-resolved spherical deconvolution, *NeuroImage*. 35 (2007) 1459–1472. doi:10.1016/j.neuroimage.2007.02.016.
- [38] E. Martínez-Heras, F. Varriano, V. Prčkovska, C. Laredo, M. Andorrà, E.H. Martínez-Lapiscina, A. Calvo, E. Lampert, P. Villoslada, A. Saiz, A. Prats-Galino, S. Llufríu, Improved Framework for Tractography Reconstruction of the Optic Radiation, *PloS One*. 10 (2015) e0137064. doi:10.1371/journal.pone.0137064.
- [39] J.C. Lim, P.M. Phal, P.M. Desmond, A.D. Nichols, C. Kokkinos, H.V. Danesh-Meyer, A.H. Kaye, B.A. Moffat, Probabilistic MRI Tractography of the Optic Radiation Using Constrained Spherical Deconvolution: A Feasibility Study, *PLOS ONE*. 10 (2015) e0118948. doi:10.1371/journal.pone.0118948.
- [40] J.D. Yeatman, R.F. Dougherty, N.J. Myall, B.A. Wandell, H.M. Feldman, Tract profiles of white matter properties: automating fiber-tract quantification, *PloS One*. 7 (2012) e49790. doi:10.1371/journal.pone.0049790.
- [41] A.J. Sherbondy, R.F. Dougherty, M. Ben-Shachar, S. Napel, B.A. Wandell, ConTrack: finding the most likely pathways between brain regions using diffusion

tractography, *J. Vis.* 8 (2008) 15.1-16. doi:10.1167/8.9.15.

[42] S.M. Smith, M. Jenkinson, H. Johansen-Berg, D. Rueckert, T.E. Nichols, C.E. Mackay, K.E. Watkins, O. Ciccarelli, M.Z. Cader, P.M. Matthews, T.E.J. Behrens, Tract-based spatial statistics: voxelwise analysis of multi-subject diffusion data, *NeuroImage*. 31 (2006) 1487–1505. doi:10.1016/j.neuroimage.2006.02.024.

[43] J.N. Ratchford, M.E. Quigg, A. Conger, T. Frohman, E.M. Frohman, L.J. Balcer, P.A. Calabresi, D.A. Kerr, Optical coherence tomography helps differentiate neuromyelitis optica and MS optic neuropathies, *Neurology*. 73 (2009) 302–308. doi:10.1212/WNL.0b013e3181af78b8.

[44] R Development Core Team, R: a language and environment for statistical computing, R Foundation for Statistical Computing, Vienna, Austria, 2008. <http://www.R-project.org>.

[45] A.J. Green, B. a. C. Cree, Distinctive retinal nerve fibre layer and vascular changes in neuromyelitis optica following optic neuritis, *J. Neurol. Neurosurg. Psychiatry*. 80 (2009) 1002–1005. doi:10.1136/jnnp.2008.166207.

[46] F. Pache, H. Zimmermann, C. Finke, A. Lacheta, S. Papazoglou, J. Kuchling, J. Wuerfel, B. Hamm, K. Ruprecht, F. Paul, A.U. Brandt, M. Scheel, Brain parenchymal damage in neuromyelitis optica spectrum disorder - A multimodal MRI study, *Eur. Radiol.* (2016). doi:10.1007/s00330-016-4282-x.

[47] E. Schneider, H. Zimmermann, T. Oberwahrenbrock, F. Kaufhold, E.M. Kadas, A. Petzold, F. Bilger, N. Borisow, S. Jarius, B. Wildemann, K. Ruprecht, A.U. Brandt, F. Paul, Optical Coherence Tomography Reveals Distinct Patterns of Retinal Damage in Neuromyelitis Optica and Multiple Sclerosis, *PLoS ONE*. 8 (2013). doi:10.1371/journal.pone.0066151.

[48] E. Vecino, F.D. Rodriguez, N. Ruzafa, X. Pereiro, S.C. Sharma, Glia–neuron interactions in the mammalian retina, *Prog. Retin. Eye Res.* 51 (2016) 1–40. doi:10.1016/j.preteyeres.2015.06.003.

[49] K. Kurosawa, T. Misu, Y. Takai, D.K. Sato, T. Takahashi, Y. Abe, H. Iwanari, R. Ogawa, I. Nakashima, K. Fujihara, T. Hamakubo, M. Yasui, M. Aoki, Severely exacerbated neuromyelitis optica rat model with extensive astrocytopathy by high affinity anti-aquaporin-4 monoclonal antibody, *Acta Neuropathol. Commun.* 3 (2015) 82. doi:10.1186/s40478-015-0259-2.

[50] T. Yamamura, I. Nakashima, Foveal thinning in neuromyelitis optica: A sign of retinal astrocytopathy?, *Neurol. Neuroimmunol. Neuroinflammation*. 4 (2017) e347.

doi:10.1212/NXI.0000000000000347.

[51] M. Bouyon, N. Collongues, H. Zéphir, L. Ballonzoli, L. Jeanjean, C. Lebrun, J. Chanson, F. Blanc, M. Fleury, O. Outteryck, S. Defoort, P. Labauge, P. Vermersch, C. Speeg, J. De Seze, Longitudinal follow-up of vision in a neuromyelitis optica cohort, *Mult. Scler. Houndmills Basingstoke Engl.* 19 (2013) 1320–1322.

doi:10.1177/1352458513476562.

[52] P. Manogaran, A.L. Trabouisee, A.P. Lange, Longitudinal Study of Retinal Nerve Fiber Layer Thickness and Macular Volume in Patients With Neuromyelitis Optica Spectrum Disorder, *J. Neuro-Ophthalmol. Off. J. North Am. Neuro-Ophthalmol. Soc.* 36 (2016) 363–368. doi:10.1097/WNO.0000000000000404.

[53] D.K. Sato, D. Callegaro, M.A. Lana-Peixoto, P.J. Waters, F.M. de H. Jorge, T. Takahashi, I. Nakashima, S.L. Apostolos-Pereira, N. Talim, R.F. Simm, A.M.M. Lino, T. Misu, M.I. Leite, M. Aoki, K. Fujihara, Distinction between MOG antibody-positive and AQP4 antibody-positive NMO spectrum disorders, *Neurology.* 82 (2014) 474–481.

doi:10.1212/WNL.0000000000000101.

[54] J. Kitley, P. Waters, M. Woodhall, M.I. Leite, A. Murchison, J. George, W. Küker, S. Chandratre, A. Vincent, J. Palace, Neuromyelitis optica spectrum disorders with aquaporin-4 and myelin-oligodendrocyte glycoprotein antibodies: a comparative study, *JAMA Neurol.* 71 (2014) 276–283. doi:10.1001/jamaneurol.2013.5857.

[55] S. Jarius, K. Ruprecht, B. Wildemann, T. Kuempfel, M. Ringelstein, C. Geis, I. Kleiter, C. Kleinschnitz, A. Berthele, J. Brettschneider, K. Hellwig, B. Hemmer, R.A. Linker, F. Lauda, C.A. Mayer, H. Tumani, A. Melms, C. Trebst, M. Stangel, M. Marziniak, F. Hoffmann, S. Schippling, J.H. Faiss, O. Neuhaus, B. Ettrich, C. Zentner, K. Guthke, U. Hofstadt-van Oy, R. Reuss, H. Pellkofer, U. Ziemann, P. Kern, K.P. Wandinger, F.T. Bergh, T. Boettcher, S. Langel, M. Liebetrau, P.S. Rommer, S. Niehaus, C. Münch, A. Winkelmann, U.K. Zettl U, I. Metz, C. Veauthier, J.P. Sieb, C. Wilke, H.P. Hartung, O. Aktas, F. Paul, Contrasting disease patterns in seropositive and seronegative neuromyelitis optica: A multicentre study of 175 patients, *J. Neuroinflammation.* 9 (2012) 14. doi:10.1186/1742-2094-9-14.

doi:10.1186/1742-2094-9-14.

[56] T. Akaishi, D.K. Sato, I. Nakashima, T. Takeshita, T. Takahashi, H. Doi, K. Kurosawa, K. Kaneko, H. Kuroda, S. Nishiyama, T. Misu, T. Nakazawa, K. Fujihara, M. Aoki, MRI and retinal abnormalities in isolated optic neuritis with myelin oligodendrocyte glycoprotein and aquaporin-4 antibodies: a comparative study, *J. Neurol. Neurosurg. Psychiatry.* 87 (2016) 446–448. doi:10.1136/jnnp-2014-310206.

- [57] K. Chalmoukou, H. Alexopoulos, S. Akrivou, P. Stathopoulos, M. Reindl, M.C. Dalakas, Anti-MOG antibodies are frequently associated with steroid-sensitive recurrent optic neuritis, *Neurol. Neuroimmunol. Neuroinflammation*. 2 (2015) e131. doi:10.1212/NXI.000000000000131.
- [58] S. Ramanathan, S.W. Reddel, A. Henderson, J.D.E. Parratt, M. Barnett, P.N. Gatt, V. Merheb, R.-Y.A. Kumaran, K. Pathmanandavel, N. Sinmaz, M. Ghadiri, C. Yiannikas, S. Vucic, G. Stewart, A.F. Bleasel, D. Booth, V.S.C. Fung, R.C. Dale, F. Brilot, Antibodies to myelin oligodendrocyte glycoprotein in bilateral and recurrent optic neuritis, *Neurol. Neuroimmunol. Neuroinflammation*. 1 (2014) e40. doi:10.1212/NXI.000000000000040.
- [59] L.J. Balk, A. Cruz-Herranz, P. Albrecht, S. Arnow, J.M. Gelfand, P. Tewarie, J. Killestein, B.M.J. Uitdehaag, A. Petzold, A.J. Green, Timing of retinal neuronal and axonal loss in MS: a longitudinal OCT study, *J. Neurol*. 263 (2016) 1323–1331. doi:10.1007/s00415-016-8127-y.
- [60] S. Zhao, K. Mutch, L. Elson, T. Nurmikko, A. Jacob, Neuropathic pain in neuromyelitis optica affects activities of daily living and quality of life, *Mult. Scler. Houndmills Basingstoke Engl*. 20 (2014) 1658–1661. doi:10.1177/1352458514522103.
- [61] J.-P. Stellmann, M. Krumbholz, T. Friede, A. Gahlen, N. Borisow, K. Fischer, K. Hellwig, F. Pache, K. Ruprecht, J. Havla, T. Kümpfel, O. Aktas, H.-P. Hartung, M. Ringelstein, C. Geis, C. Kleinschnitz, A. Berthele, B. Hemmer, K. Angstwurm, K.L. Young, S. Schuster, M. Stangel, F. Lauda, H. Tumani, C. Mayer, L. Zeltner, U. Ziemann, R.A. Linker, M. Schwab, M. Marziniak, F. Then Bergh, U. Hofstadt-van Oy, O. Neuhaus, U. Zettl, J. Faiss, B. Wildemann, F. Paul, S. Jarius, C. Trebst, I. Kleiter, NEMOS (Neuromyelitis Optica Study Group), Immunotherapies in neuromyelitis optica spectrum disorder: efficacy and predictors of response, *J. Neurol. Neurosurg. Psychiatry*. 88 (2017) 639–647. doi:10.1136/jnnp-2017-315603.

9. Statutory Declaration

I, **Frederike Cosima Oertel**, by personally signing this document in lieu of an oath, hereby affirm that I prepared the submitted dissertation on the topic **“Afferent visual system changes in patients with Neuromyelitis Optica Spectrum Disorders” / “Veränderungen des afferenten visuellen Systems bei Patienten mit Neuromyelitis Optica Spektrum- Erkrankungen”** independently and without the support of third parties, and that I used no other sources and aids than those stated.

All parts which are based on the publications or presentations of other authors, either in letter or in spirit, are specified as such in accordance with the citing guidelines. The sections on methodology (in particular regarding practical work, laboratory regulations, statistical processing) and results (in particular regarding figures, charts and tables) are exclusively my responsibility.

My contributions to any publications to this dissertation correspond to those stated in the below joint declaration made together with the first supervisor. All publications created within the scope of the dissertation comply with the guidelines of the ICMJE (International Committee of Medical Journal Editors; www.icmje.org) on authorship. In addition, I declare that I am aware of the regulations of Charité – Universitätsmedizin Berlin on ensuring good scientific practice and that I commit to comply with these regulations.

The significance of this statutory declaration and the consequences of a false statutory declaration under criminal law (Sections 156, 161 of the German Criminal Code) are known to me.”

Date

Frederike Cosima Oertel

10. Contributions

METHOD-OCT [18]

Frederike Cosima Oertel*, Hanna Zimmermann*, Janine Mikolajczak, Maria Weinhold, Ella Maria Kadas, Timm Oberwahrenbrock, Florence Pache, Friedemann Paul, Alexander U. Brandt: **Contribution of blood vessels to retinal nerve fiber layer thickness in NMOSD**. Neurology: Neuroimmunology & Neuroinflammation, 2017

Contribution: data collection, OCT segmentation, blood vessel segmentation, parts of the statistical analysis, interpretation of results, writing of the manuscript (results and discussion)

METHOD-DTI [19]

Joseph Kuchling*, Yael Backner*, **Frederike C Oertel**, Noa Raz, Judith Bellmann-Strobl, Klemens Ruprecht, Friedemann Paul, Netta Levin, Alexander U Brandt, Michael Scheel: **Comparison of probabilistic tractography and tract-based spatial statistics for assessing optic radiation damage in patients with autoimmune inflammatory disorders of the central nervous system**. NeuroImage Clinical, 2018

Contribution: data collection, OCT quality check, OCT segmentation, parts of the statistical analysis, contributed to the interpretation of results, revision of the manuscript

AQP4-CROSS-SECTIONAL [20]

Frederike C. Oertel*, Joseph Kuchling*, Hanna Zimmermann, Claudia Chien, Felix Schmidt, Benjamin Knier, Judith Bellmann-Strobl, Thomas Korn, Michael Scheel, Alexander Klistorner, Klemens Ruprecht, Friedemann Paul, Alexander U. Brandt: **Microstructural visual system changes in AQP4-antibody seropositive NMOSD** Neurology: Neuroimmunology & Neuroinflammation, 2017

Contribution: data collection and OCT segmentation (Berlin data), CSD-PROB analysis, statistical analysis, interpretation of results, writing of the manuscript

AQP4-LONGITUDINAL [21]

Frederike C Oertel*, Joachim Havla*, Adriana Roca-Fernández, Nathaniel Lizak, Hanna Zimmermann, Seyedamirhosein Motamedi, Nadja Borisow, Owen White, Judith Bellmann-Strobl, Philipp Albrecht, Klemens Ruprecht, Sven Jarius, Jacqueline Palace,

Maria Leite, Tania Kümpfel, Friedemann Paul, Alexander U Brandt: **Retinal Ganglion Cell Loss in Neuromyelitis Optica: A Longitudinal Study.** Journal of Neurology, Neurosurgery and Psychiatry, 2018

Contribution: data collection and OCT quality check (Berlin data), OCT segmentation, statistical analysis, interpretation of results, writing of the manuscript

MOG-CROSS-SECTIONAL [22]

Florence Pache*, Hanna Zimmermann*, Janine Mikolajczak, Sophie Schumacher, Anna Lacheta, **Frederike C Oertel**, Judith Bellmann-Strobel, Sven Jarius, Brigitte Wildemann, Markus Reindl, Amy Waldman, Kerstin Soelberg, Nasrin Asgari, Marius Ringelstein, Orhan Aktas, Nikolai Gross, Mathias Buttman, Thomas Ach, Klemens Ruprecht, Friedemann Paul, Alexander U Brandt, **MOG-IgG in NMO and related disorders: a multicenter study of 50 patients. Part 4: Afferent visual system damage after optic neuritis in MOG-IgG-seropositive versus AQP4-IgG-seropositive patients,** Journal of Neuroinflammation, 2016.

Contribution: data collection, data quality check, contribution to the interpretation of results, revision of the manuscript

MOG-LONGITUDINAL [23]

Frederike C Oertel*, Olivier Outteryck, Benjamin Knier, Hanna Zimmermann, Nadja Borisow, Judith Bellmann-Strobl, Astrid Blaschek, Sven Jarius, Markus Reindl, Klemens Ruprecht, Edgar Meinel, Reinhard Hohlfeld, Friedemann Paul, Alexander U Brandt, Tania Kümpfel, Joachim Havla: **Optical Coherence Tomography in Myelin-Oligodendrocyte-Glycoprotein Antibody-Seropositive Patients: A Longitudinal Study.** Journal of Neuroinflammation, 2019.

Contribution: data collection and OCT quality check (Berlin data), statistical analysis, interpretation of results, writing of the manuscript.

Signature, Date and Stamp of the supervisor

Signature of the doctoral candidate

11. Publications

11.1 METHOD-OCT [18]

Frederike Cosima Oertel*, Hanna Zimmermann*, Janine Mikolajczak, Maria Weinhold, Ella Maria Kadas, Timm Oberwahrenbrock, Florence Pache, Friedemann Paul, Alexander U. Brandt: *Contribution of blood vessels to retinal nerve fiber layer thickness in NMOSD*. Neurology: Neuroimmunology & Neuroinflammation, 2017

“Neurology: Neuroimmunology & Neuroinflammation” was not part of the Journal Summary List in 2017.

Frederike C. Oertel*
Hanna Zimmermann,
MEng*
Janine Mikolajczak, MSc
Maria Weinhold, BSc
Ella Maria Kadas, PhD
Timm Oberwahrenbrock,
PhD
Florence Pache, MD
Judith Bellmann-Strobl,
MD
Klemens Ruprecht, MD
Friedemann Paul, MD
Alexander U. Brandt, MD

*Neurol Neuroimmunol
Neuroinflamm*
2017;4:e338; doi: 10.1212/
NXL.0000000000000338

CONTRIBUTION OF BLOOD VESSELS TO RETINAL NERVE FIBER LAYER THICKNESS IN NMOSD

OPEN

Neuromyelitis optica spectrum disorders (NMOSDs) are relapsing inflammatory demyelinating disorders with optic neuritis (ON) as the hallmark. ON causes neuroaxonal damage to the optic nerve and retina, regularly leading to severely impaired visual acuity (VA).¹

Peripapillary retinal nerve fiber layer (pRNFL) thickness measured by optical coherence tomography (OCT) has been increasingly recognized as a marker for neuroaxonal damage and correlate of visual dysfunction.¹ As such, pRNFL is implemented as an outcome in clinical trials of ON-associated disorders. Blood vessels (BVs) running within the pRNFL contribute approximately 13% to an average RNFL thickness² and could present an important confounder when tracking small pRNFL changes or in diseases with severe thinning such as NMOSD.¹ Against this background, the objective of this study was to investigate the influence of retinal BVs on pRNFL measurements in an NMOSD cohort.

Methods. Forty patients from a prospective observational cohort study at the NCRC at Charité–Universitätsmedizin Berlin were enrolled (women/men: 39/1, age: 44.7 ± 15.4 years, 42 ON eyes). Inclusion criteria were a minimum age of 18 years and diagnosis of NMOSD according to the 2015 IPND criteria³ ($n = 37$, aquaporin-4 antibody seropositive $n = 28$) or myelin oligodendrocyte glycoprotein-IgG-associated encephalomyelitis ($n = 3$).⁴ Exclusion criteria were any other diseases which could influence OCT results.

All patients were examined with a Spectralis SD-OCT (Heidelberg Engineering, Heidelberg, Germany) using automatic real time (ART) function for image averaging. pRNFL was measured with a 3.4 mm ring scan around the optic nerve head (12° , 1536 A scans $16 \leq \text{ART} \leq 100$) and segmented semiautomatically (Eye Explorer 1.9.10.0 with viewing module 6.0.9.0) and manually corrected by an experienced grader. BV positions were automatically detected by OCTSEG⁵ (figure, A and B) and manually corrected. Three eyes were

excluded because of insufficient image quality based on OSCAR-IB criteria.

High-contrast VA was examined monocularly under habitual correction and photopic conditions with ETDRS charts at a simulated 20 ft distance using the Optec 6500 P System (Stereo Optical, Chicago, IL).

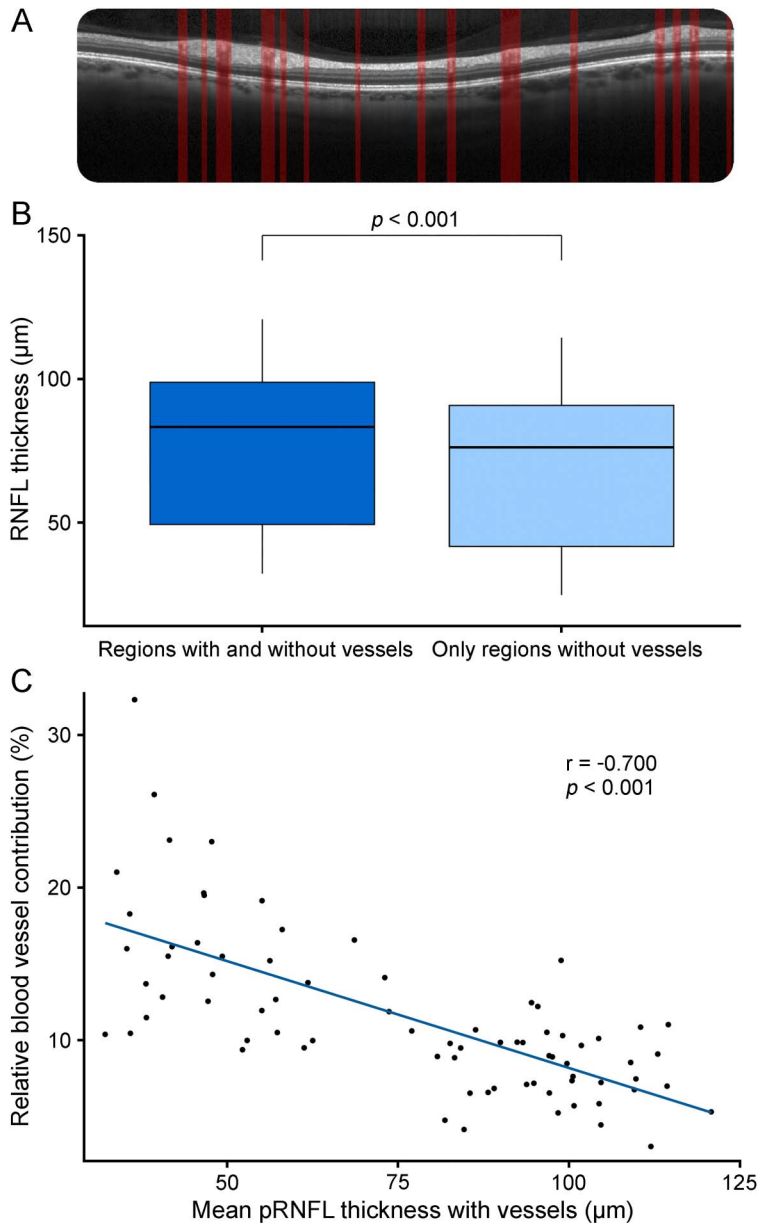
pRNFL without vessels was calculated as mean thickness of all ring scan positions not marked as part of vessels and was compared with pRNFL with vessels using paired *t* tests. We performed Pearson correlation analyses for evaluation of the relationship between pRNFL and VA and Fisher z test for correlation comparison. The relative BV contribution in percentage was calculated as $([\text{pRNFL}_{\text{with vessels}} - \text{pRNFL}_{\text{without vessels}}] / \text{pRNFL}_{\text{with vessels}} \times 100\%)$. All statistical tests were performed using R 3.1 with significance established at $p < 0.05$. The study was approved by the local Ethics Committee at Charité–Universitätsmedizin Berlin and was conducted in accordance with the Declaration of Helsinki.

Results. pRNFL measurements were thinner without including BVs ($76.1 \pm 26.6 \mu\text{m}$ with, $68.3 \pm 26.2 \mu\text{m}$ without, $p < 2e^{-16}$; figure, C). Relative BV contribution increased with lower pRNFL ($r = -0.700$, $p = 1e^{-12}$) (figure, D). When only considering eyes with pRNFL thickness below $60 \mu\text{m}$, the mean relative BV contribution was significantly higher with $16\% \pm 5\%$ compared with $9\% \pm 3\%$ in eyes with RNFL $>60 \mu\text{m}$ ($p = 8e^{-8}$).

VA (36 ± 19 ETDRS letters) was associated with pRNFL including BV ($r = 0.621$, $p = 2e^{-9}$) and without BV ($r = 0.618$, $p = 2e^{-9}$). In eyes with pRNFL measurements below $60 \mu\text{m}$, pRNFL-VA correlation was numerically higher for pRNFL excluding BV ($r = 0.495$, $p = 0.007$) than pRNFL including BV ($r = 0.482$, $p = 0.009$), but the difference was not significant ($p = 0.476$). There were no influences of antibody status, disease duration and therapy on pRNFL, relative BV contribution, or enlargement of BV areas with pRNFL thinning (data not shown).⁶

Discussion. BV contribution to average pRNFL measurements is higher in thin compared with normal/high pRNFL measurements.

Figure Contribution of blood vessels to retinal nerve fiber layer thickness



(A) pRNFL scanned by optical coherence tomography, segmented with vessel detection. (B) Mean pRNFL thickness in μm ; all regions including vessels and only regions without vessels. (C) Correlation of the relative blood vessel contribution to the pRNFL including vessels. pRNFL = peripapillary retinal nerve fiber layer.

A previous study reported an average BV contribution of 13% to pRNFL measurements.² Our study expands these findings by showing that BV contribution is increased in low pRNFL measurements like the ones regularly found in NMOSD patients with severe ON.

A relevant contribution of BV artifacts to measurement noise has been reported.⁷ Although our results did not show a structure–function correlation improvement for vessel-corrected measurements, they suggest a downgrade in pRNFL measurement sensitivity. In NMOSD cohorts, a wide range of pRNFL

thickness measurements are seen, including those lower than $60 \mu\text{m}$.¹ Typically, pRNFL differences of only a few micrometers are used to evaluate drug efficacy in ON trials.⁸ Thus, in longitudinal studies, vessel artifacts potentially interfere with the comparability of an absolute thickness change because the relative vessel contribution increases with thinner pRNFL.

We propose analyzing OCT data in studies including NMOSD and other conditions with low pRNFL measurements in addition to vessel correction. Further studies of retrospective and prospective data and larger cohorts are required to confirm and specify BV influence and to identify reliable surrogates for tracking ON-related damage in NMOSD.

*These authors contributed equally to this work.

From the NeuroCure Clinical Research Center (F.C.O., H.Z., J.M., M.W., E.M.K., T.O., F. Pache, J.B.-S., F. Paul, A.U.B.), Department of Neurology (F. Pache, J.B.-S., K.R., F. Paul), Charité–Universitätsmedizin Berlin; and Experimental and Clinical Research Center (J.B.-S., F. Paul), Max Delbrueck Center for Molecular Medicine and Charité–Universitätsmedizin Berlin, Germany.

Author contributions: F.C.O. and H.Z.: analysis/interpretation of data, statistical analysis, and drafting of the manuscript. J.M.: analysis/interpretation of data and acquisition of data. M.W. and E.M.K.: analysis/interpretation of data. T.O.: drafting/revision of the manuscript and statistical analysis. F. Pache: study concept/design and acquisition of data. J.B.-S.: study concept/design, acquisition of data, and study coordination. K.R.: drafting/revision of the manuscript for content and study supervision/coordination. F. Paul: drafting/revision of the manuscript and study supervision/coordination. A.U.B.: drafting/revision of the manuscript, study concept/design, analysis/interpretation of data, statistical analysis, and study supervision/coordination.

Study funding: No targeted funding reported.

Disclosure: F.C. Oertel reports no disclosures. H. Zimmermann received speaker honoraria from Teva and Bayer. J. Mikolajczak received travel funding and/or speaker honoraria from TEVA GmbH Germany, Biogen Idec Germany, and Bayer Vital GmbH Germany. M. Weinhold received speaker honoraria from TEVA GmbH Germany. E.M. Kadas has a patent application describing the optic nerve head volume analysis used in this study. T. Oberwahrenbrock received speaker honoraria from TEVA GmbH Germany and Bayer Germany and received research support from Federal Ministry of Education and Research. F. Pache received travel funding and/or speaker honoraria from Genzyme, a Sanofi Company, Bayer, Biogen Idec, and ECTRIMS; received research support from Charité–Universitätsmedizin Berlin, Berlin Institute of Health, KKNMS-Bundesministerium für Bildung und Forschung, and Novartis. J. Bellmann-Strobl received travel funding and/or speaker honoraria from Bayer Healthcare, Sanofi-Aventis/Genzyme, and Teva Pharmaceuticals. K. Ruprecht served on the scientific advisory board for Sanofi-Aventis/Genzyme, Novartis, and Roche; received travel funding and/or speaker honoraria from Bayer Healthcare, Biogen Idec, Merck Serono, Sanofi-Aventis/Genzyme, Teva Pharmaceuticals, Novartis, and Guthy Jackson Charitable Foundation; is an academic editor for PLoS One; receives publishing royalties from Elsevier; and received research support from Novartis and German Ministry of Education and Research. F. Paul serves on the scientific advisory board for Novartis; received speaker honoraria and travel funding from Bayer, Novartis, Biogen Idec, Teva, Sanofi-Aventis/Genzyme, Merck Serono, Alexion, Chugai, MedImmune, and Shire; is an academic editor for PLoS One, is an associate editor for Neurology® Neuroimmunology & Neuroinflammation; consulted for Sanofi-

Genzyme, Biogen Idec, MedImmune, Shire, and Alexion; received research support from Bayer, Novartis, Biogen Idec, Teva, Sanofi-Aventis/Genzyme, Alexion, Merck Serono, German Research Council, Werth Stiftung of the City of Cologne, German Ministry of Education and Research, Arthur Arnstein Stiftung Berlin, EU FP7 Framework Program, Arthur Arnstein Foundation Berlin, Guthy Jackson Charitable Foundation, and National Multiple Sclerosis of the USA. A.U. Brandt served on the scientific advisory board for Biogen; received travel funding and/or speaker honoraria from Novartis and Biogen; has patents pending from Method and System for Optic Nerve Head Shape Quantification, perceptive visual computing based postural control analysis, multiple sclerosis biomarker, and perceptive sleep motion analysis; consulted for Nexus and Motognosis; and received research support from Novartis Pharma, Biogen Idec, BMWi, BMBF, and Guthy Jackson Charitable Foundation. Go to Neurology.org/nn for full disclosure forms. The Article Processing Charge was funded by the authors.

This is an open access article distributed under the terms of the Creative Commons Attribution-NonCommercial-NoDerivatives License 4.0 (CC BY-NC-ND), which permits downloading and sharing the work provided it is properly cited. The work cannot be changed in any way or used commercially without permission from the journal.

Received February 8, 2016. Accepted in final form January 17, 2017.

Correspondence to Dr. Brandt: alexander.brandt@charite.de

1. Bennett JL, de Seze J, Lana-Peixoto M, et al. Neuromyelitis optica and multiple sclerosis: seeing differences through optical coherence tomography. *Mult Scler* 2015;21:678–688.

2. Hood DC, Fortune B, Arthur SN, et al. Blood vessel contributions to retinal nerve fiber layer thickness profiles measured with optical coherence tomography. *J Glaucoma* 2008;17:519–528.
3. Wingerchuk DM, Banwell B, Bennett JL, et al. International consensus diagnostic criteria for neuromyelitis optica spectrum disorders. *Neurology* 2015;85:177–189.
4. Pache F, Zimmermann H, Mikolajczak J, et al. MOG-IgG in NMO and related disorders: a multicenter study of 50 patients: part 4: afferent visual system damage after optic neuritis in MOG-IgG-seropositive versus AQP4-IgG-seropositive patients. *J Neuroinflammation* 2016;13:282.
5. Mayer MA, Hornegger J, Mardin CY, Tornow RP. Retinal nerve fiber layer segmentation on FD-OCT scans of normal subjects and glaucoma patients. *Biomed Opt Express* 2010;1:1358–1383.
6. Green AJ, Cree BAC. Distinctive retinal nerve fibre layer and vascular changes in neuromyelitis optica following optic neuritis. *J Neurol Neurosurg Psychiatry* 2009;80:1002–1005.
7. Balk LJ, Mayer M, Uitdehaag BMJ, Petzold A. Retinal hyperaemia-related blood vessel artifacts are relevant to automated OCT layer segmentation. *J Neurol* 2014;261:511–517.
8. Sühs KW, Hein K, Sättler MB, et al. A randomized, double-blind, phase 2 study of erythropoietin in optic neuritis. *Ann Neurol* 2012;72:199–210.

11.2 METHOD-DTI [19]

Joseph Kuchling*, Yael Backner*, **Frederike C Oertel**, Noa Raz, Judith Bellmann-Strobl, Klemens Ruprecht, Friedemann Paul, Netta Levin, Alexander U Brandt, Michael Scheel: *Comparison of probabilistic tractography and tract-based spatial statistics for assessing optic radiation damage in patients with autoimmune inflammatory disorders of the central nervous system*. NeuroImage Clinical, 2018

Journal Data Filtered By: **Selected JCR Year: 2018** Selected Editions: SCIE,SSCI
 Selected Categories: **"NEUROIMAGING"** Selected Category Scheme: WoS
Gesamtanzahl: 14 Journale

Rank	Full Journal Title	Total Cites	Journal Impact Factor	Eigenfactor Score
1	NEUROIMAGE	99,720	5.812	0.132720
2	HUMAN BRAIN MAPPING	22,040	4.554	0.043230
3	NeuroImage-Clinical	5,762	3.943	0.022670
4	Journal of NeuroInterventional Surgery	4,407	3.925	0.011860
5	Brain Imaging and Behavior	2,464	3.418	0.006610
6	AMERICAN JOURNAL OF NEURORADIOLOGY	23,231	3.256	0.028010
7	NEURORADIOLOGY	5,656	2.504	0.007020
8	JOURNAL OF NEURORADIOLOGY	985	2.467	0.001440
9	PSYCHIATRY RESEARCH-NEUROIMAGING	5,503	2.270	0.008330
10	JOURNAL OF NEUROIMAGING	2,081	2.080	0.004270
11	NEUROIMAGING CLINICS OF NORTH AMERICA	1,173	2.046	0.001310
12	STEREOTACTIC AND FUNCTIONAL NEUROSURGERY	1,807	1.905	0.002220
13	CLINICAL EEG AND NEUROSCIENCE	1,018	1.822	0.001510
14	KLINISCHE NEUROPHYSIOLOGIE	40	0.325	0.000030

Copyright © 2019 Clarivate Analytics



Comparison of probabilistic tractography and tract-based spatial statistics for assessing optic radiation damage in patients with autoimmune inflammatory disorders of the central nervous system

Joseph Kuchling^{a,b,1}, Yael Backner^{c,1}, Frederike C. Oertel^a, Noa Raz^c, Judith Bellmann-Strobl^{a,d}, Klemens Ruprecht^b, Friedemann Paul^{a,b,d,*}, Netta Levin^c, Alexander U. Brandt^{a,e,2}, Michael Scheel^{a,2}

^a Charité – Universitätsmedizin Berlin, corporate member of Freie Universität Berlin, Humboldt-Universität zu Berlin, and Berlin Institute of Health, NeuroCure Cluster of Excellence, NeuroCure Clinical Research Center, NCRC Charité, Charitéplatz 1, 10117 Berlin, Germany

^b Department of Neurology, Charité – Universitätsmedizin Berlin, Charitéplatz 1, 10117 Berlin, Germany

^c Department of Neurology, The Agnes Ginges Center for Human Neurogenetics, Hadassah-Hebrew-University Medical Center, Kiryat Hadassah Ein kerem, Jerusalem 91120, Israel

^d Experimental and Clinical Research Center, Max Delbrueck Center for Molecular Medicine and Charité – Universitätsmedizin Berlin, Charitéplatz 1, 10117 Berlin, Germany

^e Department of Neurology, University of California, 1001 Health Sciences Road, Irvine Hall, Irvine, CA 92697, USA

ARTICLE INFO

Keywords:

DTI
Neuromyelitis optica
Multiple sclerosis
TBSS
Probabilistic tractography
Optic radiation

ABSTRACT

Background: Diffusion Tensor Imaging (DTI) can evaluate microstructural tissue damage in the optic radiation (OR) of patients with clinically isolated syndrome (CIS), early relapsing-remitting multiple sclerosis and neuromyelitis optica spectrum disorders (NMOSD). Different post-processing techniques, e.g. tract-based spatial statistics (TBSS) and probabilistic tractography, exist to quantify this damage.

Objective: To evaluate the capacity of TBSS-based atlas region-of-interest (ROI) combination with 1) posterior thalamic radiation ROIs from the Johns Hopkins University atlas (JHU-TBSS), 2) Juelich Probabilistic ROIs (JUEL-TBSS) and tractography methods using 3) ConTrack (CON-PROB) and 4) constrained spherical deconvolution tractography (CSD-PROB) to detect OR damage in patients with a) NMOSD with prior ON (NMOSD-ON), b) CIS and early RRMS patients with ON (CIS/RRMS-ON) and c) CIS and early RRMS patients without prior ON (CIS/RRMS-NON) against healthy controls (HCs).

Methods: Twenty-three NMOSD-ON, 18 CIS/RRMS-ON, 21 CIS/RRMS-NON, and 26 HCs underwent 3 T MRI. DTI data analysis was carried out using JUEL-TBSS, JHU-TBSS, CON-PROB and CSD-PROB. Optical coherence tomography (OCT) and visual acuity testing was performed in the majority of patients and HCs.

Results: Absolute OR fractional anisotropy (FA) values differed between all methods but showed good correlation and agreement in Bland-Altman analysis. OR FA values between NMOSD and HC differed throughout the methodologies (p-values ranging from $p < 0.0001$ to 0.0043). ROC-analysis and effect size estimation revealed higher AUCs and R^2 for CSD-PROB (AUC = 0.812; $R^2 = 0.282$) and JHU-TBSS (AUC = 0.756; $R^2 = 0.262$), compared to CON-PROB (AUC = 0.742; $R^2 = 0.179$) and JUEL-TBSS (AUC = 0.719; $R^2 = 0.161$). Differences between CIS/RRMS-NON and HC were only observable in CSD-PROB (AUC = 0.796; $R^2 = 0.094$). No significant differences between CIS/RRMS-ON and HC were detected by any of the methods.

Conclusions: All DTI post-processing techniques facilitated the detection of OR damage in patient groups with

Abbreviations: AD, axial diffusivity; AUC, area under the curve; CIS, clinically isolated syndrome; CON, Contrack; CSD, constrained spherical deconvolution; DTI, diffusion tensor imaging; DWI, diffusion weighted imaging; DW-MRI, diffusion weighted magnetic resonance imaging; FA, fractional anisotropy; FOD, fiber orientation distribution; HC, Healthy Control; JHU, Johns Hopkins University DTI white matter atlas; JUEL, Juelich histological atlas; LGN, lateral geniculate nucleus; MD, mean diffusivity; MS, multiple sclerosis; NMOSD, neuromyelitis optica spectrum disorder; OCT, optical coherence tomography; ON, optic neuritis; OR, optic radiation; PROB, probabilistic tractography; RD, radial diffusivity; RNFL, retinal nerve fiber layer thickness; ROC, receiver operating characteristic; ROI, region of interest; RRMS, relapsing-remitting multiple sclerosis; SD, standard deviation; SEM, standard error of the mean; TBSS, tract-based spatial statistics

* Corresponding author at: NeuroCure Clinical Research Center, Charité - Universitätsmedizin Berlin, Charitéplatz 1, 10117 Berlin, Germany.

E-mail addresses: joseph.kuchling@charite.de (J. Kuchling), yael.backner@mail.huji.ac.il (Y. Backner), frederike-cosima.oertel@charite.de (F.C. Oertel), noa.raz@mail.huji.ac.il (N. Raz), judith.bellmann-strobl@charite.de (J. Bellmann-Strobl), klemens.ruprecht@charite.de (K. Ruprecht), friedemann.paul@charite.de (F. Paul), netta@hadassah.org.il (N. Levin), alexander.brandt@charite.de (A.U. Brandt), michael.scheel@charite.de (M. Scheel).

¹ Equally contributing first authors.

² Equally contributing senior authors.

<https://doi.org/10.1016/j.nicl.2018.05.004>

Received 1 February 2018; Received in revised form 3 May 2018; Accepted 6 May 2018

Available online 08 May 2018

2213-1582/ © 2018 The Authors. Published by Elsevier Inc. This is an open access article under the CC BY license (<http://creativecommons.org/licenses/by/4.0/>).

severe microstructural OR degradation. The comparison of distinct disease groups by use of different methods may lead to different - either false-positive or false-negative - results. Since different DTI post-processing approaches seem to provide complementary information on OR damage, application of distinct methods may depend on the relevant research question.

1. Introduction

The optic radiation (OR) is an integral part of the afferent visual system and belongs to the most frequently affected white matter pathways in autoimmune neuroinflammatory disorders of the central nervous system, i.e. multiple sclerosis (MS) and neuromyelitis optica spectrum disorders (NMOSD) (Backner et al., 2018; Balcer et al., 2015; Bennett et al., 2015; Finke et al., 2018; Martínez-Lapiscina et al., 2014; Pache et al., 2016a, 2016b; Pache et al., 2016a, 2016b; Petzold et al., 2014; Pfueller and Paul, 2011; Scheel et al., 2014; Schmidt et al., 2017; Sinnecker et al., 2015b; Wingerchuk et al., 2015). Diffusion-weighted magnetic resonance imaging (DW-MRI) yields the potential to non-invasively investigate microstructural OR integrity (Assaf and Pasternak, 2008; Filippi et al., 2013).

A multitude of DW-MRI post-processing techniques have been used in recent studies to investigate OR damage in neuroinflammatory disorders (Hasan et al., 2011). TBSS is a widely used fully automated method to perform whole brain tract diffusion tensor imaging (DTI) analyses. ConTrack (CON-PROB) (Sherbondy et al., 2008a, 2008b) and CSD-based probabilistic tractography (CSD-PROB) (Lim et al., 2015; Martínez-Heras et al., 2015; Tournier et al., 2007) provide high sensitivity to delineate tracts through crossing fiber regions (Auriat et al., 2015), facilitate the selection of pathways that connect two regions (Sherbondy et al., 2008b) and allow subsequent in-depth analysis, for example tract profiling, by calculating DTI values at different nodes along the OR. However, implementation of probabilistic tractography algorithms in the individual patient is frequently more time consuming due to manual predefinition of seed and target regions as well as manual or semi-automated cleaning of tractography results. Moreover, accurate OR delineation in vivo is hampered by its complex structure with the sharp bending in the Meyer's loop (Martínez-Heras et al., 2015), the reduced fiber density in this area compared to the body of the OR (Lim et al., 2015; Wu et al., 2012) and the presence of crossing fibers along the pathway (Sherbondy et al., 2008b).

Previous investigations using CON-PROB found OR DTI metrics to be altered in long-standing MS patients compared to healthy controls with correlations between OR FA and OR T2 lesion volume (Klistorner et al., 2014). A study investigating clinically isolated ON patients with CON-PROB found reduced fractional anisotropy (FA) and elevated radial diffusivity (RD) to be associated with OR lesions. No correlation between OR DTI and retinal nerve fiber layer thickness (RNFL) measured by optical coherence tomography (OCT) was found (Raz et al., 2015). By contrast, investigations using TBSS in MS patients with and without prior ON found strong correlations between RNFL and FA

within the OR, suggesting trans-synaptic neurodegeneration after ON to explain the link between low RNFL thickness and low FA values in the OR (Scheel et al., 2014). These contradictory results fall in line with previous studies either favoring (Oertel et al., 2017; Pache et al., 2016a, 2016b; Reich et al., 2009; Rocca et al., 2013) or disfavoring (Dasenbrock et al., 2011) evidence on trans-neuronal changes in neuroinflammatory disorders. The conflicting diversity of published DTI studies might be partially owing to cohort inhomogeneities with regards to time from disease onset, severity of structural damage and clinical deficit as well as total and region-specific lesion load. Beyond this, the heterogeneous usage of different DTI post-processing techniques and their specific inherent limitations may account for inconsistent reports.

Validation studies of sensitivity, specificity and technical advantages and disadvantages of different DTI post-processing methods are thus highly required. Unfortunately, there is no “gold-standard” for non-invasive DTI-based OR tract-probing (Lim et al., 2015; Thomas et al., 2014), making comparability between methods and validation of techniques difficult. To overcome these limitations, different methods need to be compared against each other under one specific research question.

The purpose of our study was to compare distinct TBSS-based and probabilistic tractography-based approaches in the delineation of OR and the detection of OR damage. We therefore investigated OR damage with different severity levels and compared a) NMOSD patients with prior ON with suspected severe OR damage, b) clinically isolated syndrome (CIS) and early relapsing-remitting multiple sclerosis (RRMS) patients with ON and suspected moderate OR damage and c) CIS and early RRMS patients without prior ON and potential OR damage against healthy controls (HCs). We evaluated inter-method agreement of FA values and compared the capacity of all methods to detect OR FA differences in all patient cohorts compared to HCs.

2. Material and methods

2.1. Subjects

Sixty-two patients were retrospectively analyzed from our research database. This included CIS and early RRMS with ON (CIS/RRMS-ON), CIS and early RRMS without ON (CIS/RRMS-NON), NMOSD with ON (NMOSD-ON) as well as 26 HCs (see Table 1). All patients were examined under supervision of a board-certified neurologist at the NeuroCure Clinical Research Center, Charité-Universitätsmedizin Berlin between January 2011 and July 2015.

Table 1
Study cohort description.

	HC	CIS/RRMS-NON	CIS/RRMS-ON	NMOSD-ON
Subjects [n]	26	21	18	23
Sex [f(m)]	22(4)	11(10)	11(7)	20(3)
Age [years; mean ± SD]	43.7 ± 15.7	33.4 ± 8.6	31.2 ± 7.7	46.7 ± 14.5
Disease duration [months; mean ± SD]	n.a.	5.40 ± 6.67	4.63 ± 5.15	94.17 ± 95.72
EDSS [median; range]	n.a.	1.5 (0–4.0)	1.5 (0–3.5)	4.0 (0–6.5)
RRMS diagnosis [n]	n.a.	5 (23.8%)	3 (16.7%)	n.a.
AQP4-ab-positive [n]	n.a.	n.a.	n.a.	19
History of bilateral optic neuritis	n.a.	n.a.	0	4

HC = healthy control; CIS/RRMS-NON = clinically isolated syndrome without prior optic neuritis; CIS/RRMS-ON = clinically isolated syndrome with prior optic neuritis; NMOSD-ON = neuromyelitis optica spectrum disorder with prior optic neuritis; EDSS = expanded disability status scale; RRMS = relapsing-remitting multiple sclerosis; AQP4-ab-positive = Aquaporin-4-antibody positive.

We included 18 CIS/RRMS-ON patients from the time of analysis 110 participants of the Berlin CIS Cohort study ([ClinicalTrials.gov](https://clinicaltrials.gov/ct2/show/study/NCT01371071) Identifier: NCT01371071; EA1/182/10). CIS/RRMS-ON patients were investigated following a first-time ON attack after 4.61 ± 5.51 months on average (range: 1–24 months) and showed no other neurological symptoms than ON-related visual dysfunction. All CIS/RRMS-ON patients presented with unilateral optic neuritis as their first clinical symptom. At the time of MRI examination, 3 of these patients fulfilled the 2010 revised McDonald criteria for MS ([Polman et al., 2011](#)) while the other 15 patients had a CIS. Twenty-one CIS/RRMS-NON patients from the same study were diagnosed as CIS ($n = 16$) or early RRMS ($n = 5$) according to the 2010 revised McDonald criteria and had a history of only one neurological attack distinct from ON (e.g. myelitis). Additionally, 23 patients meeting the international consensus diagnostic criteria for NMOSD ([Wingerchuk et al., 2015](#)) (19 Aquaporin-4-antibody-positive: 82.6%) ([Jarvis et al., 2014](#); [Metz et al., 2016](#); [Zekeridou and Lennon, 2015](#)) with a clinically definitive episode of at least one ON (NMOSD-ON) were included from the time of analysis 53 patients of our neuromyelitis optica observational study (EA1/041/14). NMOSD-ON patients had a time lapse from last ON of 73.2 ± 87.1 months (range: 5–404 months). We enrolled 26 HCs from our imaging research database. Patients were excluded if they 1) were outside age range of 18–70, 2) suffered from ophthalmological defects other than ON, 3) had a history of neurological diseases distinct from MS or NMOSD, 4) had no available DTI acquisition. Further exclusion criteria were similar to general exclusion criteria valid for MRI at 3 T. Part of NMOSD-ON patients' and HCs' DTI data have been investigated and published in a previous study ([Oertel et al., 2017](#)). All participants provided written informed consent prior to their inclusion in the study. The study was approved by the local ethics committee and was performed in accordance with the 1964 Declaration of Helsinki in its currently applicable version.

2.2. MRI acquisition and analysis

All MRI data were acquired on the same 3 T scanner (Tim Trio Siemens, Erlangen, Germany) using a single-shot echo planar imaging DTI sequence (TR/TE = 7500/86 ms; FOV = 240×240 mm²; matrix 96×96 , 61 slices no gap, slice thickness 2.3 mm, 64 non-collinear directions, b -value = 1000 s/mm²), a volumetric high-resolution T1 weighted magnetization prepared rapid acquisition gradient echo (MPRAGE) sequence (TR/TE/TI = 1900/2.55/900 ms, FOV = 240×240 mm², matrix 240×240 , 176 slices, slice thickness 1 mm) as well as a volumetric high-resolution fluid-attenuated inversion recovery sequence (3D FLAIR) (TR/TE/TI = 6000/388/2100 ms; FOV = 256×256 mm², slice thickness 1.0 mm). 3D FLAIR images of all patients were checked and verified for total lesion volume and OR-specific lesion volume by three expert raters under the supervision of a board-certified radiologist. Whole-brain segmentation and quantification of lesions of FLAIR images were performed using ITK-SNAP (www.itksnap.org) ([Yushkevich et al., 2006](#)).

2.3. Image processing

2.3.1. Tract-based spatial statistics analysis (TBSS)

DTI data analysis was carried out using TBSS ([Smith et al., 2006](#)) with tools from the FMRIB Software Library (FSL 5.0.9).

First, eddy-current and motion correction were run in FSL, then FA images were created by fitting a tensor model to the raw diffusion data using a least-squares algorithm in FDT, and then brain-extracted using BET ([Smith, 2002](#)). FA data were then aligned into a common space using the nonlinear registration tool FNIRT which uses a b-spline representation of the registration warp field. Next, the mean FA image was created and thinned to produce a mean FA skeleton that represents the centres of all tracts common to the group. Each subject's aligned FA data was then projected onto this skeleton (Supplemental Fig. S1A and B; see Supplemental material for further method description).

TBSS skeleton masks were overlaid with two different atlas masks: (A) OR ROIs derived from the Juelich 1 mm probabilistic atlas optic radiation ROI thresholded to exclude the lowest 10% (JUEL-TBSS) and (B) Johns Hopkins University 1 mm white matter tractography probabilistic atlas' posterior thalamic radiation ROI (JHU-TBSS) ([Hua et al., 2008](#); [Wakana et al., 2007](#)).

2.3.2. ConTrack probabilistic tractography and Vistalab tract profiling

DTI data analysis was performed using the open-source mrVista package (<http://vistalab.stanford.edu/software>). Probabilistic fiber tracking was performed using the Contrack algorithm (CON-PROB) ([Sherbondy et al., 2008a, 2008b](#)), designed to identify the most likely pathway between two ROIs. Prior to tractography, Eddy current-induced distortion correction and motion correction were performed in all subjects within the vistalab framework. The schematic diagram is shown in Supplemental Fig. S1C (see also Supplemental material for pipeline details). Fiber tensors were fitted using a least-squares algorithm. The eigenvalue decomposition of the diffusion tensors was computed and FA measures were derived along the OR bundles, at 50 equally-spaced positions, resulting in an FA tract profile ([Raz et al., 2015](#)). Measurements were calculated by taking a weighted average of the measurements of each individual fiber at the node (so called "fiber core") ([Yeatman et al., 2012](#)) to combine measures throughout the length of the fibers across different subjects.

2.3.3. CSD-based probabilistic tractography and Vistalab tract profiling

We applied a combination of previously published OR tractography based on high order fiber orientation distributions estimated with CSD (CSD-PROB) ([Lim et al., 2015](#); [Martínez-Heras et al., 2015](#)) and weighted mean diffusivity calculation as well as tract profiling performance in Vistalab ([Yeatman et al., 2012](#)). Probabilistic tractography from seed to target masks was performed in each hemisphere using the MRtrix3 package (<http://www.mrtrix.org/>) ([Tournier et al., 2004, 2007, 2008](#)). First, diffusion image preprocessing was performed, including eddy current-induced distortion correction and inter-volume subject motion correction by the use of MRtrix3-in-built usage of FSL's eddy tool ([Andersson and Sotiropoulos, 2016](#); [Smith et al., 2004](#)).

Maps of the fiber orientation distributions (FODs) were calculated using CSD with a maximum harmonic order of 6 (CSD algorithm). OR reconstruction pipeline was modified after Martínez-Heras et al. and Lim et al. ([Lim et al., 2015](#); [Martínez-Heras et al., 2015](#)) with non-linear transformation of atlas ROIs in MNI space to individual T1 space using FSL FNIRT ([Smith et al., 2004](#)) and subsequent registration of ROIs from individual T1 space to individual DWI space using FSL FLIRT ([Jenkinson et al., 2002](#)). The tensors were fitted using a linear least squares approach. The schematic diagram of the pipeline is presented in Supplemental Fig. S1D (see also Supplemental material for pipeline details). We then used the resulting fibers to transfer them into the Vistalab environment and compute tract profiling and weighted mean FA of each tract modified after the procedure outlined in the CON-PROB and Vistalab profiling section.

2.4. Optical coherence tomography and visual acuity assessment

Optical coherence tomography (OCT) investigations were performed in all CIS/RRMS-NON patients, in 17 out of 18 CIS/RRMS-ON patients, in 22 out of 23 NMOSD-ON patients and in 21 out of 26 HC using a Heidelberg Engineering Spectralis spectral domain OCT (Heidelberg Engineering, Heidelberg, Germany) with automatic real-time (ART) function for image averaging. The peripapillary retinal nerve fiber layer (pRNFL) was measured with activated eye tracker using 3.4-mm ring scans around the optic nerve head (12° , 1536 A-scans $16 \leq \text{ART} \leq 100$). Segmentation of global RNFL was performed semiautomatically using software provided by the OCT manufacturer (Eye Explorer 1.9.10.0 with viewing module 6.0.9.0; Heidelberg Engineering). Visual acuity tests were performed by either using ETDRS

charts or the Traditional Snellen Eye Chart in all CIS/RRMS-NON, in 17 out of 18 CIS/RRMS-ON patients, in 21 out of 23 NMOSD-ON patients and in 21 out of 26 HC. Visual testing outcomes were converted in decimals.

2.5. Statistical analysis

For statistical analysis we used Graphpad Prism 6.0 (Graphpad Software, San Diego, CA, USA) software and R version 3.1.2 with packages psych, geepack, irr, ICC, lme4, ROct and ggplot. For comparison and correlation of absolute FA values between methods we used separate FA values of left and right OR and conducted a two-way repeated measures ANOVA to account for the effect of 1) method choice and 2) OR side on FA values within each patient group and an intraclass correlation coefficient (ICC) analysis. Agreement of FA values between methods was evaluated by Pearson's correlation coefficient analysis and Bland-Altman plots (BA-analysis within Graphpad Prism 6.0).

Exploratory comparisons of patient groups regarding T2 lesion volume, RNFL and visual acuity of worse eye were conducted using one-way ANOVA. For group comparisons and correlation analyses with clinical data, we combined FA measures of left and right optic radiation and calculated the simple mean of both values in JHU-TBSS, JUEL-TBSS and CON-PROB. Since OR volumes differed between right and left side in CSD-PROB, we used weighted mean of both values for CSD-PROB

based group comparison and correlation analyses. Comparisons of patient groups regarding FA values were assessed using linear model analyses to account for FA values with subsequent R² effect size measures estimation. A receiver operating characteristic (ROC) analysis was used to assess sensitivity and specificity of methods to discriminate each patient group from healthy controls corrected for age. Comparison of tract profiles was conducted using two-way ANOVA comparing FA values of patient groups in every node against HC group. Correction for multiple comparison was performed using Bonferroni correction. Correlations between OR FA values and OR T2 lesion volume, RNFL and visual acuity were performed using linear model analysis. For all statistical analyses, a p-value of < 0.05 was regarded as significant. Data are presented as mean ± SD, except for tract profiling results that are displayed in mean ± standard error of the mean (SEM).

3. Results

3.1. Method comparison

3.1.1. Image processing quality

All four methods successfully generated visually appropriate OR tracts, with the exception of one subject in the CIS/RRMS-ON group using the CSD-PROB method.

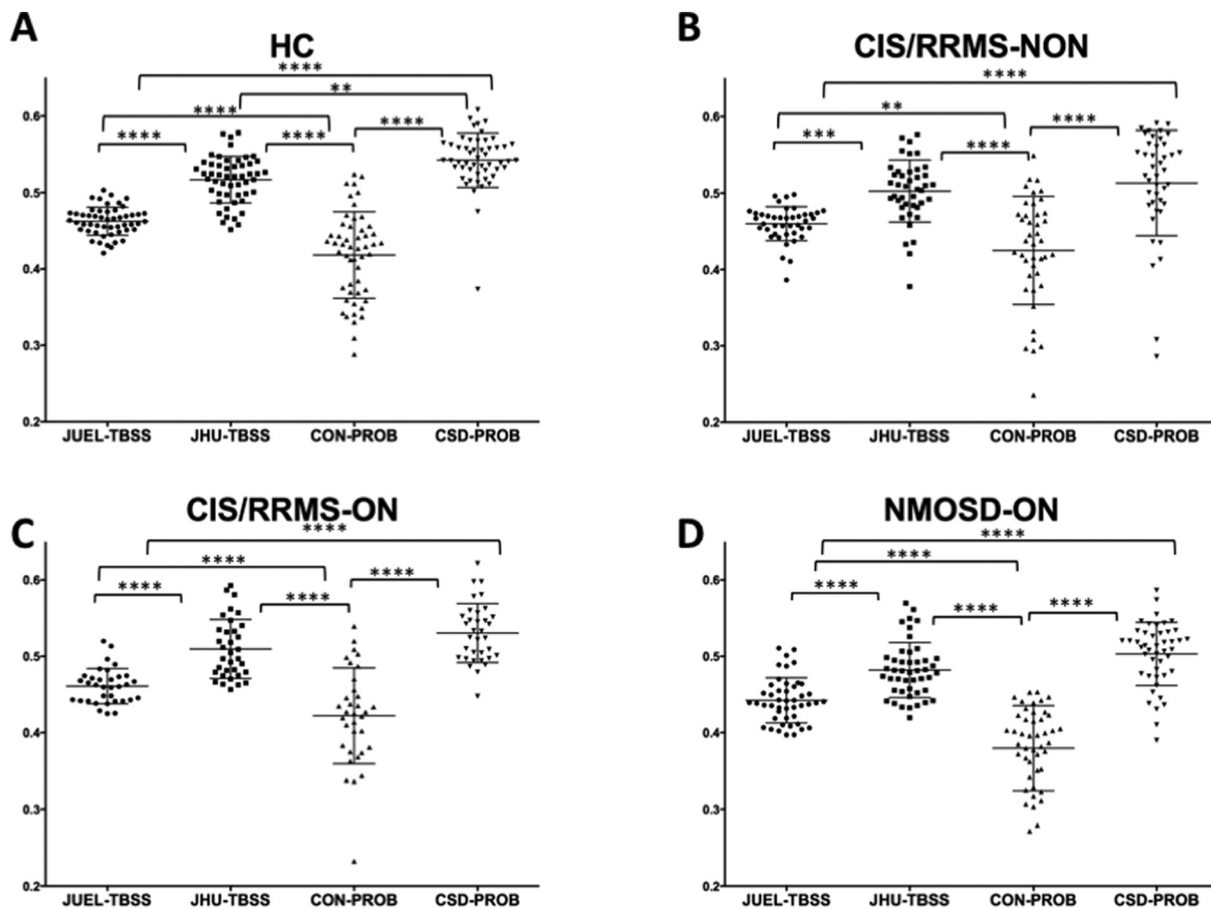


Fig. 1. Absolute FA values of different DTI post-processing methods. Optic radiation FA values are shown for A healthy controls (HC), B CIS patients without prior optic neuritis, C CIS patients with optic neuritis in their medical history and D NMOSD-ON patients. Comparison of FA distribution yielded significant differences between all methods except for the comparison of JHU-TBSS and CSD-PROB in CIS/RRMS-NON, CIS/RRMS-ON and NMOSD-ON patients. JUEL-TBSS = Juelich-based atlas ROI TBSS approach; JHU-TBSS = Johns-Hopkins University posterior thalamic radiation ROI TBSS approach; CON-PROB = ConTrack-based probabilistic tractography. CSD-PROB = constrained spherical deconvolution based probabilistic tractography. TBSS = tract-based spatial statistics.

3.1.2. Coefficient of variation in healthy controls

Coefficient of variation in HC group was lowest in JUEL-TBSS (3.99%) and highest in CON-PROB (13.54%) with comparable coefficients of variation in JHU-TBSS (5.88%) and CSD-PROB (7.21%).

3.1.3. Comparison of FA values between methods

Absolute FA value distribution of the different methods for ORs of both sides within each subject group are shown in Fig. 1 (separate left and right OR FA values are shown in Fig. S2). Two-way repeated measures ANOVA revealed a significant impact of 1) method choice and 2) OR side on FA values (see supplementary material, Table S1). Post-hoc tests with Bonferroni correction revealed significant differences between all methods except for the comparison of JHU-TBSS and CSD-PROB in CIS/RRMS-NON, CIS/RRMS-ON and NMOSD-ON. ICC analysis of absolute agreement of all FA values between methods showed poor agreement between methods with ICC values ranging from 0.112 to 0.432 (see Table 2). Lower ICC values were found in patient groups with no suspected visual system damage (HC) and in NMOSD-ON with highest suspected OR damage whereas higher ICC agreement was found in patient groups with suspected moderate damage (CIS/RRMS-ON and CIS/RRMS-NON-group).

3.1.4. Inter-method agreement of FA values

Pearson correlation analysis revealed significant correlations when analyzing all methods against each other with Pearson's *r* ranging from 0.2730 (JUEL-TBSS vs. CON-PROB) to 0.8714 (JUEL-TBSS vs. JHU-TBSS; see Table 3, Fig. 2, Fig. S3).

Bland-Altman plots showed good agreement between all methods with most FA values ranging within the 95% confidence interval from average of differences. Best limits of agreement (LOA) were observed

between values of both TBSS-based approaches (LOA distance: 0.0934; see Supplemental Fig. S4A; Table 4). Comparison of probabilistic tractography based methods with TBSS based methods generally showed a proportional error with overestimation of high FA values and underestimation of low FA values in probabilistic tractography (Fig. S4C and E). Best agreement of relative and absolute FA values between all methods were seen at medium FA values (0.45–0.5) suggesting good agreement in methods in identifying minimal to medium damage.

3.2. Comparison of patient groups against healthy controls

3.2.1. Patient group differences from HC and effect size

Comparison of patient groups against healthy controls regarding T2 lesion volume, OCT RNFL, visual acuity and optic radiation FA values are shown in Table 5. All patient groups showed higher T2 lesion volume and increased OR specific T2 lesion volume compared to HC. RNFL was significantly decreased compared to HC in CIS/RRMS-ON and NMOSD-ON, while visual impairment was only seen in NMOSD-ON group. Linear model analysis of FA differences between each patient group and healthy controls showed FA differences between NMOSD-ON and HCs throughout all methodologies (JUEL-TBSS: *p* = 0.0043; JHU-TBSS: *p* = 0.0002; CON-PROB: *p* = 0.0024; CSD-PROB: *p* < 0.0001; Fig. 3). *p*-Values and *R*² as the effect size and proportion of variance explained by the method are displayed in Table 6. Highest effect size in the discrimination of HC and NMOSD was seen in CSD-PROB (*R*² = 0.282). CSD-PROB revealed significant FA differences between CIS/RRMS-ON patients and HCs, that were not observable when other methods were applied.

Table 2
ICC analysis results of method comparisons by patient group.

	All patients	HC	CIS/RRMS-NON	CIS/RRMS-ON	NMOSD-ON
All methods ^a	0.155*	0.024	0.208*	0.252*	0.074*
JUEL-TBSS vs. JHU-TBSS	0.389	0.215	0.391	0.350	0.527
JUEL-TBSS vs. CON-PROB	0.129*	−0.084	0.236*	0.300*	−0.006
JUEL-TBSS vs. CSD-PROB	0.140	0.048	0.175	0.162	0.100
JHU-TBSS vs. CON-PROB	0.122	0.004	0.205	0.260	−0.003
JHU-TBSS vs. CSD-PROB	0.432*	0.232*	0.447*	0.578*	0.246*
CON-PROB vs. CSD-PROB	0.165	−0.014	0.085	0.155	0.061

HC = healthy control; CIS/RRMS-NON = clinically isolated syndrome without prior optic neuritis; CIS/RRMS-ON = clinically isolated syndrome with prior optic neuritis; NMOSD-ON = neuromyelitis optica spectrum disorder with prior optic neuritis; JUEL-TBSS = Juelich histological atlas optic radiation ROI based tract-based spatial statistics; JHU-TBSS = Johns Hopkins University atlas posterior thalamic ROI based tract-based spatial statistics; CON-PROB = Contrack-based probabilistic tractography; CSD-PROB = constrained spherical deconvolution based probabilistic tractography.

* *p* < 0.05.

^a ICC analysis of all 4 methods (JUEL-TBSS, JHU-TBSS, CON-PROB and CSD-PROB).

Table 3
Pearson correlation analysis between all methods by patient groups.

	All patients		HC		CIS/RRMS-NON		CIS/RRMS-ON		NMOSD-ON	
	Pearson's <i>r</i>	<i>p</i> -Value	Pearson's <i>r</i>	<i>p</i> -Value	Pearson's <i>r</i>	<i>p</i> -Value	Pearson's <i>r</i>	<i>p</i> -Value	Pearson's <i>r</i>	<i>p</i> -Value
JUEL-TBSS vs. JHU-TBSS	0.8714	< 0.0001*	0.8076	< 0.0001*	0.8523	< 0.0001*	0.8683	< 0.0001*	0.9272	< 0.0001*
JUEL-TBSS vs. CON-PROB	0.2730	0.0003*	−0.2188	0.1191	0.4967	0.0008*	0.6002	0.0001*	−0.0151	0.9207
JUEL-TBSS vs. CSD-PROB	0.4186	< 0.0001*	0.2707	0.0523	0.4543	0.0025*	0.6094	0.0002*	0.2614	0.0864
JHU-TBSS vs. CON-PROB	0.3508	< 0.0001*	0.0164	0.9084	0.4494	0.0028*	0.7063	< 0.0001*	−0.0119	0.9372
JHU-TBSS vs. CSD-PROB	0.4883	< 0.0001*	0.2940	0.0344*	0.5134	0.0005*	0.6428	< 0.0001*	0.2836	0.0621
CON-PROB vs. CSD-PROB	0.2270	0.003*	−0.0629	0.6576	0.1509	0.3398	0.5423	0.0013*	0.2695	0.0769

HC = healthy control; CIS/RRMS-NON = clinically isolated syndrome without prior optic neuritis; CIS/RRMS-ON = clinically isolated syndrome with prior optic neuritis; NMOSD-ON = neuromyelitis optica spectrum disorder with prior optic neuritis; JUEL-TBSS = Juelich histological atlas optic radiation ROI based tract-based spatial statistics; JHU-TBSS = Johns Hopkins University atlas posterior thalamic ROI based tract-based spatial statistics; CON-PROB = Contrack-based probabilistic tractography; CSD-PROB = constrained spherical deconvolution based probabilistic tractography.

* *p* < 0.05.

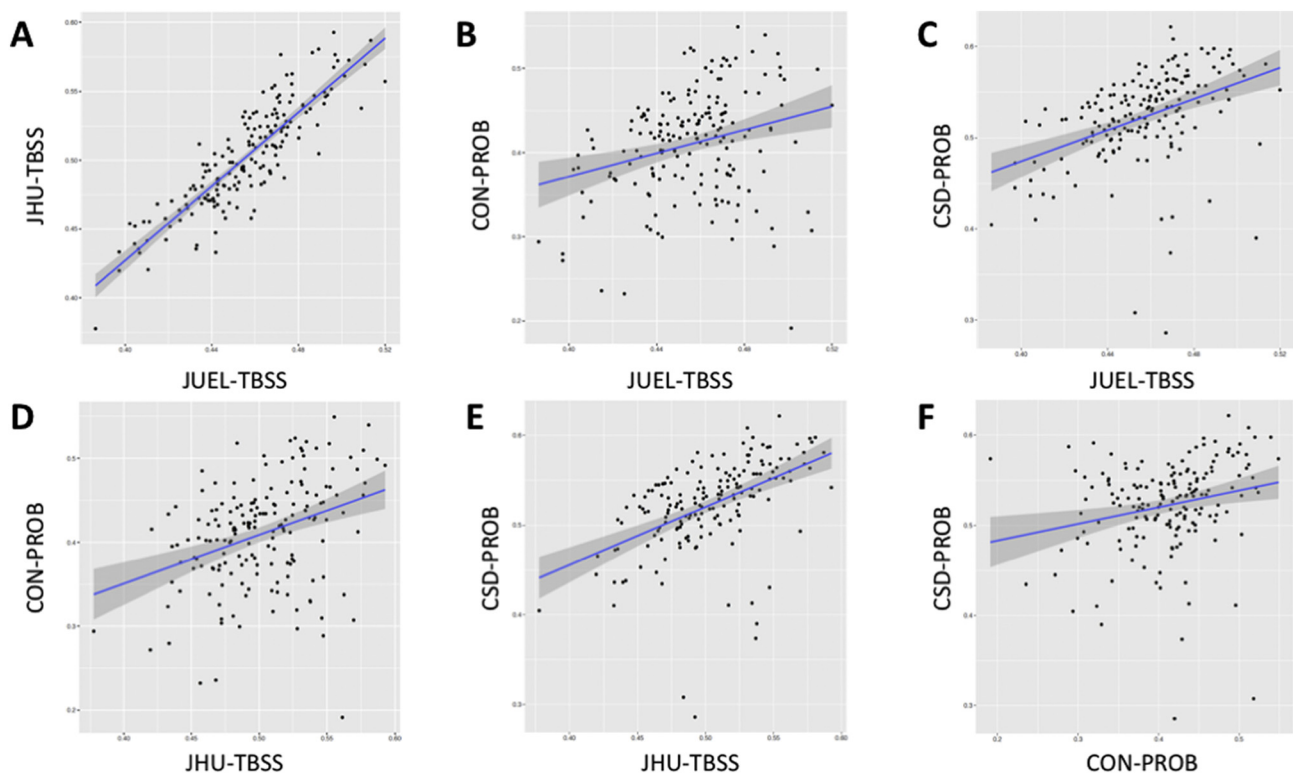


Fig. 2. Correlation of all FA values regarding each method.

Correlation of all OR FA values assessing **A** JUEL-TBSS vs. JHU-TBSS, **B** JUEL-TBSS vs. CON-PROB, **C** JUEL-TBSS vs. CSD-PROB, **D** JHU-TBSS vs. CON-PROB, **E** JHU-TBSS vs. CSD-PROB, **F** CON-PROB vs. CSD-PROB.

JUEL-TBSS = Juelich-based atlas ROI TBSS approach; JHU-TBSS = Johns-Hopkins University posterior thalamic radiation ROI TBSS approach; CON-PROB = ConTrack-based probabilistic tractography. CSD-PROB = constrained spherical deconvolution based probabilistic tractography. TBSS = tract-based spatial statistics; OR = optic radiation.

Table 4

Bias and limits of agreement of Bland-Altman analysis.

	Estimation of bias		95% Limits of agreement (LOA)	
	Bias	SD of bias	From	To
JUEL-TBSS vs. JHU-TBSS	0.0466	0.0206	0.0063	0.0871
JUEL-TBSS vs. CON-PROB	0.0218	0.0728	-0.1209	0.1646
JUEL-TBSS vs. CSD-PROB	-0.0664	0.0452	-0.1550	0.0221
JHU-TBSS vs. CON-PROB	0.0922	0.0612	-0.0279	0.2123
JHU-TBSS vs. CSD-PROB	-0.0198	0.0453	-0.1085	0.0689
CSD-PROB vs. CON-PROB	0.1121	0.0708	-0.0266	0.2508

SD = standard deviation; JUEL-TBSS = Juelich histological atlas optic radiation ROI based tract-based spatial statistics; JHU-TBSS = Johns Hopkins University atlas posterior thalamic ROI based tract-based spatial statistics; CON-PROB = Contrack-based probabilistic tractography; CSD-PROB = constrained spherical deconvolution based probabilistic tractography.

Table 5

Comparison of patient groups against healthy controls regarding T2 lesion volume, visual parameters and optic radiation FA values.

	HC	CIS/RRMS-NON	CIS/RRMS-ON	NMOSD-ON	ANOVA p
Total T2 lesion volume [ml; mean ± sd]	0.38 ± 0.66	2.87* ± 4.39	2.59* ± 3.17	2.15* ± 3.07	0.084
OR-specific T2 lesion volume [ml; mean ± sd]	0.04 ± 0.07	0.70* ± 1.02	0.57* ± 0.70	0.44* ± 0.87	0.017*
RNFL [µm; mean ± sd]	96.90 ± 7.50	98.21 ± 12.16	87.92* ± 14.76	67.12* ± 19.72	< 0.001*
Visual acuity of worse eye [mean ± sd]	1.02 ± 0.31	1.00 ± 0.37	0.96 ± 0.29	0.74* ± 0.47	0.003*
FA [JUEL-TBSS]	0.46 ± 0.02	0.46 ± 0.02	0.46 ± 0.02	0.44* ± 0.03	0.012*
FA [JHU-TBSS]	0.52 ± 0.03	0.50 ± 0.04	0.51 ± 0.04	0.48* ± 0.04	0.004*
FA [CON-PROB]	0.42 ± 0.06	0.43 ± 0.07	0.42 ± 0.06	0.38* ± 0.06	0.010*
FA [CSD-PROB]	0.54 ± 0.03	0.52* ± 0.04	0.53 ± 0.03	0.50* ± 0.04	0.001*

HC = healthy control; CIS/RRMS-NON = clinically isolated syndrome without prior optic neuritis; CIS/RRMS-ON = clinically isolated syndrome with prior optic neuritis; NMOSD-ON = neuromyelitis optica spectrum disorder with prior optic neuritis; FA = fractional anisotropy; JUEL-TBSS = Juelich histological atlas optic radiation ROI based tract-based spatial statistics; JHU-TBSS = Johns Hopkins University atlas posterior thalamic ROI based tract-based spatial statistics; CON-PROB = Contrack-based probabilistic tractography; CSD-PROB = constrained spherical deconvolution based probabilistic tractography.

Exploratory ANOVA and subsequent *t*-test *p*-values.

* *p* < 0.05 (significant from HC).

3.2.2. ROC-analysis

AUC values to discriminate HCs from NMOSD-ON were highest in CSD-PROB (AUC = 0.812), while slightly lower in CON-PROB (AUC = 0.742), JHU-TBSS (AUC = 0.756) and JUEL-TBSS (AUC = 0.719; Fig. 4). ROC-analysis results of comparison between HC vs. CIS/RRMS-ON and HC vs. CIS/RRMS-NON are shown in Table 7.

3.2.3. Tract profiling – subject group comparison

Tract profiles comparing patient groups are shown in Fig. 5. Significant differences between NMOSD-were seen in both methods (CON-PROB: nodes 26–47; CSD-PROB: nodes 20–25 and 48–50; Fig. 5).

3.2.4. OR-specific lesions and OR FA

We investigated possible correlations between OR FA values and optic radiation specific lesion volume. JUEL-TBSS, JHU-TBSS and CSD-PROB showed significant correlations between FA and OR T2 lesion

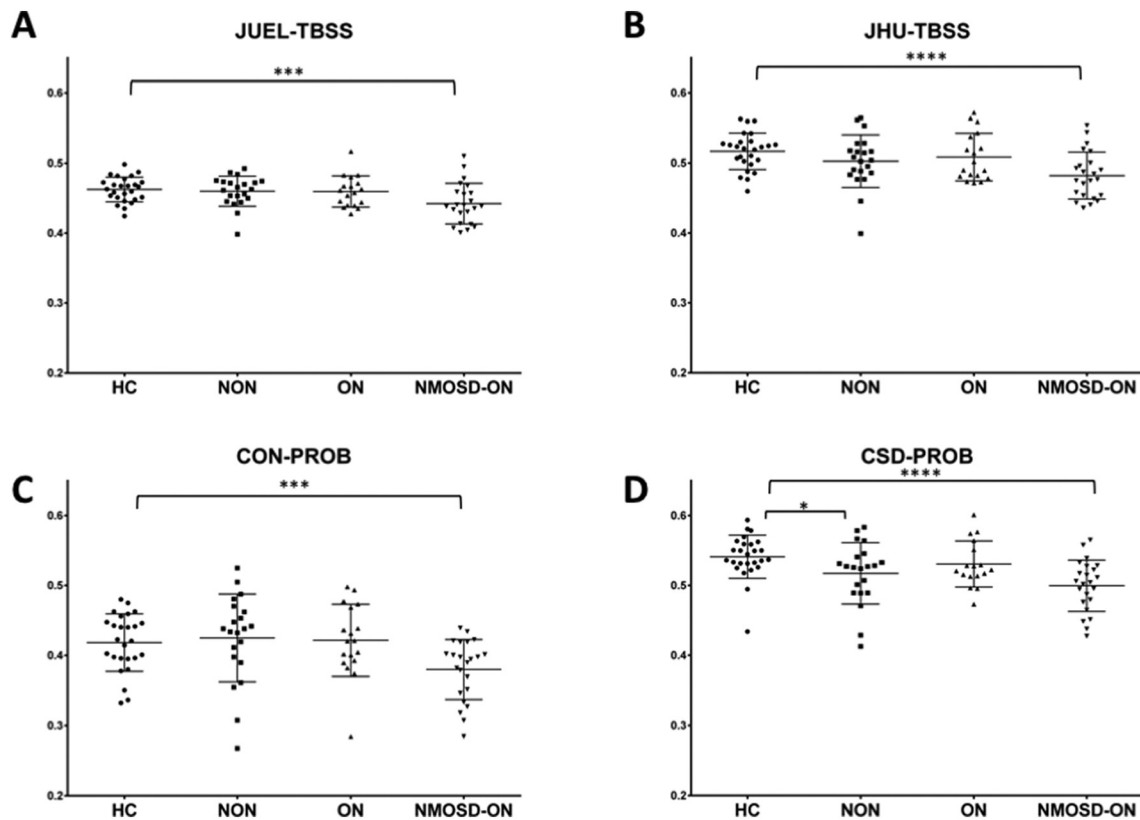


Fig. 3. OR mean FA comparison of patient groups and HCs arranged by methods. Mean FA distribution of individual TBSS skeletons within JUEL-TBSS (A) and JHU-TBSS (B). Both approaches show significant differences between HC and NMOSD group. JHU also shows significant differences between NMOSD and all CIS groups and differences between HC and CIS and HC and CIS/RRMS-NON. Comparison of weighted mean FA distribution within CON-PROB tracts (C) and CSD-PROB OR fibers (D) reveal similar significant differences between HC and NMOSD and NMOSD with all CIS/RRMS-subgroups. CSD-PROB also reveals significant differences between HC and all CIS-subgroups. FA = fractional anisotropy; HC = healthy controls; OR = optic radiation; TBSS = tract-based spatial statistics; JHU = Johns Hopkins University; ROI = region of interest; CSD = constrained spherical deconvolution; NMOSD = neuromyelitis optica spectrum disorder. * $p < 0.05$; ** $p < 0.005$; *** $p < 0.0005$; **** $p < 0.0001$.

Table 6
FA differences between patient groups and healthy controls.

	CIS/RRMS-NON vs. HC		CIS/RRMS-ON vs. HC		NMOSD-ON vs. HC	
	p-Value	R ²	p-Value	R ²	p-Value	R ²
JUEL-TBSS	0.661	0.004	0.628	0.005	0.004*	0.161
JHU-TBSS	0.134	0.049	0.362	0.020	< 0.001*	0.262
CON-PROB	0.663	0.004	0.818	0.001	0.002*	0.179
CSD-PROB	0.035	0.094	0.298	0.026	< 0.001*	0.282

HC = healthy control; CIS/RRMS-NON = clinically isolated syndrome without prior optic neuritis; CIS/RRMS-ON = clinically isolated syndrome with prior optic neuritis; NMOSD-ON = neuromyelitis optica spectrum disorder with prior optic neuritis; JUEL-TBSS = Juelich histological atlas optic radiation ROI based tract-based spatial statistics; JHU-TBSS = Johns Hopkins University atlas posterior thalamic ROI based tract-based spatial statistics; CON-PROB = Contrack-based probabilistic tractography; CSD-PROB = constrained spherical deconvolution based probabilistic tractography.
* $p < 0.05$.

volume in the CIS/RRMS-NON group (see Table 8).

3.2.5. RNFL and OR FA

Associations between RNFL and OR FA were exclusively shown in the CIS/RRMS-NON group by all methods (see Table 8).

3.2.6. Visually acuity and OR FA

Associations between visual acuity and OR FA were exclusively shown in the CIS/RRMS-NON group by JUEL-TBSS and JHU-TBSS. (see Table 8).

4. Discussion

Our study compared TBSS and probabilistic tractography based approaches to quantify OR damage in patients with NMOSD-ON and CIS with and without ON. While the distribution of absolute FA values differed among methods, correlation analyses and Bland-Altman plots revealed good agreement of FA values, especially in FA magnitudes of suspected mild OR damage, reflected by OR-specific lesion load and RNFL decrease (CIS/RRMS-ON and CIS/RRMS-NON). Both, TBSS and probabilistic tractography methods detected microstructural damage in NMOSD-ON patients compared to HCs.

4.1. Robustness of methods

CSD-PROB failed to generate OR tracts in one CIS/RRMS-ON patient, while successfully generating tracts in all other subjects. All other methods successfully identified the ORs in all subjects. It has been reported, that extensive white matter lesions in neurological disorders, such as stroke or multiple sclerosis, may lead to erroneous termination of the tracking algorithm or may cause a deviation of the bundles at the level of the lesions (Ciccarelli et al., 2008). A previous study in stroke patients showed that a CSD-based approach resulted in successful

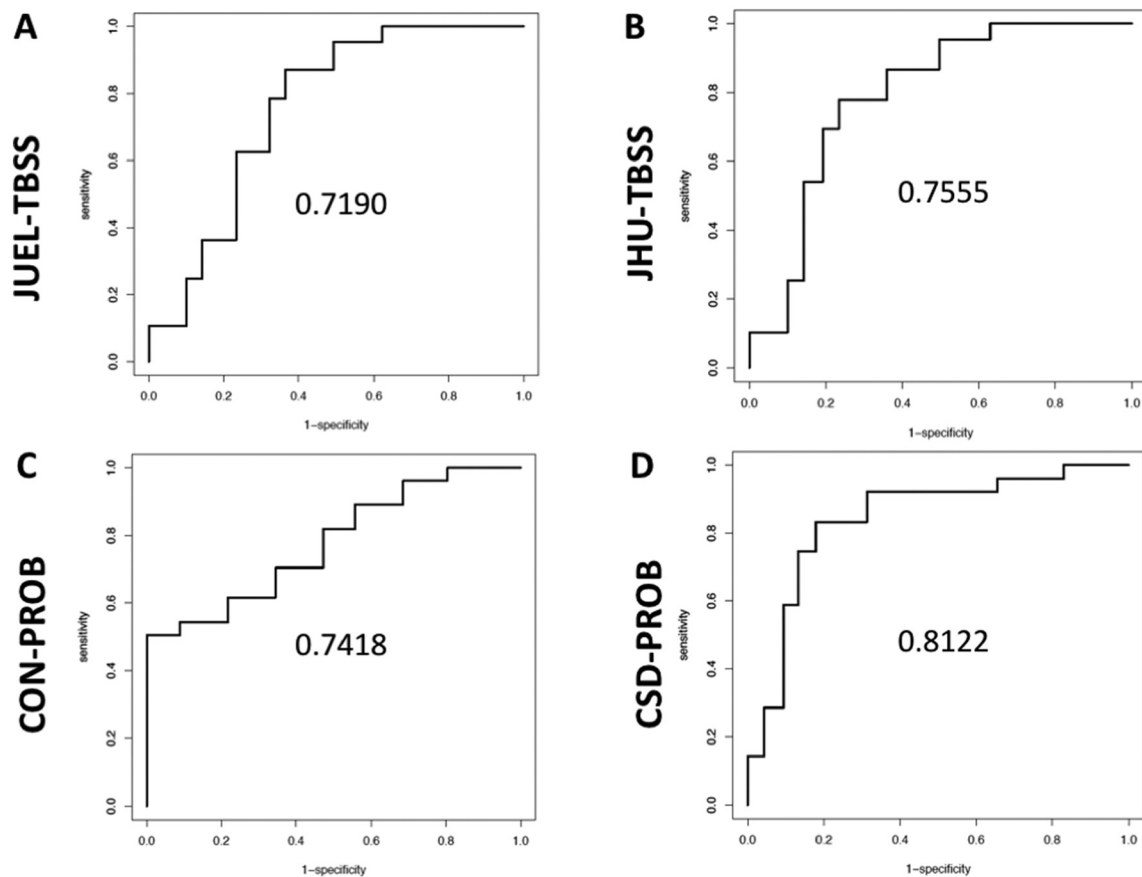


Fig. 4. ROC curves and AUCs for TBSS and CSD-based analysis methods.

ROC curves and AUCs are displayed comparing HC with NMOSD corrected for age by use of A JUJEL-TBSS, B JHU-TBSS, C CON-PROB and D CSD-PROB.

ROC = receiver operating characteristics; AUC = area under the curve; HC = healthy controls; NMOSD = neuromyelitis optica spectrum disorder; TBSS = tract-based spatial statistics; CSD = constrained spherical deconvolution; JHU = Johns Hopkins University.

Table 7

AUC values for the comparison of patient groups against healthy controls by each method corrected for age.

Method	Group 1	Group 2	AUC
JUEL-TBSS	HC	CIS/RRMS-NON	0.611
JUEL-TBSS	HC	CIS/RRMS-ON	0.625
JUEL-TBSS	HC	NMOSD-ON	0.719
JHU-TBSS	HC	CIS/RRMS-NON	0.743
JHU-TBSS	HC	CIS/RRMS-ON	0.704
JHU-TBSS	HC	NMOSD-ON	0.756
CON-PROB	HC	CIS/RRMS-NON	0.704
CON-PROB	HC	CIS/RRMS-ON	0.523
CON-PROB	HC	NMOSD-ON	0.742
CSD-PROB	HC	CIS/RRMS-NON	0.796
CSD-PROB	HC	CIS/RRMS-ON	0.626
CSD-PROB	HC	NMOSD-ON	0.812

HC = healthy control; CIS/RRMS-NON = clinically isolated syndrome without prior optic neuritis; CIS/RRMS-ON = clinically isolated syndrome with prior optic neuritis; NMOSD-ON = neuromyelitis optica spectrum disorder with prior optic neuritis; JUEL-TBSS = Juelich histological atlas optic radiation ROI based tract-based spatial statistics; JHU-TBSS = Johns Hopkins University atlas posterior thalamic ROI based tract-based spatial statistics; CON-PROB = Contrack-based probabilistic tractography; CSD-PROB = constrained spherical deconvolution based probabilistic tractography.

corticospinal tract reconstruction in 76 out of 78 tracts, while a comparative DTI-based fiber tractography resulted in the corticospinal tract reconstruction in 67 out of 78 potential tracts (Auriat et al., 2015). For both approaches unsuccessful fiber tract reconstruction occurred in the ipsilesional hemisphere of participants, indicating lesions to be

responsible for insufficient tract generation and different tractography to yield distinct susceptibilities towards lesion-associated tract generation failure (Auriat et al., 2015). In our study, unsatisfactory tract generation in our CIS/RRMS-ON patient using CSD-PROB might be caused by extensive white matter lesions that were observed in the patient's optic radiations.

4.2. Inter-method comparison of FA distribution

In our study, CON-PROB showed highest coefficient of variation of FA in HC, while JUEL-TBSS showed lowest coefficient of variation. Supposing that a homogeneous and normally distributed cohort was investigated, low coefficients of variation may suggest a correlate of good method quality. High coefficients of variation in HCs in CON-PROB, possibly caused by the mainly manual approach, might impair the validity of the method. However, high coefficients may on the other hand indicate higher method sensitivity. A recently published study compared a) individual CON-PROB with b) healthy control-based CON-PROB template OR reconstructions and c) Juelich histological atlas-based OR ROI approach in 35 healthy controls and 70 MS patients (Wang et al., 2018). Despite differences in the reconstructed OR volumes, both OR lesion volume and OR diffusivity measurements in MS subjects were highly comparable in this study. The authors found diffusivity differences between different OR segmentation techniques to be consistently small across low and high values.

By contrast, the distribution of absolute OR FA values significantly differed in our study between nearly all methods in all patient groups and showed poor absolute agreement in the ICC analysis, except for JHU-TBSS and CSD-PROB. We conclude that differences between

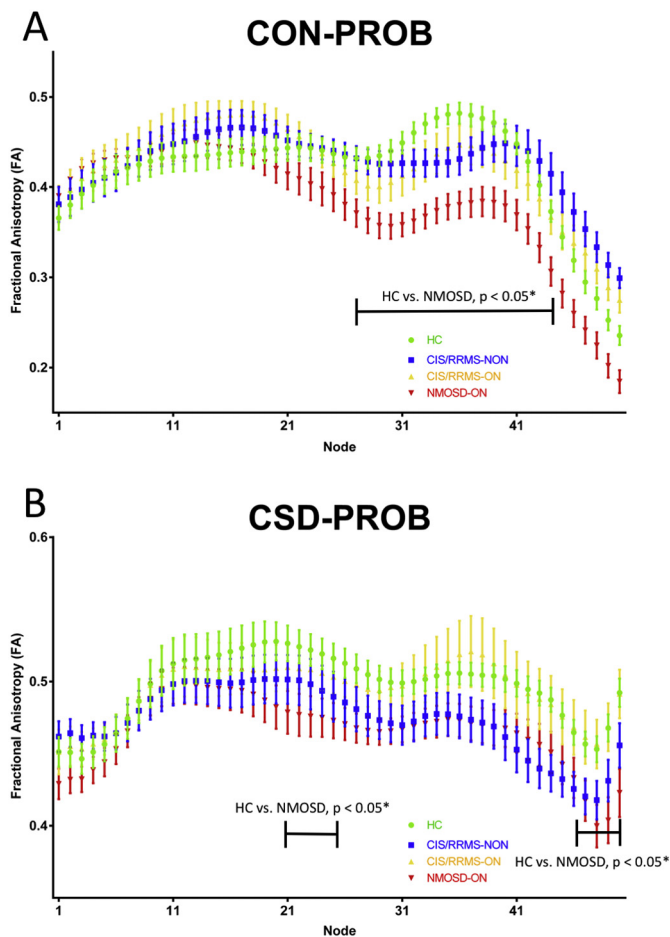


Fig. 5. Tract profiles of the optic radiation in different patient groups. OR partitioning into 50 equally divided nodes in NMOSD (red), CIS/RRMS-ON (orange) and CIS/RRMS-NON (yellow) patients and Healthy controls (green) using (A) Contrack-based probabilistic tractography (B) CSD-based tractography. OR = optic radiation; CIS = clinically isolated syndrome; ON = optic neuritis; CSD = constrained spherical deconvolution; NMOSD = neuromyelitis optica spectrum disorder; FA = fractional anisotropy.

Table 8

Correlations of optic radiation specific lesion volume, RNFL and visual acuity with optic radiation FA values by method.

	JUEL-TBSS			JHU-TBSS			CON-PROB			CSD-PROB		
	Estimate	Std error	p-Value	Estimate	Std error	p-Value	Estimate	Std error	p-Value	Estimate	Std error	p-Value
OR T2 Lesion volume												
HC	-0.073	0.060	0.23	-0.124	0.089	0.17	0.152	0.142	0.29	0.026	0.108	0.24
CIS/RRMS-NON	-0.022	0.005	< 0.01*	-0.044	0.008	< 0.01*	-0.022	0.017	0.21	-0.031	0.012	0.01*
CIS/RRMS-ON	-0.011	0.009	0.26	-0.022	0.015	0.15	-0.014	0.023	0.54	-0.027	0.014	0.06
NMOSD-ON	-0.010	0.007	0.18	-0.013	0.008	0.15	-0.016	0.011	0.15	-0.003	0.009	0.76
RNFL												
HC	0.001	0.000	0.57	0.001	0.000	0.98	0.001	0.000	0.37	0.001	0.000	0.21
CIS/RRMS-NON	0.001	0.000	< 0.01*	0.002	0.000	< 0.01*	0.002	0.000	0.01*	0.001	0.001	0.01*
CIS/RRMS-ON	0.001	0.000	0.06	0.001	0.000	0.24	0.001	0.000	0.10	0.001	0.000	0.07
NMOSD-ON	0.000	0.000	0.52	0.001	0.000	0.74	0.001	0.000	0.32	0.001	0.000	0.44
Visual acuity												
HC	0.022	0.008	0.01*	0.019	0.019	0.12	-0.055	0.019	< 0.01*	0.024	0.011	0.03*
CIS/RRMS-NON	0.026	0.008	< 0.01*	0.041	0.015	0.01*	0.021	0.027	0.44	0.010	0.017	0.55
CIS/RRMS-ON	0.012	0.011	0.30	0.014	0.017	0.45	0.033	0.024	0.17	0.011	0.019	0.56
NMOSD-ON	0.016	0.001	0.10	0.012	0.011	0.28	0.006	0.014	0.68	0.003	0.012	0.77

JUEL-TBSS = Juelich histological atlas optic radiation ROI based tract-based spatial statistics; JHU-TBSS = Johns Hopkins University atlas posterior thalamic ROI based tract-based spatial statistics; CON-PROB = Contrack-based probabilistic tractography; CSD-PROB = constrained spherical deconvolution based probabilistic tractography. RNFL = retinal nerve fiber layer thickness. Significant p-values are displayed in bold.

* p < 0.05.

absolute OR FA values may impede comparisons of previous and future DTI study results investigating microstructural OR damage. The application of the exact same method is therefore necessary to allow for any statements on possible differences between OR FA values within a specific cohort of patients. These findings may be of particular significance in any case of OR DTI comparison, regardless of within-study analyses or comparisons of OR DTI results between studies, for example in meta-analyses. Comparisons of absolute OR DTI values that did not use the same post-processing approach are not valid and must therefore be avoided.

4.3. Inter-method comparison of FA correlations and agreement

OR FA values of all methods showed significant correlations suggesting underlying associations of FA values and actual OR specific microstructural damage regardless of method choice. Subgroup analyses of Pearson correlation coefficient analyses revealed best correlations of OR FA values in CIS/RRMS-ON and CIS/RRMS-NON. These findings are in line with a recent study reporting on good agreement between CON-PROB, template-based OR reconstruction and a Juelich OR ROI-based approach in HC and MS measured by Pearson correlation coefficients and Bland-Altman analysis (Wang et al., 2018).

By contrast, only limited correlations of OR FA values were seen in our study in the non-damage group (HC) and patients with suspected extensive OR damage (NMOSD-ON).

In a recent study, CSD-PROB was investigated in ten HCs and five MS patients to compare tractography results with histological masks. It showed a good sensitivity ranging from 65% to 81% and a specificity up to 100% (Martínez-Heras et al., 2015). Another recent study compared CSD-PROB with Juelich histological atlas in 20 patients with various neurological conditions, showing a good match of the probabilistic tractography approach with a mean AUC of 0.87 (Lim et al., 2015). These findings are in line with our study showing relatively little bias between JUEL-TBSS masking approach and CSD-PROB in the conducted Bland-Altman analysis. Bland-Altman analysis revealed best agreement between all methods at medium FA values (0.45–0.5) suggesting good agreement of methods in identifying damage of medium magnitude (CIS/RRMS-ON and CIS/RRMS-NON). These findings might – at least to a certain extent – suggest the convertibility of results by different DTI post-processing methods when applied to patient groups with OR damage of mild to moderate magnitude. Concrete research approaches to

patient groups with suspected mild OR damage, for example CIS patients, could be sufficiently tackled by all investigated methods, while investigations regarding HCs or severely affected patient groups (NMOSD-ON) might lead to different results, highly dependent of the chosen method.

The presence of systematic bias and proportional errors in the comparison of DTI TBSS-based and tractography based methods may lead to false positive or false negative results when different patient groups are compared by different methods. While one method might produce significant differences in group comparison due to underestimation of low FA values, another method may yield non-significant results due to relative overestimation of low FA values. These findings might be a causative factor of today's equivocal findings (Assaf and Pasternak, 2008) of previous DTI visual pathway analyses that impede the evaluation of DTI as a potential biomarker (Inglese and Bester, 2010).

4.4. NMOSD vs. HC group comparison

Group comparison showed FA differences between NMOSD-ON and HCs throughout all TBSS and probabilistic tractography based methods. Best effect size and AUC values to distinguish both groups were observed for CSD-PROB. JHU-TBSS, JUEL-TBSS and CON-PROB showed slightly lower AUC values and effect size. Our study results are in line with previous investigations using DTI reporting on microstructural degradation with significant FA reduction within the OR (Oertel et al., 2017; Pache et al., 2016a, 2016b; Rueda Lopes et al., 2012; Yu et al., 2006). A previous study in NMOSD patients, using TBSS, found FA values to be exclusively reduced in regions associated to the visual system by making use of a TBSS ROI and a multivariate comparison approach. These results provide evidence of anterograde trans-synaptic degeneration due to ON (Pache et al., 2016a, 2016b). By contrast, one TBSS-based study demonstrated reduced FA involving not only the OR but also diffuse subcortical white matter structures in frontal, parietal, temporal, occipital and limbic regions (von Glehn et al., 2014). Another study used CSD-PROB OR tractography and revealed FA reductions within the OR of 25 AQP4-antibody seropositive NMOSD patients (Oertel et al., 2017). Notably, OR FA was not only reduced in NMOSD patients with previous ON but FA reductions were also detectable in 6 NMOSD patients with longitudinally extensive transverse myelitis (LETM) without evidence of prior ON. These results were corroborated by another study that used FSL-based probabilistic tractography (FSL's probtrackx) to delineate the OR and found FA reduction within the OR of 24 NMOSD patients with prior ON (58.3% AQP4-antibody seropositive) as well as in 12 NMOSD patients without prior ON (66.6% AQP4-antibody positive) (Tian et al., 2017). These findings suggest microstructural changes in the afferent visual system independent of ON attack-related mechanisms.

Although clinical history of our NMOSD patients with prior unilateral or bilateral ON, long disease duration and pronounced visual impairment and OCT RNFL thinning suggests the presence of attack-related optic radiation FA decrease in our NMOSD cohort, we did not find any direct associations between OCT RNFL or visual acuity and optic radiation FA, irrespective of the method. However, our data mirror the clinical experience as well as findings from conventional imaging studies showing that neurological disability and tissue damage in the visual pathway are on average more pronounced in NMOSD as compared to MS/CIS, as it can be seen in the relatively frequent bilateral manifestation of optic neuritis in our NMOSD-cohort compared to CIS/RRMS-ON (Bennett et al., 2015; Kim et al., 2015; Schmidt et al., 2017).

4.5. CIS/RRMS-ON and CIS/RRMS-NON vs. HC

No difference of OR FA between CIS/RRMS-ON and HC was seen in any of the methods used. CSD-PROB showed differences between HC and CIS/RRMS-NON. In CIS and early stages of MS, OR microstructural

damage is most likely caused by 1) trans-synaptic neurodegeneration after ON (Gabilondo et al., 2014) and 2) impact of T2 inflammatory lesions within the OR (Graham and Klistorner, 2017; Sinnecker et al., 2015a, 2015b).

Damage in the OR of ON patients due to inflammatory T2 lesions has been investigated previously. Raz et al. reported on reduced OR FA by making use of CON-PROB in patients with clinically isolated ON compared to healthy controls. In this study, reduced OR FA was associated with OR specific T2 lesion volume suggesting FA differences to be explained by intrabundle lesions (Raz et al., 2015). In our CIS/RRMS-NON cohort, OR FA in JUEL-TBSS, JHU-TBSS and CSD-PROB was associated with OR specific T2 lesion volume, indicating TBSS approaches to be more sensitive to lesional damage than probabilistic tractography approaches. These findings indicate lesional damage to be at least partly responsible for damage within the ORs of CIS/RRMS patients without prior ON. However, recent findings indicated the presence of a measurable, time-dependent trans-synaptic neurodegeneration effect on the OR after ON, independent of T2 lesion load. Longitudinal investigations using an atlas-based OR template ROI in 38 acute ON patients over 12 months showed FA reduction at baseline and subsequent additional FA decrease at an average rate of -2.6% per year (Kolbe et al., 2016). Another study investigated twenty-eight acute ON patients by use of the FSL based probabilistic tractography algorithm and found no difference between patients' and controls' mean OR FA at baseline but a constant decrease over time after 3, 6 and 12 months (Tur et al., 2016). No associations between RNFL and OR FA were found in CIS/RRMS-ON patients. Given the relatively short time after ON in our CIS/RRMS-ON cohort with a mean disease duration of 4.63 ± 5.15 months after ON, we presume that the early timepoint of MRI acquisition after ON makes the determination of any trans-synaptic effect on the optic radiations unlikely.

4.6. Tract profiling using probabilistic tractography methods

Tract-profiling group differences between HC and NMOSD were seen in higher proportion of nodes in CON-PROB compared to CSD-PROB, indicating CON-PROB tract-profiling to yield higher sensitivity for the detection of microstructural OR damage in NMOSD compared to CSD-PROB tract profiling. Using CON-PROB, tract-profiling enabled the distinction between OR fibers affected by T2 lesions and non-lesional OR fibers. Radial diffusivity, mean diffusivity and FA changes were detected along the entire OR, while axial diffusivity changes were confined to the posterior half of the OR. This discrepancy implied distinct pathophysiologic processes to be detectable by DTI tract profiling (Klistorner et al., 2015).

In our study, tract profiling showed middle and posterior parts of the OR to be more affected than anterior OR sections in NMOSD compared to HC. These findings may suggest distinct regions of the OR to exhibit more pronounced damage by trans-synaptic neurodegeneration or distinct OR T2 lesional damage affecting only specific regions of the OR due to Wallerian degeneration (Klistorner et al., 2015). However, in our analysis overall NMOSD OR FA was not associated with optic radiation T2 lesion volume. Distinct regions of the OR are supposed to be less affected by contamination from craniocaudally oriented crossing fibers to the optic radiation. Neighbouring and crossing white matter pathways may additionally lead to a reduced FA in OR fiber regions (Kamali et al., 2014). Exclusive microstructural OR damage is more likely to be observable by DTI in regions that are not affected by crossing or kissing fibers, which are represented by distinct middle and posterior parts of the OR. Both, the affection of the OR by crossing and kissing fibers, as well as distinct damage patterns caused by the localization of OR-specific T2 lesions or trans-synaptic neurodegeneration damage patterns may therefore be the cause of different levels in FA decrease along OR regions.

4.7. Technical aspects

TBSS can be implemented fully-automated requiring no manual intervention. In TBSS, the average FA may be affected by surrounding structures due to partial voluming (Smith et al., 2006). Probabilistic tractography is more time-consuming due to manual and calculation processes inherent to the specific algorithm (Wang et al., 2018). Tractography algorithms are known to be - at least to a certain extent - susceptible to image artifacts with possible insufficient tract generation (Auriat et al., 2015). However, the CSD-PROB approach used in our study represents a feasible and fully-automated probabilistic tractography method, requiring no manual intervention compared to previously used CON-PROB (Wang et al., 2018).

4.8. Limitations

Given the multitude of methods that exist for tractography and the comparison of DWI measures, our study naturally fails to comprehensively include all alternative methods for comparison. Our study is limited by the small sample size of the respective subpopulations mitigating validity of our cross-method comparison.

5. Conclusion

To our knowledge, this is the first study to compare multiple probabilistic tractography and TBSS-based approaches to quantify microstructural OR damage in patients with neuroinflammatory visual pathway damage. We proved TBSS-based and probabilistic tractography based DWI processing techniques to be feasible in detecting microstructural damage within the OR. Absolute FA values differed between the methods, preventing comparisons of OR FA analyses of previous and future studies with different post-processing approaches. Correlation and agreement of all methods' FA values were best in patients with suggested mild to moderate OR FA damage (CIS/RRMS patients), indicating methods to be exchangeable - at least to a certain extent - in the analysis of CIS/RRMS patients but not if healthy controls or patients with suspected severe damage (NMOSD-ON) are investigated. Due to systematic bias and proportional errors of FA between methods, the comparison of subject groups by use of different methods leads to different (either false-positive or false-negative) results. Although the pattern of differences between the patient cohorts was similar in our study, CSD-PROB showed significant FA differences between HC and CIS/RRMS-NON patients. Although these CSD-PROB derived differences between the groups could result from the above-mentioned systematic bias, we suggest CSD-PROB to be more sensitive to early neuroinflammatory damage, partially associated with lesions. All methods were successful in differentiating NMOSD-ON patients from HCs. Given that CSD-PROB showed highest AUC and effect size followed by JHU-TBSS, JUEL-TBSS and CON-PROB, CSD-PROB approach might be the method of choice to further investigate differential diagnostic aspects between HC and NMOSD. Tract-profiling differences between HC and NMOSD were more pronounced in CON-PROB, which might be the method of choice for tract profiling assessments. In our study, TBSS-based approaches showed better correlations with OR specific lesions, which could favor them as the method of choice for future studies to investigate the relationship between T2 lesions and DTI. Given the lack of a "gold-standard" for non-invasive DW-MRI OR delineation (Kuchling et al., 2017; Lim et al., 2015; Thomas et al., 2014), future studies are required to fully validate the capacity and limitations of different post-processing methods with regards not only to differential diagnosis and T2 lesional impact on DTI, but also concerning longitudinal FA assessment and OR DTI relationships with visual function.

Supplementary data to this article can be found online at <https://doi.org/10.1016/j.nicl.2018.05.004>.

Acknowledgments

We acknowledge support from the German Research Foundation (DFG) and the Open Access Publication Fund of Charité-Universitätsmedizin Berlin. MR-imaging for this study was performed at the Berlin Center for Advanced Neuroimaging (BCAN).

We thank Susan Pikol, Cynthia Kraut and Karl Bormann for their excellent technical support.

Funding

This work was supported by the BIH-Charité Medical Student Research Program to FCO, and by Deutsche Forschungsgemeinschaft (DFG Exc 257) to FP.

Conflicts of interest

JK received conference registration fees from Biogen and financial research support from Krankheitsbezogenes Kompetenznetzwerk Multiple Sklerose (KKNMS), not related to this work. YB has nothing to disclose. FCO received BIH-Charité Medical Student Research Program funding, not related to this work. NR has nothing to disclose. JBS received travel funding and speaking fees from Bayer Healthcare, Sanofi-Aventis/Genzyme, and Teva Pharmaceuticals. KR received research grants from German Ministry of Education and Research (BMBF/KKNMS, Competence Network Multiple Sclerosis), Novartis, Merck-Serono, and the Charite Research Fund, personal fees from Novartis, Bayer Healthcare, Biogen Idec, Merck Serono, sanofi-aventis/Genzyme, Teva Pharmaceuticals, and from Guthy Jackson Charitable Foundation. FP, NL and AU have nothing to disclose. MS holds a patent for manufacturing of phantoms for computed tomography imaging with 3D printing technology and received research support from Federal Ministry of Economics and Technology.

References

- Andersson, J.L.R., Sotiropoulos, S.N., 2016. An integrated approach to correction for off-resonance effects and subject movement in diffusion MR imaging. *NeuroImage* 125, 1063–1078. <http://dx.doi.org/10.1016/j.neuroimage.2015.10.019>.
- Assaf, Y., Pasternak, O., 2008. Diffusion tensor imaging (DTI)-based white matter mapping in brain research: a review. *J. Mol. Neurosci.* 34, 51–61. <http://dx.doi.org/10.1007/s12031-007-0029-0>.
- Auriat, A.M., Borich, M.R., Snow, N.J., Wadden, K.P., Boyd, L.A., 2015. Comparing a diffusion tensor and non-tensor approach to white matter fiber tractography in chronic stroke. *NeuroImage Clin.* 7, 771–781. <http://dx.doi.org/10.1016/j.nicl.2015.03.007>.
- Backner, Y., Kuchling, J., Massarwa, S., Oberwahrenbrock, T., Finke, C., Bellmann-Strobl, J., Ruprecht, K., Brandt, A.U., Zimmermann, H., Raz, N., Paul, F., Levin, N., 2018. Anatomical wiring and functional networking changes in the visual system following optic neuritis. *JAMA Neurol.* <http://dx.doi.org/10.1001/jamaneurol.2017.3880>.
- Balcer, L.J., Miller, D.H., Reingold, S.C., Cohen, J.A., 2015. Vision and vision-related outcome measures in multiple sclerosis. *Brain* 138, 11–27. <http://dx.doi.org/10.1093/brain/awu335>.
- Bennett, J.L., de Seze, J., Lana-Peixoto, M., Palace, J., Waldman, A., Schippling, S., Tenenbaum, S., Banwell, B., Greenberg, B., Levy, M., et al., 2015. Neuromyelitis optica and multiple sclerosis: Seeing differences through optical coherence tomography. *Mult. Scler. J.* 21 (6), 678–688 (1352458514567216).
- Ciccarelli, O., Catani, M., Johansen-Berg, H., Clark, C., Thompson, A., 2008. Diffusion-based tractography in neurological disorders: concepts, applications, and future developments. *Lancet Neurol.* 7, 715–727. [http://dx.doi.org/10.1016/S1474-4422\(08\)70163-7](http://dx.doi.org/10.1016/S1474-4422(08)70163-7).
- Dasenbrock, H.H., Smith, S.A., Ozturk, A., Farrell, S.K., Calabresi, P.A., Reich, D.S., 2011. Diffusion tensor imaging of the optic tracts in multiple sclerosis: association with retinal thinning and visual disability. *J. Neuroimaging* 21, e41–e49. <http://dx.doi.org/10.1111/j.1552-6569.2010.00468.x>.
- Filippi, M., Absinta, M., Rocca, M.A., 2013. Future MRI tools in multiple sclerosis. *J. Neurol. Sci.* 331, 14–18. <http://dx.doi.org/10.1016/j.jns.2013.04.025>.
- Finke, C., Zimmermann, H., Pache, F., Oertel, F.C., Chavarro, V.S., Kramarenko, Y., Bellmann-Strobl, J., Ruprecht, K., Brandt, A.U., Paul, F., 2018. Association of visual impairment in neuromyelitis optica spectrum disorder with visual network reorganization. *JAMA Neurol.* 75, 296–303. <http://dx.doi.org/10.1001/jamaneurol.2017.3890>.
- Gabilondo, I., Martínez-Lapiscina, E.H., Martínez-Heras, E., Fraga-Pumar, E., Llufríu, S., Ortiz, S., Bullich, S., Sepulveda, M., Falcon, C., Berenguer, J., Saiz, A., Sanchez-Dalmau, B., Villoslada, P., 2014. Trans-synaptic axonal degeneration in the visual

- pathway in multiple sclerosis: axonal degeneration in MS. *Ann. Neurol.* 75, 98–107. <http://dx.doi.org/10.1002/ana.24030>.
- Graham, S.L., Klistorner, A., 2017. Afferent visual pathways in multiple sclerosis: a review. *Clin. Exp. Ophthalmol.* 45, 62–72. <http://dx.doi.org/10.1111/ceo.12751>.
- Hasan, K.M., Walimuni, I.S., Abid, H., Hahn, K.R., 2011. A review of diffusion tensor magnetic resonance imaging computational methods and software tools. *Comput. Biol. Med.* 41, 1062–1072. <http://dx.doi.org/10.1016/j.combiomed.2010.10.008>.
- Hua, K., Zhang, J., Wakana, S., Jiang, H., Li, X., Reich, D.S., Calabresi, P.A., Pekar, J.J., van Zijl, P.C.M., Mori, S., 2008. Tract probability maps in stereotaxic spaces: analyses of white matter anatomy and tract-specific quantification. *NeuroImage* 39, 336–347. <http://dx.doi.org/10.1016/j.neuroimage.2007.07.053>.
- Inglese, M., Bester, M., 2010. Diffusion imaging in multiple sclerosis: research and clinical implications. *NMR Biomed.* 23, 865–872. <http://dx.doi.org/10.1002/nbm.1515>.
- Jarius, S., Wildemann, B., Paul, F., 2014. Neuromyelitis optica: clinical features, immunopathogenesis and treatment. *Clin. Exp. Immunol.* 176, 149–164. <http://dx.doi.org/10.1111/cei.12271>.
- Jenkinson, M., Bannister, P., Brady, M., Smith, S., 2002. Improved optimization for the robust and accurate linear registration and motion correction of brain images. *NeuroImage* 17, 825–841.
- Kamali, A., Hasan, K.M., Adapa, P., Razmandi, A., Keser, Z., Lincoln, J., Kramer, L.A., 2014. Distinguishing and quantification of the human visual pathways using high spatial resolution diffusion tensor tractography. *Magn. Reson. Imaging* 32, 796–803. <http://dx.doi.org/10.1016/j.mri.2014.04.002>.
- Kim, H.J., Paul, F., Lana-Peixoto, M.A., Tenembaum, S., Asgari, N., Palace, J., Klawiter, E.C., Sato, D.K., de Seze, J., Wuerfel, J., et al., 2015. MRI characteristics of neuromyelitis optica spectrum disorder: an international update. *Neurology* 84, 1165–1173.
- Klistorner, A., Sriram, P., Vootakuru, N., Wang, C., Barnett, M.H., Garrick, R., Parratt, J., Levin, N., Raz, N., Van der Walt, A., Masters, L., Graham, S.L., Yiannikas, C., 2014. Axonal loss of retinal neurons in multiple sclerosis associated with optic radiation lesions. *Neurology* 82, 2165–2172. <http://dx.doi.org/10.1212/WNL.0000000000000522>.
- Klistorner, A., Vootakuru, N., Wang, C., Yiannikas, C., Graham, S.L., Parratt, J., Garrick, R., Levin, N., Masters, L., Lagopoulos, J., Barnett, M.H., 2015. Decoding diffusivity in multiple sclerosis: analysis of optic radiation lesion and non-lesional white matter. *PLoS One* 10, e0122114. <http://dx.doi.org/10.1371/journal.pone.0122114>.
- Kolbe, S., van der Walt, A., Butzkueven, H., 2016. Serial diffusion tensor imaging of the optic radiations after acute optic neuritis. *J. Ophthalmol.* 2016, 6.
- Kuchling, J., Brandt, A.U., Paul, F., Scheel, M., 2017. Diffusion tensor imaging for multilevel assessment of the visual pathway: possibilities for personalized outcome prediction in autoimmune disorders of the central nervous system. *EPMA J.* 8, 279–294. <http://dx.doi.org/10.1007/s13167-017-0102-x>.
- Lim, J.C., Phal, P.M., Desmond, P.M., Nichols, A.D., Kokkinos, C., Danesh-Meyer, H.V., Kaye, A.H., Moffat, B.A., 2015. Probabilistic MRI tractography of the optic radiation using constrained spherical deconvolution: a feasibility study. *PLoS One* 10, e0118948. <http://dx.doi.org/10.1371/journal.pone.0118948>.
- Martínez-Heras, E., Varriano, F., Prčková, V., Laredo, C., Andorra, M., Martínez-Lapiscina, E.H., Calvo, A., Lampert, E., Villoslada, P., Saiz, A., Prats-Galino, A., Llufríu, S., 2015. Improved framework for tractography reconstruction of the optic radiation. *PLoS One* 10, e0137064. <http://dx.doi.org/10.1371/journal.pone.0137064>.
- Martínez-Lapiscina, E.H., Sanchez-Dalmau, B., Fraga-Pumar, E., Ortiz-Perez, S., Tercero-Urbe, A.I., Torres-Torres, R., Villoslada, P., 2014. The visual pathway as a model to understand brain damage in multiple sclerosis. *Mult. Scler.* 20, 1678–1685.
- Metz, I., Beißbarth, T., Ellenberger, D., Pache, F., Stork, L., Ringelstein, M., Aktas, O., Jarius, S., Wildemann, B., Dihazi, H., Friede, T., Brück, W., Ruprecht, K., Paul, F., 2016. Serum peptide reactivities may distinguish neuromyelitis optica subgroups and multiple sclerosis. *Neurol. Neuroimmunol. Neuroinflammation* 3, e204. <http://dx.doi.org/10.1212/NXI.0000000000000204>.
- Oertel, F.C., Kuchling, J., Zimmermann, H., Chien, C., Schmidt, F., Knier, B., Bellmann-Strobl, J., Korn, T., Scheel, M., Klistorner, A., Ruprecht, K., Paul, F., Brandt, A.U., 2017. Microstructural visual system changes in AQP4-antibody-seropositive NMO/MS. *Neurol. Neuroimmunol. Neuroinflammation* 4, e334. <http://dx.doi.org/10.1212/NXI.0000000000000334>.
- Pache, F., Zimmermann, H., Mikolajczak, J., Schumacher, S., Lacheta, A., Oertel, F.C., Bellmann-Strobl, J., Jarius, S., Wildemann, B., Reindl, M., Waldman, A., Soelberg, K., Asgari, N., Ringelstein, M., Aktas, O., Gross, N., Buttman, M., Ach, T., Ruprecht, K., Paul, F., Brandt, A.U., in cooperation with the Neuromyelitis Optica Study Group (NEMOS), 2016a. MOG-IgG in NMO and related disorders: a multicenter study of 50 patients. part 4: afferent visual system damage after optic neuritis in MOG-IgG-seropositive versus AQP4-IgG-seropositive patients. *J. Neuroinflammation* 13, 282. <http://dx.doi.org/10.1186/s12974-016-0720-6>.
- Pache, F., Zimmermann, H., Finke, C., Lacheta, A., Papazoglou, S., Kuchling, J., Wuerfel, J., Hamm, B., Ruprecht, K., Paul, F., Brandt, A.U., Scheel, M., 2016b. Brain parenchymal damage in neuromyelitis optica spectrum disorder - a multimodal MRI study. *Eur. Radiol.* 26, 4413–4422. <http://dx.doi.org/10.1007/s00330-016-4282-x>.
- Petzold, A., Wattjes, M.P., Costello, F., Flores-Rivera, J., Fraser, C.L., Fujihara, K., Leavitt, J., Marignier, R., Paul, F., Schippling, S., Sindic, C., Villoslada, P., Weinschenker, B., Plant, G.T., 2014. The investigation of acute optic neuritis: a review and proposed protocol. *Nat. Rev. Neurol.* 10, 447–458. <http://dx.doi.org/10.1038/nrneurol.2014.108>.
- Pfeller, C.F., Paul, F., 2011. Imaging the visual pathway in Neuromyelitis Optica. *Mult. Scler. Int.* 2011, 1–5. <http://dx.doi.org/10.1155/2011/869814>.
- Polman, C.H., Reingold, S.C., Banwell, B., Clanet, M., Cohen, J.A., Filippi, M., Fujihara, K., Havrdova, E., Hutchinson, M., Kappos, L., Lublin, F.D., Montalban, X., O'Connor, P., Sandberg-Wollheim, M., Thompson, A.J., Waubant, E., Weinschenker, B., Wolinsky, J.S., 2011. Diagnostic criteria for multiple sclerosis: 2010 revisions to the McDonald criteria. *Ann. Neurol.* 69, 292–302. <http://dx.doi.org/10.1002/ana.22366>.
- Raz, N., Bick, A.S., Ben-Hur, T., Levin, N., 2015. Focal demyelinating damage and neighboring white matter integrity: an optic neuritis study. *Mult. Scler.* 21, 562–571. <http://dx.doi.org/10.1177/1352458514551452>.
- Reich, D.S., Smith, S.A., Gordon-Lipkin, E.M., Ozturk, A., Caffo, B.S., Balcer, L.J., Calabresi, P.A., 2009. Damage to the optic radiation in multiple sclerosis is associated with retinal injury and visual disability. *Arch. Neurol.* 66. <http://dx.doi.org/10.1001/archneurol.2009.107>.
- Rocca, M.A., Mesaros, S., Preziosa, P., Pagani, E., Stosic-Opincal, T., Dujmovic-Basuroski, L., Druлович, J., Filippi, M., 2013. Wallerian and trans-synaptic degeneration contribute to optic radiation damage in multiple sclerosis: a diffusion tensor MRI study. *Mult. Scler.* 19, 1610–1617.
- Rueda Lopes, F.C., Doring, T., Martins, C., Cabral, F.C., Malfetano, F.R., Pereira, V.C., Alves-Leon, S., Gasparetto, E.L., 2012. The role of demyelination in neuromyelitis optica damage: diffusion-tensor MR imaging study. *Radiology* 263, 235–242.
- Scheel, M., Finke, C., Oberwahrenbrock, T., Freing, A., Pech, L.-M., Schlichting, J., Sömmer, C., Wuerfel, J., Paul, F., Brandt, A.U., 2014. Retinal nerve fibre layer thickness correlates with brain white matter damage in multiple sclerosis: a combined optical coherence tomography and diffusion tensor imaging study. *Mult. Scler. Houndmills Basingstoke Engl.* 20, 1904–1907. <http://dx.doi.org/10.1177/1352458514535128>.
- Schmidt, F., Zimmermann, H., Mikolajczak, J., Oertel, F.C., Pache, F., Weinhold, M., Schinzel, J., Bellmann-Strobl, J., Ruprecht, K., Paul, F., Brandt, A.U., 2017. Severe structural and functional visual system damage leads to profound loss of vision-related quality of life in patients with neuromyelitis optica spectrum disorders. *Mult. Scler. Relat. Disord.* 11, 45–50. <http://dx.doi.org/10.1016/j.msard.2016.11.008>.
- Sherbondy, A.J., Dougherty, R.F., Ben-Shachar, M., Napel, S., Wandell, B.A., 2008a. ConTrack: finding the most likely pathways between brain regions using diffusion tractography. *J. Vis.* 8, 1–16. <http://dx.doi.org/10.1167/8.9.15>.
- Sherbondy, A.J., Dougherty, R.F., Napel, S., Wandell, B.A., 2008b. Identifying the human optic radiation using diffusion imaging and fiber tractography. *J. Vis.* 8, 1–12. <http://dx.doi.org/10.1167/8.10.12>.
- Sinneker, T., Kuchling, J., Dusek, P., Dörr, J., Niendorf, T., Paul, F., Wuerfel, J., 2015a. Ultrahigh field MRI in clinical neuroimmunology: a potential contribution to improved diagnostics and personalised disease management. *EPMA J.* 6 (16). <http://dx.doi.org/10.1186/s13167-015-0038-y>.
- Sinneker, T., Oberwahrenbrock, T., Metz, I., Zimmermann, H., Pfueller, C.F., Harms, L., Ruprecht, K., Ramien, C., Hahn, K., Brück, W., Niendorf, T., Paul, F., Brandt, A.U., Dörr, J., Wuerfel, J., 2015b. Optic radiation damage in multiple sclerosis is associated with visual dysfunction and retinal thinning – an ultrahigh-field MR pilot study. *Eur. Radiol.* 25, 122–131. <http://dx.doi.org/10.1007/s00330-014-3358-8>.
- Smith, S.M., 2002. Fast robust automated brain extraction. *Hum. Brain Mapp.* 17, 143–155. <http://dx.doi.org/10.1002/hbm.10062>.
- Smith, S.M., Jenkinson, M., Woolrich, M.W., Beckmann, C.F., Behrens, T.E.J., Johansen-Berg, H., Bannister, P.R., De Luca, M., Drobnjak, I., Flitney, D.E., Niazy, R.K., Saunders, J., Vickers, J., Zhang, Y., De Stefano, N., Brady, J.M., Matthews, P.M., 2004. Advances in functional and structural MR image analysis and implementation as FSL. *NeuroImage* 23 (Suppl. 1), S208–219. <http://dx.doi.org/10.1016/j.neuroimage.2004.07.051>.
- Smith, S.M., Jenkinson, M., Johansen-Berg, H., Rueckert, D., Nichols, T.E., Mackay, C.E., Watkins, K.E., Ciccarelli, O., Cader, M.Z., Matthews, P.M., Behrens, T.E.J., 2006. Tract-based spatial statistics: Voxelwise analysis of multi-subject diffusion data. *NeuroImage* 31, 1487–1505. <http://dx.doi.org/10.1016/j.neuroimage.2006.02.024>.
- Thomas, C., Ye, F.Q., Irfanoglu, M.O., Modi, P., Saleem, K.S., Leopold, D.A., Pierpaoli, C., 2014. Anatomical accuracy of brain connections derived from diffusion MRI tractography is inherently limited. *Proc. Natl. Acad. Sci. U. S. A.* 111, 16574–16579. <http://dx.doi.org/10.1073/pnas.1405672111>.
- Tian, D.-C., Su, L., Fan, M., Yang, J., Zhang, R., Wen, P., Han, Y., Yu, C., Zhang, C., Ren, H., Shi, K., Zhu, Z., Dong, Y., Liu, Y., Shi, F.-D., 2017. Bidirectional degeneration in the visual pathway in neuromyelitis optica spectrum disorder (NMO/MS). *Mult. Scler. Houndmills Basingstoke Engl.* 1352458517727604. <https://doi.org/10.1177/1352458517727604>.
- Tournier, J.-D., Calamante, F., Gadian, D.G., Connelly, A., 2004. Direct estimation of the fiber orientation density function from diffusion-weighted MRI data using spherical deconvolution. *NeuroImage* 23, 1176–1185. <http://dx.doi.org/10.1016/j.neuroimage.2004.07.037>.
- Tournier, J.-D., Calamante, F., Connelly, A., 2007. Robust determination of the fibre orientation distribution in diffusion MRI: non-negativity constrained super-resolved spherical deconvolution. *NeuroImage* 35, 1459–1472. <http://dx.doi.org/10.1016/j.neuroimage.2007.02.016>.
- Tournier, J.-D., Yeh, C.-H., Calamante, F., Cho, K.-H., Connelly, A., Lin, C.-P., 2008. Resolving crossing fibres using constrained spherical deconvolution: validation using diffusion-weighted imaging phantom data. *NeuroImage* 42, 617–625. <http://dx.doi.org/10.1016/j.neuroimage.2008.05.002>.
- Tur, C., Goodkin, O., Altmann, D.R., Jenkins, T.M., Miszkiewicz, K., Mirigiani, A., Fini, C., Gandini Wheeler-Kingshott, C.A.M., Thompson, A.J., Ciccarelli, O., Toosy, A.T., 2016. Longitudinal evidence for anterograde trans-synaptic degeneration after optic neuritis. *Brain J. Neurol.* 139, 816–828. <http://dx.doi.org/10.1093/brain/awv396>.
- von Glehn, F., Jarius, S., Lira, R.P.C., Ferreira, M.C.A., von Glehn, F.H.R., e Castro, S.M.C., Beltrami, G.C., Bergo, F.P., Farias, A.S., Brandão, C.O., et al., 2014. Structural brain abnormalities are related to retinal nerve fiber layer thinning and disease duration in neuromyelitis optica spectrum disorders. *Mult. Scler. J.* 20, 1189–1197. <http://dx.doi.org/10.1177/1352458513519838>.
- Wakana, S., Caprihan, A., Panzenboeck, M.M., Fallon, J.H., Perry, M., Gollub, R.L., Hua, K., Zhang, J., Jiang, H., Dubey, P., Blitz, A., van Zijl, P., Mori, S., 2007.

- Reproducibility of quantitative tractography methods applied to cerebral white matter. *NeuroImage* 36, 630–644. <http://dx.doi.org/10.1016/j.neuroimage.2007.02.049>.
- Wang, C., Klistorner, A., Ly, L., Barnett, M.H., 2018. White matter tract-specific quantitative analysis in multiple sclerosis: comparison of optic radiation reconstruction techniques. *PLoS One* 13, e0191131. <http://dx.doi.org/10.1371/journal.pone.0191131>.
- Wingerchuk, D.M., Banwell, B., Bennett, J.L., Cabre, P., Carroll, W., Chitnis, T., de Seze, J., Fujihara, K., Greenberg, B., Jacob, A., Jarius, S., Lana-Peixoto, M., Levy, M., Simon, J.H., Tenembaum, S., Traboulsee, A.L., Waters, P., Wellik, K.E., Weinschenker, B.G., 2015. International consensus diagnostic criteria for neuromyelitis optica spectrum disorders. *Neurology* 85, 177–189. <http://dx.doi.org/10.1212/WNL.0000000000001729>.
- Wu, W., Rigolo, L., O'Donnell, L.J., Norton, I., Shriver, S., Golby, A.J., 2012. Visual pathway study using in vivo diffusion tensor imaging tractography to complement classic anatomy. *Neurosurgery* 70, 145–156. discussion 156. <https://doi.org/10.1227/NEU.0b013e31822efcae>.
- Yeatman, J.D., Dougherty, R.F., Myall, N.J., Wandell, B.A., Feldman, H.M., 2012. Tract profiles of white matter properties: automating fiber-tract quantification. *PLoS One* 7. <http://dx.doi.org/10.1371/journal.pone.0049790>.
- Yu, C.S., Lin, F.C., Li, K.C., Jiang, T.Z., Zhu, C.Z., Qin, W., Sun, H., Chan, P., 2006. Diffusion tensor imaging in the assessment of normal-appearing brain tissue damage in relapsing neuromyelitis optica. *Am. J. Neuroradiol.* 27, 1009–1015.
- Yushkevich, P.A., Piven, J., Hazlett, H.C., Smith, R.G., Ho, S., Gee, J.C., Gerig, G., 2006. User-guided 3D active contour segmentation of anatomical structures: significantly improved efficiency and reliability. *NeuroImage* 31, 1116–1128. <http://dx.doi.org/10.1016/j.neuroimage.2006.01.015>.
- Zekeridou, A., Lennon, V.A., 2015. Aquaporin-4 autoimmunity. *Neurol. Neuroimmunol. Neuroinflammation* 2, e110. <http://dx.doi.org/10.1212/NXI.0000000000000110>.

11.3 AQP4-CROSS-SECTIONAL [20]

Frederike C. Oertel*, Joseph Kuchling*, Hanna Zimmermann, Claudia Chien, Felix Schmidt, Benjamin Knier, Judith Bellmann-Strobl, Thomas Korn, Michael Scheel, Alexander Klistorner, Klemens Ruprecht, Friedemann Paul, Alexander U. Brandt:
Microstructural visual system changes in AQP4-antibody seropositive NMOSD.
Neurology: Neuroimmunology & Neuroinflammation, 2017

“Neurology: Neuroimmunology & Neuroinflammation” was not part of the Journal Summary List in 2017.

Microstructural visual system changes in AQP4-antibody-seropositive NMOSD

OPEN

Frederike C. Oertel*
Joseph Kuchling, MD*
Hanna Zimmermann,
MEng
Claudia Chien, MSc
Felix Schmidt, MD
Benjamin Knier, MD
Judith Bellmann-Strobl,
MD
Thomas Korn, MD
Michael Scheel, MD
Alexander Klistorner, MD
Klemens Ruprecht, MD
Friedemann Paul, MD
Alexander U. Brandt, MD

Correspondence to
Dr. Brandt:
alexander.brandt@charite.de

ABSTRACT

Objective: To trace microstructural changes in patients with aquaporin-4 antibody (AQP4-ab)-seropositive neuromyelitis optica spectrum disorders (NMOSDs) by investigating the afferent visual system in patients without clinically overt visual symptoms or visual pathway lesions.

Methods: Of 51 screened patients with NMOSD from a longitudinal observational cohort study, we compared 6 AQP4-ab-seropositive NMOSD patients with longitudinally extensive transverse myelitis (LETM) but no history of optic neuritis (ON) or other bout (NMOSD-LETM) to 19 AQP4-ab-seropositive NMOSD patients with previous ON (NMOSD-ON) and 26 healthy controls (HCs). Foveal thickness (FT), peripapillary retinal nerve fiber layer (pRNFL) thickness, and ganglion cell and inner plexiform layer (GCIPL) thickness were measured with optical coherence tomography (OCT). Microstructural changes in the optic radiation (OR) were investigated using diffusion tensor imaging (DTI). Visual function was determined by high-contrast visual acuity (VA). OCT results were confirmed in a second independent cohort.

Results: FT was reduced in both patients with NMOSD-LETM ($p = 3.52e^{-14}$) and NMOSD-ON ($p = 1.24e^{-16}$) in comparison with HC. Probabilistic tractography showed fractional anisotropy reduction in the OR in patients with NMOSD-LETM ($p = 0.046$) and NMOSD-ON ($p = 1.50e^{-5}$) compared with HC. Only patients with NMOSD-ON but not NMOSD-LETM showed neuroaxonal damage in the form of pRNFL and GCIPL thinning. VA was normal in patients with NMOSD-LETM and was not associated with OCT or DTI parameters.

Conclusions: Patients with AQP4-ab-seropositive NMOSD without a history of ON have microstructural changes in the afferent visual system. The localization of retinal changes around the Müller-cell rich fovea supports a retinal astrocytopathy. *Neurol Neuroimmunol Neuroinflamm* 2017;4:e334; doi: 10.1212/NXI.0000000000000334

GLOSSARY

AD = axial diffusivity; **ART** = automatic real time; **DTI** = diffusion tensor imaging; **FT** = foveal thickness; **GCIPL** = ganglion cell and inner plexiform layer; **GEE** = general estimate equation; **HC** = healthy control; **LETM** = longitudinally extensive transverse myelitis; **LGN** = lateral geniculate nucleus; **LPA** = lesion prediction algorithm; **LST** = Lesion Segmentation Toolbox; **MD** = mean diffusivity; **NMOSD** = neuromyelitis optica spectrum disorder; **OCT** = optical coherence tomography; **ON** = optic neuritis; **OR** = optic radiation; **pRNFL** = peripapillary retinal nerve fiber layer; **RD** = radial diffusivity; **ROI** = region of interest; **VA** = visual acuity.

Neuromyelitis optica spectrum disorders (NMOSDs) are relapsing inflammatory conditions of the CNS presenting with optic neuritis (ON) and longitudinally extensive transverse myelitis (LETM) as key clinical features and less frequently brainstem and cerebral involvement.¹ NMOSD is associated with serum antibodies to the astrocytic water channel aquaporin-4 (AQP4), which can be detected in 60%–80% of patients.^{2,3} The remainder may not only

*These authors contributed equally to this work.

From the NeuroCure Clinical Research Center (F.C.O., J.K., H.Z., C.C., F.S., J.B.-S., M.S., F.P., A.U.B.), and Department of Neurology (J.K., F.S., J.B.-S., K.R., F.P.), Charité—Universitätsmedizin Berlin; Department of Neurology (B.K., T.K.), Klinikum rechts der Isar, and Department of Experimental Neuroimmunology (T.K.), Technische Universität München; Munich Cluster for Systems Neurology (SyNergy) (T.K.), Germany; Clinical Ophthalmology and Eye Health (A.K.), Central Clinical School, Save Sight Institute, Sydney, Australia; and Experimental and Clinical Research Center (F.P.), Max Delbrück Center for Molecular Medicine and Charité—Universitätsmedizin Berlin, Germany.

Funding information and disclosures are provided at the end of the article. Go to Neurology.org/nn for full disclosure forms. The Article Processing Charge was paid by the authors.

This is an open access article distributed under the terms of the Creative Commons Attribution-NonCommercial-NoDerivatives License 4.0 (CC BY-NC-ND), which permits downloading and sharing the work provided it is properly cited. The work cannot be changed in any way or used commercially without permission from the journal.

Table 1 Demographic data of HCs and patients with NMOSD (mean ± SD)

	HC	NMOSD-LETM	NMOSD-ON
Subject, n	26	6	19
Sex, female/male	22/4	6/0	17/2
Age, y	43.6 ± 15.7	43.1 ± 9.83	43.7 ± 12.5
Disease duration, y		3.0 ± 3.7	9.5 ± 8.9
EDSS, median (min-max)		3.5 (1.5-6.5)	4 (0-6)

Abbreviations: EDSS = Expanded Disability Status Scale; HC = healthy control; LETM = longitudinally extensive transverse myelitis; NMOSD = neuromyelitis optica spectrum disorder; NMOSD-LETM = NMOSD patients with a history of LETM but no history of ON; NMOSD-ON = NMOSD patients with a history of ON; ON = optic neuritis.

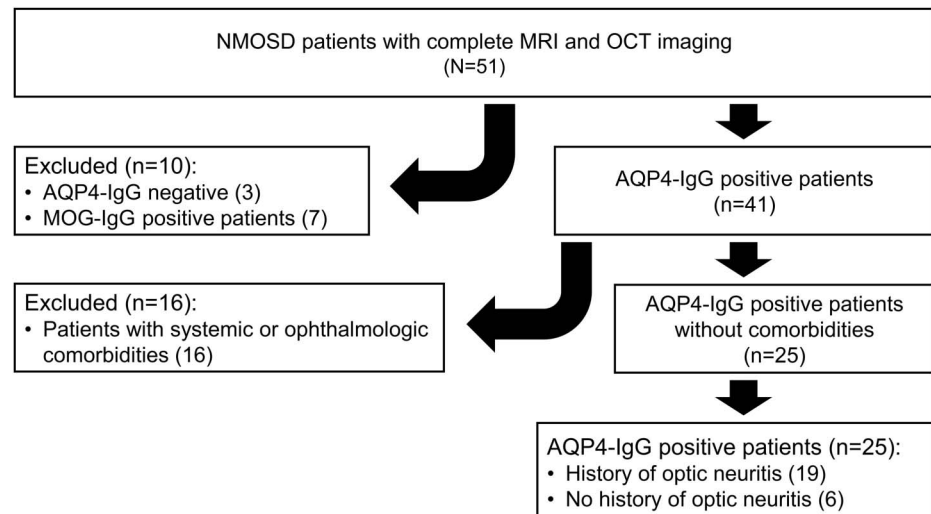
comprise patients with false-negative AQP4-antibody tests but also true AQP4 seronegatives that may harbor other autoantibodies (e.g., myelin oligodendrocyte glycoprotein) and may thus suffer from distinct disease entities.^{4,5}

In contrast to MS, patients with NMOSD virtually never present clinically with progressive disease.⁶ However, advanced imaging and histopathologic studies have shown conflicting results as to whether covert tissue damage can occur independent of attack-associated lesions in patients with NMOSD.⁷⁻⁹ One possible explanation for these discrepancies may be the heterogeneity of previously investigated cohorts comprising both AQP4-antibody (AQP4-ab) positive and negative patients. Also on clinical examination, it may be difficult to identify subtle findings beyond the

overtly affected functional system (i.e., optic nerve or spinal cord).

Against this background, we investigated microstructural and lesion-independent CNS tissue changes in a homogeneous cohort of exclusively AQP4-ab-seropositive NMOSD patients. To exclude any focal attack-related damage, we limited our study to patients who were only presenting with LETM but were otherwise asymptomatic. We used 2 imaging techniques: optical coherence tomography (OCT) to measure retinal thickness and diffusion tensor imaging (DTI)-based probabilistic tractography to analyze the optic radiation (OR).

METHODS Patients. We screened 51 patients with NMOSD participating in an ongoing prospective observational cohort study at the NeuroCure Clinical Research Center at the Charité—Universitätsmedizin Berlin. Six patients with a history of LETM but no other attack (i.e., history of ON) (NMOSD-LETM), 19 NMOSD-ON, and 26 age- and sex-matched healthy controls (HCs) were enrolled (table 1). In a previous study including nineteen (76%) of the 25 patients with NMOSD, normal subcortical gray matter volumes and microstructural changes were found.¹⁰ Inclusion criteria were a minimum age of 18 years and a definite diagnosis of AQP4-ab-seropositive NMOSD according to the 2015 International Consensus Diagnostic Criteria.¹¹ AQP4-ab were determined by a cell-based assay (Euroimmun, Lübeck, Germany). Patients exhibiting ophthalmologic (e.g., glaucoma, myopia >5 dpt) or systemic diseases (e.g., systemic lupus erythematosus), which can potentially influence OCT or DTI results, were excluded from the study (figure 1). Visual function was tested monocularly with habitual correction and under photopic conditions. For high-contrast visual acuity (VA), Early Treatment in Diabetes

Figure 1 Flowchart of cohort selection

AQP4 = aquaporin-4; MOG = myelin oligodendrocyte glycoprotein; NMOSD = neuromyelitis optica spectrum disorder; OCT = optical coherence tomography.

Retinopathy Study charts were used at a 20-ft distance with an Optec 6500 P system (Stereo Optical, Chicago, IL).¹²

We additionally included a confirmatory OCT cohort consisting of 3 patients with AQP4-ab-seropositive NMOSD-LETM (women/men: 3/0; age: 41.3 ± 10.7 years; disease duration: 2.8 ± 2.1 years), 3 patients with AQP4-ab-seropositive NMOSD-ON (women/men: 3/0; age: 44.0 ± 1.0 years; disease duration: 2.9 ± 0.8 years), and 8 HCs (women/men: 8/0; age: 42.3 ± 1.7 years) following the same inclusion and exclusion criteria from a longitudinal prospective observational cohort study at the Department of Neurology, Klinikum rechts der Isar at the Technical University of Munich, Germany.

Ethics statement. The local ethics committee of the Charité—Universitätsmedizin Berlin approved this study (EA1/131/09). OCT data from the confirmatory cohort were collected under an ethics vote from the ethics committee at the Technical University of Munich (166/16S). The study was conducted in accordance with the Declaration of Helsinki in its currently applicable version and the applicable German laws. All patients provided written informed consent.

Optical coherence tomography. All retinal examinations were performed using a Heidelberg Engineering Spectralis spectral domain OCT (Heidelberg Engineering, Heidelberg, Germany) with automatic real-time (ART) function for image averaging. The peripapillary retinal nerve fiber layer (pRNFL) was measured with activated eye tracker using 3.4-mm ring scans around the optic nerve head (12°, 1,536 A-scans 16 ≤ ART ≤ 100). The combined ganglion cell and inner plexiform layer (GCIPL) volume was measured using a 6-mm diameter cylinder around the fovea from a macular volume scan (25° × 30°, 61 vertical B-scans, 768 A-scans per B-scan, ART = 15).¹³ Segmentation of pRNFL and GCIPL was performed semiautomatically using software provided by the OCT manufacturer (Eye Explorer 1.9.10.0 with viewing module 6.0.9.0; Heidelberg Engineering). All measurements were checked for segmentation errors and corrected if necessary by an experienced rater. Foveal thickness (FT) was measured as

the mean thickness of a 1-mm diameter cylinder around the fovea from each collected macular scan. We report our quantitative OCT data in line with the APOSTEL recommendations.¹⁴

Magnet resonance imaging. All MRI data were acquired on the same 3T scanner (MAGNETOM Trio Siemens, Erlangen, Germany) using a single-shot echo planar, DTI sequence (repetition time [TR]/echo time [TE] = 7,500/86 ms; field-of-view [FOV] = 240 × 240 mm²; matrix 96 × 96, slice thickness 2.3 mm, 64 noncollinear directions, b-value = 1,000 s/mm²), as well as a volumetric high-resolution fluid-attenuated inversion recovery sequence (3D FLAIR) (TR/TE/TI = 6,000/388/2,100 ms; FOV = 256 × 256 mm², slice thickness 1.0 mm). 3D FLAIR images of patients with NMOSD-LETM were checked and verified for OR lesions by a board-certified radiologist. Whole-brain segmentation and quantification of lesions of FLAIR images were performed using lesion prediction algorithm in the Lesion Segmentation Toolbox (LST) for MATLAB 2013a (MathWorks, Inc., Natick, MA).¹⁵

Probabilistic tractography. Diffusion tensors on the DTI images were fitted by a linear-least square approach. MRtrix package 0.2 (J-D Tournier; Brain Research Institute, Melbourne, Australia) was used to perform probabilistic tractography from seed to target mask.¹⁶ Fiber orientation distribution was estimated with constrained spherical deconvolution and mapped with a maximum harmonic order of 6. The OR reconstruction pipeline was modified from the Martinez-Heras et al.¹⁷ and Lim et al.¹⁸ pipeline. The Juelich probabilistic atlas was used to generate binary masks of lateral geniculate nucleus (LGN) as the seed region of interest (ROI) and primary visual cortex (V1) as the target ROI. For binary exclusion masks, a midline sagittal exclusion plane, a termination coronal plane 20 mm posterior to the temporal pole, and a gray matter segmentation mask were created in the 3D coordinate system of the Montreal Neurological Institute (MNI-152). These were subsequently registered to individual DTI space, serving as a binary exclusion ROI for tractography. Ten thousand

Table 2 OCT and DTI results from HC and NMOSD subgroups (mean ± SD)

	HCs	NMOSD-LETM	NMOSD-ON	NMOSD-LETM vs HC			NMOSD-ON vs LETM			NMOSD-ON vs HC		
				B	SE	p Value	B	SE	p Value	B	SE	p Value
FT, μm	280 ± 21	260 ± 18	262 ± 18	-20.38	8.233	1.5e ⁻²	0.952	7.890	9.0e ⁻¹	-20.32	5.540	2.4e ⁻⁴
pRNFL, μm	97.1 ± 7.4	105.0 ± 6.9	71.7 ± 22.8	-8.28	2.968	5.3e ⁻³	-33.03	5.066	7.0e ⁻¹¹	-25.6	4.045	2.4e ⁻¹⁰
GCIPL, mm ³	1.87 ± 0.15	1.93 ± 0.11	1.54 ± 0.30	0.061	0.049	2.1e ⁻¹	-0.389	0.071	3.9e ⁻⁸	-0.333	0.062	8.3e ⁻⁸
FA	0.57 ± 0.04	0.54 ± 0.03	0.53 ± 0.04	-0.029	0.015	4.6e ⁻²	-0.014	0.015	3.2e ⁻¹	-0.046	0.011	1.5e ⁻⁵
MD	0.83 ± 0.07	0.90 ± 0.06	0.87 ± 0.05	0.050	0.032	1.2e ⁻¹	-0.020	0.026	4.5e ⁻¹	0.003	0.016	3.7e ⁻²
AD	1.43 ± 0.08	1.49 ± 0.09	1.43 ± 0.06	0.044	0.040	2.7e ⁻¹	-0.048	0.036	1.8e ⁻¹	-0.003	0.020	8.7e ⁻¹
RD	0.53 ± 0.08	0.61 ± 0.06	0.59 ± 0.06	0.054	0.031	8.3e ⁻²	-0.006	0.026	8.2e ⁻¹	0.053	0.018	2.7e ⁻³
Confirmatory cohort												
FT, μm	286 ± 10	257 ± 4	246 ± 4	-27.89	3.72	6.6e ⁻¹⁴	-11.36	2.62	1.4e ⁻⁵	-40.62	4.60	<2.0e ⁻¹⁶
pRNFL, μm	98.2 ± 4.6	114.0 ± 7.2	66.70 ± 14.9	15.68	2.77	1.5e ⁻⁸	-46.51	5.15	<2.0e ⁻¹⁶	-32.04	4.98	1.3e ⁻¹⁰
GCIPL, mm ³	2.04 ± 0.09	2.07 ± 0.07	1.37 ± 0.14	0.04	0.05	5.1e ⁻¹	-0.70	0.05	<2.0e ⁻¹⁶	-0.69	0.03	<2.0e ⁻¹⁶

Abbreviations: AD = axial diffusivity; B = estimate; FA = fractional anisotropy; FT = foveal thickness; GCIPL = ganglion cell and inner plexiform layer volume; HC = healthy control; LETM = longitudinally extensive transverse myelitis; MD = mean diffusivity; NMOSD = neuromyelitis optica spectrum disorder; NMOSD-LETM = NMOSD patients with a history of LETM but no history of ON; NMOSD-ON = NMOSD patients with a history of ON; OCT = optical coherence tomography; ON = optic neuritis; pRNFL = peripapillary retinal nerve fiber layer thickness; RD = radial diffusivity.

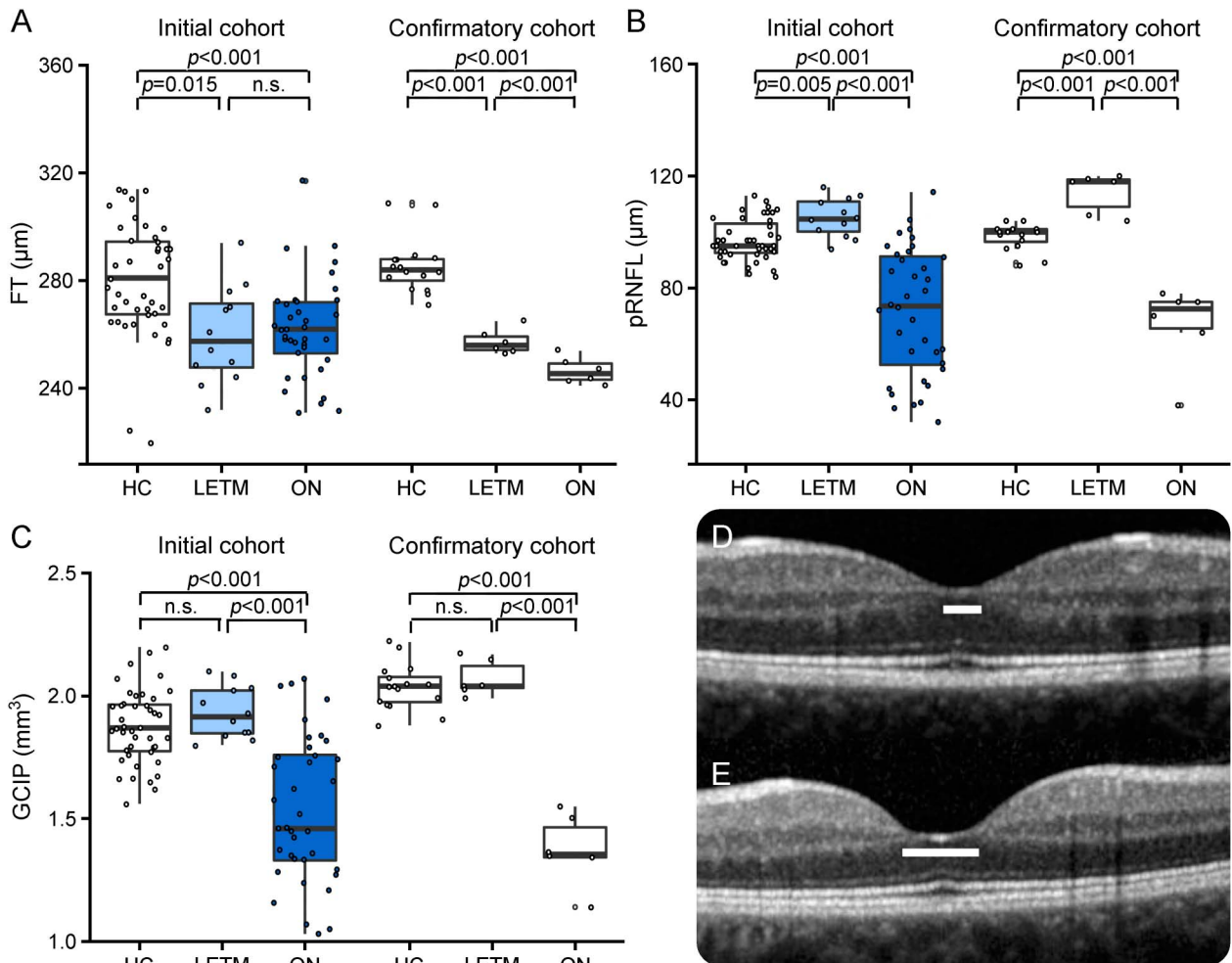
unidirectional streamlines from the LGN to V1 were generated (fractional anisotropy (FA) threshold: 0.1; curvature threshold: 25%; step size: 0.2 mm) for each OR. Streamlines were thresholded for 25% of the maximum value. Resulting fibers were transferred to the Vistalab environment (vistalab.stanford.edu/, Vistalab, Stanford University, Stanford, CA) to compute tract profiles of weighted mean DTI values of FA, mean diffusivity (MD), radial diffusivity (RD), and axial diffusivity at 50 equally spaced positions. We used the middle 30 of the 50 positions for statistical analysis for the exclusion of potential confounders from the LGN to V1 and to have a pure OR volume only.

Statistical analysis. Group differences were tested with a χ^2 test for sex and a Wilcoxon-Mann-Whitney *U* test for age. Group differences in OCT, DTI, and VA were evaluated by general estimate equation (GEE) models accounting for within-subject intereye dependencies and correcting for age and sex. Relationships between structural and functional parameters were analyzed using GEE models and correcting for age and

sex. Combined *p* values of exploratory and confirmatory cohort results were calculated by Fisher combined probability test. All tests were performed with R version 3.1.2 with packages psych, geepack, and ggplot2. Graphical representations were created with R and Graphpad Prism 6.0 (Graphpad Software, San Diego, CA). For all calculations, statistical significance was established at *p* < 0.05.

RESULTS OCT analysis. The fovea is a region rich in AQP4-positive Müller cells, and foveal thinning has previously been reported in eyes from patients with NMOSD without ON.¹⁹ We found that FT in eyes from patients with NMOSD-LETM was lower than that in HC, as was FT in patients with NMOSD-ON patients. Remarkably, FT in eyes from patients with NMOSD-LETM never experiencing visual symptoms was comparable to FT in eyes from patients with NMOSD-ON (table 2 and figure 2).

Figure 2 OCT results



Boxplots of mean OCT values with values of individual eyes (jitter) in HC (left, white), NMOSD-LETM (middle, light blue), NMOSD-ON (right, dark blue), and for each confirmatory cohort (without color) for (A) FT values (μm); (B) pRNFL thickness (μm); (C) GCIP volume (mm^3); (D) FT in a representative macular scan of right eye from an HC; (E) FT changes in a representative macular scan of right eye from a patient with NMOSD-LETM. FT = foveal thickness; GCIP = combined ganglion cell and inner plexiform layer volume; HC = healthy control; LETM = longitudinally extensive transverse myelitis; NMOSD-LETM = NMOSD patients with a history of LETM but no history of ON; NMOSD-ON = NMOSD patients with a history of ON; OCT = optical coherence tomography; ON = optic neuritis; pRNFL = peripapillary retinal nerve fiber layer thickness.

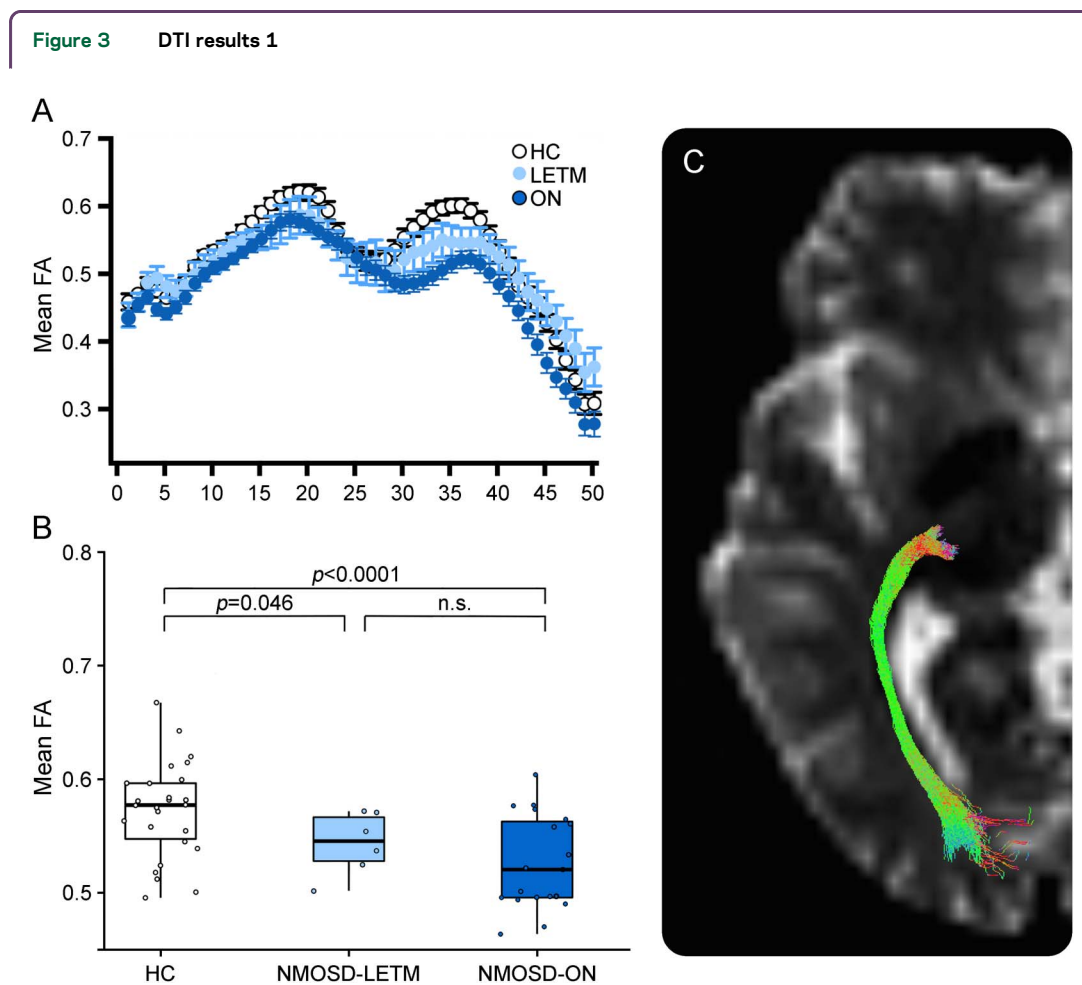
The FT reduction reflected a change in foveal shape, from an open V-shape in eyes from HCs to a wide U-shape in eyes from patients with NMOSD (figure 2, D–E).

In eyes from patients with NMOSD-LETM, pRNFL and GCIPL as markers of retinal neuroaxonal degeneration were not reduced but pRNFL instead increased in comparison with HC (table 1 and figure 2). By contrast and as expected, eyes with previous ON in the NMOSD-ON group presented with severe pRNFL and GCIPL loss, indicating ON-dependent neuroaxonal damage.^{20,21} All OCT results were confirmed in a second independent cohort (figure 2). Statistical combination of *p* values from the initial and confirmatory cohorts produced immense FT and pRNFL differences between NMOSD-LETM and HC (FT $p = 3.52e^{-14}$, pRNFL $p = 1.93e^{-9}$, and GCIPL n.s.) as well as NMOSD-ON and HC (FT $p = 1.24e^{-16}$, pRNFL $p = 1.43e^{-18}$, and GCIPL $p = 8.87e^{-22}$), supporting a high

likelihood of true-positive results, despite the low sample size in either cohort.

MRI analysis. Microstructural white matter changes in the OR were analyzed using DTI-based probabilistic tractography. Patients with NMOSD-LETM presented with FA reduction in comparison with HC ($p = 0.046$), which suggests structural changes in the OR of patients with NMOSD-LETM (table 2 and figures 3 and 4). Patients with NMOSD-ON expectedly showed pathologic changes in comparison with HCs (FA: $p = 1.5e^{-5}$; MD: $p = 0.037$; and RD: $p = 0.003$).

To ascertain that patients with NMOSD-LETM were indeed asymptomatic with respect to their visual system, we analyzed lesion distribution and volume on brain MRI. Whole-brain lesion volume did not differ between NMOSD-ON (0.95 ± 1.23 mL) and NMOSD-LETM (0.95 ± 1.30 mL; $p > 0.999$). Two patients with NMOSD-LETM had



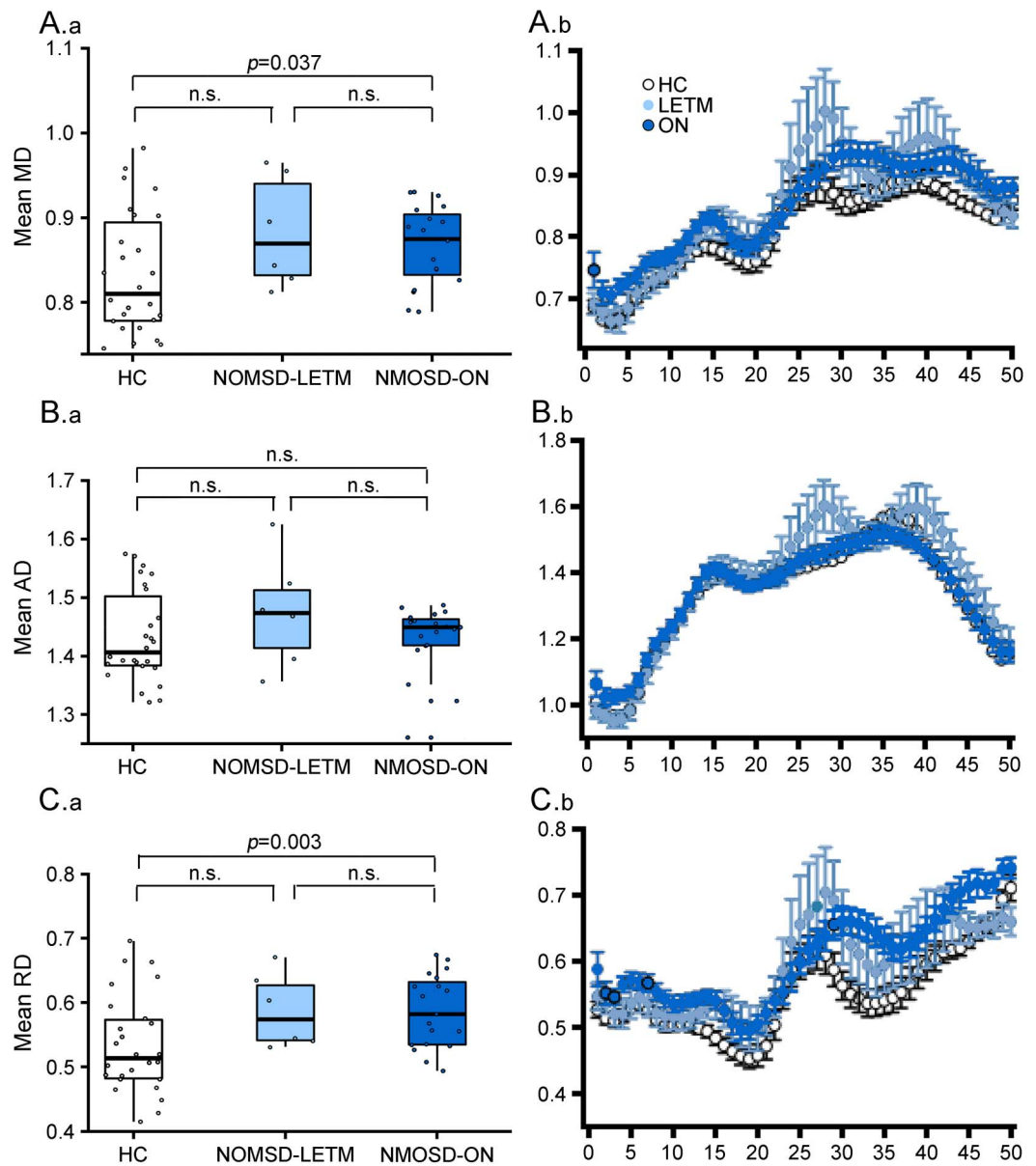
(A) Tract presentation of OR from LGN to V1 for averaged weight-mean DTI values of 50 segments in HC (white), NMOSD-LETM (light blue), and NMOSD-ON (dark blue) for FA (mean \pm SEM). (B) Boxplot of mean FA values for middle 3/5 of the OR in HC (left, white), NMOSD-LETM (middle, light blue), and NMOSD-ON (right, dark blue). (C) Example of resulting fibers from tractography analysis. DTI = diffusion tensor imaging; FA = fractional anisotropy; HC = healthy control; LETM = longitudinally extensive transverse myelitis; LGN = lateral geniculate nucleus; NMOSD = neuromyelitis optica spectrum disorder; NMOSD-LETM = NMOSD patients with a history of LETM but no history of ON; NMOSD-ON = NMOSD patients with a history of ON; ON = optic neuritis; OR = optic radiation; V1 = primary visual cortex.

unspecific small dot-like lesions in the OR unilaterally. All confirmatory patients with NMOSD-LETM presented without any lesions in the OR. In patients with NMOSD-LETM, OR FA did not correlate with FT ($r = 0.066$, $p = 0.800$), pRNFL ($r = -0.204$, $p = 0.500$), or GCIPL ($r = 0.261$, $p = 0.400$), suggesting a structurally independent alteration without dependency on the observed foveal changes or covert retinal neuroaxonal damage. In patients with NMOSD-ON, reduced OR FA correlated with

reduced GCIP ($r = 0.361$, $p = 0.030$), but not with FT ($r = 0.210$, $p = 0.200$).

Functional measurements. VA ([logMAR]: -0.02 ± 0.10) was normal in all patients with NMOSD-LETM. As expected, patients with NMOSD-ON had worse mean VA of all eyes ([logMAR]: 0.22 ± 0.37 ; $p = 0.002$). In patients with NMOSD-LETM and NMOSD-ON, VA did not correlate with FT (NMOSD-LETM: $r = -0.312$, $p = 0.300$;

Figure 4 DTI results 2



(A.a-C.a) Boxplots of mean DTI values for middle 3/5 of the OR and (A.b-C.b) Tract presentation of OR from the LGN to V1 for averaged weight-mean DTI values of 50 segments in HC (white), NMOSD-LETM (light blue), and NMOSD-ON (dark blue) for (A) MD, (B) AD, and (C) RD (mean \pm SEM for all). AD = axial diffusivity; DTI = diffusion tensor imaging; FA = fractional anisotropy; HC = healthy control; LETM = longitudinally extensive transverse myelitis; LGN = lateral geniculate nucleus; MD = mean diffusivity; NMOSD = neuromyelitis optica spectrum disorder; NMOSD-LETM = NMOSD patients with a history of LETM but no history of ON; NMOSD-ON = NMOSD patients with a history of ON; ON = optic neuritis; OR = optic radiation; RD = radial diffusivity; V1 = primary visual cortex.

NMOSD-ON: $r = 0.082$, $p = 0.700$) and OR FA (NMOSD-LETM: VA: $r = -0.445$, $p = 0.100$; NMOSD-ON: $r = 0.073$, $p = 0.700$).

DISCUSSION Patients with AQP4-ab-positive NMOSD without a history of ON and with normal visual function and otherwise normal neuroaxonal retinal measurements (pRNFL, GCIPL) have foveal thinning and reduced OR fractional anisotropy, suggesting microstructural changes in the afferent visual pathway in the absence of clinical attacks of ON.

In NMOSD, 55% of all first clinical events are ONs,²² which in conjunction with subsequent attacks cause damage to the optic nerve with resultant visual impairment.^{20,21,23–25} However, subclinical tissue alterations in NMOSD affecting the afferent visual system have been controversially discussed.^{19–21} For example, while one study reported axonal damage in eyes that never experienced ON,¹⁹ another study did not find any signs of neuroaxonal damage in eyes without ON in patients with NMOSD.²¹

Our study now clearly demonstrates structural retinal and OR changes outside attack-related lesions.²⁶ The parafoveal area is characterized by a high density of retinal astrocytic Müller cells, which express AQP4 and may thus serve as retinal targets in NMOSD.^{19,27–29} Müller cells regulate the retinal water balance and have a relevant role in neurotransmitter and photopigment recycling, as well as in energy and lipid metabolism.²⁷ Müller cell dysfunction or degeneration could thus lead to impaired retinal function including changes in water homeostasis. Of interest, both the initial cohort and the confirmatory cohort showed a mild increase of pRNFL thickness, which could indicate tissue swelling. These findings are supported by animal studies showing retraction of astrocytic end feet in some and astrocyte death in other cases, suggesting a primary astrocytopathy in NMOSD also outside acute lesions.^{30–32} The changes we identified in the OR in this study furthermore indicate that a presumptive astrocytopathy may not be confined to the retina.^{10,23,25} This is in line with astrocytic end feet changes reported in biopsies from LETM spinal cord lesions and spinal cord atrophy in AQP4-ab-positive patients without previous myelitis.^{9,33} Whether these changes lead to subtle clinical manifestations should be further investigated using more sensitive functional measures such as visual evoked potentials or low-contrast VA. If confirmed, this would be in line with a preferential affection of the visual system, even without apparent clinical symptoms in NMOSD.

Reduction of FT in patients with NMOSD without overt clinical evidence of optic nerve involvement (normal VA, normal pRNFL, and GCIPL values) was

comparable with that of patients with previous ON. To assure that we were only detecting AQP4-ab-associated pathologies, we rigorously excluded potential confounders. Most importantly, we only included a homogeneous group of AQP4-ab-seropositive patients who are expected to display a well-defined astrocytopathy phenotype.³⁴ Patients were only eligible if they presented with LETM and no history of ON, visual symptoms, or other typical NMOSD-associated bouts. Since our patients with NMOSD-LETM did not show pRNFL and GCIPL thinning, a previous subclinical ON is highly unlikely. However, a potential pRNFL swelling might have masked a mild subclinical neurodegeneration, but the effects would likely be small and would not be able to explain the observed changes, which are comparable to eyes after severe ON.²¹ In light of a recent animal study,³² it is conceivable that AQP4-specific T cells also contribute to foveal astrocytopathy. However, disease-independent factors in NMOSD, such as prematurity and environmental conditions,³⁵ may also play a role in foveal thinning.

Previous studies investigating retinal changes in patients with NMOSD regularly included measurements from unaffected fellow eyes from patients with unilateral ON. This is problematic since ON in NMOSD often involves the optic chiasm, and carry-over effects by chiasmic involvement of symptomatically unilateral ON have been reported in up to 64% of patients with AQP4-ab-positive NMOSD.²² This sets our study apart from a previous study reporting FT reduction in eyes without previous ON in a cohort of patients with NMOSD, which could have been alternatively explained by both non-AQP4 pathologies and chiasmic carry-over effects.¹⁹ Furthermore, none of the patients with NMOSD-LETM had NMOSD-related attacks other than LETM, minimizing the potential of attack- or lesion-related tissue alteration as the cause of the observed changes. Attack-related tissue alteration could have been the case in a recent study reporting spinal cord atrophy in AQP4-ab-positive NMOSD patients with ON.⁹ Of interest, despite all patients in the NMOSD-LETM group reporting and showing no symptoms of visual dysfunction, a few patients showed small lesions near the OR. Measurements from these patients were not outliers but well positioned within the data distribution of the whole cohort (not shown).

One important limitation of our study, which we share with the majority of other studies published in NMOSD, is the small sample size. We were able to confirm our results, however, in a second independent cohort. Furthermore, our study cannot answer whether the reported changes are attack related or attack independent (e.g., due to circulating

antibodies). That at least some occult changes might be caused during acute attacks was suggested by a study reporting a correlation of brain volumes and perfusion change with the number of ON attacks in patients with NMOSD.³⁶

We found microstructural changes in the afferent visual system in visually asymptomatic patients with AQP4-ab–positive NMOSD-LETM, which were most apparent in the fovea, a region rich in AQP-expressing Müller cells. Localization and extent of these changes are suggestive of an astrocytopathy without apparent neuroaxonal damage. Identifying occult brain changes in patients with NMOSD is important for a number of reasons. These occult changes could be relevant for symptoms that are not directly related to attacks, e.g., cognitive dysfunction, fatigue, and depression^{37–39} and could predispose to full attacks causing severe astrocytic damage, demyelination, and neuroaxonal damage. As such, occult CNS including retinal changes in NMOSD may be an important diagnostic and target. Retinal imaging of NMOSD-specific changes could aid in early differential diagnosis of NMOSD and help to identify patients in need of an NMOSD-specific therapy. Although highly specific, antibody testing takes too much time during an initial attack of a de novo NMOSD patient, making acute attack-related therapeutic diversification currently difficult. Future research should thus focus on the sensitivity and specificity of the retinal findings in NMOSD also in contrast to relevant differential diagnoses such as myelin oligodendrocyte glycoprotein antibody (MOG-ab)-associated encephalomyelopathy or MS.⁴⁰ Finally, retinal assessment could aid as therapy response marker during novel drug development.

AUTHOR CONTRIBUTIONS

F.C.O. and J.K.: data collection and analysis. F.C.O.: writing of the manuscript. H.Z.: OCT and data analysis. C.C.: lesion segmentation and data analysis. F.S. and J.B.-S.: study coordination and data acquisition. B.K. and T.K.: data collection and analysis. M.S.: data analysis, lesion segmentation, and tractography. A.K.: tractography. K.R. and F.P.: study coordination. A.U.B.: study concept, design, coordination, data analysis, and writing of the manuscript. All authors revised the manuscript for intellectual content and read and approved the final manuscript.

ACKNOWLEDGMENT

The authors thank Janine Mikolajczak, Charlotte Kiepert, Susan Pikol, Cynthia Kraut, and Karl Bormann for their excellent technical support.

STUDY FUNDING

This study was funded by research support from the German Research Foundation (DFG Exc. 257 to F.P.), the German Federal Ministry of Economic Affairs and Energy (EXIST 03EFEBE079 to A.U.B. and M.S.) and the Guthy Jackson Charitable Foundation.

DISCLOSURE

F. Oertel reports no disclosures. J. Kuchling received congress registration fee from Biogen and research support from Krankheitsbezogenes Kompetenznetz Multiple Sklerose. H. Zimmermann received speaker honoraria from Teva and Bayer. C. Chien reports no disclosures. F. Schmidt received speaker honoraria from Genzyme. B. Knier received travel funding from

Bayer, Merck Serono, ECTRIMS, and Neurowind; and received research support from Kompetenznetz Multiple Sklerose, Bundesministerium für Bildung und Forschung, Kommission für Klinische Forschung, and Technical University of Munich. J. Bellman-Strobl received travel funding and speaking fees from Bayer Healthcare, Sanofi-Aventis/Genzyme, and Teva Pharmaceuticals. T. Korn served on the scientific advisory board for German MS Society, Merck Serono, Novartis, and Biogen; received travel funding and/or speaker honoraria from Biogen, Novartis, Merck Serono, and Bayer; and received research support from Biogen, German Research Council, German Ministry of Education and Research, European Research Council, and Else-Kroner-Fresenius Foundation. M. Scheel holds a patent for manufacturing of phantoms for computed tomography imaging with 3D printing technology and received research support from Federal Ministry of Economics and Technology. A. Klitschner holds patents for Electrophysiological visual field measurement, Method and apparatus for objective electrophysiological assessment of visual function, Stimulus method for multifocal visual evoked potential, Flexible electrode assembly and apparatus for measuring electrophysiological signals, Apparatus for measuring electrophysiological signals, and Flexible printed circuit board electrode assembly; and received research support from Sydney University Foundation for Medical Research and Sydney Eye Hospital Foundation. K. Ruprecht served on the scientific advisory board for Sanofi-Aventis/Genzyme, Novartis, and Roche; received travel funding and/or speaker honoraria from Bayer Healthcare, Biogen Idec, Merck Serono, Sanofi-Aventis/Genzyme, Teva Pharmaceuticals, Novartis, and Guthy Jackson Charitable Foundation; is an academic editor for *PLoS ONE*; receives publishing royalties from Elsevier; and received research support from Novartis and German Ministry of Education and Research. F. Paul serves on the scientific advisory board for Novartis; received speaker honoraria and travel funding from Bayer, Novartis, Biogen Idec, Teva, Sanofi-Aventis/Genzyme, Merck Serono, Alexion, Chugai, MedImmune, and Shire; is an academic editor for *PLoS ONE*; is an associate editor for *Neurology*, *Neuroimmunology & Neuroinflammation*; consulted for Sanofi/Genzyme, Biogen Idec, MedImmune, Shire, and Alexion; and received research support from Bayer, Novartis, Biogen Idec, Teva, Sanofi-Aventis/Genzyme, Alexion, Merck Serono, German Research Council, Werth Stiftung of the City of Cologne, German Ministry of Education and Research, Arthur Arnstein Stiftung Berlin, EU FP7 Framework Program, Arthur Arnstein Foundation Berlin, Guthy Jackson Charitable Foundation, and National Multiple Sclerosis of the USA. A.U. Brandt served on the scientific advisory board for Biogen; received travel funding and/or speaker honoraria from Novartis and Biogen; has patents pending from method and system for optic nerve head shape quantification, perceptive visual computing based postural control analysis, multiple sclerosis biomarker, and perceptive sleep motion analysis; has consulted for Nexus and Motognosis; and received research support from Novartis Pharma, Biogen Idec, BMWi, BMBF, and Guthy Jackson Charitable Foundation. Go to Neurology.org/nn for full disclosure forms.

Received December 1, 2016. Accepted in final form January 10, 2017.

REFERENCES

1. Jarius S, Wildemann B, Paul F. Neuromyelitis optica: clinical features, immunopathogenesis and treatment. *Clin Exp Immunol* 2014;176:149–164.
2. Metz I, Beißbarth T, Ellenberger D, et al. Serum peptide reactivities may distinguish neuromyelitis optica subgroups and multiple sclerosis. *Neurol Neuroimmunol Neuroinflamm* 2016;3:e204. doi: 10.1212/NXI.0000000000000204.
3. Zekeridou A, Lennon VA. Aquaporin-4 autoimmunity. *Neurol Neuroimmunol Neuroinflamm* 2015;2:e110. doi: 10.1212/NXI.0000000000000110.
4. Waters P, Reindl M, Saiz A, et al. Multicentre comparison of a diagnostic assay: aquaporin-4 antibodies in neuromyelitis optica. *J Neurol Neurosurg Psychiatry* 2016;87:1005–1015.
5. Zamvil SS, Slavin AJ. Does MOG Ig-positive AQP4-seronegative opticospinal inflammatory disease justify a diagnosis of NMO spectrum disorder? *Neurol*

- Neuroimmunol Neuroinflamm 2015;2:e62. doi: 10.1212/NXI.0000000000000062.
6. Wingerchuk DM, Pittock SJ, Lucchinetti CF, Lennon VA, Weinshenker BG. A secondary progressive clinical course is uncommon in neuromyelitis optica. *Neurology* 2007;68:603–605.
 7. Kremer S, Renard F, Achard S, et al. Use of advanced magnetic resonance imaging techniques in neuromyelitis optica spectrum disorder. *JAMA Neurol* 2015;72:815–822.
 8. Lucchinetti CF, Guo Y, Popescu BFG, Fujihara K, Itoyama Y, Misu T. The pathology of an autoimmune astrocytopathy: lessons learned from neuromyelitis optica. *Brain Pathol* 2014;24:83–97.
 9. Ventura RE, Kister I, Chung S, Babb JS, Shepherd TM. Cervical spinal cord atrophy in NMOSD without a history of myelitis or MRI-visible lesions. *Neurol Neuroimmunol Neuroinflamm* 2016;3:e224. doi: 10.1212/NXI.0000000000000224.
 10. Finke C, Heine J, Pache F, et al. Normal volumes and microstructural integrity of deep gray matter structures in AQP4+ NMOSD. *Neurol Neuroimmunol Neuroinflamm* 2016;3:e229. doi: 10.1212/NXI.0000000000000229.
 11. Wingerchuk DM, Banwell B, Bennett JL, et al. International consensus diagnostic criteria for neuromyelitis optica spectrum disorders. *Neurology* 2015;85:177–189.
 12. Bock M, Brandt AU, Kuchenbecker J, et al. Impairment of contrast visual acuity as a functional correlate of retinal nerve fibre layer thinning and total macular volume reduction in multiple sclerosis. *Br J Ophthalmol* 2012;96:62–67.
 13. Oberwahrenbrock T, Weinhold M, Mikolajczak J, et al. Reliability of intra-retinal layer thickness estimates. *PLoS One* 2015;10:e0137316.
 14. Cruz-Herranz A, Balk LJ, Oberwahrenbrock T, et al. The APOSTEL recommendations for reporting quantitative optical coherence tomography studies. *Neurology* 2016; 86:2303–2309.
 15. Schmidt P, Gaser C, Arsic M, et al. An automated tool for detection of FLAIR-hyperintense white-matter lesions in multiple sclerosis. *Neuroimage* 2012;59:3774–3783.
 16. Tournier JD, Calamante F, Connelly A. Robust determination of the fibre orientation distribution in diffusion MRI: non-negativity constrained super-resolved spherical deconvolution. *Neuroimage* 2007;35:1459–1472.
 17. Martínez-Heras E, Varriano F, Prčková V, et al. Improved framework for tractography reconstruction of the optic radiation. *PLoS One* 2015;10:e0137064.
 18. Lim JC, Phal PM, Desmond PM, et al. Probabilistic MRI tractography of the optic radiation using constrained spherical deconvolution: a feasibility study. *PLoS One* 2015;10:e0118948.
 19. Jeong IH, Kim HJ, Kim NH, Jeong KS, Park CY. Sub-clinical primary retinal pathology in neuromyelitis optica spectrum disorder. *J Neurol* 2016;263:1343–1348.
 20. Syc SB, Saidha S, Newsome SD, et al. Optical coherence tomography segmentation reveals ganglion cell layer pathology after optic neuritis. *Brain* 2012;135:521–533.
 21. Schneider E, Zimmermann H, Oberwahrenbrock T, et al. Optical coherence tomography reveals distinct patterns of retinal damage in neuromyelitis optica and multiple sclerosis. *PLoS One* 2013;8:e66151.
 22. Ramanathan S, Prelog K, Barnes EH, et al. Radiological differentiation of optic neuritis with myelin oligodendrocyte glycoprotein antibodies, aquaporin-4 antibodies, and multiple sclerosis. *Mult Scler J* 2016;22:470–482.
 23. Pache F, Zimmermann H, Finke C, et al. Brain parenchymal damage in neuromyelitis optica spectrum disorder: a multi-modal MRI study. *Eur Radiol* 2016;26:4413–4422.
 24. Rueda Lopes FC, Doring T, Martins C, et al. The role of demyelination in neuromyelitis optica damage: diffusion-tensor MR imaging study. *Radiology* 2012;263:235–242.
 25. Zhao DD, Zhou HY, Wu QZ, et al. Diffusion tensor imaging characterization of occult brain damage in relapsing neuromyelitis optica using 3.0T magnetic resonance imaging techniques. *Neuroimage* 2012;59:3173–3177.
 26. Kim HJ, Paul F, Lana-Peixoto MA, et al. MRI characteristics of neuromyelitis optica spectrum disorder: an international update. *Neurology* 2015;84:1165–1173.
 27. Reichenbach A, Bringmann A. *Müller Cells in the Healthy and Diseased Retina*. New York: Springer; 2010.
 28. Nicchia GP, Pisani F, Simone L, et al. Glio-vascular modifications caused by Aquaporin-4 deletion in the mouse retina. *Exp Eye Res* 2016;146:259–268.
 29. Felix CM, Levin MH, Verkman AS. Complement-independent retinal pathology produced by intravitreal injection of neuromyelitis optica immunoglobulin G. *J Neuroinflammation* 2016;13:275.
 30. Kurosawa K, Misu T, Takai Y, et al. Severely exacerbated neuromyelitis optica rat model with extensive astrocytopathy by high affinity anti-aquaporin-4 monoclonal antibody. *Acta Neuropathol Commun* 2015;3:82.
 31. Misu T, Fujihara K, Kakita A, et al. Loss of aquaporin 4 in lesions of neuromyelitis optica: distinction from multiple sclerosis. *Brain* 2007;130:1224–1234.
 32. Zeka B, Hastermann M, Kaufmann N, et al. Aquaporin 4-specific T cells and NMO-IgG cause primary retinal damage in experimental NMO/SD. *Acta Neuropathol Commun* 2016;4:82.
 33. Hayashida S, Masaki K, Yonekawa T, et al. Early and extensive spinal white matter involvement in neuromyelitis optica. *Brain Pathol Epub* 2016 Apr 15.
 34. Hinson SR, Pittock SJ, Lucchinetti CF, et al. Pathogenic potential of IgG binding to water channel extracellular domain in neuromyelitis optica. *Neurology* 2007;69: 2221–2231.
 35. Provis JM, Dubis AM, Maddess T, Carroll J. Adaptation of the central retina for high acuity vision: cones, the fovea and the avascular zone. *Prog Retin Eye Res* 2013;35:63–81.
 36. Sánchez-Catasús CA, Cabrera-Gomez J, Almaguer Melián W, et al. Brain tissue volumes and perfusion change with the number of optic neuritis attacks in relapsing neuromyelitis optica: a voxel-based correlation study. *PLoS One* 2013;8:e66271.
 37. Liu Y, Duan Y, He Y, et al. A tract-based diffusion study of cerebral white matter in neuromyelitis optica reveals widespread pathological alterations. *Mult Scler J* 2012; 18:1013–1021.
 38. Finke C, Schlichting J, Papazoglou S, et al. Altered basal ganglia functional connectivity in multiple sclerosis patients with fatigue. *Mult Scler J* 2015;21:925–934.
 39. Chavarro VS, Mealy MA, Simpson A, et al. Insufficient treatment of severe depression in neuromyelitis optica spectrum disorder. *Neurol Neuroimmunol Neuroinflamm* 2016;3:e286. doi: 10.1212/NXI.0000000000000286.
 40. Pache F, Zimmermann H, Mikolajczak J, et al. MOG-IgG in NMO and related disorders: a multicenter study of 50 patients: part 4: afferent visual system damage after optic neuritis in MOG-IgG-seropositive versus AQP4-IgG-seropositive patients. *J Neuroinflammation* 2016;13:282.

11.4 AQP4-LONGITUDINAL [21]

Frederike C Oertel*, Joachim Havla*, Adriana Roca-Fernández, Nathaniel Lizak, Hanna Zimmermann, Seyedamirhosein Motamedi, Nadja Borisow, Owen White, Judith Bellmann-Strobl, Philipp Albrecht, Klemens Ruprecht, Sven Jarius, Jacqueline Palace, Maria Leite, Tania Kümpfel, Friedemann Paul, Alexander U Brandt: *Retinal Ganglion Cell Loss in Neuromyelitis Optica: A Longitudinal Study*. Journal of Neurology, Neurosurgery and Psychiatry, 2018

<http://dx.doi.org/10.1136/jnnp-2018-318382>

Journal Data Filtered By: **Selected JCR Year: 2018** Selected Editions: SCIE,SSCI
 Selected Categories: **"CLINICAL NEUROLOGY"** Selected Category
 Scheme: WoS

Gesamtanzahl: 199 Journale

Rank	Full Journal Title	Total Cites	Journal Impact Factor	Eigenfactor Score
1	LANCET NEUROLOGY	30,748	28.755	0.069460
2	Nature Reviews Neurology	9,548	21.155	0.031060
3	ACTA NEUROPATHOLOGICA	20,206	18.174	0.041660
4	Alzheimers & Dementia	13,341	14.423	0.036340
5	JAMA Neurology	8,683	12.321	0.042040
6	BRAIN	52,970	11.814	0.074030
7	SLEEP MEDICINE REVIEWS	6,920	10.517	0.010920
8	NEURO-ONCOLOGY	11,858	10.091	0.029150
9	ANNALS OF NEUROLOGY	37,336	9.496	0.048630
10	NEUROLOGY	89,258	8.689	0.115200
11	JOURNAL OF NEUROLOGY NEUROSURGERY AND PSYCHIATRY	29,660	8.272	0.030730
12	MOVEMENT DISORDERS	26,964	8.061	0.037650
13	Neurology-Neuroimmunology & Neuroinflammation	1,996	7.353	0.008220
14	Brain Stimulation	5,457	6.919	0.014470
15	Epilepsy Currents	799	6.909	0.001560
16	NEUROPATHOLOGY AND APPLIED NEUROBIOLOGY	3,876	6.878	0.006420
17	NEUROSCIENTIST	4,986	6.791	0.008520
18	BRAIN PATHOLOGY	5,263	6.155	0.007880
19	Alzheimers Research & Therapy	3,160	6.142	0.010700
20	STROKE	64,814	6.046	0.082630

11.5 MOG-CROSS-SECTIONAL [22]

Florence Pache*, Hanna Zimmermann*, Janine Mikolajczak, Sophie Schumacher, Anna Lacheta, **Frederike C Oertel**, Judith Bellmann-Strobel, Sven Jarius, Brigitte Wildemann, Markus Reindl, Amy Waldman, Kerstin Soelberg, Nasrin Asgari, Marius Ringelstein, Orhan Aktas, Nikolai Gross, Mathias Buttmann, Thomas Ach, Klemens Ruprecht, Friedemann Paul, Alexander U Brandt, **MOG-IgG in NMO and related disorders: a multicenter study of 50 patients. Part 4: Afferent visual system damage after optic neuritis in MOG-IgG-seropositive versus AQP4-IgG-seropositive patients**, Journal of Neuroinflammation, 2016.

Journal Data Filtered By: **Selected JCR Year: 2016** Selected Editions: SCIE,SSCI
 Selected Categories: **“NEUROSCIENCES”** Selected Category Scheme: WoS
Gesamtanzahl: 258 Journale

Rank	Full Journal Title	Total Cites	Journal Impact Factor	Eigenfactor Score
1	NATURE REVIEWS NEUROSCIENCE	36,952	28.880	0.071380
2	NATURE NEUROSCIENCE	54,399	17.839	0.160740
3	Annual Review of Neuroscience	13,211	15.630	0.020660
4	TRENDS IN COGNITIVE SCIENCES	23,273	15.402	0.046360
5	BEHAVIORAL AND BRAIN SCIENCES	8,195	14.200	0.010940
6	NEURON	82,253	14.024	0.227070
7	PROGRESS IN NEUROBIOLOGY	12,163	13.217	0.018020
8	MOLECULAR PSYCHIATRY	17,452	13.204	0.049670
9	ACTA NEUROPATHOLOGICA	16,462	12.213	0.037060
10	BIOLOGICAL PSYCHIATRY	41,859	11.412	0.067400
11	TRENDS IN NEUROSCIENCES	19,178	11.124	0.029690
12	JOURNAL OF PINEAL RESEARCH	7,278	10.391	0.008040
13	BRAIN	48,061	10.292	0.077590
14	ANNALS OF NEUROLOGY	34,215	9.890	0.057310
15	FRONTIERS IN NEUROENDOCRINOLOGY	3,516	9.425	0.006600
16	SLEEP MEDICINE REVIEWS	4,980	8.958	0.009730
17	NEUROSCIENCE AND BIOBEHAVIORAL REVIEWS	20,452	8.299	0.047230
18	NEUROSCIENTIST	4,325	7.391	0.009890
19	Molecular Neurodegeneration	2,946	6.780	0.009540
20	CEREBRAL CORTEX	27,496	6.559	0.063240
21	NEUROPSYCHOPHARMACOLOGY	23,920	6.403	0.046670
22	NEUROPSYCHOLOGY REVIEW	2,478	6.352	0.004650
23	GLIA	12,781	6.200	0.021920
24	Alzheimers Research & Therapy	1,699	6.196	0.007180
25	MOLECULAR NEUROBIOLOGY	7,338	6.190	0.017440
26	NEURO SIGNALS	653	6.143	0.000670
27	CURRENT OPINION IN NEUROBIOLOGY	13,188	6.133	0.036730
28	Brain Stimulation	3,905	6.078	0.013020
29	JOURNAL OF NEUROSCIENCE	171,800	5.988	0.319910
30	BRAIN BEHAVIOR AND IMMUNITY	10,719	5.964	0.026460
31	NEUROIMAGE	85,630	5.835	0.173210
32	PAIN	35,333	5.445	0.044460
33	NEUROPATHOLOGY AND APPLIED NEUROBIOLOGY	3,413	5.347	0.006400
34	NEURAL NETWORKS	8,741	5.287	0.010250
35	BRAIN PATHOLOGY	4,580	5.272	0.008450
36	JOURNAL OF NEUROTRAUMA	12,787	5.190	0.021640
37	Neurotherapeutics	3,451	5.166	0.008220
38	JOURNAL OF PSYCHIATRY & NEUROSCIENCE	2,759	5.165	0.004970
39	NEUROBIOLOGY OF AGING	20,010	5.117	0.046250

Rank	Full Journal Title	Total Cites	Journal Impact Factor	Eigenfactor Score
40	Journal of Neuroinflammation	7,946	5.102	0.023970
41	JOURNAL OF CEREBRAL BLOOD FLOW AND METABOLISM	16,998	5.081	0.029520
42	Frontiers in Molecular Neuroscience	1,979	5.076	0.008520
43	NEUROBIOLOGY OF DISEASE	14,554	5.020	0.031140
44	NEUROPHARMACOLOGY	18,559	5.012	0.040280
45	SLEEP	18,127	4.923	0.026090
46	Multiple Sclerosis Journal	9,727	4.840	0.023240
47	Molecular Autism	1,294	4.833	0.006320
48	PSYCHONEUROENDOCRINOLOGY	14,409	4.788	0.028830
49	Neuropsychiatry	149	4.778	0.000740
50	JOURNAL OF PHYSIOLOGY-LONDON	48,567	4.739	0.047830
51	INTERNATIONAL JOURNAL OF NEUROPSYCHOPHARMACOLOGY	6,082	4.712	0.015310
52	EXPERIMENTAL NEUROLOGY	19,445	4.706	0.027440
53	CURRENT OPINION IN NEUROLOGY	5,258	4.699	0.011490
54	Brain Structure & Function	4,325	4.698	0.014300
55	Frontiers in Cellular Neuroscience	6,088	4.555	0.027500
56	BIPOLAR DISORDERS	5,323	4.531	0.009660
57	HUMAN BRAIN MAPPING	18,139	4.530	0.041900
58	JOURNAL OF PAIN	8,312	4.519	0.018540
59	Frontiers in Aging Neuroscience	3,477	4.504	0.013020
60	Developmental Cognitive Neuroscience	1,483	4.321	0.007490
61	CORTEX	8,200	4.279	0.021370
62	EUROPEAN NEUROPSYCHOPHARMACOLOGY	6,575	4.239	0.015920
63	PROGRESS IN NEUROPSYCHOPHARMACOLOGY & BIOLOGICAL PSYCHIATRY	9,740	4.187	0.016310
64	JOURNAL OF PSYCHOPHARMACOLOGY	5,518	4.179	0.012020
65	JOURNAL OF NEUROCHEMISTRY	35,279	4.083	0.030170
66	EUROPEAN JOURNAL OF NEUROLOGY	9,137	3.988	0.018850
67	Dialogues in Clinical Neuroscience	2,348	3.976	0.005480
68	HIPPOCAMPUS	8,694	3.945	0.016170
69	Social Cognitive and Affective Neuroscience	5,263	3.937	0.020160
70	CNS Neuroscience & Therapeutics	2,615	3.919	0.007370
71	Annals of Clinical and Translational Neurology	902	3.901	0.004880
72	ACS Chemical Neuroscience	3,084	3.883	0.011020
73	Frontiers in Neuroinformatics	1,377	3.870	0.006310
74	CLINICAL NEUROPHYSIOLOGY	17,871	3.866	0.021920
75	NUTRITIONAL NEUROSCIENCE	1,192	3.765	0.001900
76	GENES BRAIN AND BEHAVIOR	3,385	3.743	0.006820
77	JOURNAL OF ALZHEIMERS DISEASE	14,542	3.731	0.036370

RESEARCH

Open Access



MOG-IgG in NMO and related disorders: a multicenter study of 50 patients. Part 4: Afferent visual system damage after optic neuritis in MOG-IgG-seropositive versus AQP4-IgG-seropositive patients

Florence Pache^{1,2†}, Hanna Zimmermann^{1,2†}, Janine Mikolajczak¹, Sophie Schumacher¹, Anna Lacheta¹, Frederike C. Oertel¹, Judith Bellmann-Strobl^{1,12}, Sven Jarius³, Brigitte Wildemann³, Markus Reindl⁴, Amy Waldman⁵, Kerstin Soelberg^{6,7}, Nasrin Asgari^{6,7}, Marius Ringelstein⁸, Orhan Aktas⁸, Nikolai Gross⁹, Mathias Buttman¹⁰, Thomas Ach¹¹, Klemens Ruprecht², Friedemann Paul^{1,2,12†}, and Alexander U. Brandt^{1*†}; in cooperation with the Neuromyelitis Optica Study Group (NEMOS)

Abstract

Background: Antibodies against myelin oligodendrocyte glycoprotein (MOG-IgG) have been reported in patients with aquaporin-4 antibody (AQP4-IgG)-negative neuromyelitis optica spectrum disorders (NMOSD). The objective of this study was to describe optic neuritis (ON)-induced neuro-axonal damage in the retina of MOG-IgG-positive patients in comparison with AQP4-IgG-positive NMOSD patients.

Methods: Afferent visual system damage following ON was bilaterally assessed in 16 MOG-IgG-positive patients with a history of ON and compared with that in 16 AQP4-IgG-positive NMOSD patients. In addition, 16 healthy controls matched for age, sex, and disease duration were analyzed. Study data included ON history, retinal optical coherence tomography, visual acuity, and visual evoked potentials.

Results: Eight MOG-IgG-positive patients had a previous diagnosis of AQP4-IgG-negative NMOSD with ON and myelitis, and eight of (mainly recurrent) ON. Twenty-nine of the 32 eyes of the MOG-IgG-positive patients had been affected by at least one episode of ON. Peripapillary retinal nerve fiber layer thickness (pRNFL) and ganglion cell and inner plexiform layer volume (GCIP) were significantly reduced in ON eyes of MOG-IgG-positive patients (pRNFL = 59 ± 23 μm ; GCIP = 1.50 ± 0.34 mm^3) compared with healthy controls (pRNFL = 99 ± 6 μm , $p < 0.001$; GCIP = 1.97 ± 0.11 mm^3 , $p < 0.001$). Visual acuity was impaired in eyes after ON in MOG-IgG-positive patients (0.35 ± 0.88 logMAR). There were no significant differences in any structural or functional visual parameters between MOG-IgG-positive and AQP4-IgG-positive patients (pRNFL: 59 ± 21 μm ; GCIP: 1.41 ± 0.27 mm^3 ; Visual acuity = 0.72 ± 1.09 logMAR). Importantly, MOG-IgG-positive patients had a significantly higher annual ON relapse rate than AQP4-IgG-positive patients (median 0.69 vs. 0.29 attacks/year, $p = 0.004$), meaning that on average a single ON episode caused less damage in MOG-IgG-positive than in AQP4-IgG-positive patients. pRNFL and GCIP loss correlated with the number of ON episodes in MOG-IgG-positive patients ($p < 0.001$), but not in AQP4-IgG-positive patients.

(Continued on next page)

* Correspondence: Alexander.Brandt@charite.de

†Equal contributors

Friedemann Paul and Alexander U Brandt are equally contributing senior authors.

Florence Pache and Hanna Zimmermann are equally contributing first authors.

¹NeuroCure Clinical Research Center (NCRC), Charité – Universitätsmedizin Berlin, Charitéplatz 1, 10117 Berlin, Germany

Full list of author information is available at the end of the article



(Continued from previous page)

Conclusions: Retinal neuro-axonal damage and visual impairment after ON in MOG-IgG-positive patients are as severe as in AQP4-IgG-positive NMOSD patients. In MOG-IgG-positive patients, damage accrual may be driven by higher relapse rates, whereas AQP4-IgG-positive patients showed fewer but more severe episodes of ON. Given the marked damage in some of our MOG-IgG-positive patients, early diagnosis and timely initiation and close monitoring of immunosuppressive therapy are important.

Keywords: Myelin oligodendrocyte glycoprotein antibodies (MOG-IgG), aquaporin-4 antibodies (AQP4-IgG), NMO-IgG, neuromyelitis optica, Devic syndrome, neuromyelitis optica spectrum disorders (NMOSD), optic neuritis, optical coherence tomography, visual evoked potentials, visual acuity, retinal neuro-axonal damage

Background

Myelin oligodendrocyte glycoprotein (MOG) is expressed on the outer surface of oligodendrocytic myelin sheaths, representing approximately 0.05 % of all myelin-constituting proteins [1]. Antibodies against MOG (MOG-IgG) have been detected in a proportion of aquaporin-4 (AQP4)-IgG-seronegative patients with neuromyelitis optica spectrum disorder (NMOSD) phenotype [2–6]. MOG-IgG have further been reported in children with acute and relapsing-remitting inflammatory demyelinating encephalomyelitis as well as in a proportion of adults with inflammatory demyelinating diseases such as optic neuritis (ON) [7–9].

Currently it is debated whether MOG-IgG-associated encephalomyelitis should be classified as an NMOSD subtype or as a separate disease entity [10–12]. MOG-IgG-seropositive patients from NMOSD cohorts can show clinical features of recurrent transverse myelitis and ON, similar to AQP4-IgG-seropositive patients [4]. However, the cellular target of AQP4-IgG is an astrocytic water channel, suggesting a different mechanism of injury from MOG-IgG. This is supported by a recent case study of a MOG-IgG-seropositive patient who showed severe demyelination with no evidence of astrocytopathy [13] and by further brain biopsy case studies [14–16].

ON in NMOSD patients is often severe with marked retinal nerve fiber layer and ganglion cell layer loss, severe visual impairment including blindness, and a high frequency of bilateral events [17, 18]. In around 20 % of affected eyes, macular microcysts are found in the inner nuclear layer as a sign of severe ON-related retinal injury [19, 20]. In comparison, the extent of afferent visual system damage following ON in MOG-IgG-seropositive patients is less well understood.

Some previous studies, employing either structural or clinical assessment of visual function, suggested that MOG-IgG-positive patients have fewer attacks, better recovery from relapses, and less neuro-axonal retinal damage than AQP4-IgG-positive patients [4, 21, 22]. However, it is a potential drawback that observation periods were relatively short and sample sizes low in those

studies. Moreover, some included mostly or exclusively Asian patients [4, 22]; this could be relevant in that genetic factors have been proposed to play a role in NMOSD pathogenesis [17]. By contrast, more recent studies by others [23, 24] and us [25] demonstrate that the disease follows a relapsing course in the long run in most MOG-IgG-positive patients.

The objective of this retrospective multicenter study was to investigate visual system damage after ON in a larger cohort of Caucasian patients with MOG-IgG-associated encephalomyelitis and long-term follow-up using a comprehensive assessment of the afferent visual system including structural, functional, and clinical parameters, and to compare it with that in AQP4-IgG-positive NMOSD patients.

Methods

Patients

MOG-IgG-seropositive patients with a history of ON and available optical coherence tomography (OCT) data were recruited from a large retrospective study [25, 26]. Sixteen patients (15 female; mean age 44.0 ± 15.2 years) were enrolled from six university hospitals in Europe (Germany: Berlin, Freiburg, Düsseldorf, Heidelberg, Würzburg; Denmark: Vejle). The inclusion criteria were age ≥ 18 years, a confirmed history of ON (more than 3 months prior to visual assessments), and seropositivity for MOG-IgG. A MOG-antibody serum titer of $\geq 1:160$ was classified as positive [26]. Clinical and paraclinical data on disease onset, relapse history, expanded disability status scale (EDSS) [27], visual acuity, OCT, magnetic resonance imaging (MRI), and immunotherapy were retrospectively collected. Annualized relapse rate was calculated as the ratio of number of attacks and years since disease onset, excluding patients with disease duration of less than 1 year. All patients were of Caucasian descent; all MOG-IgG-positive patients tested seronegative for AQP4-IgG, and vice versa (Table 1). Eight (50 %) MOG-IgG-positive patients had a previous diagnosis of—mainly recurrent—ON, and eight (50 %) had been diagnosed with NMOSD based on the clinical symptoms of ON and myelitis before anti-MOG-IgG was tested.

Table 1 Demographic data

		MOG-IgG	AQP4-IgG	MOG-IgG vs. AQP4-IgG (MWU/Chi ²) <i>p</i>
Patients	<i>N</i>	16	16	
Age (years)	Mean ± SD	44.0 ± 15.2	43.2 ± 13.9	0.838
Sex (f/m)		15/1	16/0	>0.999
Ophthalmologic comorbidities	<i>N</i>	2 ^{a)} (13 %)	0 (0 %)	
Age at onset (years)	Mean ± SD	37.2 ± 15.1	34.7 ± 14.8	0.669
Time since onset (years)	Mean ± SD	6.9 ± 6.5	8.4 ± 6.8	0.287
ON eyes	<i>N</i> (%)	29 (91.6 %)	25 (78.1 %)	
Number of ON episodes	Median (range)	4.5 (1–13)	2 (1–4)	0.012
Myelitis prevalence	<i>N</i> (%)	8 (50 %)	15 (93.8 %)	0.018
ARR	Median (range)	1.25 (0.38–7.14)	0.64 (0.17–1.44)	0.026
ON ARR	Median (range)	0.69 (0.17–7.14)	0.29 (0.07–0.96)	0.004
EDSS	Median (range)	3.0 (1.0–7.5)	4.0 (1.0–6.5)	0.064

Abbreviations: AQP4-IgG aquaporin-4 antibody-seropositive NMOSD patients, ARR annualized relapse rate, EDSS expanded disability status scale, f female, m male, MOG-IgG myelin oligodendrocyte glycoprotein antibody-seropositive patients, MWU Wilcoxon-Mann-Whitney U test, ON optic neuritis, SD standard deviation

^{a)}Early stage dry macular degeneration in both eyes and suspect for early stage glaucoma, respectively
p-values in bold emphasis depict significant values ($p < 0.05$)

AQP4-IgG-positive NMOSD patients [28] ($n = 16$, all female, mean age 43.2 ± 13.9 years) and healthy controls (HC, $n = 16$, 15 female, mean age 43.9 ± 15.4 years) were randomly selected from the research database of the NeuroCure Clinical Research Center (Charité – Universitätsmedizin Berlin, Berlin, Germany), matched for sex and age on cohort basis. Two MOG-IgG-positive patients had co-occurring ophthalmologic conditions in both eyes: one had early-stage dry macular degeneration, and glaucoma was suspected in the other patient. These two patients and their matched AQP4-IgG-positive patients and HC were included in the case descriptions but excluded from statistical analyses of OCT and visual function parameters. Furthermore, only eyes with a previous ON were included in statistical analyses. The local ethics committees approved the study protocol in accordance with the Declaration of Helsinki (1964) in its currently applicable version. All participants provided informed written consent.

MOG-IgG and AQP4-IgG assay

MOG-IgG antibodies were detected using a live cell-based assay and a fixed cell-based assay, both employing HEK293 cells transfected with human full-length MOG; mock-transfected cells were used as control substrates (see part 1 for details [26]). AQP4-IgG were detected using a commercially available cell-based assay (EUROIMMUN, Lübeck, Germany) [29, 30].

Optical coherence tomography

OCT was performed using the Spectralis SD-OCT device (Heidelberg Engineering, Heidelberg, Germany) with the automatic real time function for image averaging.

Peripapillary retinal nerve fiber layer thickness (pRNFL) was derived from a standard ring scan around the optic nerve head (12° , 768 or 1536 A-scans, $16 \leq \text{ART} \leq 100$). A macular volume scan ($25^\circ \times 30^\circ$, 61 vertical or horizontal B-scans, 768 A-scans per B-scan, $9 \leq \text{ART} \leq 15$) was acquired for retinal layer analysis. All scans underwent quality control [31] and post-processing by one experienced rater in a standardized manner. Layer segmentation was performed with the device's software (Eye Explorer 1.9.10.0 with viewing module 6.0.9.0). Automatic segmentation results were carefully checked for errors and corrected if necessary by an experienced rater masked for the diagnosis of the subjects. Combined ganglion cell and inner plexiform layer volume (GCIP), inner nuclear layer volume, and outer retinal layers volume including the outer plexiform and nuclear layer, inner and outer photoreceptor segments, and retinal pigment epithelium, were extracted from a 6-mm-diameter cylinder around the fovea [32]. Furthermore, all scans were examined for macular microcysts [19] and other retinal pathologies. The OCT parameters are visualized in Fig. 1.

Visual function testing

Visual function testing was performed in MOG-IgG-positive and AQP4-IgG-positive patients at the same visit as OCT, except for one patient (see Additional file 1: Table S1). Visual evoked potentials (VEP) were recorded with checkerboard stimulation (1°) with the device routinely used at the sites. P100 peak latency was included in analysis and considered as abnormal when higher than 112 ms [33] or when no clear signal could be evoked. Habitually corrected visual acuity was tested with letter charts obtained as part of routine clinical care

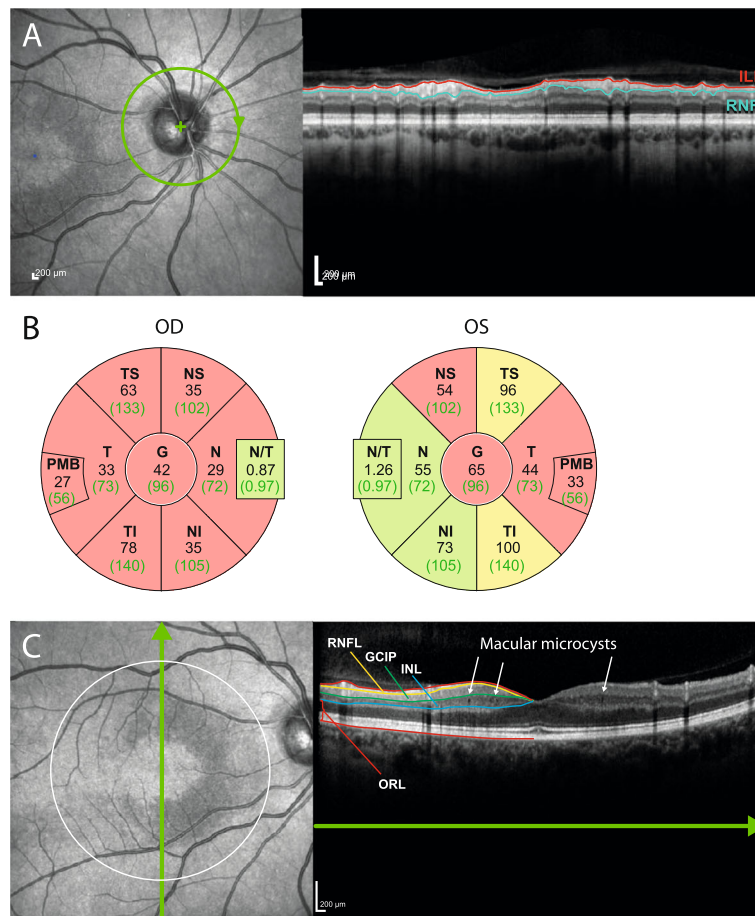


Fig. 1 Sample images from patient 1. **a** Sample images from a peripapillary ring scan. On the left, a scanning laser ophthalmoscopy image shows scan positioning (in green). On the right, an OCT scan shows severe peripapillary retinal nerve fiber layer (pRNFL) loss (between the inner limiting membrane [ILM], shown in red, and the lower border, in turquoise). **b** Ring-scan data in comparison with normative device data from both eyes of this patient. Black numbers display the thickness measurements (in μm) of the subject, green numbers the average thickness in the age-matched reference group. Sectors are classified in comparison with the reference group: green, thickness values within the 5th and 95th percentile range; yellow, 1st to 5th percentile range; red, below the 1st percentile. Abbreviations: G global, NS nasal-superior, N nasal, NI nasal-inferior, TI temporal-inferior, T temporal, TS temporal-superior. **c** Macular scan of the same patient. On the left, the dark, sickle-shaped area on and around the macula represents tissue with microcysts in the inner nuclear layer (INL). The white circle indicates the 6-mm-diameter cylinder in which intraretinal layers are analyzed. The green line with arrow shows the scanning position of the OCT scan on the right. Here, the defined layers are the RNFL, the ganglion cell and inner plexiform layer (GCIP), then INL and the outer retinal layers (ORL). Macular microcysts can be seen as small black dots in the INL

and converted into logMAR units. A visual acuity of 0.2 logMAR and worse was considered abnormal. When no letter could be recognized by the patient, visual acuity was registered with 2.0 logMAR for finger counting and 3.0 logMAR for hand motion recognition [34].

Data analysis

Statistics were performed in R version 3.1.2 [35] using the packages psych, MASS, geepack and ggplot. Differences in demographics between the cohorts were tested with Pearson chi-square test and non-parametric tests (Mann-Whitney U for two cohorts and Kruskal-Wallis for three cohorts). Comparisons of visual system data between cohorts were performed using generalized

estimating equation (GEE) models accounting for intra-subject inter-eye dependencies. GEE results are provided with regression coefficient (B) and standard error (SE). To investigate the extent of damage caused by subsequent ON episodes we employed a linear spline regression model as proposed by Ratchford et al. [36]. Due to the exploratory nature of this study, no correction for multiple comparisons was performed.

Results

The demographic and clinical features of MOG-IgG-positive patients are presented in Table 1 and case-by-case clinical details are provided in Additional file 1: Table S1. One patient had pediatric onset of the disease,

at 6 years of age; her case has been reported in an earlier publication [11]. All other patients had adult onset. All MOG-IgG-positive patients had experienced at least one episode of ON (median 4.5, range 1–13) and, except for one with a short follow-up period (8 months, patient 8), presented with an unequivocally relapsing disease course. Age at onset and disease duration at the time of examination did not differ between MOG-IgG-positive and AQP4-IgG-positive patients (Table 1). Detailed case studies, including therapy, are provided in parts 2 and 3 of this series of articles [25, 37].

OCT and visual function in MOG-IgG-positive ON

Two eyes from two patients had to be excluded from the analysis owing to acute ON at the time of assessment. Thus, 23 eyes from 14 MOG-IgG-positive patients were analyzed at a median time of 16.4 months (range 3–125 months) since the most recent episode of ON. Detailed afferent visual system parameters of all patients are given in Table 2, and case-by-case descriptions are provided in Additional file 2: Table S2.

Reduced pRNFL thickness compared with the manufacturer’s normative data was found in 18 of the 23 (78.2 %) ON-affected eyes of the MOG-IgG-positive group (mean 59 ± 23 μm). In addition, two fellow eyes without clinically evident previous ON and with normal VEPs showed reduced RNFL thickness (51 μm and 75 μm, respectively). Five ON eyes (21.7 %) but none of the non-ON eyes had macular microcysts in the inner

nuclear layer. Of 20 ON eyes with available VEP data, 12 (60 %) eyes had abnormal P100 latencies—two (10 %) of them despite normal pRNFL—while all four non-ON fellow eyes had normal VEPs. Visual acuity was on average reduced in ON eyes (mean 0.35 ± 0.88 logMAR), with three eyes being legally blind at a visual acuity of 1.0 logMAR and worse. On the other hand, 16 of 23 ON eyes (70 %) preserved visual acuity of 0.1 logMAR or better.

There were no significant differences in OCT and visual function measurements between MOG-IgG-positive patients with a history of both ON and myelitis (n = 8) and MOG-IgG-positive patients with a history only of recurrent ON (n = 8) (not shown).

Comparison with HC and AQP4-IgG-positive NMOSD patients

We then compared the afferent visual system damage in ON eyes of MOG-IgG-positive patients with age- and sex-matched HC and with ON eyes of AQP4-IgG-positive NMOSD patients (Table 2, Fig. 2). As expected, pRNFL and GCIP were significantly lower than in HC both in the MOG-IgG-positive group (both p < 0.001) and in the AQP4-IgG-positive group (both p < 0.001). Furthermore, inner nuclear layer volume was significantly greater than HC in the MOG-IgG-positive subgroup (p = 0.009), but not in the AQP4-IgG-positive NMOSD subgroup. By contrast, no significant difference was noted between MOG-IgG-positive and AQP4-IgG-positive patients regarding retinal layer measures. Macular

Table 2 Structural and functional data of MOG-IgG-positive patients’ ON eyes in comparison to AQP4-IgG-positive patients and control data

	MOG-IgG positive ON (n = 23 eyes from 14 subjects)	AQP4-IgG positive ON (n = 21 eyes from 14 subjects)	HC (n = 28 eyes from 14 subjects)	MOG-IgG positive vs. AQP4-IgG positive (GEE)			MOG-IgG positive vs. HC (GEE)		
				B	SE	p	B	SE	p
Retinal OCT									
Average pRNFL (μm)	59 ± 23	59 ± 21	99 ± 6	-0.6	7.58	0.94	39.0	6.01	<0.001
Nasal pRNFL (μm)	44 ± 21	45 ± 24	74 ± 12	0.2	7.85	0.98	28.6	6.01	<0.001
Temporal pRNFL (μm)	44 ± 16	40 ± 15	71 ± 10	-3.0	4.51	0.50	27.6	4.26	<0.001
GCIP (mm ³)	1.50 ± 0.34	1.41 ± 0.27	1.97 ± 0.11	-0.10	0.10	0.35	0.47	0.08	<0.001
INL (mm ³)	1.03 ± 0.10	1.01 ± 0.11	0.95 ± 0.04	-0.02	0.04	0.55	-0.07	0.03	0.009
ORL (mm ³)	4.86 ± 0.26	4.93 ± 0.26	4.73 ± 0.21	0.04	0.09	0.70	-0.13	0.09	0.14
Eyes with macular microcysts (n)	5 (21.7 %)	4 (19.0 %)		Chi ²		>0.99			
Visual function									
Visual acuity/logMAR	0.35 ± 0.88	0.72 ± 1.09	-	0.33	0.32	0.30			
Abnormal P100 latency*	12 (57 %)	10 (50 %)	-	Chi ²		0.88			

OCT and visual function results are not including data from the two patients with early stage dry macular degeneration in both eyes and glaucoma, respectively, and their respective AQP4-IgG-positive controls and healthy controls. Furthermore, two eyes of two MOG-IgG positive patients were excluded due to acute ON at time of examination. Explanations: All data are given as mean ± standard deviation (minimum – maximum), if not declared different

AQP4-IgG aquaporin-4 antibody-seropositive NMOSD patients, GCIP ganglion cell and inner plexiform layer, HC healthy controls, INL inner nuclear layer, ON eyes with history of optic neuritis, MOG-IgG myelin oligodendrocyte glycoprotein antibody-seropositive patients, ORL outer retinal layers including layer from outer plexiform layer to Bruch’s membrane, pRNFL peripapillary retinal nerve fiber layer

p-values in bold emphasis depict significant values (p < 0.05)

* VEP data were available for 20 out of 23 ON eyes of MOG-IgG positive patients and 20 out of 21 eyes of AQP4-IgG positive patients

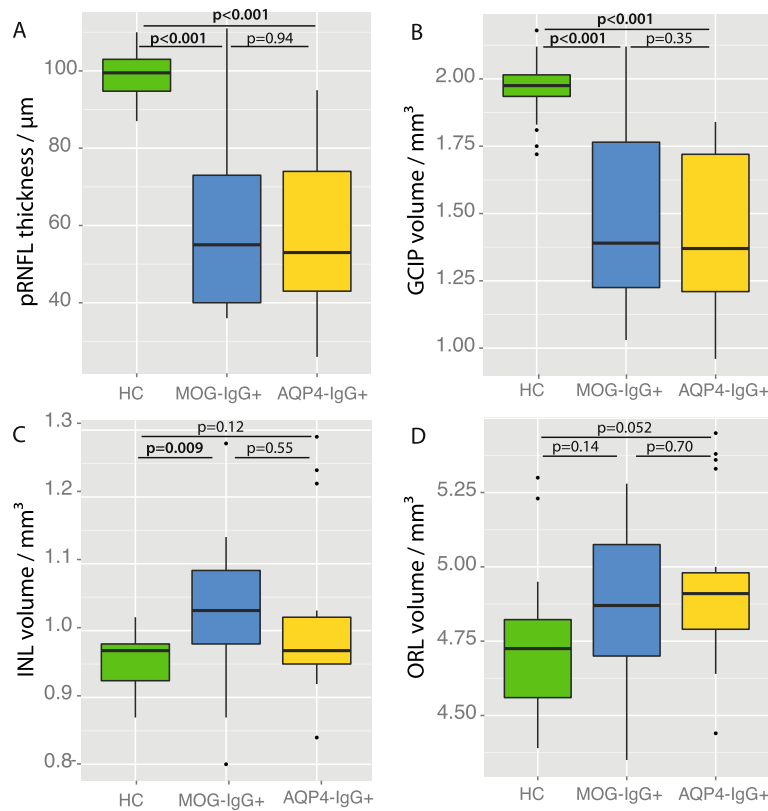


Fig. 2 Retinal layer measures of MOG-IgG-positive and AQP4-IgG-positive ON eyes. *Boxplots* for the comparison of retinal layer measures of the eyes in the healthy control group and the ON eyes of MOG-IgG-positive (MOG-IgG+) and AQP4-IgG-positive (AQP4-IgG+) NMOSD patients. **(a)** Peripapillary retinal nerve fiber layer thickness derived from a ring scan (pRNFL); **(b-d)** Intraretinal layer volumes quantified in a 6-mm-diameter cylinder around the fovea centralis: **(b)** ganglion cell and inner plexiform layer volume (GCIP); **(c)** inner nuclear layer volume (INL); **(d)** outer retinal layer volume comprising all layers from outer plexiform layer to Bruch’s membrane

microcysts were found in both subgroups in similar prevalence, but differences in microcyst size or extend might have led to a high variability of inner nuclear layer volume values (Table 2). Visual acuity was less impaired in the MOG-IgG-positive subgroup (mean 0.35 ± 0.88 logMAR) than in the AQP4-IgG-positive subgroup (0.72 ± 1.09); however, the difference was not significant ($p = 0.30$).

Of note, the MOG-IgG-positive patients showed a significantly higher annualized relapse rate both for all relapses and—even higher—for ON than the AQP4-IgG-positive patients ($p = 0.026$ and $p = 0.004$, respectively), despite similar disease duration (Table 1).

Retinal damage and number of ON episodes

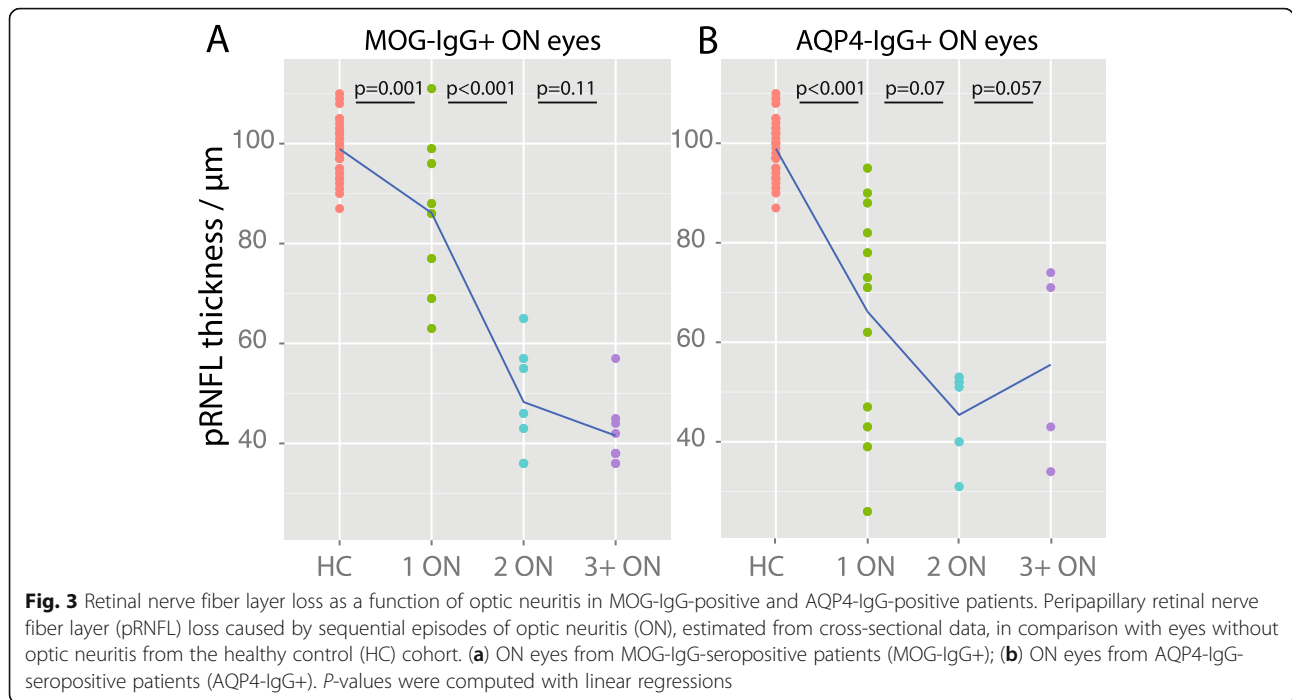
In MOG-IgG-positive patients, a higher number of ON episodes was associated with more severe pRNFL and GCIP loss (GEE: pRNFL $B = -4.9$, $SE = 1.40$, $p < 0.001$; GCIP $B = -0.07$, $SE = 0.02$, $p < 0.001$), but not with changes of the inner nuclear layer or outer retinal layers. By contrast, in AQP4-IgG-positive patients the extent of retinal layer changes did not correlate with the number of ON attacks.

In our cross-sectional data, the first ON episode caused a mean pRNFL loss of $12.8 \mu\text{m}$ ($p = 0.001$) in MOG-IgG-positive patients and $32.8 \mu\text{m}$ ($p < 0.001$) in AQP4-IgG-positive patients in comparison with HC eyes. In contrast, a second episode of ON caused additional pRNFL loss of $37.8 \mu\text{m}$ ($p < 0.001$) in MOG-IgG-positive patients and $20.8 \mu\text{m}$ in AQP4-IgG-positive patients, although that difference was not significant ($p = 0.07$) (Fig. 3). A similar association was found for GCIP volume (data not shown).

Discussion

This study shows that ON in MOG-IgG-positive patients leads to severe pRNFL and GCIP thinning and visual function impairment, the extent of which is comparable to ON in patients with AQP4-IgG. Moreover, it suggests that the damage accrual may be driven by higher relapse rates in MOG-IgG-positive patients, in contrast to more severe ON-associated damage during a single ON episode in AQP4-IgG-positive patients.

Some earlier studies of MOG-IgG-positive patients, which were characterized by relatively short observation



periods, suggested that MOG-IgG-seropositive patients present more often with monophasic disease and have a milder clinical phenotype and better recovery than patients with AQP4-IgG-seropositive NMO [4, 5, 38]. By contrast, all but one of our patients showed a relapsing disease course with a high frequency of attacks, protracted ON episodes, and, in some cases, severe visual impairment. In line with our findings, two more recent studies have also demonstrated that MOG-IgG seropositivity is frequently associated with a recurrent disease course in patients with ON [23, 24]. Concerning neuro-axonal damage of the retina, a recent study including 19 MOG-IgG-positive patients reported less retinal nerve fiber and ganglion cell layer damage than in AQP4-IgG-positive patients following ON [22]. As a limitation, however, that study included exclusively monophasic patients. By contrast, in our study we demonstrated that retinal neuro-axonal damage after ON in MOG-IgG-positive patients is at least as severe as in AQP4-IgG-positive NMO patients, compared with our own control cohort as well as with previously published AQP4-IgG-positive cohorts [39, 40] when patients with long-term follow-up (mean ~7 years) and, accordingly, relapsing disease course are included in the analysis.

Notably, although average visual function was impaired in relapsing ON of both MOG-IgG-positive and AQP4-IgG-positive patients, some MOG-IgG-positive patients performed comparably well on high-contrast visual acuity testing despite severe neuro-axonal retinal damage: 70 % of ON eyes retained a visual acuity of 0.1 logMAR or better after ON. However, visual acuity was obtained in non-standardized manner as high-contrast letter acuity in

clinical routine; thus the reliance on functional testing may underestimate the actual extent of damage to the afferent visual system. The impact of structural damage as demonstrated in the present study should be further investigated with low-contrast letter acuity, color vision testing, visual fields, and quality of life scales.

Our study features strengths and limitations. Among its strengths we count the relatively high number of patients included, given the low prevalence of the disease, the fact that reliable assays for detecting antibodies to full-length human MOG have become available only relatively recently, and the fact that OCT is not yet routinely and generally available. A further potential strength is that our cohort was genetically homogeneous with all patients and controls being of Caucasian origin. As a potential limitation, not all patients were systematically tested for other optic neuropathies, such as Leber's hereditary optic neuropathy (LHON). While a mitochondrial mutation may have contributed to the marked pRNFL thinning in the female patient with pediatric onset of disease (patient 4 in Additional file 1: Table S1), the time course (approximately 10 years before the contralateral eye demonstrated a mild decrease in visual acuity) is unusual for LHON, a condition which typically affects both eyes within months of each other without a relapsing and remitting course. Finally, data were collected retrospectively in a multicenter approach. As a result, additional data, e.g., the Multiple Sclerosis Function Composite or OCT scans obtained during acute optic neuritis, were not available. Moreover, we were not able to systematically correlate optic nerve MRI [23, 41] and OCT in this study,

which would require highly standardized MRI protocols and a prospective study design. However, prospective studies as well as single-center studies in MOG-IgG-positive patients are difficult to perform due to the condition's rarity and the currently limited access to MOG-IgG testing. Moreover, all patients with available data seen at the various centers were included in the analysis, thereby reducing the risk of referral bias. Nonetheless, the preliminary evidence derived from this retrospective exploratory study needs to be confirmed in further prospective and independent studies.

Conclusions

In summary, we demonstrate (a) that a substantial proportion of MOG-IgG-seropositive patients develop retinal neuro-axonal damage; (b) that visual impairment and structural damage increase with the number of attacks and thus with disease duration; and, importantly, (c) that the extent of neuro-axonal damage in MOG-IgG-positive patients with ON is not different from that in patients with AQP4-IgG-positive ON in the long-term course of the disease, i.e., when patients with relapsing rather than monophasic ON are taken into account. Given the marked structural and functional damage in some of our ON patients, early diagnosis, timely initiation of immunosuppressive therapy, and close monitoring of treatment efficacy seem paramount. Although no systematic investigations of drugs for relapse prevention in this condition have yet been conducted, retrospective data on treatment responses (see part 2 of this series [25]), as well as available evidence in favor of a pathogenic role of MOG-IgG [16, 30], suggest that—in accordance with treatment recommendations for AQP4-IgG-positive NMOSD [42]—patients with MOG-IgG-positive ON may benefit from high-dose intravenous methylprednisolone treatment and, possibly, plasma exchange for acute attacks as well as from immunosuppression for attack prevention.

Additional files

Additional file 1: Table S1. Demographic, clinical and serological data.

^{a)} Early stage dry macular degeneration in both eyes; ^{b)} Suspected early stage glaucoma. ^{c)} Visual assessments were performed during acute ON OS. Abbreviations: ON: optic neuritis. VEP P100: visually evoked potential P100 latency. n.e.: not evocable; pRNFL: peripapillary retinal nerve fiber layer thickness. GCIP: combined ganglion cell and inner plexiform layer volume. INL: inner nuclear layer volume. ORL: outer retinal layers volume including layers from outer plexiform layer to Bruch's membrane. (DOCX 21 kb)

Additional file 2: Table S2. Visual evoked potentials, visual acuity, and OCT results. ^{a)} Protracted relapses were registered as one episode; ^{b)} Early stage dry macular degeneration in both eyes; ^{c)} Suspected early stage glaucoma; ^{d)} Medication other than acute relapse therapy (immunotherapy). Abbreviations: AQP4-IgG = aquaporin-4 antibodies; CRION = chronic relapsing inflammatory optic neuropathy; EDSS = expanded disability status scale; F = female; MOG-IgG = myelin oligodendrocyte glycoprotein antibodies; NMOSD = neuromyelitis optica spectrum disorders; (r)ON = (recurrent) optic neuritis. (DOC 59 kb)

Abbreviations

AQP4-IgG: Aquaporin-4 immunoglobulin G; ARR: Annualized relapse rate; EDSS: Expanded disability status scale; GCIP: Ganglion cell and inner plexiform layer volume; GEE: Generalized estimating equation; LHON: Leber's hereditary optic neuropathy; MOG-IgG: Myelin oligodendrocyte glycoprotein antibody-seropositive patients; MWU: Wilcoxon-Mann-Whitney *U* test; OCT: Optical coherence tomography; ON: Optic neuritis; pRNFL: Peripapillary retinal nerve fiber layer thickness; SD: Standard deviation; SE: Standard error; VEP: Visual evoked potentials

Acknowledgments

BW and SJ are grateful to the Dietmar Hopp Foundation and to Merck Serono for funding research on NMO and related disorders at the Molecular Neuroimmunology Group, Department of Neurology, University of Heidelberg, and to Mrs. Anna Eschbeck and the Nikon Imaging Center at the University of Heidelberg for excellent technical assistance. FrP would like to acknowledge research support by the German Research Council (DFG Exc 257) and by the Federal Ministry for Education and Research (Competence Network Multiple Sclerosis; N2-ADVISIM). AUB is grateful to the German Federal Ministry of Economic Affairs and Technology (EXIST-Forschungstransfer RETINEU). MRe would like to thank the Eugene Devic European Network (EDEN) project (ERA-Net ERARE 2; Austrian Science Fund FWF project I916) and the Austrian Federal Ministry of Science, Research and Economy (grant Big Wig MS).

Funding

This work was supported by the Dietmar Hopp Stiftung (BW), Merck Serono (BW), the German Federal Ministry of Education and Research (BMBF/KKNMS, Competence Network Multiple Sclerosis, FrP, KR and OA; N2-ADVISIMs, FrP and AB), the German Federal Ministry for Economic Affairs and Technology (EXIST-Forschungstransfer RETINEU, AB), the German Research Foundation (DFG Exc 257, FP), the Austrian Federal Ministry of Science, Research and Economy (grant Big Wig MS, MRe), the Eugene Devic European Network (EDEN) project (European Research Area-Net ERARE 2, MRe); the Austrian Science Fund (FWF project I916; MRe).

Availability of data and materials

The datasets during and/or analysed during the current study available from the corresponding author on reasonable request.

Authors' contributions

FIP participated in the design of the study, acquired clinical information, and drafted the manuscript. HZ performed OCT post-processing and statistical analysis and drafted the manuscript. JM acquired OCT and visual function data. SS, AL, and FCO. acquired clinical and visual function data. JBS participated in the design of the study and acquired clinical data. MRe and SJ provided MOG-IgG results and contributed to interpretation of the data. SJ and BW contributed OCT and clinical data and contributed to interpretation of the data. AW contributed to interpretation of the data. KS acquired OCT and visual function data. NA acquired clinical data and contributed to interpretation of the data. MRI acquired OCT, clinical, and visual function data. OA acquired clinical data. NG acquired OCT, clinical, and visual function data. KR participated in the design of the study and contributed to interpretation of the data. MB acquired clinical data, contributed to interpretation of the data, and edited the manuscript. TA acquired OCT and visual function data. FrP contributed to the interpretation of the data and drafted the manuscript. AUB conceived the study and participated in its design and coordination contributed to analysis, and drafted the manuscript. All authors were involved in revising the manuscript for intellectual content and read and approved the final manuscript.

Competing interests

FIP received a research grant from Novartis Pharmaceuticals and travel grants from Genzyme, a Sanofi company. HZ has received speaking fees from Teva and Bayer. JM has received speaking fees from Teva and Biogen Idec. B.W. has received speaking/consultation honoraria and travel grants from Bayer Healthcare, Biogen Idec, Merck Serono, and Genzyme, a Sanofi company. ATW has received support from the National Institutes of Health and Biogen Idec. MRI has received speaker honoraria from Novartis and Bayer and travel reimbursements from Bayer Schering, Biogen Idec, and Genzyme. OA has received advisor fees or honoraria from Bayer HealthCare,

Biogen, Chugai, Genzyme, MedImmune, Novartis, and Teva; and research support from Bayer HealthCare, Biogen, Novartis, and Teva. KR has received research support from Novartis as well as speaking fees or travel grants from Bayer Healthcare, Biogen Idec, Merck Serono, Sanofi/Genzyme, Teva, Roche, and Novartis. FrP has received research grants and speaker honoraria from Bayer, Teva, Genzyme, Merck, Novartis, and MedImmune and is a member of the steering committee of the OCTIMS study (Novartis). AUB. has received consulting fees from Biogen, Novartis, Teva, Nexus, and Motognosis and funding for research from Novartis and Biogen. All other authors report nothing to disclose. None of the reported disclosures interfered with the present study.

Consent for publication

All participants provided informed written consent for publication.

Ethics approval and consent to participate

The study was approved by the local ethics committees of the participating centers. All participants provided informed written consent.

Author details

¹NeuroCure Clinical Research Center (NCRC), Charité – Universitätsmedizin Berlin, Charitéplatz 1, 10117 Berlin, Germany. ²Department of Neurology, Charité – Universitätsmedizin Berlin, Berlin, Germany. ³Molecular Neuroimmunology Group, Department of Neurology, University of Heidelberg, Heidelberg, Germany. ⁴Clinical Department of Neurology, Medical University of Innsbruck, Innsbruck, Austria. ⁵Division of Neurology, Children's Hospital of Philadelphia, Pennsylvania, USA. ⁶Department of Neurology, Vejle Hospital, Vejle, Denmark. ⁷Department of Neurobiology, Institute of Molecular Medicine, University of Southern Denmark, Odense, Denmark. ⁸Department of Neurology, Medical Faculty, Heinrich Heine University, Düsseldorf, Germany. ⁹Department of Ophthalmology, Medical Faculty, University of Freiburg, Freiburg, Germany. ¹⁰Department of Neurology, University of Würzburg, Würzburg, Germany. ¹¹Department of Ophthalmology, University of Würzburg, Würzburg, Germany. ¹²Experimental and Clinical Research Center, Max Delbrück Center for Molecular Medicine and Charité – Universitätsmedizin Berlin, Berlin, Germany.

Received: 1 April 2016 Accepted: 9 September 2016

Published online: 01 November 2016

References

- Reindl M, Di Pauli F, Rostásy K, Berger T. The spectrum of MOG autoantibody-associated demyelinating diseases. *Nat Rev Neurol*. 2013;9:455–61.
- Mader S, Gredler V, Schanda K, Rostásy K, Dujmovic I, Pfäller K, et al. Complement activating antibodies to myelin oligodendrocyte glycoprotein in neuromyelitis optica and related disorders. *J Neuroinflammation*. 2011;8:184.
- Rostásy K, Mader S, Hennes EM, Schanda K, Gredler V, Guenther A, et al. Persisting myelin oligodendrocyte glycoprotein antibodies in aquaporin-4 antibody negative pediatric neuromyelitis optica. *Mult Scler J*. 2013;19:1052–9.
- Sato DK, Callegaro D, Lana-Peixoto MA, Waters PJ, Jorge FM, de H, Takahashi T, et al. Distinction between MOG antibody-positive and AQP4 antibody-positive NMO spectrum disorders. *Neurology*. 2014;82:474–81.
- Kitley J, Waters P, Woodhall M, Leite MI, Murchison A, George J, et al. Neuromyelitis optica spectrum disorders with aquaporin-4 and myelin oligodendrocyte glycoprotein antibodies: a comparative study. *JAMA Neurol*. 2014;71:276–83.
- Saadoun S, Waters P, Owens GP, Bennett JL, Vincent A, Papadopoulos MC. Neuromyelitis optica MOG-IgG causes reversible lesions in mouse brain. *Acta Neuropathol Commun*. 2014;2:35.
- Baumann M, Sahin K, Lechner C, Hennes EM, Schanda K, Mader S, et al. Clinical and neuroradiological differences of paediatric acute disseminating encephalomyelitis with and without antibodies to the myelin oligodendrocyte glycoprotein. *J Neurol Neurosurg Psychiatry*. 2015;86:265–72.
- Kim S-M, Woodhall MR, Kim J-S, Kim S-J, Park KS, Vincent A, et al. Antibodies to MOG in adults with inflammatory demyelinating disease of the CNS. *Neurol Neuroimmunol Neuroinflammation* [Internet]. 2015 [cited 2016 Feb 18];2. Available from: <http://www.ncbi.nlm.nih.gov/pmc/articles/PMC4608758/>
- Höftberger R, Sepulveda M, Armangue T, Blanco Y, Rostásy K, Cobo Calvo A, et al. Antibodies to MOG and AQP4 in adults with neuromyelitis optica and suspected limited forms of the disease. *Mult Scler J*. 2015;21:866–74.
- Zamvil SS, Slavin AJ. Does MOG Ig-positive AQP4-seronegative opticospinal inflammatory disease justify a diagnosis of NMO spectrum disorder? *Neurol Neuroimmunol Neuroinflammation* [Internet]. 2015 [cited 2015 Feb 23];2. Available from: <http://www.ncbi.nlm.nih.gov/pmc/articles/PMC4309526/>
- Reindl M, Rostásy K. MOG antibody-associated diseases. *Neurol Neuroimmunol Neuroinflammation* [Internet]. 2015 [cited 2015 Dec 16];2. Available from: <http://www.ncbi.nlm.nih.gov/pmc/articles/PMC4309525/>
- Aktas O. Collateral benefit: the comeback of MOG antibodies as a biomarker in neurological practice. *J Neurol Neurosurg Psychiatry*. 2015;86:243.
- Ikedá K, Kiyota N, Kuroda H, Sato DK, Nishiyama S, Takahashi T, et al. Severe demyelination but no astrocytopathy in clinically definite neuromyelitis optica with anti-myelin-oligodendrocyte glycoprotein antibody. *Mult Scler J*. 2015;21:656–9.
- Spadaro M, Gerdes LA, Mayer MC, Ertl-Wagner B, Laurent S, Krumbholz M, et al. Histopathology and clinical course of MOG-antibody-associated encephalomyelitis. *Ann Clin Transl Neurol*. 2015;2:295–301.
- Di Pauli F, Höftberger R, Reindl M, Beer R, Rhomberg P, Schanda K, et al. Fulminant demyelinating encephalomyelitis: Insights from antibody studies and neuropathology. *Neurol Neuroimmunol Neuroinflammation*. 2015;2:e175.
- Jarius S, Metz I, König FB, Ruprecht K, Reindl M, Paul F, et al. Screening for MOG-IgG and 27 other anti-gial and anti-neuronal autoantibodies in "pattern II multiple sclerosis" and brain biopsy findings in a MOG-IgG-positive case. *Mult Scler J*. 2016. doi:10.1177/1352458515622986.
- Jarius S, Wildemann B, Paul F. Neuromyelitis optica: clinical features, immunopathogenesis and treatment. *Clin Exp Immunol*. 2014;176:149–64.
- Bennett JL, de Seze J, Lana-Peixoto M, Palace J, Waldman A, Schippling S, et al. Neuromyelitis optica and multiple sclerosis: Seeing differences through optical coherence tomography. *Mult Scler J*. 2015;21:678–88.
- Kaufhold F, Zimmermann H, Schneider E, Ruprecht K, Paul F, Oberwahrenbrock T, et al. Optic Neuritis Is Associated with Inner Nuclear Layer Thickening and Microcystic Macular Edema Independently of Multiple Sclerosis. *PLoS One*. 2013;8:e71145.
- Sotirchos ES, Saidha S, Byraiah G, Mealy MA, Ibrahim MA, Sepah YJ, et al. In vivo identification of morphologic retinal abnormalities in neuromyelitis optica. *Neurology*. 2013;80:1406–14.
- Martinez-Hernandez E, Sepulveda M, Rostásy K, et al. Antibodies to aquaporin 4, myelin-oligodendrocyte glycoprotein, and the glycine receptor $\alpha 1$ subunit in patients with isolated optic neuritis. *JAMA Neurol*. 2015;72:187–93.
- Akaishi T, Sato DK, Nakashima I, Takeshita T, Takahashi T, Doi H, et al. MRI and retinal abnormalities in isolated optic neuritis with myelin oligodendrocyte glycoprotein and aquaporin-4 antibodies: a comparative study. *J Neurol Neurosurg Psychiatry*. 2016;87(4):446–8.
- Ramanathan S, Reddel SW, Henderson A, Parratt JDE, Barnett M, Gatt PN, et al. Antibodies to myelin oligodendrocyte glycoprotein in bilateral and recurrent optic neuritis. *Neurol Neuroimmunol Neuroinflammation*. 2014;1:e40.
- Chalmoukou K, Alexopoulos H, Akrivou S, Stathopoulos P, Reindl M, Dalakas MC. Anti-MOG antibodies are frequently associated with steroid-sensitive recurrent optic neuritis. *Neurol Neuroimmunol Neuroinflammation*. 2015;2:e131.
- Jarius S, Ruprecht K, Kleiter I, Borisow N, Asgari N, Pitarokoli K, et al. MOG-IgG in NMO and related disorders: a multicenter study of 50 patients. Part 2: Epidemiology, clinical presentation, radiological and laboratory features, treatment responses, and long-term outcome. *J Neuroinflammation*. 2016. doi:10.1186/s12974-016-0718-0.
- Jarius S, Ruprecht K, Kleiter I, Borisow N, Asgari N, Pitarokoli K, et al. MOG-IgG in NMO and related disorders: a multicenter study of 50 patients. Part 1: Frequency, syndrome specificity, influence of disease activity, long-term course, association with AQP4-IgG, and origin. *J Neuroinflammation*. 2016. doi:10.1186/s12974-016-0717-1.
- Kurtzke JF. Rating neurologic impairment in multiple sclerosis: an expanded disability status scale (EDSS). *Neurology*. 1983;33:1444–52.
- Wingerchuk DM, Banwell B, Bennett JL, Cabre P, Carroll W, Chitnis T, et al. International consensus diagnostic criteria for neuromyelitis optica spectrum disorders. *Neurology*. 2015;85:177–89.
- Jarius S, Probst C, Borowski K, Franciotta D, Wildemann B, Stoecker W, et al. Standardized method for the detection of antibodies to aquaporin-4 based

- on a highly sensitive immunofluorescence assay employing recombinant target antigen. *J Neurol Sci.* 2010;291:52–6.
30. Jarius S, Wildemann B. Aquaporin-4 Antibodies (NMO-IgG) as a Serological Marker of Neuromyelitis Optica: A Critical Review of the Literature. *Brain Pathol.* 2013;23:661–83.
 31. Tewarie P, Balk L, Costello F, Green A, Martin R, Schippling S, et al. The OSCAR-IB Consensus Criteria for Retinal OCT Quality Assessment. *PLoS One.* 2012;7:e34823.
 32. Oberwahrenbrock T, Weinhold M, Mikolajczak J, Zimmermann H, Paul F, Beckers J, et al. Reliability of Intra-Retinal Layer Thickness Estimates. *PLoS One.* 2015;10:e0137316.
 33. Emmerson-Hanover R, Shearer DE, Creel DJ, Dustman RE. Pattern reversal evoked potentials: gender differences and age-related changes in amplitude and latency. *Electroencephalogr Clin Neurophysiol.* 1994;92:93–101.
 34. Holladay JT. Proper method for calculating average visual acuity. *J Refract Surg Thorofare NJ.* 1997;13:388–91.
 35. R Development Core Team. R: a language and environment for statistical computing [Internet]. Vienna, Austria: R Foundation for Statistical Computing; 2010. Available from: <http://www.R-project.org>
 36. Ratchford JN, Quigg ME, Conger A, Frohman T, Frohman EM, Balcer LJ, et al. Optical coherence tomography helps differentiate neuromyelitis optica and MS optic neuropathies. *Neurology.* 2009;73:302–8.
 37. Jarius S, Kleiter I, Ruprecht K, Asgari N, Pitarokoili K, Borisow N, et al. MOG-IgG in NMO and related disorders: a multicenter study of 50 patients. Part 3: Brainstem involvement - frequency, presentation and outcome. *J Neuroinflammation.* 2016. doi:10.1186/s12974-016-0719-z.
 38. Jarius S, Ruprecht K, Wildemann B, Kuempfel T, Ringelstein M, Geis C, et al. Contrasting disease patterns in seropositive and seronegative neuromyelitis optica: A multicentre study of 175 patients. *J Neuroinflammation.* 2012;9:14.
 39. Schneider E, Zimmermann H, Oberwahrenbrock T, Kaufhold F, Kadas EM, Petzold A, et al. Optical Coherence Tomography Reveals Distinct Patterns of Retinal Damage in Neuromyelitis Optica and Multiple Sclerosis. *PLoS One.* 2013;8:e66151.
 40. Bennett JL, de Seze J, Lana-Peixoto M, Palace J, Waldman A, Schippling S, et al. Neuromyelitis optica and multiple sclerosis: Seeing differences through optical coherence tomography. *Mult Scler.* 2015;21(6):678–88.
 41. Galetta SL, Villoslada P, Levin N, Shindler K, Ishikawa H, Parr E, et al. Acute optic neuritis. *Neurol Neuroimmunol Neuroinflammation* [Internet]. 2015 [cited 2016 Jun 2];2. Available from: <http://www.ncbi.nlm.nih.gov/pmc/articles/PMC4516397/>
 42. Trebst C, Jarius S, Berthele A, Paul F, Schippling S, Wildemann B, et al. Update on the diagnosis and treatment of neuromyelitis optica: Recommendations of the Neuromyelitis Optica Study Group (NEMOS). *J Neurol.* 2013;261:1–16.

Submit your next manuscript to BioMed Central and we will help you at every step:

- We accept pre-submission inquiries
- Our selector tool helps you to find the most relevant journal
- We provide round the clock customer support
- Convenient online submission
- Thorough peer review
- Inclusion in PubMed and all major indexing services
- Maximum visibility for your research

Submit your manuscript at
www.biomedcentral.com/submit



11.6 MOG-LONGITUDINAL [23]

Frederike C Oertel*, Olivier Outteryck, Benjamin Knier, Hanna Zimmermann, Nadja Borisow, Judith Bellmann-Strobl, Astrid Blaschek, Sven Jarius, Markus Reindl, Klemens Ruprecht, Edgar Meinel, Reinhard Hohlfeld, Friedemann Paul, Alexander U Brandt, Tania Kümpfel, Joachim Havla: **Optical Coherence Tomography in Myelin-Oligodendrocyte-Glycoprotein Antibody-Seropositive Patients: A Longitudinal Study**. Journal of Neuroinflammation, 2019.

Journal Data Filtered By: **Selected JCR Year: 2018** Selected Editions: SCIE,SSCI
 Selected Categories: **"NEUROSCIENCES"** Selected Category Scheme: WoS
Gesamtanzahl: 267 Journale

Rank	Full Journal Title	Total Cites	Journal Impact Factor	Eigenfactor Score
1	NATURE REVIEWS NEUROSCIENCE	43,107	33.162	0.068480
2	NATURE NEUROSCIENCE	63,390	21.126	0.164700
3	ACTA NEUROPATHOLOGICA	20,206	18.174	0.041660
4	BEHAVIORAL AND BRAIN SCIENCES	9,377	17.194	0.010240
5	TRENDS IN COGNITIVE SCIENCES	27,095	16.173	0.040040
6	JOURNAL OF PINEAL RESEARCH	10,695	15.221	0.010560
7	NEURON	95,348	14.403	0.218680
8	TRENDS IN NEUROSCIENCES	20,163	12.314	0.024480
9	Annual Review of Neuroscience	14,042	12.043	0.015020
10	MOLECULAR PSYCHIATRY	20,353	11.973	0.049290
11	BRAIN	52,970	11.814	0.074030
12	BIOLOGICAL PSYCHIATRY	43,122	11.501	0.053320
13	PROGRESS IN NEUROBIOLOGY	12,929	10.658	0.013230
14	Nature Human Behaviour	1,230	10.575	0.006550
15	SLEEP MEDICINE REVIEWS	6,920	10.517	0.010920
16	ANNALS OF NEUROLOGY	37,336	9.496	0.048630
17	Molecular Neurodegeneration	4,248	8.274	0.011350
18	NEUROSCIENCE AND BIOBEHAVIORAL REVIEWS	26,724	8.002	0.051580
19	FRONTIERS IN NEUROENDOCRINOLOGY	4,196	7.852	0.005490
20	Neurology-Neuroimmunology & Neuroinflammation	1,996	7.353	0.008220
21	NEUROPSYCHOPHARMACOLOGY	25,672	7.160	0.039090


Rank	Full Journal Title	Total Cites	Journal Impact Factor	Eigenfactor Score
22	Brain Stimulation	5,457	6.919	0.014470
23	NEUROPATHOLOGY AND APPLIED NEUROBIOLOGY	3,876	6.878	0.006420
24	NEUROENDOCRINOLOGY	5,046	6.804	0.005690
25	NEUROSCIENTIST	4,986	6.791	0.008520
26	BRAIN BEHAVIOR AND IMMUNITY	14,533	6.170	0.025700
27	BRAIN PATHOLOGY	5,263	6.155	0.007880
28	Alzheimers Research & Therapy	3,160	6.142	0.010700
29	JOURNAL OF NEUROSCIENCE	175,046	6.074	0.233460
30	JOURNAL OF CEREBRAL BLOOD FLOW AND METABOLISM	19,766	6.040	0.028050
31	PAIN	38,312	6.029	0.039070
32	CURRENT OPINION IN NEUROBIOLOGY	15,090	6.014	0.033650
33	Acta Neuropathologica Communications	3,063	5.883	0.014190
34	Translational Stroke Research	1,955	5.847	0.004330
35	GLIA	14,003	5.829	0.018760
36	NEUROIMAGE	99,720	5.812	0.132720
37	NEURAL NETWORKS	13,063	5.785	0.016060
38	NEUROPSYCHOLOGY REVIEW	2,971	5.739	0.003940
39	Molecular Autism	2,107	5.712	0.008000
40	Journal of Neuroinflammation	11,767	5.700	0.023240
41	Multiple Sclerosis Journal	11,501	5.649	0.022750
42	Annual Review of Vision Science	458	5.622	0.003300
43	Neurotherapeutics	4,475	5.552	0.009060
44	Translational Neurodegeneration	810	5.534	0.002420

RESEARCH

Open Access



Optical coherence tomography in myelin-oligodendrocyte-glycoprotein antibody-seropositive patients: a longitudinal study

Frederike C. Oertel^{1,2}, Olivier Outteryck³, Benjamin Knier⁴, Hanna Zimmermann^{1,2}, Nadja Borisow^{1,2}, Judith Bellmann-Strobl^{1,2}, Astrid Blaschek⁶, Sven Jarius⁷, Markus Reindl⁸, Klemens Ruprecht⁹, Edgar Meinl¹⁰, Reinhard Hohlfeld^{5,10}, Friedemann Paul^{1,2,9}, Alexander U. Brandt^{1,2,11*} , Tania Kümpfel¹⁰ and Joachim Havla^{10,12}

Abstract

Background: Serum antibodies against myelin-oligodendrocyte-glycoprotein (MOG-IgG) are detectable in a proportion of patients with acute or relapsing neuroinflammation. It is unclear, if neuro-axonal damage occurs only in an attack-dependent manner or also progressively. Therefore, this study aimed to investigate longitudinally intra-retinal layer changes in eyes without new optic neuritis (ON) in MOG-IgG-seropositive patients.

Methods: We included 38 eyes of 24 patients without ON during follow-up (F/U) [median years (IQR)] 1.9 (1.0–2.2) and 56 eyes of 28 age- and sex-matched healthy controls (HC). The patient group's eyes included 18 eyes without (Eye^{ON-}) and 20 eyes with history of ON (Eye^{ON+}). Using spectral domain optical coherence tomography (OCT), we acquired peripapillary retinal nerve fiber layer thickness (pRNFL) and volumes of combined ganglion cell and inner plexiform layer (GCIP), inner nuclear layer (INL), and macular volume (MV). High-contrast visual acuity (VA) was assessed at baseline.

Results: At baseline in Eye^{ON-}, pRNFL ($94.3 \pm 15.9 \mu\text{m}$, $p = 0.36$), INL ($0.26 \pm 0.03 \text{ mm}^3$, $p = 0.11$), and MV ($2.34 \pm 0.11 \text{ mm}^3$, $p = 0.29$) were not reduced compared to HC; GCIP showed thinning ($0.57 \pm 0.07 \text{ mm}^3$; $p = 0.008$), and VA was reduced ($\log\text{MAR } 0.05 \pm 0.15$ vs. -0.09 ± 0.14 , $p = 0.008$) in comparison to HC. Longitudinally, we observed pRNFL thinning in models including all patient eyes (annual reduction $-2.20 \pm 4.29 \mu\text{m}$ vs. $-0.35 \pm 1.17 \mu\text{m}$, $p = 0.009$) in comparison to HC. Twelve Eye^{ON-} with other than ipsilateral ON attacks ≤ 6 months before baseline showed thicker pRNFL at baseline and more severe pRNFL thinning in comparison to 6 Eye^{ON-} without other clinical relapses.

Conclusions: We observed pRNFL thinning in patients with MOG-IgG during F/U, which was not accompanied by progressive GCIP reduction. This effect could be caused by a small number of Eye^{ON-} with other than ipsilateral ON attacks within 6 months before baseline. One possible interpretation could be a reduction of the swelling, which could mean that MOG-IgG patients show immune-related swelling in the CNS also outside of an attack's target area.

Keywords: Optical coherence tomography, Optic neuritis, Myelin-oligodendrocyte-glycoprotein

Background

Antibodies against conformation-dependent epitopes of myelin-oligodendrocyte-glycoprotein (MOG-IgG) have

been described in patients with central nervous system (CNS) inflammation of putative autoimmune etiology [1–4]. MOG is also the dominant antigen for demyelinating antibodies in experimental autoimmune encephalomyelitis (EAE), the predominant animal model of multiple sclerosis (MS), and MOG-IgG can augment demyelination by cell-mediated and humoral immune responses [1]. In neuropathology studies, MOG-IgG are associated with MS-like pathology directed against myelin and oligodendrocytes and biopsies present a MS pattern II [5, 6]. MOG-IgG affinity-purified from the blood of patients with

* Correspondence: alexander.brandt@charite.de

¹Experimental and Clinical Research Center, Max Delbrueck Center for Molecular Medicine and Charité – Universitätsmedizin Berlin, Freie Universität Berlin, Humboldt-Universität zu Berlin and Berlin Institute of Health, Robert-Rössle-Straße 10, 13125 Berlin, Germany

²NeuroCure Clinical Research Center, Charité – Universitätsmedizin Berlin, Freie Universität Berlin, Humboldt-Universität zu Berlin and Berlin Institute of Health, Charitéplatz 1, 10117 Berlin, Germany

Full list of author information is available at the end of the article



optic neuritis (ON) enhanced inflammation and induced demyelination upon transfer into experimental animals indicating the pathogenic potential of MOG-IgG detected in the blood of these patients [7]. It is discussed whether MOG-IgG define a separate disease entity tentatively called MOG-IgG-associated diseases, MOG-IgG autoimmunity or MOG-IgG seropositive encephalomyelitis rather than being part of several autoimmune disorders, especially neuromyelitis optica spectrum disorders (NMOSD) [1, 3, 8, 9]. However, the bouquet of clinical phenotypes in MOG-IgG-associated diseases at clinical onset is not easy to differentiate and overlaps with aquaporin-4-IgG (AQP4-IgG)-seropositive NMOSD and in rare cases with MS [2, 10–12], although distinct clinical features such as seizures have been described [13–15]. ON is the most common manifestation and can lead to substantial neuro-axonal damage after multiple relapses, as shown in different cohorts [11, 16]. The pattern of retinal degeneration after ON seems to be similar in all MOG-IgG-seropositive cohorts as shown by optical coherence tomography (OCT) studies [11, 16]. OCT proved to be a precise and reproducible method for non-invasive visualization and quantification of retinal layers and plays a crucial role in analyzing retinal changes in various neuroinflammatory disorders [17–20]. In a cross-sectional study, MOG-IgG-related OCT features indicated subclinical pathology in eyes without a history of ON (Eye^{ON-}) [16]. However, no longitudinal OCT data is reported in MOG-IgG-associated diseases so far and the pattern of longitudinal retinal damage still remains elusive. Using OCT, we assessed retinal layer thinning as a marker of neuro-axonal damage in a cohort of MOG-IgG-seropositive patients without ON during follow-up (F/U). We aimed to investigate at baseline and longitudinally microstructural changes in MOG-IgG-seropositive patients, extending previous work in AQP4-IgG-seropositive NMOSD [21, 22].

Methods

Study populations

Twenty-four patients were seen and followed [F/U (years; median (inter-quartile-range (IQR))) 1.9 (1.0–2.2)] at four university tertiary care centers specialized in neuroimmunological diseases (Institute of Clinical Neuroimmunology, Ludwig Maximilians University (LMU), Munich, Germany, $N = 11$; NeuroCure Clinical Research Center, Charité – Universitätsmedizin Berlin, Germany, $N = 10$; Department of Neurology, University of Lille Hospital, Lille, France, $N = 1$; Department of Neurology, Klinikum Rechts der Isar, Technische Universität München (TUM), Munich, Germany, $N = 2$). Written informed consent was obtained from all patients participating in the study. The local ethics committees approved the study protocol in accordance with the Declaration of Helsinki

(1964) in its currently applicable version. All patients were matched by age ($W = 370$, $p = 0.542$) and sex ($\chi^2 = 0.937$, $p = 0.333$) to 56 eyes of 28 healthy controls (HC; F/U [years; median (IQR)] 1.9 (1.9–2.3) from the NeuroCure Clinical Research Center, Charité – Universitätsmedizin Berlin, Germany. Inclusion criteria were the detection of MOG-IgG, complete longitudinal clinical and OCT imaging data with minimum F/U of 8 months and age between 15 and 75 years at baseline. Only eyes without concomitant potentially confounding diseases (glaucoma, diabetes mellitus, retinal surgery, retinal disease, ametropia > 6 diopters) were included. Eyes with a history of ON ≤ 5 months before baseline were excluded. Clinical data (diagnosis, disease onset, number of ON, date last ON, brain attacks, myelitis, EDSS, relapses, treatment history) were collected for all patients. For detection of MOG-IgG, serum samples from all patients were analyzed at least once by established cell-based assays at the discretion of each center using the laboratory's cutoffs (MOG IFT, EUROIMMUN, Laboratory Stöcker, Germany; Molecular Neuroimmunology Group, University Heidelberg, Heidelberg, Germany; Reindl Lab, Medical University of Innsbruck, Innsbruck, Austria; Meinel Lab, LMU, Munich, Hemmer Lab, TUM, Munich) [3, 7, 23].

Optical coherence tomography

All centers used SPECTRALIS spectral-domain OCT (Heidelberg Engineering, Heidelberg, Germany) with automatic real-time (ART) function for image averaging. We acquired peripapillary retinal nerve fiber layer thickness (pRNFL) and volumes of combined ganglion cell and inner plexiform layer (GCIP), inner nuclear layer (INL) and macular volume (MV) by OCT. GCIP, INL and MV were calculated as a 3 mm diameter cylinder around the fovea from a macular volume scan ($25^\circ \times 30^\circ$, 61 vertical B-scans, $12 \leq \text{ART} \leq 18$; $20^\circ \times 20^\circ$, 25 vertical B-scans, $27 \leq \text{ART} \leq 49$). The peripapillary RNFL (pRNFL) was measured with activated eye tracker using ring scans around the optic nerve (12° , 1536 A-scans, $57 \leq \text{ART} \leq 100$) or the most inner ring of a star-and-ring scan around the optic nerve (12° , 768 A-scans, $27 \leq \text{ART} \leq 33$). For two patients (8.3%), the ring scan protocol changed during the acquisition period (ring scan to inner ring of a star-and-ring scan). Segmentation of all layers was performed semi-automatically using software provided by the OCT manufacturer (Eye Explorer 1.9.10.0 with viewing module 6.3.4.0, Heidelberg Engineering, Heidelberg, Germany). Experienced raters (BK for TU Munich data, JH for all other data) carefully checked all scans for sufficient quality and segmentation errors and corrected if necessary. OCT data in this study is reported and analyzed according to the APOSTEL and OSCAR-IB recommendations

[24, 25]. Macular microcysts were defined as the presence of cystic lesions on at least one scan detected by experienced raters (BK for TU Munich scans, JH for all other scans). Additionally, we collected habitually corrected monocular high-contrast visual acuity (VA) using ETDRS (Early Treatment Diabetic Retinopathy Study) charts at baseline in 20 ft distance for a subset of patients ($N = 15$).

Statistical methods

Group differences between MOG-IgG patients and HC were tested by chi-squared test for sex and Wilcoxon rank-sum test for age. Main outcomes were change of GCIP, pRNFL, INL and MV and VA over F/U. Cross-sectional differences of OCT values and VA between all groups were analyzed pairwise by generalized estimating equation (GEE) models to account for inter-eye within-patient correlations of monocular measurements. Longitudinal analyses of OCT and VA were performed with linear mixed effects models using time from baseline and group as fixed effects and patient-ID and eye-ID as random effects; results are reported for effect “Time from Baseline * Group”, which reflects the group-specific change over time. Annual loss was estimated for each individual as change to baseline at last visit divided by F/U time in years. All tests and graphical representations were performed with R version 3.3.1 [<http://www.R-project.org>]. Statistical significance was established at $p < 0.05$, and all results were interpreted in the context of an exploratory analysis and therefore not adjusted for multiple comparison.

Results

Cohort description and follow-up

We included 38 eyes of 24 patients without ON during F/U. 70% of the patients from Berlin [7/10] and 64% of the patients from LMU Munich [7/11] have been included in previous cross-sectional studies [7, 10, 16]. MOG-IgG-seropositive patients had the following diagnosis: recurrent ON ($N = 7$), MOG-IgG-seropositive NMOSD ($N = 12$) meeting the 2015 IPND (International Panel for Neuromyelitis Optica Diagnosis) criteria for seronegative NMOSD [26], MOG-IgG-seropositive MS ($N = 3$) and MOG-IgG-seropositive meningoencephalomyelitis ($N = 2$). All patients had ≥ 1 F/U visit(s) [median (range) 2 visits (2–7)]. The MOG-IgG-seropositive cohort included 18 eyes without (Eye^{ON^-}) and 20 eyes with a history of ON (Eye^{ON^+}) (number of ONs [median (range)] 0 (0 – 8); time since ON in years [median (range)] 2.2 (0.4 – 14.9)). From the 18 Eye^{ON^-} , we identified 12 eyes with other than ipsilateral ON attacks within 6 months before baseline (five eyes of three patients with a myelitis, four eyes of two patients with myelitis and brainstem attacks, one eye of one patient

with myelitis and contralateral ON and 2 eyes of 2 patients with contralateral ON; age 40 ± 9 , male/female 5/3, EDSS 2.5, median follow-up 14 ± 5.9 months) and six eyes without other attacks (age 39.0 ± 21.0 , male/female 1/4, EDSS 3.5, median follow-up 26 ± 4.5 months). Retrospectively, one patient (2 eyes) could not be included in the study analysis because he had ONs on both sides during F/U and another patient (2 eyes) could not be included because he had insufficient follow-up less than 8 months. Data of further 8 eyes had to be excluded (five eyes with ON during F/U, one eye with ON less than 5 months before study inclusion, one eye with missing data, one eye with OCT-confounding disease). Clinical characteristics of all included patients are shown in Table 1.

Group differences at baseline

First, we analyzed group differences at baseline between MOG-IgG-seropositive patient eyes with a history of ON (Eye^{ON^+}), patient eyes without previous ON (Eye^{ON^-}) and eyes from HC. At baseline, in Eye^{ON^-} , pRNFL, INL and MV were not significantly different, but GCIP was significantly thinner in comparison to HC ($p = 0.008$) (Table 2, Fig. 1). VA was lower in Eye^{ON^-} in comparison to HC ($p = 0.013$).

In Eye^{ON^+} at baseline pRNFL, GCIP and MV were significantly lower in comparison to HC (pRNFL $p < 0.0001$, GCIP $p < 0.0001$, MV $p < 0.0001$). In contrast, INL was significantly thicker in Eye^{ON^+} (INL 0.30 ± 0.05 mm³ vs. 0.27 ± 0.03 mm³ ($p = 0.046$)). VA was also lower in Eye^{ON^+} (0.55 ± 0.81) in comparison to HC [-0.09 (0.14), $p = 0.01$] and Eye^{ON^-} [0.05 (0.15), $p = 0.058$].

One Eye^{ON^-} showed a massive thinness of the pRNFL at baseline despite a missing history of ON. We found macular microcysts within the INL in 6/20 (30%) Eye^{ON^+} .

OCT changes during F/U

Longitudinally, we observed pRNFL thinning, which was not accompanied by progressive GCIP reduction, in eyes without ON during F/U (annual loss: -2.20 ± 4.29 μm vs. HC -0.35 ± 1.17 μm , $p = 0.009$) (Fig. 2; individual changes in Additional file 1). There were no longitudinal group differences between Eye^{ON^+} and Eye^{ON^-} for GCIP, pRNFL, INL and MV as well as between MOG-IgG-seropositive NMOSD and other MOG-IgG-seropositive patients (Table 3). In a previous study investigating spinal cord changes in MOG-IgG patients, we suspected edematous changes in patients close to a clinical attack [27]. We therefore investigated patients with a non-ipsilateral ON attack within 6 months of the baseline visit in a subgroup analysis. At baseline, the pRNFL in 12 Eye^{ON^-} with a non-ipsilateral ON attack within the 6 months before baseline was thicker in comparison to 6 Eye^{ON^-} without a non-ipsilateral ON attack within the 6

Table 1 Clinical characteristics of patients. Age ($W = 370$, $p = 0.542$) and sex ($\chi^2 = 0.937$, $p = 0.333$) did not differ between MOG-IgG-seropositive patients and HCs

	HC	MOG-IgG-seropositive patients
Subjects [N]	28	24
Number of eyes [N]	56	38
F/U [median years (min, max)]	1.9 (0.8–3.3)	1.9 (0.6–2.8)
Age [mean (SD)]; [range at baseline]	43.12 (9.76); [11–68]	40.66 (13.53); [15–68]
Sex [male (%)]	6 (21.4)	9 (37.5)
Clinical phenotypes (MOG-IgG-associated diseases)	–	ON ($N = 7$), NMOSD ($N = 12$), MS ($N = 3$), meningoencephalomyelitis ($N = 2$)
EDSS at baseline [median (IQR)]	–	2.5 (2.0; 3.0)
Disease duration at baseline in years [median (IQR)]	–	3.0(1.1; 8.8)
Eyes with a history of ON [Eye ^{ON+} , N (%)]	–	20 (52.6%)
Patients with a history of ON [N (%)]	–	15 (62.5%)
Number of ON in Eye ^{ON+} [median (range)]	–	2 (1–8)
Eyes without a history of ON [Eye ^{ON-} , N (%)]	–	18 (47.4%)
Time since ON [years; median (range)]	–	2.2 (0.4–14.9)
Eyes with contralateral ON during F/U [N (%)]	–	5 (13.2)
Treatment at baseline [N]	–	AZA [4], MTX [1], NAT [1], RIX [8], IVIG [1], PRED [2], NONE [7]

Abbreviations: HC healthy controls, N number, SD standard deviation, F/U follow-up, AZA azathioprine, MTX methotrexate, NAT natalizumab, RIX rituximab, IVG intravenous immunoglobulins, PRED prednisone, TOC tocilizumab, MMF mycophenolate mofetil, NONE no treatment

months before baseline (pRNFL $100.2 \pm 12.7 \mu\text{m}$ vs. $82.7 \pm 16.2 \mu\text{m}$ ($p = 0.019$)) (Fig. 3A). Reduction of pRNFL thickness was seen mainly in 3 eyes of the subgroup analysis. Two of the 3 eyes had no clinical evidence of unilateral ON attacks of the contralateral eye within the 6 months prior to inclusion in the study. One of the 3 eyes had a relapse complex with myelitis, brain attack and contralateral ON within 6 months prior to baseline. An ON-affection of these 12 Eye^{ON-} with a non-ipsilateral ON attack was further ruled out by a stable high-contrast visual acuity (HCVA) without a change during F/U (HCVA as decimal, median (range): at baseline 1.0 (0.6–1.1); at last visit 1.0 (0.6–1.6)). A

longitudinal graphical display of Eye^{ON-} showed the pRNFL thinning to be predominantly present in Eye^{ON-} with an attack before baseline (Fig. 3B). However, due to the small sample size, no statistical analysis could be performed.

Discussion

In this study, we investigated longitudinally, MOG-IgG-seropositive patients for potential progressive or covert damage in the retina in the absence of new clinical ON. We could not detect progressive GCIP thinning during F/U in MOG-IgG-seropositive patients, which is in contrast to progressive GCIP

Table 2 Baseline OCT results of MOG-IgG-seropositive patients and HCs

Baseline results	HC	MOG-IgG-seropositive patients Eye ^{ON-}	MOG-IgG-seropositive patients Eye ^{ON+}	HC vs Eye ^{ON-}			HC vs Eye ^{ON+}			Eye ^{ON-} vs Eye ^{ON+}		
	N (eyes) = 56	N (eyes) = 18	N (eyes) = 20	[β]	[SE]	[p]	[β]	[SE]	[p]	[β]	[SE]	[p]
GCIP [mean (SD)]	0.63 (0.04)	0.57 (0.07)	0.39 (0.12)	-0.057	0.022	0.008	-0.235	0.033	< 0.0001	-0.178	0.037	< 0.0001
pRNFL [mean (SD)]	98.50 (9.17)	94.33 (15.92)	58.25 (22.56)	-4.167	4.577	0.360	-40.25	5.864	< 0.0001	-36.08	6.311	< 0.0001
INL [mean (SD)]	0.27 (0.03)	0.26 (0.03)	0.30 (0.05)	-0.014	0.009	0.110	0.026	0.013	0.046	0.041	0.014	0.004
MV [mean (SD)]	2.37 (0.10)	2.34 (0.11)	2.19 (0.13)	-0.036	0.034	0.290	-0.183	0.039	< 0.0001	-0.147	0.042	0.0005
HCVA in logMAR [mean (SD)]	-0.09 (0.14)	0.05 (0.15)	0.55 (0.81)	0.146	0.059	0.013	0.394	0.134	0.0032	0.248	0.131	0.058

Abbreviations: B estimate, GCIP combined ganglion cell and inner plexiform layer, HC healthy control, INL inner nuclear layer, Eye^{ON-} MOG-IgG-seropositive patients without a history of ON, Eye^{ON+} MOG-IgG-seropositive patients with a history of ON, OCT optical coherence tomography, ON optic neuritis, p p value, pRNFL peripapillary retinal nerve fiber layer, SD standard deviation, SE standard error, MV macular volume, vs versus, N number of eyes

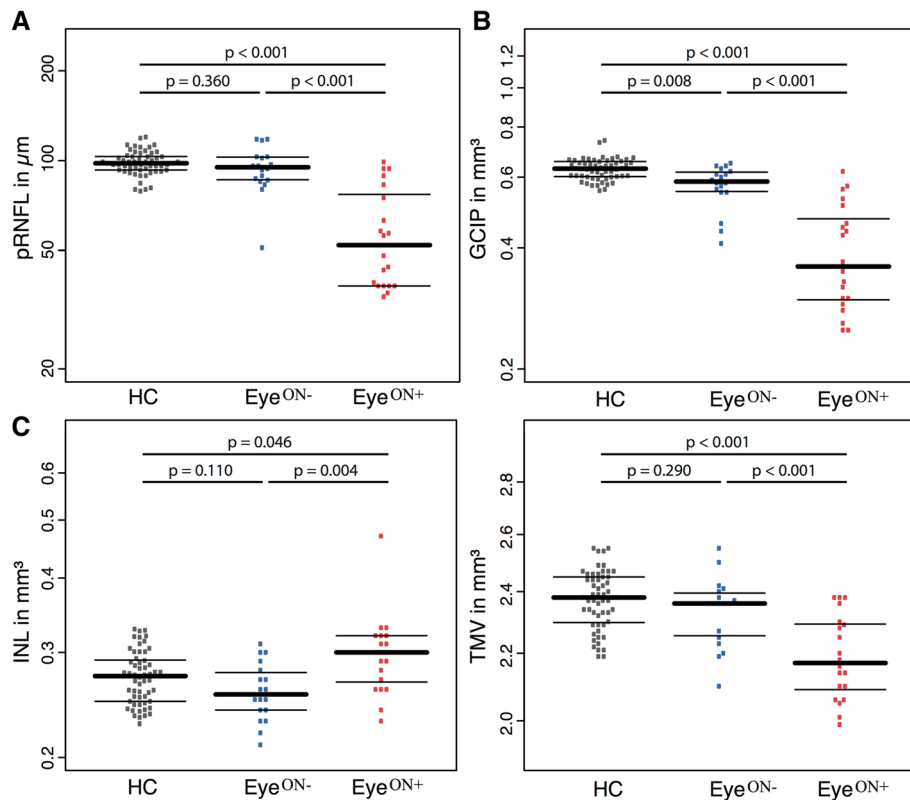


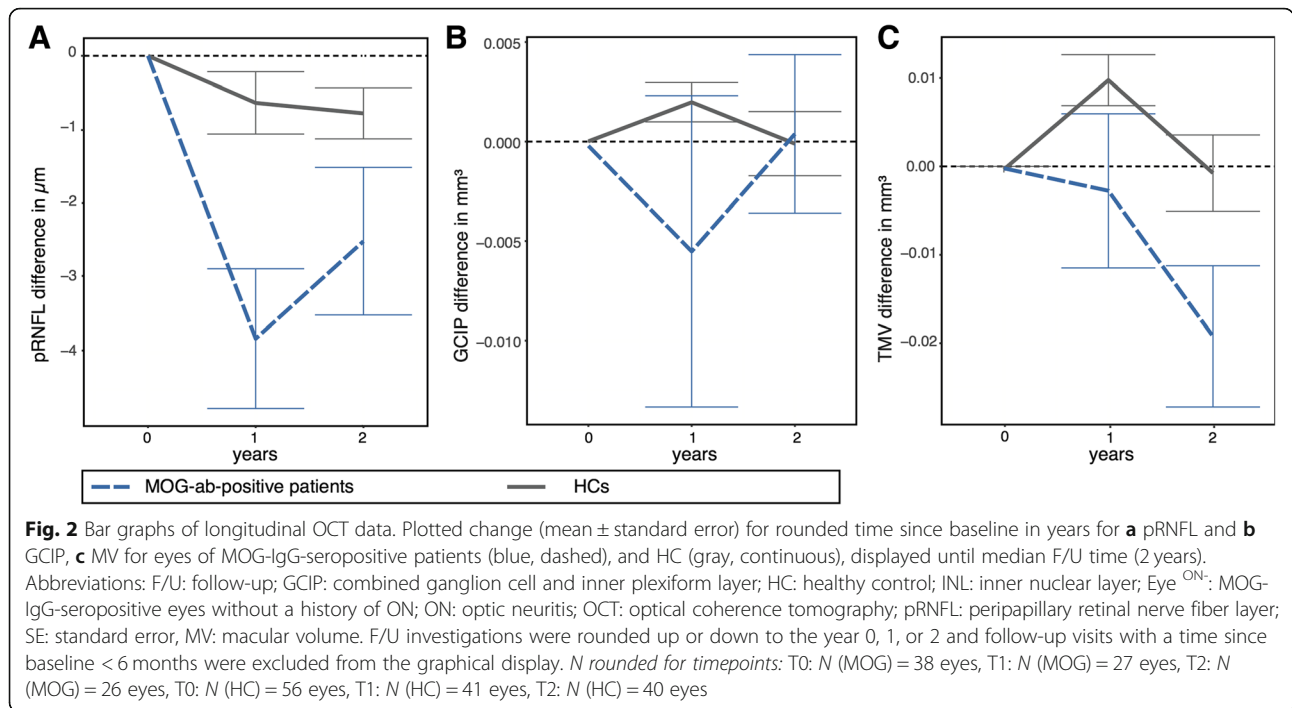
Fig. 1 Baseline data: bee swarm plots of cross-sectional OCT data for HC (gray, left), MOG-IgG-seropositive Eye^{ON-} (blue, middle) and MOG-IgG-seropositive Eye^{ON+} (red, right) (median \pm IQR, single eyes as dots) for **a** pRNFL, **b** GCIP, **c** INL, and **d** MV. Abbreviations: Eye^{ON-}: MOG-IgG-seropositive eyes without a history of ON; Eye^{ON+}: MOG-IgG-seropositive eyes with a history of ON; GCIP: combined ganglion cell and inner plexiform layer; HC: Healthy control; INL: inner nuclear layer; IQR: inter-quartile range; OCT: Optical coherence tomography; p: *p* value; pRNFL: peripapillary retinal nerve fiber layer; MV: macular volume

reduction in AQP4-IgG-seropositive NMOSD and MS [22, 27]. Instead, we observed a longitudinal pRNFL reduction, which in a consequent subgroup analysis appeared to primarily occur in patients with non-ipsilateral ON attacks within 6 months before baseline. A hypothetical explanation of this finding could be a remission of pRNFL edema.

Cross-sectional retinal imaging studies have shown conflicting results as to whether MOG-IgG-associated diseases have a more favorable outcome compared to patients with ON in other disease contexts [28–34]. The presumed higher relapse rates in MOG-IgG-seropositive patients could be associated with a severe retinal neuroaxonal loss and an unfavorable visual outcome [11]. Although OCT data regarding MOG-IgG-associated retinal damage are inconsistent [11, 16, 30, 35], neuroaxonal retinal damage may occur as a consequence of clinical episode(s) of ON or of subclinical involvement [11, 16]. ON was associated with macular microcysts, a biomarker suggestive of severe optic neuropathy [16, 36,

37]. A previous study investigating a smaller cohort of MOG-IgG-positive patients showed a significant reduction of the pRNFL and the ganglion cell layer in Eye^{ON-} compared to HC cross-sectionally [16]. By contrast, in our current study, we could only confirm a significant GCIP reduction in Eye^{ON-} at baseline but no significant reduction of the pRNFL as a hint towards subclinical retinal pathology. However, pRNFL edema as a marker of immune-related swelling in the CNS after relapses and also outside of relapses could have contributed to this finding. The GCIP reduction at baseline could be discussed as progressive neurodegenerative retinal involvement, subclinical optic nerve pathology, chiasmal crossover of ON in contralateral eyes, or as an expression of subclinical ON in the previous patient's history. However, according to Ramanathan et al., only 5% of ONs in MOG-IgG-seropositive patients shows chiasmal involvement [38].

Longitudinally, we observed pRNFL but not GCIP thinning. We hypothesize that this can be explained not only



by subclinical retinal or optic nerve involvement or drug-induced retinal damage related to immunosuppressive treatment, but also by a remission of non-ipsilateral ON attacks that has occurred in Eye^{ON-} within 6 months before baseline since patients without clinical attacks ≤ 6 months before baseline did not present significant pRNFL or GCIP loss during F/U. This is clearly in contrast to our recently published data about longitudinal GCIP thinning in AQP4-IgG-seropositive NMOSD [22] or earlier studies reporting GCIP loss in MS [27] and might be an important hint towards the differentiation of MOG-IgG-associated diseases from AQP4-IgG-seropositive NMOSD. AQP4-IgG-seropositive NMOSD is an astrocytopathy, and a primary retinopathy caused by antibody-mediated

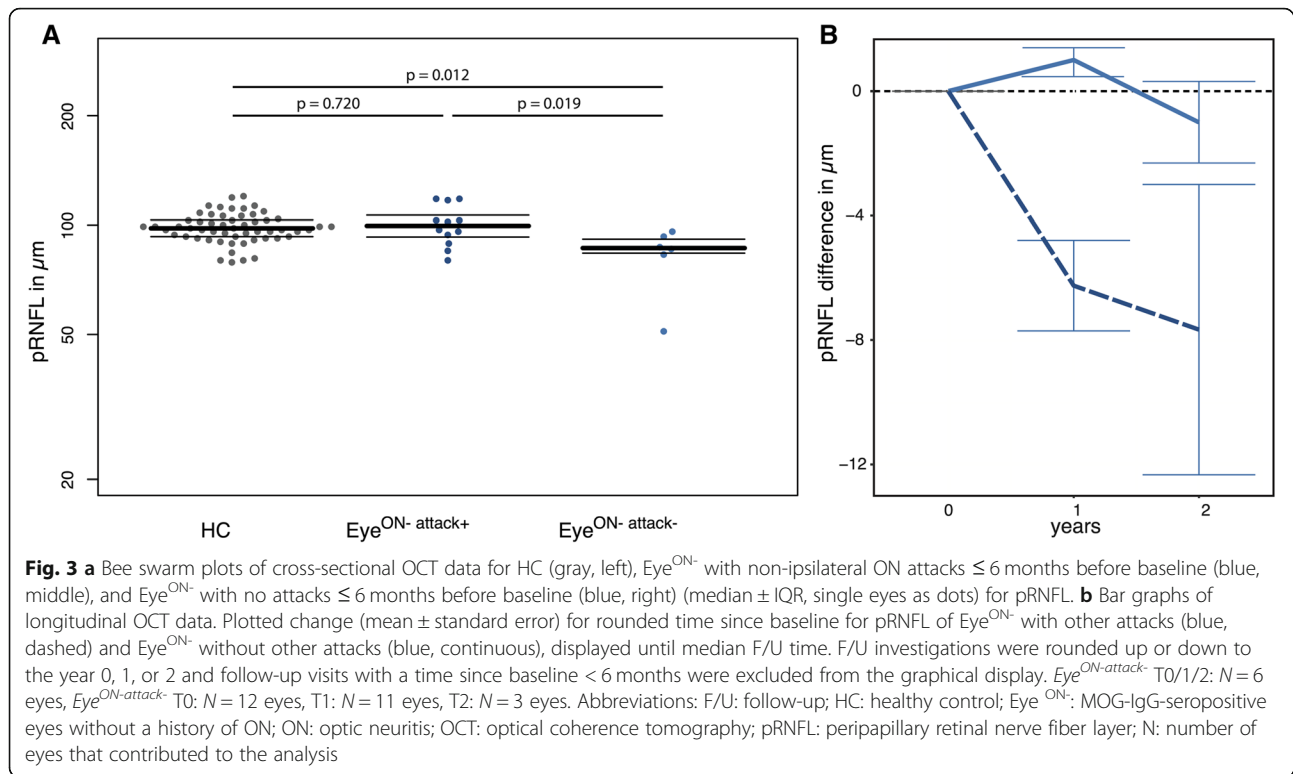
damage is supported by animal studies and recently also clinical studies [22, 39]. In contrast, the retina does not harbor myelin-producing oligodendrocytes and an expression of MOG has not been shown, making a primary retinopathy unlikely.

Further, data showing clear differences between AQP4-IgG-seropositive NMOSD and MOG-IgG-associated diseases were presented recently by Chien et al. [40]. Spinal cord imaging data showed differences in spinal cord affection patterns and disability accumulation. A higher prevalence of myelitis with clinical attacks and chronic spinal cord lesions was detected for AQP4-IgG-seropositive NMOSD patients in comparison to MOG-IgG-associated diseases [40]. Interestingly, MOG-IgG-seropositive

Table 3 Longitudinal OCT results of MOG-IgG-seropositive patients and HCs

Longitudinal OCT data	HC	MOG-IgG-seropositive patients Eye ^{ON-}	MOG-IgG-seropositive patients Eye ^{ON+}	HC vs MOG-IgG-seropositive patients (Eye ^{ON-} and Eye ^{ON+})				Eye ^{ON-} vs Eye ^{ON+}			
				[B]	[95%CI]	[SE]	[p]	[B]	[95%CI]	[SE]	[p]
Absolute change to baseline											
	<i>N</i> (eyes) = 56	<i>N</i> (eyes) = 18	<i>N</i> (eyes) = 20								
GCIP [mean (SD)]	0.00 (0.01)	0.00 (0.01)	0.00 (0.05)	-0.000	-0.004; 0.005	0.002	0.884	-0.006	-0.016; 0.003	0.005	0.214
pRNFL [mean (SD)]	-0.61 (2.00)	-4.5 (5.89)	-1.60 (4.48)	-1.645	-2.819; -0.471	0.599	0.009	0.168	-1.380; 1.717	0.790	0.832
INL [mean (SD)]	0.00 (0.01)	0.01 (0.02)	0.00 (0.03)	0.002	-0.002; 0.005	0.002	0.312	-0.003	-0.011; 0.004	0.004	0.381
MV [mean (SD)]	0.00 (0.02)	-0.01 (0.04)	-0.01 (0.05)	-0.008	-0.016; 0.0013	0.004	0.103	0.002	-0.013; 0.018	0.008	0.769

Abbreviations: 95%CI 95% confidence interval, B Estimate (beta-coefficient), GCIP combined ganglion cell and inner plexiform layer, HC healthy control, INL inner nuclear layer, Eye^{ON-} MOG-IgG-seropositive patients without a history of ON, Eye^{ON+} MOG-IgG-seropositive patients with a history of ON, OCT optical coherence tomography, p p value, pRNFL peripapillary retinal nerve fiber layer, SD standard deviation, SE standard error, MV macular volume, vs versus, N number of eyes



patients showed a swelling of the upper cervical cord area during other non-myelitis attacks, also pointing towards a systemic inflammatory affection in MOG-IgG-associated diseases as potentially shown here in the pRNFL during different attacks [40]. Our data is in line with the conclusion that AQP4-IgG-seropositive NMOSD and MOG-IgG-associated diseases are distinct immunological disorders, but share common clinical patterns [22, 40–42].

Limitations of our study are the heterogeneity of MOG-IgG-seropositive patients with different clinical phenotypes in our cohort, the heterogeneity of immunosuppressive treatments of our patients, and due to the rarity of MOG-IgG-seropositive patients in Europe, the small sample size, which leads to outliers possibly having a larger effect on the results, short and variable F/U, and the evaluation of MOG-IgG by different labs using different assays. Additionally, our study lacks magnetic resonance imaging data on optic nerve lesion lengths and lesion volumes of the afferent visual system as well as whole-brain lesion volume to further evaluate subclinical retinal atrophy in MOG-IgG-associated diseases.

Conclusions

We report in this small explorative study of MOG-IgG-associated diseases no evidence of GCIP thinning during F/U. Additionally, we found pRNFL reduction without GCIP loss during F/U predominantly in Eye^{ON-} with

other than ipsilateral ON attacks ≤ 6 months before baseline. We will investigate in a planned longitudinal study involving more centers, whether this reduction is actually due to a remission of edema or reflects retinal neurodegenerative processes or drug-induced retinal damage related to aggressive immunosuppressive treatment.

Additional file

Additional file 1: Figure S1. Spaghetti plots of longitudinal OCT data. Plotted absolute values of all subjects for time since baseline in years for (A) pRNFL and (B) GCIP, (C) MV for eyes of MOG-IgG-seropositive patients (turquoise) and HC (red), as well as (D) plotted absolute values of all Eye^{sON-} with (green) and without (red) an attack in the 6 months before baseline. Abbreviations: GCIP: Combined ganglion cell and inner plexiform layer, HC: Healthy control, Eye^{ON-}: MOG-IgG-seropositive eyes without a history of ON, ON: Optic neuritis, OCT: Optical coherence tomography, pRNFL: Peripapillary retinal nerve fiber layer, MV: Macular volume. (TIFF 47160 kb)

Abbreviations

AQP4-IgG: Aquaporin-4 antibodies; ART: Automatic real time; B: Estimate; CNS: Central nervous system; EAE: Experimental autoimmune encephalomyelitis; EDSS: Expanded disability status scale; Eye^{ON-}: Eyes without a history of optic neuritis; Eye^{ON+}: Eyes with a history of optic neuritis; F/U: Follow-up; GCIP: Combined ganglion cell and inner plexiform layer; GEE: Generalized estimated eq.; HC: Healthy control; INL: Inner nuclear layer; IQR: Inter-quartile range; LMU: Ludwig-Maximilians University Munich; MOG-IgG: Myelin-oligodendrocyte glycoprotein antibodies; MS: Multiple sclerosis; N: Number; NCRC: NeuroCure Clinical Research Center Berlin; NMOSD: Neuromyelitis optica spectrum disorders; OCT: Optical coherence tomography; ON: Optic neuritis; *p*: *p* value; pRNFL: Peripapillary retinal nerve

fiber layer; SD: Standard deviation; SE: Standard error; MV: Macular volume; TUM: Technical University Munich; VA: Visual acuity

Acknowledgements

We acknowledge support from the German Research Foundation (DFG) and the Open Access Publication Funds of Charité-Universitätsmedizin Berlin. JH and FCO like to thank Charlotte Bereuter, Angelika Bamberger, Luise Böhm, and Ivonne Hinz for their excellent technical support. SJ would like to thank Mrs. Anna Eschlbeck and the Nikon Imaging Center at the University of Heidelberg for excellent technical assistance. MR would like to thank Mrs. Kathrin Schanda for excellent technical assistance.

Authors' contributions

FCO participated in the design of the study, collected data, performed OCT quality check (BERLIN), performed the statistical analysis, contributed to the interpretation of the results, and drafted the manuscript. OO acquired OCT and clinical and visual function data and performed OCT quality check (LILLE). BK acquired OCT and clinical and visual function data and performed OCT quality check and segmentation (TUM). HZ acquired OCT and visual function data (BERLIN). NB and JBS acquired clinical data and participated in the coordination of the cohort study (BERLIN). AB acquired OCT and visual function data and performed OCT quality check (LMU). SJ performed the MOG-IgG assays. MR, KR, EM, RH, TK, and FP participated in the study design and coordination. AUB conceived the study and participated in its design, coordination as well as contributed to the interpretation of the results and supervised the statistical analyses. JH participated in the design of the study and the coordination, collected data, acquired OCT and clinical and visual function data (LMU), performed OCT segmentation (all centers apart from TUM), contributed to the interpretation of the results, and drafted the manuscript. All authors were involved in revising the manuscript for intellectual content and read and approved the final manuscript.

Funding

The project was supported with grants from the German Ministry for Education and Research (BMBF/KKNMS; Competence Network Multiple Sclerosis (to FP, KR, EM, BK), from the Deutsche Forschungsgemeinschaft (DFG, grant Exc. 257 to FP, AUB; DFG SFB TR128 to EM, RH), from the German Federal Ministry of Economic Affairs and Energy (EXIST 03EFEBE079 to AUB), from the German Ministry of Education and Research (N2-ADVISIMS 16GW0079 to FP and AUB), from the National Multiple Sclerosis Society (to FP), from the Guthy-Jackson Charitable Foundation (to FP, AUB), from the German Federal Ministry of Education and Research under 01ZZ1603[A-D] and 01ZZ1804[A-H] (DIFUTURE) and Friedrich-Baur-Stiftung (to JH) and from Novartis (to HZ, BK), from intramural funding of the Technical University of Munich (to BK), from the Verein zur Therapieforschung für MS Kranke (to EM).

Availability of data and materials

The datasets used and/or analyzed during the current study are available from the corresponding author on reasonable request.

Ethics approval and consent to participate

Twenty-four patients were seen at four university tertiary care centers specialized in neuroimmunological diseases (Institute of clinical Neuroimmunology, Ludwig-Maximilians University (LMU), Munich, NeuroCure Clinical Research Center, Charité – Universitätsmedizin Berlin, Germany; Department of Neurology, University of Lille Hospital, Lille, France; Department of Neurology, Klinikum Rechts der Isar, Technische Universität München (TUM), Munich, Germany). Written informed consent was obtained from all patients participating in the study. The local ethics committees approved the study protocol in accordance with the Declaration of Helsinki (1964) in its currently applicable version.

Consent for publication

Not applicable

Competing interests

JH reports a grant for OCT research from the Friedrich-Baur-Stiftung; personal fees and non-financial support from Merck, Novartis, Roche, Bayer Healthcare, Santhera, Biogen, Sanofi Genzyme; and non-financial support of the Guthy-Jackson Charitable Foundation, all outside the submitted work. FCO was an employee of

Nocturne UG, unrelated to this work. OO reports grant for research from Novartis-Pharma and grants and personal fees from Biogen, Genzyme, Merck, Novartis-Pharma, and Teva-Pharma, outside the submitted work. BK reports grants from the Bundesministerium für Bildung und Forschung (Kompetenznetz Multiple Sklerose KKNMS), intramural funding from the Technical University of Munich (KKF program) and a grant from Novartis unrelated to this study. HZ reports a research grant from Novartis related to this study and speaking fees from Teva unrelated to this study. LB has nothing to disclose. JBS has received travel grants and speaking fees from Bayer Healthcare, Biogen Idec, Merck Serono, Sanofi-Aventis/Genzyme, Teva Pharmaceuticals unrelated to this study. SJ has nothing to disclose. The Neurological Research Laboratory (Medical University of Innsbruck and Tirol Kliniken, MR) receives payments for antibody assays (AQP4- and anti-neuronal antibodies) and for AQP4- and MOG-antibody validation experiments organized by Euroimmun (Germany). KR was supported by the German Ministry of Education and Research (BMBF/KKNMS, Competence Network Multiple Sclerosis) and has received research support from Novartis and Merck Serono as well as speaking fees and travel grants from Guthy Jackson Charitable Foundation, Bayer Healthcare, Biogen Idec, Merck Serono, Sanofi-Aventis/Genzyme, Teva Pharmaceuticals, Roche and Novartis. EM received an honorarium from Roche, Novartis and Genzyme, and grant support from Novartis and Genzyme. RH received research grants and/or speaker honoraria from Actelion, Genzyme-Sanofi, Novartis, Immunic, Roche. FP reports research grants and speaker honoraria from Bayer, Teva, Genzyme, Merck, Novartis, MedImmune and is a member of the steering committee of the OCTIMS study (Novartis), all unrelated to this work. AUB is the founder and holds shares of Motognosis and Nocturne. He is named as an inventor on several patent applications describing serum biomarkers for MS, perceptive visual computing for tracking of motor dysfunction and OCT image analysis. TK received travel expenses and personal compensations from Bayer Healthcare, Teva Pharma, Merck, Novartis Pharma, Sanofi-Aventis/Genzyme, Roche, and Biogen as well as grant support from Bayer-Schering AG, Novartis and Chugai Pharma, unrelated to this work.

Author details

¹Experimental and Clinical Research Center, Max Delbrück Center for Molecular Medicine and Charité – Universitätsmedizin Berlin, Freie Universität Berlin, Humboldt-Universität zu Berlin and Berlin Institute of Health, Robert-Rössle-Straße 10, 13125 Berlin, Germany. ²NeuroCure Clinical Research Center, Charité – Universitätsmedizin Berlin, Freie Universität Berlin, Humboldt-Universität zu Berlin and Berlin Institute of Health, Charitéplatz 1, 10117 Berlin, Germany. ³Department of Neurology and Neuroradiology, Roger Salengro Hospital, University of Lille, INSERM 1171, Avenue du Professeur Emile Laine, 59037 Lille, France. ⁴Department of Neurology, Klinikum Rechts der Isar, Technische Universität München, Ismaninger Straße 22, 81675, Munich, Germany. ⁵Munich Cluster for Systems Neurology, Feodor-Lynen-Str 17, 81377 Munich, Germany. ⁶Department of Pediatric Neurology and Developmental Medicine, Dr. von Hauner's Children's Hospital, University of Munich, Lindwurmstraße 4, 80337 Munich, Germany. ⁷Molecular Neuroimmunology Group, Department of Neurology, University of Heidelberg, Im Neuenheimer Feld 400, 69120 Heidelberg, Germany. ⁸Clinical Department of Neurology, Medical University of Innsbruck, Anichstraße 35, 6020 Innsbruck, Austria. ⁹Department of Neurology, Charité – Universitätsmedizin Berlin, Freie Universität Berlin, Humboldt-Universität zu Berlin and Berlin, Institute of Health, Charitéplatz 1, 10117 Berlin, Germany. ¹⁰Institute of Clinical Neuroimmunology, Ludwig-Maximilians University, Marchioninstr. 15, 81377 Munich, Germany. ¹¹Department of Neurology, University of California Irvine, 30, 101 The City Dr S, Orange, CA 92868, USA. ¹²Data Integration for Future Medicine consortium (DIFUTURE), Ludwig-Maximilians University, Marchioninstr. 15, Munich 81377, Germany.

Received: 13 November 2018 Accepted: 13 June 2019

Published online: 25 July 2019

References

- Hohlfeld R, Dornmair K, Meinl E, Wekerle H. The search for the target antigens of multiple sclerosis, part 1: autoreactive CD4+ T lymphocytes as pathogenic effectors and therapeutic targets. *Lancet Neurol*. 2016;15:198–209.
- Dos Passos GR, Oliveira LM, da Costa BK, Apostolos-Pereira SL, Callegaro D, Fujihara K, et al. MOG-IgG-associated optic neuritis, encephalitis, and myelitis: lessons learned from neuromyelitis optica spectrum disorder. *Front Neurol*. 2018;9:217.

3. Jarius S, Paul F, Aktas O, Asgari N, Dale RC, de Seze J, et al. MOG encephalomyelitis: international recommendations on diagnosis and antibody testing. *J Neuroinflammation*. 2018;15:134.
4. Peschl P, Bradl M, Höftberger R, Berger T, Reindl M. Myelin oligodendrocyte glycoprotein: deciphering a target in inflammatory demyelinating diseases. *Front Immunol*. 2017;8:529.
5. Spadaro M, Gerdes LA, Mayer MC, Ertl-Wagner B, Laurent S, Krumbholz M, et al. Histopathology and clinical course of MOG-antibody-associated encephalomyelitis. *Ann Clin Transl Neurol*. 2015;2:295–301.
6. Jarius S, Metz I, König FB, Ruprecht K, Reindl M, Paul F, et al. Screening for MOG-IgG and 27 other anti-gliar and anti-neuronal autoantibodies in “pattern II multiple sclerosis” and brain biopsy findings in a MOG-IgG-positive case. *Mult Scler*. 2016;22:1541–9.
7. Spadaro M, Winklmeier S, Beltrán E, Macrini C, Höftberger R, Schuh E, et al. Pathogenicity of human antibodies against myelin oligodendrocyte glycoprotein. *Ann Neurol*. 2018;84:315–28.
8. Narayan R, Simpson A, Fritsche K, Salama S, Pardo S, Mealy M, et al. MOG antibody disease: a review of MOG antibody seropositive neuromyelitis optica spectrum disorder. *Mult Scler Relat Disord*. 2018;25:66–72.
9. Borisow N, Mori M, Kuwabara S, Scheel M, Paul F. Diagnosis and treatment of NMO spectrum disorder and MOG-encephalomyelitis. *Front Neurol*. 2018;9:888.
10. Cobo-Calvo A, Ruiz A, Maillart E, Audoin B, Zephir H, Bourre B, et al. Clinical spectrum and prognostic value of CNS MOG autoimmunity in adults: the MOGADOR study. *Neurology*. 2018;90:e1858–69.
11. Pache F, Zimmermann H, Mikolajczak J, Schumacher S, Lacheta A, Oertel FC, et al. MOG-IgG in NMO and related disorders: a multicenter study of 50 patients. Part 4: afferent visual system damage after optic neuritis in MOG-IgG-seropositive versus AQP4-IgG-seropositive patients. *J Neuroinflammation*. 2016;13:282.
12. Zamvil SS, Slavin AJ. Does MOG Ig-positive AQP4-seronegative opticospinal inflammatory disease justify a diagnosis of NMO spectrum disorder? *Neurol Neuroimmunol Neuroinflamm*. 2015;2:e62.
13. Hamid SHM, Whittam D, Saviour M, Alorainy A, Mutch K, Linaker S, et al. Seizures and encephalitis in myelin oligodendrocyte glycoprotein IgG disease vs aquaporin 4 IgG disease. *JAMA Neurol*. 2018;75:65–71.
14. Ogawa R, Nakashima I, Takahashi T, Kaneko K, Akaishi T, Takai Y, et al. MOG antibody-positive, benign, unilateral, cerebral cortical encephalitis with epilepsy. *Neurol Neuroimmunol Neuroinflamm*. 2017;4:e322.
15. Pandit L, Mustafa S, Uppoor R, Nakashima I, Takahashi T, Kaneko K. Reversible paraspinous muscle hyperintensity in anti-MOG antibody-associated transverse myelitis. *Neurol Neuroimmunol Neuroinflamm*. 2018;5:e412.
16. Havla J, Kumpfel T, Schinner R, Spadaro M, Schuh E, Meinl E, et al. Myelin-oligodendrocyte-glycoprotein (MOG) autoantibodies as potential markers of severe optic neuritis and subclinical retinal axonal degeneration. *J Neurol*. 2017;264:139–51.
17. Bennett JL, de Seze J, Lana-Peixoto M, Palace J, Waldman A, Schippling S, et al. Neuromyelitis optica and multiple sclerosis: seeing differences through optical coherence tomography. *Mult Scler*. 2015;21:678–88.
18. Galetta SL, Villoslada P, Levin N, Shindler K, Ishikawa H, Parr E, et al. Acute optic neuritis: unmet clinical needs and model for new therapies. *Neurol Neuroimmunol Neuroinflamm*. 2015;2:e135.
19. Oberwahrenbrock T, Traber GL, Lukas S, Gabilondo I, Nolan R, Songster C, et al. Multicenter reliability of semiautomatic retinal layer segmentation using OCT. *Neurol Neuroimmunol Neuroinflamm*. 2018;5:e449.
20. Oertel FC, Zimmermann H, Paul F, Brandt AU. Optical coherence tomography in neuromyelitis optica spectrum disorders: potential advantages for individualized monitoring of progression and therapy. *EPMA J*. 2018;9:21–33.
21. Oertel FC, Kuchling J, Zimmermann H, Chien C, Schmidt F, Knier B, et al. Microstructural visual system changes in AQP4-antibody-seropositive NMOSD. *Neurol Neuroimmunol Neuroinflamm*. 2017;4:e334.
22. Oertel FC, Havla J, Roca-Fernández A, Lizak N, Zimmermann H, Motamed S, et al. Retinal ganglion cell loss in neuromyelitis optica: a longitudinal study. *J Neurol Neurosurg Psychiatry*. 2018;89(12):1259–1265.
23. Mader S, Gredler V, Schanda K, Rostasy K, Dujmovic I, Pfaller K, et al. Complement activating antibodies to myelin oligodendrocyte glycoprotein in neuromyelitis optica and related disorders. *J Neuroinflammation*. 2011;8:184.
24. Schippling S, Balk LJ, Costello F, Albrecht P, Balcer L, Calabresi PA, et al. Quality control for retinal OCT in multiple sclerosis: validation of the OSCAR-IB criteria. *Mult Scler*. 2015;21:163–70.
25. Cruz-Herranz A, Balk LJ, Oberwahrenbrock T, Saidha S, Martinez-Lapiscina EH, Lagreze WA, et al. The APOSTEL recommendations for reporting quantitative optical coherence tomography studies. *Neurology*. 2016;86:2303–9.
26. Wingerchuk DM, Banwell B, Bennett JL, Cabre P, Carroll W, Chitnis T, et al. International consensus diagnostic criteria for neuromyelitis optica spectrum disorders. *Neurology*. 2015;85:177–89.
27. Balk LJ, Cruz-Herranz A, Albrecht P, Arnov S, Gelfand JM, Tewarie P, et al. Timing of retinal neuronal and axonal loss in MS: a longitudinal OCT study. *J Neurol*. 2016;263:1323–31.
28. Sato DK, Callegaro D, Lana-Peixoto MA, Waters PJ, Jorge FM de H, Takahashi T, et al. Distinction between MOG antibody-positive and AQP4 antibody-positive NMO spectrum disorders. *Neurology*. 2014;82:474–81.
29. Höftberger R, Sepulveda M, Armangue T, Blanco Y, Rostásy K, Cobo Calvo A, et al. Antibodies to MOG and AQP4 in adults with neuromyelitis optica and suspected limited forms of the disease. *Mult Scler*. 2015;21:866–74.
30. Akaishi T, Sato DK, Nakashima I, Takeshita T, Doi H, et al. MRI and retinal abnormalities in isolated optic neuritis with myelin oligodendrocyte glycoprotein and aquaporin-4 antibodies: a comparative study. *J Neurol Neurosurg Psychiatry*. 2016;87:446–8.
31. Nakajima H, Motomura M, Tanaka K, Fujikawa A, Nakata R, Maeda Y, et al. Antibodies to myelin oligodendrocyte glycoprotein in idiopathic optic neuritis. *BMJ Open*. 2015;5:e007766.
32. Akaishi T, Nakashima I, Takeshita T, Mugikura S, Sato DK, Takahashi T, et al. Lesion length of optic neuritis impacts visual prognosis in neuromyelitis optica. *J Neuroimmunol*. 2016;293:28–33.
33. Jarius S, Ruprecht K, Kleiter I, Borisow N, Asgari N, Pitarokouli K, et al. MOG-IgG in NMO and related disorders: a multicenter study of 50 patients. Part 2: epidemiology, clinical presentation, radiological and laboratory features, treatment responses, and long-term outcome. *J Neuroinflammation*. 2017;13(1):280.
34. Jitrapaikulsan J, Chen JJ, Flanagan EP, Tobin WO, Fryer JP, Weinschenker BG, et al. Aquaporin-4 and myelin oligodendrocyte glycoprotein autoantibody status predict outcome of recurrent optic neuritis. *Ophthalmology*. 2018;125:1628–37.
35. Ramanathan S, Reddel SW, Henderson A, Parratt JDE, Barnett M, Gatt PN, et al. Antibodies to myelin oligodendrocyte glycoprotein in bilateral and recurrent optic neuritis. *Neurol Neuroimmunol Neuroinflamm*. 2014;1(4):e40.
36. Brandt AU, Oberwahrenbrock T, Kadas EM, Lagreze WA, Paul F. Dynamic formation of macular microcysts independent of vitreous traction changes. *Neurology*. 2014;83:73–7.
37. Kaufhold F, Zimmermann H, Schneider E, Ruprecht K, Paul F, Oberwahrenbrock T, et al. Optic neuritis is associated with inner nuclear layer thickening and microcystic macular edema independently of multiple sclerosis. *PLoS One*. 2013;8(8):e71145.
38. Ramanathan S, Prelog K, Barnes EH, Tantsis EM, Reddel SW, Henderson AP, et al. Radiological differentiation of optic neuritis with myelin oligodendrocyte glycoprotein antibodies, aquaporin-4 antibodies, and multiple sclerosis. *Mult Scler*. 2016;22:470–82.
39. Felix CM, Levin MH, Verkman AS. Complement-independent retinal pathology produced by intravitreal injection of neuromyelitis optica immunoglobulin G. *J Neuroinflammation*. 2016;13:275.
40. Chien C, Scheel M, Schmitz-Hübsch T, Borisow N, Ruprecht K, Bellmann-Strobl J, et al. Spinal cord lesions and atrophy in NMOSD with AQP4-IgG and MOG-IgG associated autoimmunity. *Mult Scler*. 2018;1352458518815596.
41. Spadaro M, Gerdes LA, Krumbholz M, Ertl-Wagner B, Thaler FS, Schuh E, et al. Autoantibodies to MOG in a distinct subgroup of adult multiple sclerosis. *Neurol Neuroimmunol Neuroinflamm*. 2016;3:e257.
42. Körtvélyessy P, Breu M, Pawlitzki M, Metz I, Heinze H-J, Matzke M, et al. ADEM-like presentation, anti-MOG antibodies, and MS pathology: TWO case reports. *Neurol Neuroimmunol Neuroinflamm*. 2017;4:e335.

Publisher's Note

Springer Nature remains neutral with regard to jurisdictional claims in published maps and institutional affiliations.

13. Publication list

Original Publications (first author)

Frederike C Oertel*, Olivier Outteryck, Benjamin Knier, Hanna Zimmermann, Nadja Borisow, Judith Bellmann-Strobl, Astrid Blaschek, Sven Jarius, Markus Reindl, Klemens Ruprecht, Edgar Meinl, Reinhard Hohlfeld, Friedemann Paul, Alexander U Brandt, Tania Kümpfel, Joachim Havla. *Optical coherence tomography in myelin-oligodendrocyte-glycoprotein antibody-seropositive patients: a longitudinal study*. J. Neuroinflammation. 16 (2019) 154. doi:10.1186/s12974-019-1521-5. **(IF 2018: 5.700)**

Frederike C Oertel*, Joachim Havla*, Adriana Roca-Fernández, Nathaniel Lizak, Hanna Zimmermann, Seyedamirhosein Motamedi, Nadja Borisow, Owen White, Judith Bellmann-Strobl, Philipp Albrecht, Klemens Ruprecht, Sven Jarius, Jacqueline Palace, Maria Leite, Tania Kümpfel, Friedemann Paul, Alexander U Brandt: *Retinal Ganglion Cell Loss in Neuromyelitis Optica: A Longitudinal Study*. J Neurol Neurosurg Psychiatry. 2018; doi:10.1136/jnnp-2018-318382. **(IF 2018: 8.272)**

Frederike C Oertel*, Hanna Zimmermann*, Janine Mikolajczak, Maria Weinhold, Ella Maria Kadas, Timm Oberwahrenbrock, Florence Pache, Judith Bellmann-Strobl, Klemens Ruprecht, Friedemann Paul, Alexander U Brandt: *Contribution of blood vessels to retinal nerve fiber layer thickness in NMOSD*. Neurol - Neuroimmunol Neuroinflammation. 2017;4:e338. **(IF 2017: not available)**

Frederike C Oertel*, Joseph Kuchling*, Hanna Zimmermann, Claudia Chien, Felix Schmidt, Benjamin Knier, Judith Bellmann-Strobl, Thomas Korn, Michael Scheel, Alexander Klistorner, Klemens Ruprecht, Friedemann Paul, Alexander U Brandt: *Microstructural visual system changes in AQP4-antibody seropositive NMOSD*. Neurol - Neuroimmunol Neuroinflammation. 2017;4:e334. **(IF 2017: not available)**

Original Publications (coauthor)

Athina Papadopoulou*, **Frederike C Oertel**, Laura Gaetano, Joseph Kuchling, Hanna G. Zimmermann, Claudia Chien, Nadja Borisow, Judith Bellmann-Strobl, Klemens Ruprecht, Mallar M. Chakravarty, Michael Scheel, Stefano Magon, Jens Wuerfel, Friedemann Paul, Alexander U. Brandt: *Selective, attack-related damage of thalamic nuclei in neuromyelitis optica spectrum disorders*. J Neurol Neurosurg Psychiatry. Epub 2019 <http://dx.doi.org/10.1136/jnnp-2018-320249> (**Impact Factor 2018: 8.272**)

Joseph Kuchling*, Yael Backner*, **Frederike C Oertel**, Noa Raz, Judith Bellmann-Strobl, Klemens Ruprecht, Friedemann Paul, Netta Levin, Alexander U Brandt, Michael Scheel: *Comparison of probabilistic tractography and tract-based spatial statistics for assessing optic radiation damage in patients with autoimmune inflammatory disorders of the central nervous system*. NeuroImage: Clinical. 2018; 19:538-550 (**Impact Factor 2018: 3.943**)

Carsten Finke*, Hanna Zimmermann, Florence Pache, **Frederike C Oertel**, Lisa Kramarenko, Judith Bellmann-Strobl, Klemens Ruprecht, Alexander U Brandt, Friedemann Paul: *Visual network reorganization in neuromyelitis optica*. JAMA Neurol. 2018; 75:296–303 (**Impact Factor 2018: 12.321**)

Sunil Kumar Yadav*, Seyedamirhosein Motamedi, Timm Oberwahrenbrock, **Frederike C Oertel**, Konrad Polthier, Friedemann Paul, Ella Maria Kadas, Alexander U Brandt: *CuBe: Parametric Modeling of 3D Foveal Shape using Cubic Bézier*. Biomed Opt Express. 2017; 8:4181–4199. (**Impact Factor 2017 3.482**)

Felix Schmidt*, Hanna Zimmermann*, Janine Mikolajczak, **Frederike C Oertel**, Florence Pache, Maria Weinhold, Johann Schinzel, Judith Bellmann-Strobl, Klemens Ruprecht, Friedemann Paul, Alexander U Brandt: *Severe structural and functional visual system damage leads to profound loss of vision-related quality of life in patients with neuromyelitis optica spectrum disorders*. Mult Scler Relat Disord. 2017; 11:45–50. (**Impact Factor 2017: 3.119**)

Florence Pache*, Hanna Zimmermann*, Janine Mikolajczak, Sophie Schumacher, Anna Lacheta, **Frederike C Oertel**, Judith Bellmann-Strobl, Sven Jarius, Brigitte Wildemann,

Markus Reindl, Amy Waldman, Kerstin Soelberg, Nasrin Asgari, Marius Ringelstein, Orhan Aktas, Nikolai Gross, Mathias Buttman, Thomas Ach, Klemens Ruprecht, Friedemann Paul, Alexander U Brandt: *MOG-IgG in NMO and related disorders: A multicenter study of 50 patients. Part 4: Afferent visual system damage after optic neuritis in MOG-IgG-seropositive versus AQP4-IgG-seropositive patients.* J Neuroinflammation. 2016; 13:282. **(Impact Factor 2016: 5.102)**

Case Studies and Letters to the Editor

Theodora Gkaniatsou*, Athina Papadopoulou*, Friedemann Paul, Alexander U Brandt, **Frederike C Oertel**: *Frequency of autoimmune disorders and autoantibodies in European patients with neuromyelitis optica spectrum disorders.* Acta Neurol Belg. Epub 2019; <https://doi.org/10.1007/s13760-019-01176-6> **(Impact Factor 2018: 1.612)**

Frederike C Oertel*, Francesca Bosello*, Axel Petzold: *Retinal optical coherence tomography shows optic disc changes in low intracranial pressure headaches: a case report.* Acta Neurol Belg. 2018; 118:131–133. **(Impact Factor 2018: 1.612)**

Review Articles

Frederike C Oertel*, Jana Schließeit*, Alexander U Brandt, Friedemann Paul: *Cognitive Impairment in Neuromyelitis Optica Spectrum Disorders: A Review of Clinical and Neuroradiological Features.* Front. Neurol. 2019 Epub doi: 10.3389/fneur.2019.00608. eCollection 2019. **(Impact Factor 2018: 2.635)**

Frederike C Oertel*, Hanna Zimmermann, Alexander U Brandt, Friedemann Paul: *Novel uses of retinal imaging with optical coherence tomography in multiple sclerosis.* Expert Rev Neurother. 2019 Jan;19(1):31-43. **(Impact Factor 2018: 3.453)**

Frederike C Oertel*, Hanna Zimmermann, Friedemann Paul, Alexander U Brandt: *Optical Coherence Tomography in Neuromyelitis Optica Spectrum Disorders: Potential advantages for individualized monitoring of progression and therapy.* EPMA J. 2018; 9:21–33. **(Impact Factor 2018: 4.661)**

Athina Papadopoulou*, **Frederike C Oertel**, Hanna Zimmermann, Oliver Zeitz, Alexander U Brandt, Friedemann Paul. Optische Kohärenztomographie bei Erkrankungen des zentralen Nervensystems. *Klin Monatsbl Augenheilkd.* 2018; 235:1242–1258. (**Impact Factor 2018: 0.792**)

Frederike C Oertel*, Hanna Zimmermann, Alexander U Brandt, Friedemann Paul: *Optische Kohärenztomographie bei Neuromyelitis optica-Spektrum-Erkrankungen.* *Nervenarzt.* 2017; 88:1411–1420. (**Impact Factor 2017: 0.738**)

Livia Asan*, Geerthe M Balk, Nina Bieber, Sarah Hatzenbühler, Christine Heuer, Jonas Hillebrandt, Uwe Lewin, Katharina Lichter, **Frederike C Oertel**, Anthony Petkidis, Katharina Reichel, Melanie M Weber, Vinona Wicht, Tina Pangrsic, Christian Vogel. *Shedding light on gene therapy as a future treatment for sensory disorders – from gene replacement to optogenetics.* *Z Für Audiol.* 2016; 55:94-104 (**Impact Factor 2016: not available**)

Conference Abstracts

Valentin Jünger*, Graham Cooper, Claudia Chien, Meera Chikermane, **Frederike C Oertel**, Hanna Zimmermann, Klemens Ruprecht, Sven Jarius, Nadja Siebert, Joseph Kuchling, Athina Papadopoulou, Susanna Asseger, Judith Bellmann-Strobl, Friedemann Paul, Alexander U. Brandt, Michael Scheel: *Optic Chiasm Assessment on Clinical Standard 3D T1w-MRI detects Optic Nerve Atrophy.* Poster. ARSEP – MS Meeting. Paris, France. 05/2019

Patrik Althoff*, Britta King, Daniel Drebingen, Laura Schäfer, Friederike Rosenthal, **Frederike C Oertel**, Noah Ayadi, Brian Dommisch, Karen Otte, René M Gieß, Judith Bellmann-Strobl, Christoph Heesen, Friedemann Paul, Alexander U Brandt, Jan-Patrick Stellmann, Tanja Schmitz-Hübsch, Ludwig Rasche: *Der Zusammenhang kognitiv-motorischer Interferenz mit Erkrankungssymptomen bei Multipler Sklerose.* Poster. DGN. Berlin, Germany. 11/2018

Frederike C Oertel*, Joachim Havla, Adriana Roca-Fernández, Nathaniel Lizak, Hanna Zimmermann, Seyedamirhosein Motamedi, Nadja Borisow, Owen B White, Judith

Bellmann-Strobl, Philipp Albrecht, Klemens Ruprecht, Sven Jarius, Jacqueline Palace, Maria Isabel Leite, Tania Kümpfel, Friedemann Paul, Alexander U Brandt: *Retinal Ganglion Cell Loss in Neuromyelitis Optica: A Longitudinal Study*. **Talk**. ECTRIMS. Berlin. Germany. 10/2018.

Joachim Havla*, **Frederike C Oertel***, Olivier Outteryck, Benjamin Knier, Hanna Zimmermann, Luise Böhm, Edgar Meinl, Reinhard Hohlfeld, Friedemann Paul, Alexander U Brandt, Tania Kümpfel: *Peripapillar Retinal Nerve Fiber Loss in Myelin-Oligodendrocyte-Glycoprotein Antibody-Positive Patients: A Longitudinal Study*. Poster. ECTRIMS. Berlin, Germany. 10/2018

Joseph Kuchling*, **Frederike C Oertel**, Hanna G. Zimmermann, Claudia Chien, René M. Giess, Judith Bellmann-Strobl, Klemens Ruprecht, Jens Wuerfel, Friedemann Paul, Michael Scheel, Alexander U. Brandt: *Modelling MS progression in the afferent visual system: Retinal, optic radiation and visual cortex changes after clinically isolated optic neuritis*. Poster. ECTRIMS. Berlin, Germany. 10/2018

Seyedamirhosein Motamedi*, **Frederike C Oertel**, Joachim Havla, Sunil Yadav, Ella Maria Kadas, Hanna Zimmermann, Klemens Ruprecht, Judith Bellmann-Strobl, Tania Kümpfel, Friedemann Paul, Alexander U Brandt: *3D fovea morphometry reveals distinct foveal changes in neuromyelitis optica spectrum disorders*. Poster. ECTRIMS. Berlin, Germany. 10/2018

Athina Papadopoulou*, **Frederike C Oertel**, Laura Gaetano, Joseph Kuchling, Hanna Zimmermann, Nadja Borisow, Judith Bellmann-Strobl, Klemens Ruprecht, Michael Scheel, Stefano Magon, Jens Wuerfel, Friedemann Paul, Alexander U. Brandt: *Affection of thalamic subnuclei in NMOSD: evidence of anterograde transsynaptic degeneration in the visual pathway*. Poster. ECTRIMS. Berlin, Germany. 10/2018

Noah Ayadi*, Hanna Zimmermann, Yael Backner, **Frederike C Oertel**, Nadja Borisow, René Giess, Judith Bellmann-Strobl Klemens Ruprecht, Alexander U. Brandt, Netta Levin, Friedemann Paul: *Motion perception is associated with functional and structural visual pathway damage in multiple sclerosis and neuromyelitis optica spectrum disorders*. Poster. ECTRIMS. Berlin, Germany. 10/2018

Panayiota Petrou*, Ibrahim Kassis, Netta Levin, Friedemann Paul, Michael Scheel, **Frederike C Oertel**, Michelle Hallimi, Tamir Ben Hur, Ariel Ginzberg, Dimitrios Karrusis: *A phase IIIb double blind trial to investigate the efficacy and the optimal way of administration of mesenchymal stem cells (MSC) in active and progressive multiple sclerosis (MS)*. Poster. ECTRIMS. Berlin, Germany. 10/2018

Svenja Specovius*, Hanna Zimmermann, Claudia Chien, **Frederike C Oertel**, Lawrence Cook, Elena H Martinez-Lapiscina, Marco Aurélio Lana Peixoto, Mariana Andrade Fontenelle, Jaqueline Palace, Adriana Roca-Fernandez, Alejandro Rubio Diaz, M.I. Leite, S.M. Sharma, Sasitorn Siritho, Ayse Altintas, R. Yildirim, U. Tanriverdi, Anu Jacob, Saif Huda, Romain Marignier, Elodie Nerrant, Alvaro Cobo Calvo, Jérôme de Seze, Thomas Senger, Lekha Pandit, Anitha Dcunha, Ibis Soto de Castillo, Denis Bichuetti, I. Maynard Tavares, Eugene F. May, Caryl Tongco, Joachim Havla, Letizia Leocani, Marco Pisa, M. Radaelli, Orhan Aktas, Marius Ringelstein, Jana Rybak, Philipp Albrecht, Ho Jin Kim, Jae-Won Hyun, Nasrin Asgari, Kerstin Soelberg, Yang Mao-Draayer, Hadas-Stiebel-Kalish, Ilya Kister, Zoe Rimler, Allyson Reid, Alexander U. Brandt, Friedemann Paul with the GJCF International Clinical Consortium for NMOSD: *The CROCTINO project: An international retrospective multi-center study of retinal optical coherence tomography in 501 patients with neuromyelitis optica spectrum disorders*. Poster. ECTRIMS. Berlin, Germany. 10/2018

Frederike C Oertel*, Nathaniel Lizak, Hanna Zimmermann, Timm Oberwahrenbrock, Janine Mikolajczak, Joachim Havla, Felix Schmidt, Judith Bellmann-Strobl, Tania Kümpfel, Alexander Klistorner, Klemens Ruprecht, Friedemann Paul, Alexander U Brandt: *Retinal changes in aquaporin-4 antibody seropositive Neuromyelitis Optica Spectrum Disorders: a longitudinal study*. Poster. ECTRIMS. London, UK. 10/2017

Claudia Chien*, **Frederike C Oertel**, Felix Schmidt, Michael Scheel, Klemens Ruprecht, Judith Alexander U Brandt, Friedemann Paul: *Identification of Structural Imaging Correlates of Disability in Neuromyelitis Optica: A Graph Theory-based Approach*. Poster. ECTRIMS. London, UK. 10/2017

Frederike C Oertel*, Joseph Kuchling, Hanna Zimmermann, Claudia Chien, Felix Schmidt, Judith Bellmann-Strobl, Michael Scheel, Alexander Klistorner, Klemens Ruprecht, Friedemann Paul, Alexander U Brandt: *Microstructural changes in the afferent visual system of asymptomatic patients with AQP4-antibody positive neuromyelitis optica spectrum disorders*. Poster. AAN. Boston, USA. 04/2017

Frederike C Oertel*, Hanna Zimmermann, Janine Mikolajczak, Maria Weinhold, Ella-Maria Kadas, Timm Oberwahrenbrock, Florence Pache, Friedemann Paul, Alexander U Brandt: *Influence of blood vessels on peripapillary retinal nerve fiber layer thickness measurements in patients with Neuromyelitis optica spectrum disorders*. Poster. ECTRIMS. London, UK. 09/2016

Selected invited Talks

Frederike C Oertel*: OCT zur retinalen Bildgebung bei Patienten mit Spinozerebellärer Ataxie. Deutscher Kongress für Parkinson und Bewegungsstörungen 2019. Düsseldorf, Germany. 03/08/2019

Frederike C Oertel*: Optical Coherence Tomography in Multiple Sclerosis. The International Congress on Advanced Treatments & Technologies in Multiple Sclerosis 2018. London, UK. 12/14/2018

Frederike C Oertel*: Probabilistic tractography of the optic radiation reveals microstructural visual system damage in NMOSD. Imaging Workshop: Neurodegeneration and Neuroplasticity. UKE Hamburg, Germany. 11/16/2018

Frederike C Oertel*: Neue OCT-Verfahren für die Neurologie. Neurowoche 2018 (Kongress der deutschen Gesellschaft für Neurologie). Berlin, Germany. 11/03/2018

Frederike C Oertel*: Recent research on retinal changes in NMOSD. IMSVISUAL Meeting at ECTRIMS. Paris, France. 10/27/2017

* first author

14. Acknowledgments

The time of my thesis taught me a lot about myself. It revealed my capacities and expanded them; it helped me to recognize my priorities in life and to disobey them occasionally. I sincerely thank everyone who accompanied and supported me on this path!

First, I would like to express my gratitude to my supervisors Prof. Dr. Friedemann Paul and Dr. Alexander Brandt. Thank you for the high degree of trust you have placed in me and the endless opportunities you offered. I would like to thank you for taking all my ideas seriously and always supporting me. Dear Alex, your enthusiasm and inventiveness is impressive; my great passion for research would not exist without you. I also would like to thank my third supervisor Dr. Joseph Kuchling and my secret supervisor Dr. Hanna Zimmermann, who always helped with words and deeds and seemed to have an answer to my questions at all times. Nevertheless, I am also deeply grateful to Dr. Timm Oberwahrenbrock and Dr. Michael Scheel, who always brought me back down to earth and critically challenged - and improved - my work. Moreover, this thesis would not have been possible without the everlasting helpfulness and support of the entire team of AG Paul, for which I am incredibly thankful. Last but not least, I am also much obliged to all patients, who participated in our studies, and all collaborators, who made our multi-center studies possible, especially Prof. O. Aktas, Dr. P. Albrecht, Prof. N. Asgari, Dr. B. Knier, Prof. T. Kümpfel, Dr. J. Havla, Prof. R. Hohlfeld, Dr. S. Jarius, Prof. A. Klistorner, Prof. E. Meini, Dr. O. Outteryck, Dr. J. Palace, Prof. A. Petzold, Prof. M. Reindl, and Prof. B. Wildemann as well as their colleagues, and to the Berlin Institute of Health for my M.D. Student Research Stipend.

Despite the productivity and efficiency of the last years, I am incredible thankful to all my friends and my family, who constantly reminded me that there is more to life than efficiency. It is the greatest gift for me, when you take the time to do nothing together. Your support is my strongest drive!

Thank you.